

EUROPEAN SCHOOL OF MOLECULAR MEDICINE, NAPLES SITE
Scientific coordinator Prof. Francesco Salvatore

UNIVERSITÀ DEGLI STUDI DI NAPOLI FEDERICO II

Ph.D. in Molecular Medicine

Curriculum

XX ciclo

*Title of the Thesis: **RAS ONCOGENE AND DEREGLATION OF
DIFFERENTIATION IN THYROID CELLS***

Supervisor :

Prof. Alfredo Fusco

Ph.D. student :

Dr. Maria Giuseppina Baratta

Internal Supervisor :

Prof. Tommaso Russo

External Supervisor :

Prof. Mariano Barbacid

Table of Contents

Table of Contents.....	iii
Abbreviations.....	vii
List of Figures.....	viii
ABSTRACT.....	1
1. Synopsis of Background.....	1
2. Aim of research.....	2
3. Results.....	2
INTRODUCTION.....	3
1. Ras oncogenes.....	3
1.1. Ras proteins.....	3
1.2. Ras proteins activity regulation and Ras oncoproteins.....	4
1.3. Ras proteins signal transduction pathways.....	5
1.4. Ras oncogenes and human cancers.....	8
1.5. Ras oncogenes in experimental models.....	11
2. The Thyroid Follicular Cell (TFC).....	12
2.1. The thyroid gland.....	12
2.2. TFCs differentiation.....	12
2.3. The Sodium/Iodide symporter (NIS).....	14
2.4. The TSH receptor (TSHr).....	16
2.5. The Paired-Box transcription factor 8 (Pax8).....	21
3. The TFCs derived cancers.....	25
3.1. TFCs malignancies.....	25
3.2. Multistep cancerogenesis.....	26
3.3. Genetic alterations.....	28
3.4. Role of Ras oncogenes.....	31
3.5. Thyroid cancer therapy.....	33
4. The FRTL-5 thyroid cell line.....	35
4.1. FRTL-5 cells.....	36
4.2. Transformation of FRTL-5 cells by Ras oncogene.....	36
4.3. An inducible system of Ras mediated transformation of FRTL5 cells.....	37
MATERIALS AND METHODS.....	38
1. N-terminal Multiple-Tags (TTN, DTN, MTN) gene synthesis and cloning in pCEFL expression vector.....	38
1.1. TTN Tag.....	38
1.2. DTN Tag.....	40
1.3. MTN Tag.....	42
2. C-terminal Multiple-Tags (TTC, DTC, MTC) cloning in pCEFL expression vector.....	44

2.1. TTC Tag.....	44
2.2. DTC Tag.....	45
2.3. MTC Tag.....	45
3. Expression and reporter constructs.....	48
3.1. Reporter constructs.....	48
3.2. N-terminal (TTN, DTN, MTN) tagged-Pax8 expression vectors.....	48
3.3. C-terminal (TTC, DTC, MTC) tagged-Pax8 expression vectors.....	49
3.4. GAL-Pax8 deletion derivatives expression vectors.....	49
3.5. Pax8 deletion derivatives expression vectors.....	50
3.6. Other Expression constructs.....	51
4. Cell culture.....	52
5. Transfections.....	52
6. cAMP Enzyme Immunometric assay.....	53
7. PKA kinase activity assay.....	54
8. Proteins extraction.....	54
9. Flag-Pax8 Immunoprecipitation (IP).....	55
9.1. Nuclear proteins extraction.....	55
9.2. Immunoprecipitation.....	55
9.3. Elution with 3xFLAG peptide.....	56
10. Multiple Tagged-Pax8 Affinity purification TESTs.....	56
10.1. Protein extracts preparation.....	56
10.2. Streptavidin-binding affinity purification.....	56
10.3. V5-IP.....	57
10.4. Flag-IP.....	57
10.5. Flag/V5 double IP.....	58
10.6. Aspecific elution through boiling in SDS.....	58
10.7. TEV cleavage mediated elution.....	58
10.8. Precission cleavage mediated elution.....	59
11. Monodimensional SDS-PAGE and Bidimensional electrophoresis.....	59
12. Western Blot.....	60
13. RNA extraction and Real-Time RT-PCR.....	61
14. Chromatin-IP.....	61
14.1. Crosslinked chromatin preparation.....	61
14.2. Transcription rate measurement.....	62
14.3. Pax8 binding measurement.....	63
15. Gel mobility shift.....	63
16. EMBL Compounds library.....	64
17. GFP assay for High-throughput screening (HTS-GFP assay).....	64
17.1. Cell culturing.....	64
17.2. Cell plating on 96well assay plates.....	64
17.3. Compounds addition.....	65
17.4. Plate washing.....	66
17.5. GFP fluorescence read-out.....	67
17.6. Results analysis (fold activation and determination of hits frequency).....	68
18. Luciferase assay for High-throughput screening (HTS-Luc assay).....	68
18.1. Cell culturing.....	68
18.2. Cell plating.....	69
18.3. Transfection.....	69
18.4. Compound addition.....	69

18.5. Luciferase luminescence read-out.....	70
18.6. Results analysis	70
19. ERK phosphorylation assay.....	70
RESULTS	72
1. ER-Ras ^{V12} activation induces a rapid downregulation of thyroidspecific gene expression.....	72
2. NIS downregulation is achieved through an ER-RAS ^{V12} mediated impairment of NUE (NIS Upstream enhancer)transcriptional activity.....	74
3. Activation of Ras reduces both the amount and the activity of Pax8.....	79
4. Role of the TSHr/cAMP pathway in ER-RAS ^{V12} induced dedifferentiation.....	90
4.1. TSHr downregulation is not the master event in oncogenic Ras induced de-differentiation	90
4.2. The reduction of cAMP intracellular levels induced by oncogenic Ras is not the cause of the dedifferentiated phenotype.....	91
4.3. Oncogenic Ras inhibits the TSHr/cAMP pathway by acting also downstream of cAMP production.....	91
4.4. Oncogenic Ras Inhibits PKA activity	91
5. Pax8 activity is impaired by Ras oncogene through inhibition of the cAMP/PKA pathway.....	108
5.1. Pax8 activity is regulated by PKA	108
5.2. PKA catalytic subunit over-expression restore Ras oncogene induced Pax8 inactivation and NUE activity.....	108
6. A minimal Pax8 transactivation domain is required to confer PKA responsiveness	115
6.1. Oncogenic Ras does not induce major post-translational modification on Pax8	115
6.2. Identification of Pax8 transactivation domain minimal regions responsive to ERRAS ^{V12}	115
6.3. Oncogenic Ras action is FRTL-5 specific.....	116
6.4. Identification of Pax8 transactivation domain minimal regions responsive to PKA.....	116
7. Characterization of oncogenic Ras induced modifications of Pax8 transcriptional complexes	127
7.1. Gel filtration analysis of Pax8 transcriptional complex.....	127
7.2. Generation of multiple Tags to isolate Pax8 cofactors.....	128
7.3. Evaluation of Tagged-Pax8 chimaeric proteins activity	128
7.4. Generation of stable cell lines expressing different multitag-Pax8.....	129
7.5. Testing of BirA/Avi biotinylation system and elution procedures	130
7.6. Comparison of Biotin-based purification system versus V5 and Flag epitopes based immunoprecipitations.....	131
7.7. Comparison of V5 and Flag single-step IPs versus double-step IP.....	132
7.8. Analysis of Pax8 cofactors differentially regulated by ERRAS ^{V12}	133
8. Oncogenic Ras induced de-differentiation is a reversible phenotype	145
9. Oncogenic Ras de-differentiates FRTL-5 cells through the MAPK pathway	147
10. Identification of chemical inhibitors of the MAPK pathway through a cell-based HTS assay	151
10.1. GFP expression, driven by the NIS gene enhancer, is sensitive to oncogenic Ras activation.....	151
10.2. Set-up of cell-based HTS assays	151

10.3. Pilot Screen.....	152
10.4. Lead Screen.....	153
10.5. Hits confirmation and specificity screen.....	153
10.6. EC50 determination and confirmatory screening.....	153
10.7. Hits activity on MAPK pathway and endogenous NIS gene expression	154
DISCUSSION.....	183
Bibliography.....	188

Abbreviations

The abbreviations used are: Follicular thyroid cell, **TFC**; Follicular Rat thyroid immortalized cell line, **FRTL-5**; Oncogenic human h-ras (G12V) fused to the ERTM Ligand binding domain, **ER-Ras^{V12}**; FRTL5 derived stable cell line expressing ER-Ras^{V12}, **C111**; Tamoxifen, **4OHT**; Thyroperoxidase, **TPO**; Sodium-Iodide symporter, **NIS**; thyroid oxidase, **DUOX2**; TSH receptor, **TSHr**; thyroglobulin, **Tg**; NIS upstream enhancer, **NUE**; C111 derived stable cell lines expressing Flag-Pax8, **Px clones**; Artificial promoter containing 5 Pax8 binding sites, **Cp5**; Rho-tagged human TSHr, **hTSHr**; C111 derived stable cell lines expressing hTSHr, **T clones**; Adenylyl cyclase stimulator Forskolin, **Fsk**; cAMP analogue 8-(4-Chlorophenylthio)adenosine 3',5'-cyclic monophosphate, **8-CPT**; phosphodiesterases inhibitor 3-Isobutyl-1-methylxanthine, **IBX**; Quantitative Western Blot, **QWB**; FRTL5 derived stable cell lines expressing oncogenic human h-ras (G12V), **RasV12 clones**; MAPK pathway inhibitor U-0126, **UO**; MAPK pathway inhibitor PD-98059, **PD**; C111 derived stable cell lines expressing GFP under the control of the NIS gene enhancer NUE, **NG6**; High throughput screening, **HTS**;

List of Figures

RESULTS section

<u>Figure1</u>	: ER-Ras ^{V12} activation induces a rapid downregulation of thyroid specific gene expression.....	73
<u>Figure2-4</u>	: NIS downregulation is achieved through an ER-Ras ^{V12} mediated impairment of NUE activity.....	76
<u>Figure5-13</u>	: Activation of Ras reduces both the amount and the activity of Pax8.....	81
<u>Figure14-27</u>	: Role of the TSHr/cAMP pathway in ER-Ras ^{V12} induced dedifferentiation.....	93
<u>Figure28-32</u>	: Pax8 activity is impaired by Ras oncogene through inhibition of the cAMP/PKA pathway.....	110
<u>Figure33-41</u>	: A minimal Pax8 transactivation domain is required to confer PKA responsiveness.....	118
<u>Figure42-52</u>	: Characterization of oncogenic Ras induced modification of Pax8 transcriptional complexes.....	134
<u>Figure53</u>	: Oncogenic Ras induced dedifferentiation is reversible.....	146
<u>Figure54-56</u>	: Oncogenic Ras dedifferentiate FRTL-5 cells through the MAPK pathway.....	148
<u>Figure57-71</u>	: Identification of chemical inhibitors of the MAPK pathway through a cell based HTS assay.....	156

ABSTRACT

1. Synopsis of Background

Ras gene family includes three closely related genes (K-*ras*, N-*ras* e H-*ras*). These genes encode a monomeric GTPase localized at the inner surface of the plasmatic membrane whose activity is strictly controlled by the cell (1). Ras isoforms, H-, N- e K-*ras*, share most of the known functions and represent an important convergence point in the transduction of extracellular signals regulating proliferation and differentiation. In more than 30% of all human tumours *ras* genes are interested by mutation and encode a constitutively active protein, contributing to several aspects of malignancy (2).

Today an increasing number of data suggest that tumorigenesis could arise through the generation of the so-called “Cancer Stem Cells” (CSC). The cellular origin of CSC, if they arise from tissue stem cells or from restricted progenitor/differentiated cells, has not been definitively determined. Independently from their cellular origin, CSC are staminal-like cells which give raise to tumours instead of normal tissues because of defects in the differentiation pathway (3). So far it has been demonstrated that *ras* oncogenes mediated transformation of differentiated epithelial thyroid cell lines, such as FRTL5, is coupled to suppression of the differentiated thyroid phenotype (4, 5). This cellular system represents a model in which neoplastic transformation is associated to deregulation of differentiation.

A similar deregulation of thyroid differentiation is observed, *in vivo*, in anaplastic thyroid carcinomas which are characterized by cancerous cells that lack the differentiated phenotype peculiar to the follicular thyroid cell from which they have originated. Ras oncogenic mutations occur in about 50% of these carcinomas, suggesting that they could have a role in the genesis of the anaplastic phenotype. The lack of thyroid differentiation is of particular relevance in these tumours, because is the reason why the ordinary therapeutic protocols, based on radioactive iodide, do not work. Radioactive

iodide accumulation in cancerous thyroid cells is indeed mediated by the NIS gene product whose expression is characteristic of terminally differentiated follicular thyroid cells (6).

2. Aim of research

Aim of this research was the characterization of the molecular mechanisms through which *ras* oncogene induces dedifferentiation using as a model the epithelial thyroid cell line FRTL5.

3. Results

These studies were done by using a chimeric Ras oncoprotein whose activity is Tamoxifen-dependent (4). This chimeric Ras oncoprotein (ER-HRas^{V12}) was already demonstrated capable of reproducing *ras* oncogene functions in FRTL5 cells in a Tamoxifen-dependent way (4). This inducible system allowed the analysis of the kinetic of *ras* oncogene induced transformation and the isolation of primary events, induced by the oncogene, responsible for the loss of differentiation.

Through the use of such conditional model system, I found that immediately after ER-Ras^{V12} activation Thyroid specific gene expression is downregulated and in particular NIS transcription is turned off. I demonstrate that Ras oncoprotein inactivates Pax8 transcriptional activity early on in the transformation process and induces inhibition of the TSHr pathway through a double mechanism which involves both downregulation of TSHr expression itself plus an additional interference with the TSHr signalling, the latter located downstream of cAMP production.

Such effects were reversible and induced by Ras through the MAPK pathway. I demonstrate that cAMP pathway inhibition is the cause of Pax8 inactivation and that by restoring a functional cAMP pathway I can restore both Pax8 activity and thyroid-specific gene expression

I also engineered a HTS (High-Throughput Screening) assay in order to test the re-differentiating action of 50000 compounds. I found some new structures which could be optimized in order to be used as re-differentiating agents in thyroid cancer therapy or which could be tested as general inhibitors of Ras oncogenes activity even in other kind of cancers.

INTRODUCTION

1. Ras oncogenes

Ras gene family in mammals includes three closely related genes (*K-ras*, *N-ras* e *H-ras*). These genes encode a monomeric GTPase localized at the inner surface of the plasmatic membrane whose activity is strictly controlled by the cell (1). Ras isoforms, H-, N- and K-Ras, share most of the known functions and represent an important convergence point in the transduction of extracellular signals regulating proliferation and differentiation. In more than 30% of all human tumours *ras* genes are interested by mutation and encode a constitutively active protein, which contributes to several aspects of malignancy(2).

1.1. Ras proteins

Ras proteins are extrinsic membrane-bound guanine nucleotide binding proteins which possess an intrinsic GTP hydrolysis activity that shuttles them from an active (GTP-bound) to an inactive (GDP-bound) signalling state. Reactivation of these proteins occurs when their bound GDP nucleotide is ejected making place for the binding of the more abundant cellular GTP (7).

The four mammalian Ras isoforms (H-,N- and the two alternative splicing product of the K-Ras locus K-Ras4A and KRas4B) are identical in their first 85 aminoacid and have >90% identity in the following 80 aminoacid. The principal divergence is restricted to the last 24 amino acids which contains signal sequences for post-translational modifications (8).

A key determinant of Ras functioning is indeed post-translational lipid processing of its C-terminal that is a prerequisite for membrane recruitment and its consequent biochemical activation (see paragraph 1.2). The C-terminal CAAX motif is the target of the farnesyl transferase enzyme that catalyze the addition of a farnesil isoprenoid lipid followed by proteolytic cleavage of AAX sequence

(Ras converting enzyme I) and carboxymethylation of the now terminal Cys residue by the isoprenylcysteine carboxymethyltransferase. An additional signal in the C-terminal is required for full membrane recruitment. Prenylated K-Ras-4A and H-ras require a further palmitoylation step in which a palmitol moiety is attached to upstream C-terminal Cys residues while for prenylated K-Ras-4B a string of positively charged Lys residue upstream of the C-terminus is sufficient to mediate its anchoring to the membrane(9).

The overall Ras structure consist of a hydrophobic core of six stranded β -sheets and 5 α -helices that are interconnected by a series of 10 loops. Among these loops there are three of them (L1/P-loop(aa10-15), L2/switchI(aa26-36) , and L4/switchII(aa59-64)) situated on one facet of the protein that have crucial roles in Ras function. All three loops contact infact the γ -phosphate of GTP and are involved in determining the proper conformation of the GTP-Mg²⁺ complex in the Ras protein active center thus allowing the hydrolysis reaction. In particular the switchII loop (L4) also contains the catalitically essential Gln61 residue. The structural difference between the active GTP form and the inactive GDP form can be described by position changes in SwitchI(L2) and switchII(L4) loops. These loops are indeed the ones involved in the interactions with upstream Ras regulators and downstreams Ras effectors(7).

1.2.Ras proteins activity regulation and Ras oncoproteins

The lifetime of the active, GTP-bound state of Ras proteins is of great importance since it is only in this state that the signal can be transmitted to the effector molecule next in sequence. This time window is determined by the rate of GTP hydrolysis. Considered in isolation, The Ras protein is a very inefficient enzyme since not only the rate of GDP hydrolysis is very low but also the Ras-GDP complex is very stable. The rate of both reactions however can be accelerated in the process of signal transduction through intervention of appropriate partner proteins (7).

There are two classes of proteins that accelerate such processes: the G-nucleotide exchange proteins (GEFs) and the GTPase activating proteins (GAPs). The function of GEFs is to promote dissociation of bound GDP and thus functioning as a positive regulator of Ras protein. The function of

GAPs is on the contrary to increase the rate of GTP hydrolysis thus working as a negative regulator of Ras protein activity. The coupled activity of both class of proteins, tightly controlled within the cells, determines the time window of Ras activation (7, 10).

Regulation of GEFs and GAPs activity in the cell can be achieved with very different mechanisms. Their activity can be regulated through coupling to membrane receptors or through second messengers such as DAG and Ca^{2+} (1, 9, 11). The best characterized example of such regulation is the recruitment of the GEF protein Sos by Tyrosine Kinase membrane receptors (RTK). RTKs activated by extracellular signals recruit Sos to the plasma membrane through the adaptor protein Grb2. Once recruited to the membrane, where Ras is localized, Sos protein determines Ras activation by promoting dissociation of GDP(11).

Mutated Ras proteins have been described in a variety of cancer types (see paragraph 1.4). It has been shown that oncogenic activity correlates with an increased lifetime of the GTP-bound Ras form. Oncogenic mutations of Ras proteins are found in particular at position 12, 13 and 61 (10). When Gly12, located in the P-loop as described in the previous paragraph, is replaced by other amino acids the conformation of the active site does not allow anymore the interaction with upstream positive regulators (GAP) necessary to stimulate Ras GTP-ase activity thus fixing Ras in the active GTP-bound form. The Gln at position 61, in the L4 loop, is necessary to stabilize the transition state of the GTP hydrolytic reaction. When this aminoacid is substituted the intrinsic GTP-hydrolysis activity of Ras is basically abolished and cannot be stimulated further neither by GAPs proteins(7).

1.3.Ras proteins signal transduction pathways

Once activated by appropriate signals, the conformational changes induced by GTP binding (in particular a reorientation of switchI and switchII loops) allow the interaction of Ras protein with its effectors and the thus the activation of signal cascades. An overall view of Ras effectors is shown in Figure 1.

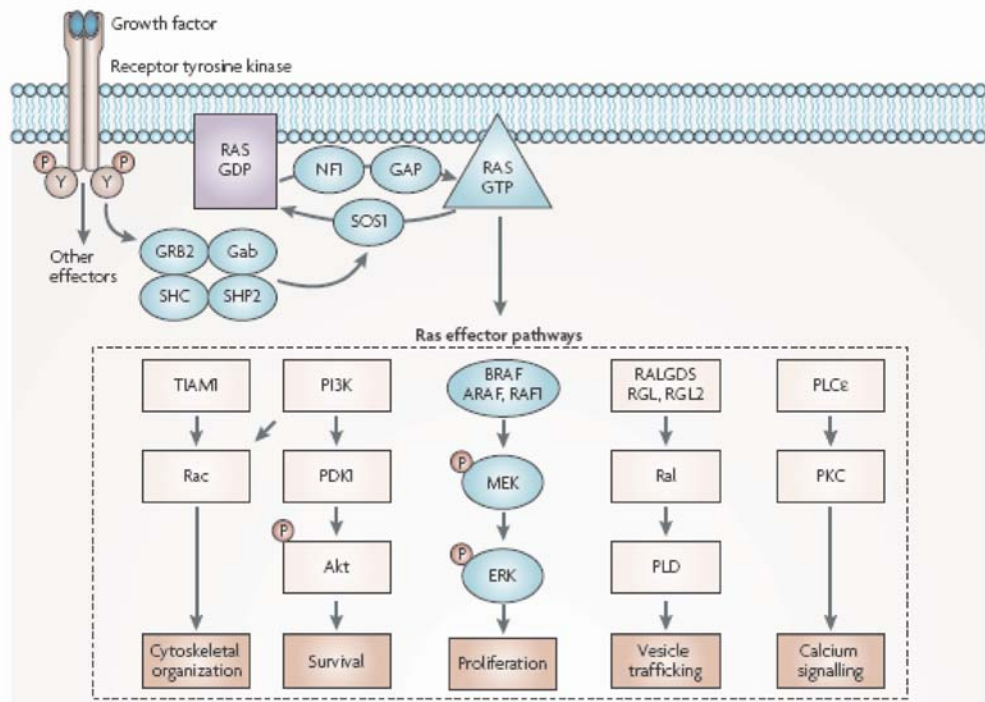


Figure 1. Schematic representation of Ras effectors

Several Ras–GTP effector pathways have been described, and some of the key effectors are depicted here. The BRAF–mitogen-activated and extracellular-signal regulated kinase kinase (MEK)–extracellular signal-regulated kinase (ERK) cascade often determines proliferation and becomes deregulated in certain cancers and in developmental disorders such as cardio-facio-cutaneous syndrome. Ras also activates the phosphatidylinositol 3-kinase (PI3K)–3-phosphoinositide-dependent protein kinase 1 (PDK1)–Akt pathway that frequently determines cellular survival. RALGDS, RALGDS-like gene (RGL), RGL2 and TIAM1 are exchange factors of Ral and Rac, respectively. Among the effectors of Ral is phospholipase D (PLD) an enzyme e that regulates vesicle trafficking. Rac regulates actin dynamics and, therefore, the cytoskeleton. Ras also binds and activates the enzyme phospholipase C ! (PLC!), the hydrolytic products of which regulate calcium signalling and the protein kinase C (PKC) family. P, phosphate; Y, receptor tyrosine. (*shubbert et al 2007*)

The Raf-MEK-ERK MAPK cascade

The first Ras effector characterized in mammals was the Ser/Thr kinase Raf. In mammals there are three Raf isoforms cRaf-1, B-Raf and A-Raf (12, 13). Activated Ras interacts with Raf kinases thus facilitating plasma membrane association of normally cytosolic Raf. Full activation of c-Raf-1 and A-Raf is a very complex phenomena that requires multiple signals involving both phosphorylation and dephosphorylation events, however Ras recruitment to the plasma membrane is a necessary pre-requisite for their activation and a sufficient event for B-Raf activation (13, 14).

Activated Raf kinase phosphorylate and activate the MEK1 and MEK2 dual-specificity protein kinases. MEK1/2 then phosphorylate and activate ERK1 and ER2 MAPKs. Activated ERKs can translocate to the nucleus where they phosphorylate and regulate various transcription factors such as Ets family transcription factors, ultimately leading to change in gene expression (15, 16). The majority of ERK substrates are nuclear proteins and are estimated to comprise over 160 proteins (17).

The Raf-MEK-ERK cascade has a key role in Ras normal and neoplastic function. It has infact been shown that constututely activated Raf and MEK can transform rodent fibroblast and that MEK and ERK are necessary for Ras-mediated transformation. Further evidences suggesting that mutationally activated Ras and Raf are functionally equivalent come from their incidence in the same types of human cancers in which mutations of the two genes are never overlapping (18).

Although all three Raf isoforms (cRaf-1, B-Raf and A-Raf) can activate both MEK1 and MEK2 *in vitro* they differs in their ability to do so and it appears that the main cellular activator of MEK kinases is B-Raf rather than the other isoforms (19, 20). Indeed B-Raf binds and phosphorylate MEK1/2 more efficiently than c-Raf1 and A-raf (20, 21) and only Mouse embryonic fibroblasts (MEFs) from B-Raf knock out mice have severely compromised ERK activity while MEFs from c-Raf and A-Raf knock out mice shows a relatively normal ERK activation (22-25). As a further confirmation of the non-equivalence of the three isoforms, only B-Raf isoform is a human oncogene up to present knowledge (26).

The PI3K pathway

A second class of Ras effectors is represented by the Phosphatidylinositol-3-kinases (PI3K) made up of a regulatory (p85) and a catalytic (p110) subunit. Ras mediated PI3K activation is obtained through recruitment of PI3K at the plasma membrane through interaction with the p110 catalytic subunit (7). Once activated PI3K converts the second messenger phosphatidylinositol (4,5)biphosphate (PIP₂) into phosphatidylinositol (3,4,5) triphosphate (PIP₃) which recruits and activates the PDK1 kinase which in turns activatre AKT kinase whose activity promotes cell proliferation and survival through activation of the mTOR kinase and inhibition of FoxO transcription factors(27).

The PI3K pathway is an important driver of cell proliferation and survival. Numerous types of human tumors, both sporadic or arising as a component of a cancer predisposition syndrome, shows upregulation of the PI3K pathway. In most cases upregulation of the PI3K pathway is the consequence of PTEN deletion or mutation. PTEN is in fact a lipid phosphatase that negatively regulate the PI3K pathway converting PIP₃ back to PIP₂(28).

In vivo data support a functional link between the ras and PI3K pathway indicating that Ras activation and PTEN loss can serve the same function during tumorigenesis(29).

The Ral pathway and other effectors

The Ras-like (Ral) guanyl nucleotide-binding proteins RALA and RALB are activated by Ras through its direct interaction with a class of GEFs (for example RalGDS) that have biochemical specificity for Ral proteins. Thus Ras activation promotes accumulation of Ral proteins in their active GTP-bound form. Ral proteins engage multiple effectors and their suggested role is to deflect induction of programmed cell death that occur in response to aberrant mitogenic signal (bodemann 2008).

The number of Ras effectors have been increasing during the years (1, 9). Some of the best characterized additional effectors are PLC ϵ and TIAM1. The phospholipase PLC ϵ once activated by Ras cleave PtdIns(4,5)P₂ into inositol-1,4,5-triphosphate (Ins (1,4,5)P₃ and diacylglycerol (DAG) promoting releasing of Ca²⁺ and activation of PKC respectively. TIAM1 is a Rho GTPase family GEF and serves as one route to activate the Rac and Rho GTPase downstream of Ras. Some of the less characterized Ras effectors are AF-6, RIN1 and the RASSF proteins (9, 18).

Although it is largely unknown whether effectors other than Raf or PI3K have a critical role in human cancer, mice models of Ras dependent tumorigenesis showed a reduced tumor incidence when PLC ϵ , TIAM1 or RalGDS are lacking (30-32).

1.4.Ras oncogenes and human cancers

Aberrant signalling through the Ras pathway occurs as the result of several different classes of mutational damage in tumor cells. The most obvious of these is the mutation of Ras genes themselves. These mutations, as described in paragraph 1.2, all compromise the GTPase activity of Ras preventing GAPs from promoting hydrolysis of GTP and therefore causing accumulation of Ras in the GTP-

bound, active form. About 30% of human tumors have activating point mutation in Ras, most frequently in K-Ras (85%of total), then N-Ras (15%) then H-Ras (1%) (Fig. 2) (11) .

Cancer type	HRAS	KRAS	NRAS
Biliary tract	0%	33%	1%
Bladder	11%	4%	3%
Breast	0%	4%	0%
Cervix	9%	9%	1%
Colon	0%	32%	3%
Endometrial	1%	15%	0%
Kidney	0%	1%	0%
Liver	0%	8%	10%
Lung	1%	19%	1%
Melanoma	6%	2%	18%
Myeloid leukaemia	0%	5%	14%
Ovarian	0%	17%	4%
Pancreas	0%	60%	2%
Thyroid	5%	4%	7%

Figure 2. HRAS, KRAS and NRAS mutations in human cancer

The mutation data were obtained from the Sanger institute Catalogue of somatic mutations in Cancer. (Scubbert et al 2007)

Mutation of Ras genes themselves is not the only way through which Ras signalling pathway can be aberrantly activated in human cancers (Fig. 3). Examples of such indirect activation are 1) deletion of GAPs protein as the NF1 gene in neurofibromatosis type 1 (33) 2) Upstream growth factor receptor activation such as EGFR and HER2 which are frequently activated by overexpression in many types of cancer including breast, ovarian and stomach carcinoma (34, 35) 3) Mutation or amplification of Ras effectors such as mutations in B-Raf gene or deletion of pTEN (26, 28).

As a consequence, the /Raf/MEK/ERK pathway is often up-regulated in many human tumors and it is emerging that the inhibition of Ras/Raf/MAPK pathway is relevant for many cancer types therapies(36-38), especially when used in combination with conventional cytotoxic agents (39). Currently inhibitors of the kinase function of Raf and MEK represent the most studied and advanced approaches for blocking ERK signalling, with several inhibitors under evaluation in clinical trials and additional ones in pre-clinical analysis(36).

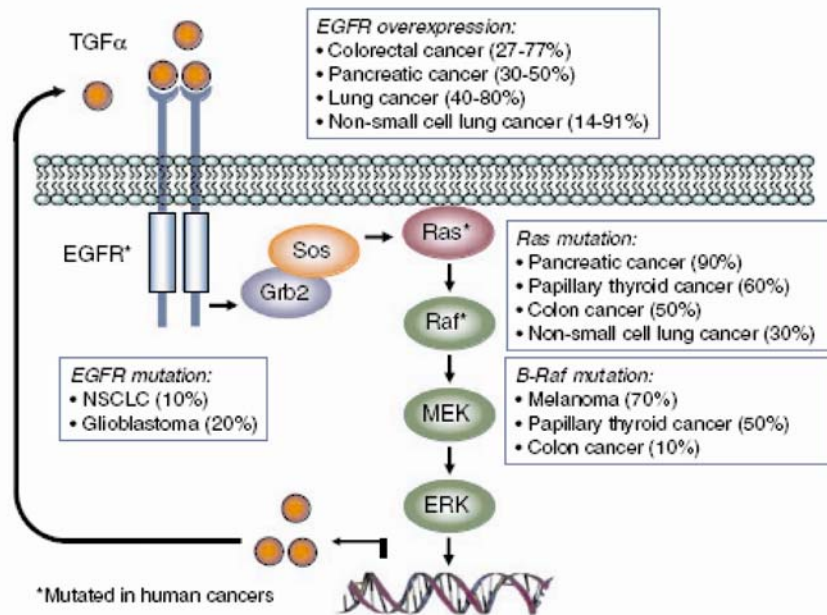


Figure 3. Oncogenic mutations that mimic activation of the Ras pathways in human cancers (Roberts et al 2007)

There is substantial evidence validating the importance of Raf and MEK in Ras promoted cancer progression and cancer growth. In particular the finding that mutationally activated Ras and B-Raf occur in a non-overlapping occurrence in melanomas, colon carcinomas, papillary thyroid carcinoma serous ovarian carcinomas and lung cancers suggests that ras function, in all these type of cancers, is facilitated primarily by activation of Raf (14, 40-43).

Recently, germline *de novo* mutational activation of H-Ras and K-Ras, B-Raf as well as MEK1 and MEK2 has been found in patient that comprise a group of related developmental disorders (Costello, Cardio-facio-cutaneous (CFC), Leopard's and Noonan's syndromes) (36), and suggest that aberrant ERK activation will contribute to other human disorders as well as cancer . The non-cancerous syndromes showed a weak activation of the MAPk pathway when compared to those seen in cancer probably because stronger activity can't be tolerated during development (10).

1.5.Ras oncogenes in experimental models

Most of the studies relative to the biological and biochemical properties of Ras oncoproteins have been typically done in rodent fibroblast. Nevertheless *ras* oncogenic mutations are found with higher frequency in tumours of haematopoietic and epithelial origin (44). It is indeed demonstrated that the cellular context and the developmental stage in which *ras* oncogenes act plays a fundamental role both when considering its ability to promote cancerogenesis or when considering the downstream pathways required to do so.

It has been observed in fact that activation of a latent *K-ras* oncogenic allele in mouse models induces exclusively lung tumours, with a complete penetrance, and thymic lymphoma and skin papillomas in the 30% of the animals, highlighting the cell-type specific tumorigenic effects of Ras oncogene activation ((45-48). Furthermore when the K-Ras oncogenic allele is activated post-natally, and not during development,, only lung tumors are observed suggesting that not only the effect of Ras oncogene are cell-type specific but are also dependent upon the developmental stage and differentiation status of the cell in which these mutations occur (46) Interestingly, despite the high frequency of K-Ras mutations in human's carcinomas of the pancreas and colon very few mice models develop neoplastic lesions in those tissues. This data suggest that in those tissues Ras oncogene mutation may not be the primary event and additional mutations are required for a full tumor phenotype (46).

The same cell-type specificity has been observed in cellular models. It has been reported, dissecting the requirements of Ras signalling for transformation, that immortalized human fibroblasts require activation of Raf and Ral-GEFs, Human embryonic kidney cells require the activation of PI3K and Ral-GEFs and human mammary epithelial cells require the activation of Raf, PI3K and Ral.-GEFs (49). It should be considered also that it has been reported that rodent cells cannot be considered completely equivalent to human cells when analysing their susceptibility to cancer(50). For example it was shown that mouse and human cells differ in their use of Ras effector pathways for transformation. In NIH-3T3 mouse fibroblasts the Raf/MEK/ERK effector pathway was shown be necessary and sufficient for their transformation while in human BJ fibroblasts the RAL-GDS but not Raf or PI3K effector pathway was shown to be required for anchorage independent-growth (51).

These data, taken together, clearly show that fibroblast studies could not be extended completely to other cellular systems and that cell type-peculiar activities relevant to tumorigenesis exerted by Ras oncoproteins should be highlighted in each cellular context.

2. The Thyroid Follicular Cell (TFC)

2.1. The thyroid gland

The mammalian thyroid gland consists of two lobes, connected by a very thin isthmus, located in front of the trachea. The thyroid parenchyma is composed of various epithelial cells. Thyroid follicular cells (TFCs), destined to produce thyroid hormones, are most abundant and are organized in particular spheroid structures known as follicles, each composed of a layer surrounding a closed cavity containing the colloid. TFCs are highly differentiated and express a number of proteins required for the synthesis and the release, in the blood, of thyroid hormones. thyroid gland is able to produce and release thyroid hormones and the regulation of its growth and function is exerted by the hypothalamic-pituitary axis.

2.2. TFCs differentiation

Both the final structure of thyroid and the differentiation of TFCs occur during embryonic life through a process, that in mice, starts around embryonic day (E) 8-8.5 and is completed by E16.5-17 (Fig. 4).

Thyroid anlage, the presumptive thyroid-forming district, is evident by E 8-8.5, as a midline thickening in the floor of the primitive pharynx (52). The thyroid bud evaginates from the floor of the pharynx and by E9.5-10 thyroid anlage begins a caudal translocation towards its final position (53)

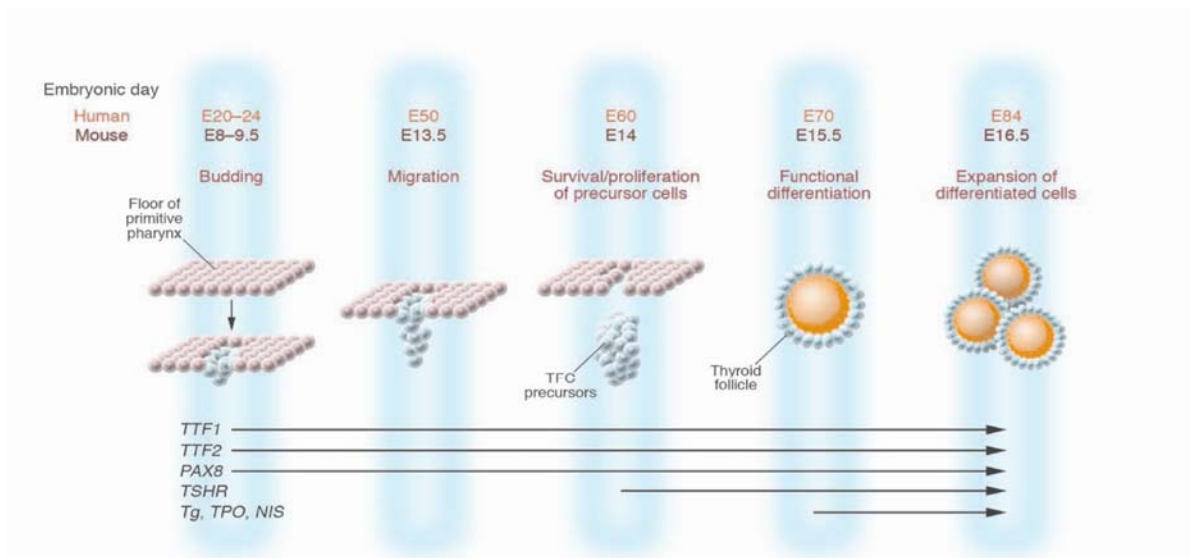


Figure 4. Schematic representation of TFCs differentiation during development

At mouse E8 the thyroid bud appears as a thickening in the pharynx floor and express a combination of transcription factors such as TTF1 , TTF2 and Pax8 necessary for subsequent expression of downstream functional thyroid genes such as Tg, TPO and NIS. At about E13.5 in mouse TFCs precursors start their migration and by E14 express TSHr. By E15.5 appears the thyroid follicular organization and the expression of a series of protein necessary for thyroid hormone biosynthesis (i.e. TPO, Tg and NIS). (Davies et al. 2005)

As soon as the thyroid anlage is visible as an endodermal thickening in the floor of the primitive pharynx, the precursors of TFCs acquire a specific molecular signature and can be distinguished by the co-expression of four transcription factors Hhex (54), Titf1 (55), Pax8 (55) and Foxe1 (56). It is worth noting that each of these transcription factors is expressed also in other tissues but such a combination is a unique hallmark of both differentiated thyroid follicular cells and their precursors (57)

On E12-12.5, the thyroid bud proliferates continuing its downward migration. At E13-14, the developing thyroid reaches its definitive position and joins with the ultimobranchial bodies that contain the precursors of calcitonin-producing cells (C cells) , originated from the neural crest (58, 59).

When the thyroid primordium reaches the sublaryngeal position, TFC precursors accomplish their functional differentiation and by E15-16 the gland acquires its definitive shape, two lobes connected by an isthmus. TFCs start organizing into cords of cells forming small rudimentary follicles. In the late fetal life, thyroid increases in size and its parenchyma is organized into small follicles, surrounded by a capillary network, enclosing thyroglobulin in their lumen (60).

The final differentiation program of TFC requires almost three days. The terminally differentiated phenotype of TFC is characterized by the expression of a number of proteins that are necessary for thyroid hormones biosynthesis, such as thyroglobulin (Tg, a colloidal protein stored in the lumen of thyroid follicles and the substrate for synthesis of thyroid hormones by iodination), thyroperoxidase (TPO; the enzyme responsible for Tg iodination) and the Sodium/Iodide symporter (NIS; which transports iodine into the thyroid cells). Tg appears around E14 (55) while thyroxine (the thyroid hormone) is first detected at E16.5 (61).

2.3. The Sodium/Iodide symporter (NIS)

The thyroid gland has the ability to uptake and concentrate iodide, which is a fundamental step in thyroid hormone biosynthesis that occur through the Na^+/I^- symporter (NIS).

NIS expression

NIS is not properly a thyroid-specific protein since its expression has been detected also in extrathyroidal tissues, such as lactating mammary gland, gastric mucosa, salivary and lacrimal glands, choroid plexus, skin, placenta, and thymus, among other tissues. In these non-thyroidal tissues NIS gene expression is under the control of different mechanisms, the majority of which have not been identified yet. Factors known to regulate NIS expression are listed in Figure 5.

FACTOR	EFFECT
TSH	Stimulates NIS gene expression, and increases iodide uptake by thyrocytes in culture and thyroid gland
Iodide	Decreases the levels of NIS mRNA and protein, and reduces NIS function at the plasma membrane. These effects seem to depend on the production of organified iodine (IX)
Estrogen	Reduces the sodium-iodide symporter gene expression and the transport of iodide into FRTL-5 thyroid cell lines. In ovariectomized rats treated with estradiol, NIS function increases
Retinoic acid	Different studies show that RA administration re-stimulates iodine uptake in about 20–50% of patients with radioiodine non-responsive thyroid carcinoma
Cytokines	Decrease NIS expression
Histone deacetylase inhibitors	Treatment of thyroid cancer cell lines with histone deacetylase inhibitors increases NIS expression as well as iodide uptake
Pax8 expression	This thyroid transcription factor is often reduced in thyroid tumors. The re-expression of Pax8 seems to be associated with the recovery of the NIS mRNA expression in rat thyroid cell line
Thyroglobulin	Thyroglobulin (TG) accumulated in the follicular lumen might reduce NIS mRNA levels secondary to decreased Pax-8 mRNA and protein levels

Figure 5. Factors that regulate NIS expression and/or function (*carvalho et al 2007*)

In thyroid follicular cells TSH is required for the maintenance of differentiation and for the proliferation. Besides the induction of other thyroid specific differentiation markers (see paragraph 2.5), TSH stimulates NIS gene expression, and increases iodide uptake by thyrocytes (62, 63). The majority of TSH actions on the thyrocytes are mediated by the intracellular increase in cyclic adenosine 3,5-monophosphate (cAMP) levels, which is secondary to adenylate cyclase activation. Both NIS expression and targeting to the plasma membrane are stimulated by TSH through the cAMP pathway, however the exact mechanism by which NIS gene promoter is regulated by cAMP has not been fully understood. Rat NIS promoter has been extensively studied so far and two important proximal regions described are a binding site for Titf1 (TTF1) and a TSH responsive element, where a putative transcription factor NTF-1 (NIS TSH responsive factor-1) interacts. The NIS upstream promoter (NUE) contains two Pax 8 binding sites and a cAMP response element-like sequence binding proteins. NUE region is essential for full responsiveness to TSH (64).

NIS protein

The rat and human (h) NIS cDNAs encode proteins composed of 618- and a 643-amino acid, respectively (65, 66). hNIS exhibits an 84% amino acid identity and 93% similarity to rat NIS. The current NIS secondary structure model depicts NIS as a protein with 13 transmembrane segments (TMS) (Fig. 6), the amino terminus facing the extracellular side, and the carboxy terminus facing the cytosol (67, 68).

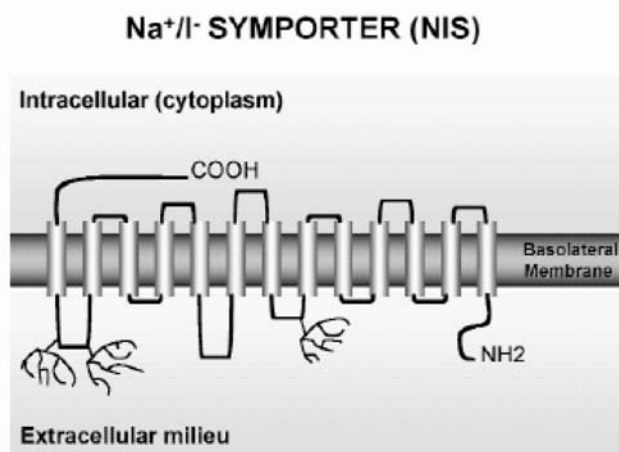


Figure 6. NIS protein structure
NIS protein is an integral plasma membrane glycoprotein containing thirteen transmembrane segments and localized on the basolateral plasma membrane of thyrocytes (carvalho et al 2007)

The Na^+/I^- symporter (NIS) is an integral plasma membrane glycoprotein localized in the basolateral membrane of thyrocytes. NIS belongs to the solute carrier family 5 (SLC5A, according to the Online Mendelian Inheritance in Man classification, OMIM). NIS is synthesized as a precursor of approximately 56 kDa and the mature glycosylated protein has 87 kDa however the lack of N-linked glycosylation of the molecule does not impair its function, stability or targeting to the cellular membrane (69, 70).

NIS function

The transport of iodide is a fundamental step in thyroid hormone biosynthesis and occurs through the Na^+/I^- symporter (NIS), an integral plasma membrane glycoprotein localized in the basolateral membrane of thyrocytes. NIS couples the inward transport of two Na^+ ions, which occurs in favor of its electrochemical gradient, to the simultaneous inward translocation of one I^- ion against its electrochemical gradient(71). After influx into thyrocytes, iodide is then translocated from the cytoplasm across the apical plasma membrane towards the follicular lumen, in a process called I^- efflux that is mediated by a protein called pendrin (a Cl^-/I^- transporter)(72).

Differently from other tissues that are able to take up iodide from the circulation, the thyroid gland accumulates iodine for a prolonged period of time. This is the result of thyroid microscopic features and the prompt oxidation and organification of iodine into selected tyrosyl residues of thyroglobulin (Tg), a reaction catalyzed by thyroperoxidase (TPO) in the presence of hydrogen peroxide generated by thyroid dual oxidase (DuOx).

Mutations in NIS protein, impairing its function, have been associated with congenital hypothyroidism due to a defect in thyroid iodide uptake(73, 74).

2.4.The TSH receptor (TSHr)

A well established regulator of adult thyroid function is the glycoprotein hormone TSH that, through its receptor (TSHr), conveys inside the thyroid cells an elevation of the second messenger cAMP, thus stimulating thyroid growth and function. Gain-of-function mutations of the TSHr gene are

indeed associated with congenital hyperthyroidism while, on the contrary, TSHr loss-of-function mutations are associated with congenital hypothyroidism (75).

TSHr expression

Tshr is expressed on the basolateral membrane of TFCs. In mouse embryo, when the developing thyroid has reached its final position, *Tg* is expressed and *Tshr* is detected in TFC precursors by E14-14.5 (55, 76). At later stages of development *Tshr* expression increases and remains expressed in adult life. Tshr has also been detected in other tissues, such as extraocular tissue, lymphocytes, adipocytes and bone (77) although physiological relevance of the expression is a topic of debate.

The TSHR promoter contains functional binding sites for several transcription factors including GABP(78), TTF1 (79), TR/RXR (80), CREB and ICER (81), nevertheless there is little fluctuation in the TSHR mRNA levels and regulation of functional TSHR is mainly exerted at the posttranslational level (82).

TSHr structure

Tshr is a member of the glycoprotein hormone receptor family (83), a subclass of rhodopsin-like G protein-coupled receptors (GPCRs). All members of GPCRs have a transmembrane serpentine domain composed of seven helices. In addition, members of glycoprotein hormone receptor subfamily, that includes TSH, LH/chorionic gonadotropin and FSH receptor, are characterized by a large extracellular amino terminal domain, responsible for hormone recognition and binding (84) (Fig. 7).

The gene, made up of 10 exons, is translated in a protein 765 amino acid long both in humans and in mice. The amino terminal of the protein, encoded by nine exons forms the extracellular domain; the 10th large exon encodes the C terminal part of the extracellular domain, the transmembrane serpentine domain and cytoplasmic tail. The extracellular domain is characterized by two cysteine-rich regions flanking nine leucine-repeats (LRRs) each made of 20-24 amino acids that form a beta strand followed by an alpha helix. TSH binds to extracellular domain while transmembrane and intracellular domains are involved in transducing signal triggered by TSH binding.

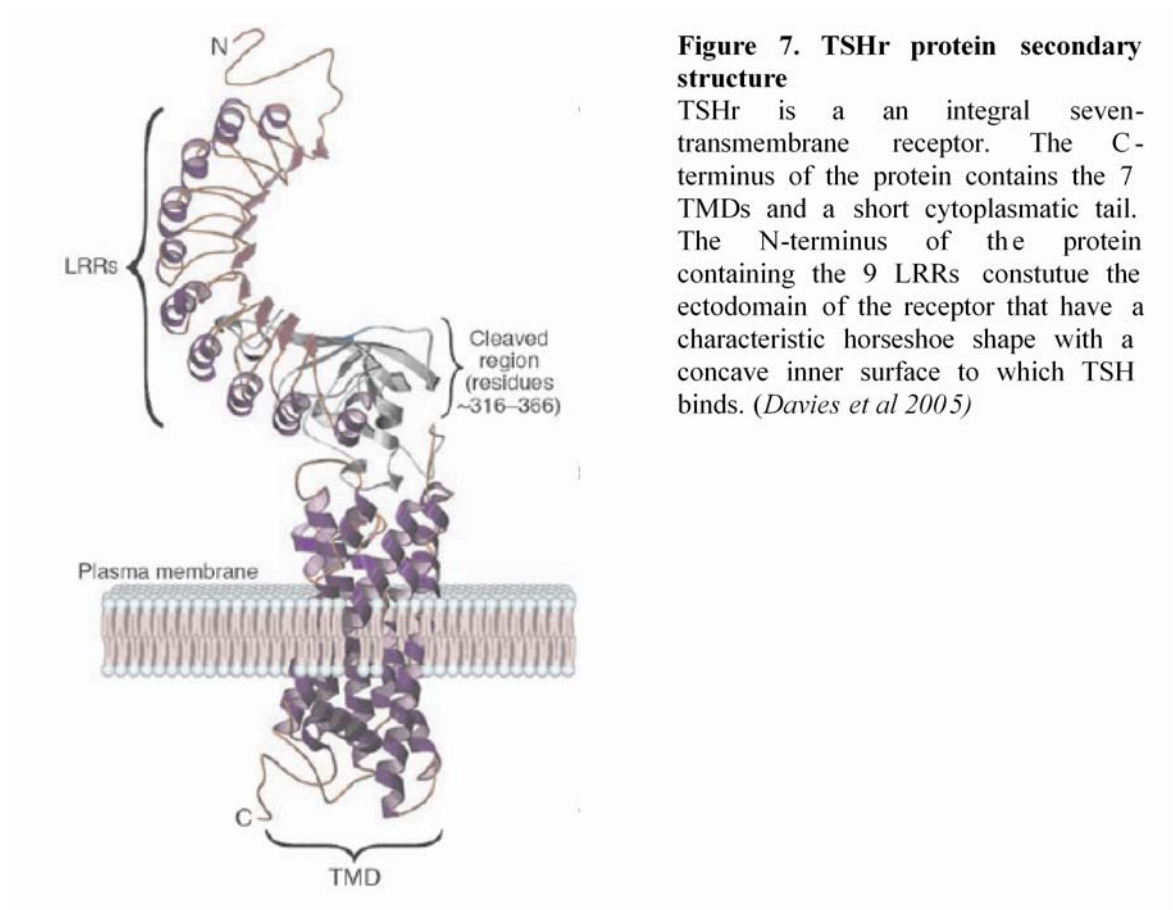


Figure 7. TSHr protein secondary structure

TSHr is an integral seven-transmembrane receptor. The C-terminus of the protein contains the 7 TMDs and a short cytoplasmic tail. The N-terminus of the protein containing the 9 LRRs constitute the ectodomain of the receptor that have a characteristic horseshoe shape with a concave inner surface to which TSH binds. (Davies et al 2005)

Tshr is translated as a monomer but undergoes intramolecular cleavage of its extracellular domain. After the cleavage, TSHR consists of two portions (the amino terminal portion and the other including the serpentine and cytoplasmic tail) held together by disulfide bonds (85). The cleavage involves two steps. In the first step a metalloprotease, acting at the cell surface, recognizes a specific sequence around AA 314. In the second step a disulfide isomerase is involved in the reduction of the disulfide bonds that hold the cleaved receptor subunits together.

TSHr signal transduction

TSHr is a G-protein coupled receptor. G-proteins are made up by three subunits (α , β and γ) among which the α -subunit (G_α) has a GTPase activity and needs to be GTP-bound in order to be active while the β - and γ - subunit exist as a tightly associated complex ($G_{\beta\gamma}$) and are active in this form. Upon binding of TSH to the extracellular domain of TSHr the cytoplasmic domain of TSHr undergoes a

conformational change that allow activation of the associated $G\alpha$ subunit and dissociation of the $G\beta\gamma$ subunit (7).

Thyrocyte growth, as well the maintenance of thyrocyte differentiated phenotype, occurs mainly through the TSHR mediated increase in cAMP (86-88) (Fig. 8).

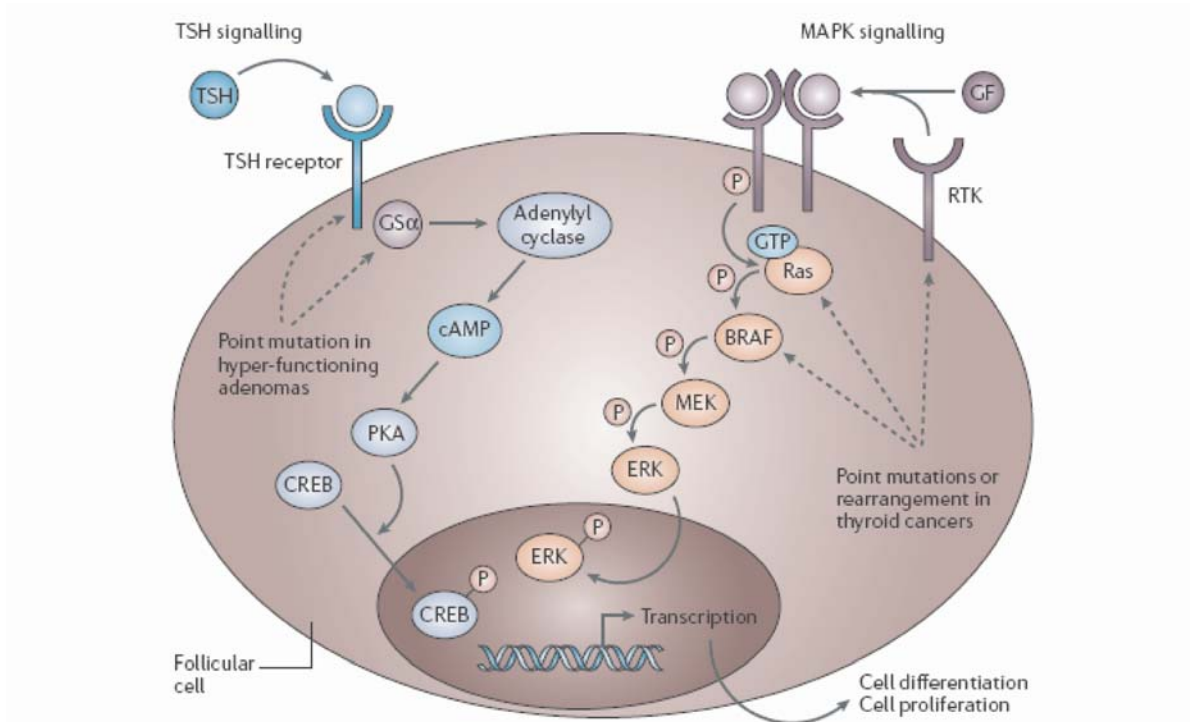


Figure 8. Cell signalling pathways in thyroid follicular cells

Thyroid follicular cells express cell-surface receptors for thyroid-stimulating hormone (TSH). TSH activates this receptor and G proteins such as $G\alpha$ at the cell surface of follicular cells, and induces intracellular production of cyclic AMP (cAMP) by adenylyl cyclase. cAMP stimulates the cAMP-dependent protein kinase A (PKA), which in turn phosphorylates cytoplasmic and nuclear target proteins. One PKA substrate is the nuclear transcription factor CREB, which activates the transcription of cAMP-responsive genes after being phosphorylated by PKA.

Growth factors (GF) induce receptor-tyrosine kinase (RTK) dimerization, resulting in phosphorylation of specific tyrosine residues within the cytoplasmic tail. In cooperation with receptor adaptors, phosphorylated RTK activates Ras by catalysing the replacement of GDP with GTP. In its GTP-bound form, Ras activates the kinase activity of BRAF and its downstream signalling cascade. BRAF phosphorylates the mitogen-activated protein kinase (MAPK) kinase (MEK), which phosphorylates and activates extracellular-signal-regulated kinase (ERK). Activated ERK migrates to the nucleus where it phosphorylates and activates various transcription factors that are involved in cell proliferation and differentiation (Kondo et al 2006)

After binding of TSH to the receptor cAMP-dependent protein kinase (PKA) activation is obtained in the following way :1) TSH stimulated TSHR dissociates the heterotrimeric G protein activating the $G\alpha$ s subunit. 2) $G\alpha$ s-dependent activation of adenylyl cyclase(AC) follows, increasing cAMP

production.3) cAMP-dependent activates PKA by dissociation of its regulatory subunits. 4) Activated PKA phosphorylates target proteins including membrane receptors, signalling molecules and transcription factors changing their activities to promote growth and differentiation (7). The variety of targets will further amplify and diversify the final outcome of this pathway. Perhaps the most classical target for PKA after translocation of its catalytic subunit to the nucleus is the transcription factor CREB, whose transcriptional activity will be promoted upon phosphorylation by PKA (89).

On the other side, $G_{\beta\gamma}$ dissociated dimers can activate additional pathways. In thyrocytes $G_{\beta\gamma}$ activation has been reported to directly activate PLC β , PKC and PI3K pathways (90). However the function of TSHr through $G_{\beta\gamma}$ signal transduction is much less characterized.

Role of TSHr in TFCs differentiation

Experiments in terminally differentiated thyroid cell lines have shown that TSH can regulate, albeit to different extents, the expression of mRNA of several thyroid specific genes such as Tg (86, 91, 92), TPO (93, 94), NIS (67, 86), Foxe1/TITF2 (95) and Pax8 (86, 96).

The role of TSH/Tshr signaling *in vivo* during embryonic life has been studied in genetically modified mice in which *Tshr* gene has been disrupted by homologous recombination (*Tshr*^{-/-}) mice (97) or in spontaneous mutant mice carrying a loss-of-function mutation in the *Tshr* gene (*Tshr*^{hyt/hyt}) (98). Loss of function mice models show that TSH/TSHr function is necessary, but not sufficient, for NIS and TPO gene expression (99). Indeed E16 mouse embryos deprived of TSH/Tshr signaling do not show defects in morphology of the gland which displays a normal size and follicular structure though both TPO and NIS are undetectable in TFCs (99). Thus TSH pathway is absolutely required for the differentiation process of the thyroid even though not sufficient since forcing its expression before E14 do not anticipate expression of NIS and TPO genes(99).

It is worth noting that nevertheless the Tshr pathway becomes active by E15 when the expansion of the lobes also begins, this signaling is not relevant for the growth of the gland. This is in contrast with the role that TSH/Tshr signals have in differentiated TFC, where the TSH-induced cAMP pathway is the main regulator of thyroid growth. Actually, both *Tshr*^{-/-} and *Tshr*^{hyt/hyt} mice display a severe hypoplastic adult thyroid (97, 99, 100).

2.5. The Paired-Box transcription factor 8 (Pax8)

In the terminally differentiated TFC transcription of thyroid functional genes relies on the coordinated action of the thyroid specific set of transcription factors (Nkx2.1/TITF1, FoxE1/TITF2, Pax8, HHex) among which the transcription factor Pax8 appears to play very relevant roles (101, 102). Pax8 belongs to a family of genes called paired box (Pax) genes which have been found in many vertebrate species such as zebrafish, frog, chick, mouse and human on the basis of sequence homology to *Drosophila* segmentation genes. Consistently with their fundamental role in development, mutations in Pax genes have been associated with a number of disease phenotypes (Fig.9) (103).





PAX family Group	Protein structure/domains		Protein family member	Embryonic Expression Domain	Expression/Mutation in human disease
	Paired	octapeptide homeodomain			
I			PAX1	Skeleton, thymus 3rd/4th pharyngeal pouch	Klippel-Feil Syndrome, Jarcho-Levin Syndrome
			PAX9	Skeleton, Teeth, Thymus	Jarcho-Levin Syndrome, Oligodentia
II			PAX2	Kidney, CNS	Hyperproliferative dysplastic kidney, Renal hyperplasia, Bladder and renal cancer, Coloboma Syndrome
			PAX5	B-Cells, CNS	Lymphomas
			PAX8	Kidney, Thyroid, CNS	Congenital hypothyroidism, Thyroid carcinomas/adenomas
III			PAX3	Neural Crest, CNS somites/muscle	Waardenburg Syndrome Types I/III, Melanoma, Rhabdomyosarcoma
			PAX7	Neural Crest, CNS somites/muscle	Rhabdomyosarcoma
IV			PAX4	Pancreas, gut	Diabetes
			PAX6	Pancreas, gut, CNS and eye	Aniridia, GI tumors Cataracts/Peter's Anomaly

Figure 9. Pax protein family

Pax genes are characterized by the presence of the paired domain (white rectangle) and are divided into groups according to the presence of an octapeptide (grey cylinder) and/or a homeodomain (grey rectangle). Embryonic expression domains are listed as well as disease phenotypes associated with each gene. (Lang *et al* 2007).

In humans, loss-of-function mutations of a single Pax8 allele are associated with congenital hypothyroidism (103). The same association can be observed also in mice models but only in the appropriate genetic background (104). Experiments in terminally differentiated thyroid cell lines have shown that PAX8 is involved in the maintenance of thyrocyte cell type and is essential for the thyrocyte-specific promoter activation of the FoxE1/TITF2, TPO, TG, and NIS genes (64, 102, 105-108).

Pax8 expression

The *Pax8* gene is expressed during mouse ontogeny in the developing CNS, thyroid gland, kidney and placenta (109, 110). Transcripts of this gene give rise to at least six alternative splice product. The longest isoform is 457 and 450 amino acids long in mice (111) and humans (112) respectively. The alternative isoforms differ in their C-terminal sequences while sharing common N-terminal regions including the paired domain. These *Pax8* isoforms consequently bind DNA in an indistinguishable manner, but exhibit distinct transactivation properties (110). Interestingly, the alternative splicing of the *Pax8* mRNA isoforms is spatially and temporally regulated during mouse embryogenesis(110).

It has been shown that in rat thyroid cell lines (113) as well as in dog thyrocytes in culture (114), *Pax8* synthesis is regulated by TSH by a cAMP-mediated mechanism. DREAM, a transcriptional repressor, seems to be a negative regulator of *Pax8* gene, binding to two consensus sequences localized in the 5' UTR of *Pax8* (115). Calcium binding to DREAM blocks its ability to associate with DNA and later also its repressive activity. TSH is known to increase the free cytosolic Ca^{++} concentration in thyroid cells; it is hypothesized that both Ca^{++} and the cAMP signal transduction pathways could participate in the control of *Pax8* expression. However it is worth noting that TSH control on *Pax8* expression seems to be effective only in adult TFCs since the *Pax8* expression is not affected in developing thyroid of mice harboring severe alterations in TSH/Tshr signalling (100)

Pax8 protein

The Pax gene family consists of tissue-specific transcriptional regulators, essential for normal embryogenesis, which share a highly conserved 128-aminoacid long unique DNA-binding domain called Paired domain. Pax genes have peculiar and defined expression patterns in mouse embryogenesis suggesting they are involved in a variety of different developmental function.

The mammalian Pax gene family consists of nine member (Pax1 to Pax9) which are not clustered together but map on different chromosomal loci (116, 117). Pax proteins, which all share the Paired DNA-binding domain, can be arranged into four groups according to the presence or absence of a conserved octapeptide motif and the presence absence or truncation of a homeodomain (Fig. 9). *Pax8* belongs to Pax protein subfamily II which also includes *Pax2* and *Pax5* (118). This subgroup is

characterized by the presence of the octapeptide motif and a rudimentary homeodomain encoding only the first α -helix of the three helixed canonical homeodomain (109, 119).

The paired domain, localized at the N-terminal of the protein, is a DNA-binding domain which is composed of two sub-domains, PAI and RED each composed of a helix–turn–helix (HTH) motif and binding to two distinct half-sites in adjacent major grooves of the DNA helix (120-122) (Fig. 10) The paired domain of all members of the Pax2/5/8 family depends on both subdomains for DNA sequence recognition (123, 124). The transcriptional activity of Pax8 depends on sequences located at the carboxy-terminal of the molecule. A serine/threonine/tyrosine-rich sequence, present in both Pax8a and Pax8b isoforms seem to be responsible for the strong transactivating properties of these two isoforms (125).

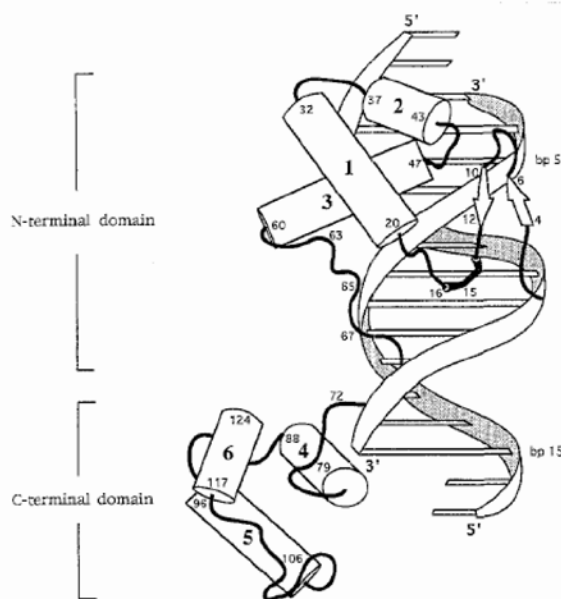


Figure 10. Overview of the Paired -domain DNA complex

Sketch of the complex of paired domain with DNA. Cylinders indicates α -helices and arrows indicate β -sheets.(Xu et al 1995)

Pax8 activity regulation and transcriptional cofactors

It has been demonstrated *in vitro* as well as in cultured cells that oxidation/reduction state of the thiol groups of cysteine residues can regulate the DNA binding activity of Pax8 (126). These effects could be mediated by the redox effector factor-1 (Ref-1). The synthesis and the translocation of Ref-1 from cytoplasm to nucleus, occurs in thyroid cells upon TSH stimulation (127). The oxidation exerts its

effects directly on the paired domain and affects its DNA-binding activity. It was demonstrated as well that Pax8 activity is dependent upon TSH in immortalized Rat thyrocytes (86).

To be considered, besides Pax8 protein activity regulation itself, is that differential association with cofactors is another way of regulating Pax8 transcriptional activity. In addition to the synergistic cooperation between Pax8 and Titf1 (107, 128), Pax8 can interact with other proteins which can be responsible for the target preferences in definite cell types or developmental stages or in response to specific stimuli. Pax8 was described to interact with p300 (129-131), Rb (132), PARP (133), Taz (134), and WBP-2 (135).

The role of Pax8 TFCs differentiation

The study on Pax8 null embryos has offered some insights on the functional role of this factor during development. At E9, the thyroid anlage is correctly formed in proper position, begins to migrate but at E11 both the morphological and molecular phenotypes of the developing thyroid change. The thyroid bud is much smaller, the expression of Foxe1 and Hhex is strongly down-regulated and TFC precursors are still not detected by E12.5 (106). These data indicate that in developing thyroid Pax8 is involved in the control of survival and/or expansion of TFC precursors though we do not know the target genes that execute this program. In addition Pax8 has a specific upper role in the genetic network that maintains the expression of other thyroid-enriched transcription factors. In TFC precursors Foxe1 is tightly regulated by Pax8, which is necessary for the onset of its expression indicating that Foxe1 can be a transcriptional target of Pax8 (106).

In Pax8 null mice mature TFCs are absent making it difficult to reveal the role of this factor in the control of adult thyroid function. All the available data on Pax8 functions in differentiated cells, come from studies on cell lines in culture. Consensus sequences recognized by Pax8 have been found in the proximal promoters of Tg and TPO and in an upstream enhancer of NIS (64). In both Tg and TPO proximal promoters, Pax8 binding sites partially overlap Titf1 binding sequences (105); in NIS enhancer the two Pax-8 sites flank a cAMP response element and recently it has been shown that Pax8 is able to bind in vitro to the 5-flanking region of Foxe1 and ThOX2 genes (107).

Functional assays carried out in non thyroid cell lines have demonstrated that Pax8 is required to activate the TPO promoter and to a less extent the Tg promoter (105) and NIS enhancer (64). In addition, it has been demonstrated that in transformed thyroid cells Pax8 is sufficient to activate expression of the endogenous genes encoding Tg, TPO and NIS. These data suggest that Pax8 has an important role in the maintenance of functional differentiation in thyroid cells (102).

In humans, heterozygous mutations in PAX8 have been reported in both sporadic and familial cases of congenital hypothyroidism. Eight different mutations, seven located in the paired domain, (136-140) and one in the C domain (141) have been described. Assays *in vitro* demonstrate that the ability of the mutated PAX8 proteins to bind to specific DNA target is either strongly reduced or absent; consistently, the transcriptional activity of proteins is lost.

3. The TFCs derived cancers

Thyroid cancers constitute the most frequent endocrine neoplasia with an incidence of one to four new cases per 100000 persons per year, remarkably with 2 to 3- fold higher prevalence in women. Diagnosis and treatment of thyroid cancer have achieved high levels of medical and technical standard. Although some forms of thyroid tumors such as papillary carcinomas show quite good prognosis others such as anaplastic tumors have a rather poor prognosis.

3.1. TFCs malignancies

The thyroid follicular epithelial cells are considered the precursors of four forms of thyroid neoplasia: thyroid adenoma, follicular (FTC), papillary (PTC) and anaplastic (ATC) carcinoma as well as some variants therefrom such as Hurthle cell carcinoma. Another way of classifying thyroid cancers is on the basis of their differentiation grade with respect to the TFCs cell from which they have originated. Follicular-cell-derived carcinomas are thus broadly divided into well-differentiated, poorly differentiated and undifferentiated types on the basis of histological and clinical parameters. Well-differentiated thyroid carcinoma includes papillary and follicular types(142).

The PTC variant is the most frequent type of thyroid malignancy (85–90% of thyroid malignancies). The diagnosis of PTC is based on a series of features such as papillary architecture and characteristic

nuclear structure that predict the propensity for metastasis to local lymph nodes. FTC is defined as a neoplasm, not belonging to papillary thyroid carcinoma, with evidence of capsular and/or vascular invasion. ATC is defined as an undifferentiated, highly aggressive neoplasm with evidence of epithelial differentiation (142, 143). Diagnosis of the follicular variant of thyroid carcinoma on the basis of morphological and structural features is not always straightforward (144).

Most well-differentiated thyroid cancers behave in an indolent manner and have an excellent prognosis. By contrast, undifferentiated or anaplastic thyroid carcinoma is a highly aggressive and lethal tumour. The presentation is dramatic, with a rapidly enlarging neck mass that invades adjacent tissues. There is currently no effective treatment and death usually occurs within 1 year of diagnosis. Poorly differentiated thyroid carcinomas are morphologically and behaviourally intermediate between well-differentiated and undifferentiated thyroid carcinomas (142).

3.2. Multistep cancerogenesis

Cancer is a genetic disease arising because of somatic mutations in cancer susceptibility genes. Cancer development depends not only on one mutation initiating tumorigenesis but also on subsequent mutations driving tumor progression toward malignancy and invasion (145).

Cancer development happens with a process that formally is analogue to Darwinian evolution and is defined "somatic evolution". The ability of cancer cells to clonally expand, genetic diversification within the expanding clone and selective pressure of the surrounding microenvironment are the factors that determine cancer progression (146).

The different type of thyroid malignancies have been considered different stages of an overall cancerogenic process toward full malignancy whose final step is represented by the Anaplastic thyroid carcinomas (ATCs). ATC, which account for less than 5% of all thyroid cancers, is the most malignant thyroid neoplasm and is almost invariably fatal (147). A large portion of ATCs are identified in patients who have longstanding goiters or incompletely treated papillary or follicular thyroid cancers (148, 149). Careful histopathologic examination of ATC reveals that many of them contain a papillary structure or follicular components in focal areas. It is believed that ATC is derived from the follicular

epithelial cells and represents a terminal dedifferentiation of preexisting differentiated carcinoma (147).

Besides the presence of pre- or co-existing well-differentiated thyroid carcinoma with less differentiated types, the theory of sequential progression of well-differentiated thyroid carcinoma through the spectrum of poorly differentiated to undifferentiated thyroid carcinoma (Fig. 11) is supported also by the identification of a the common core of genetic loci with identical allelic imbalances in co-existing well differentiated components (150).

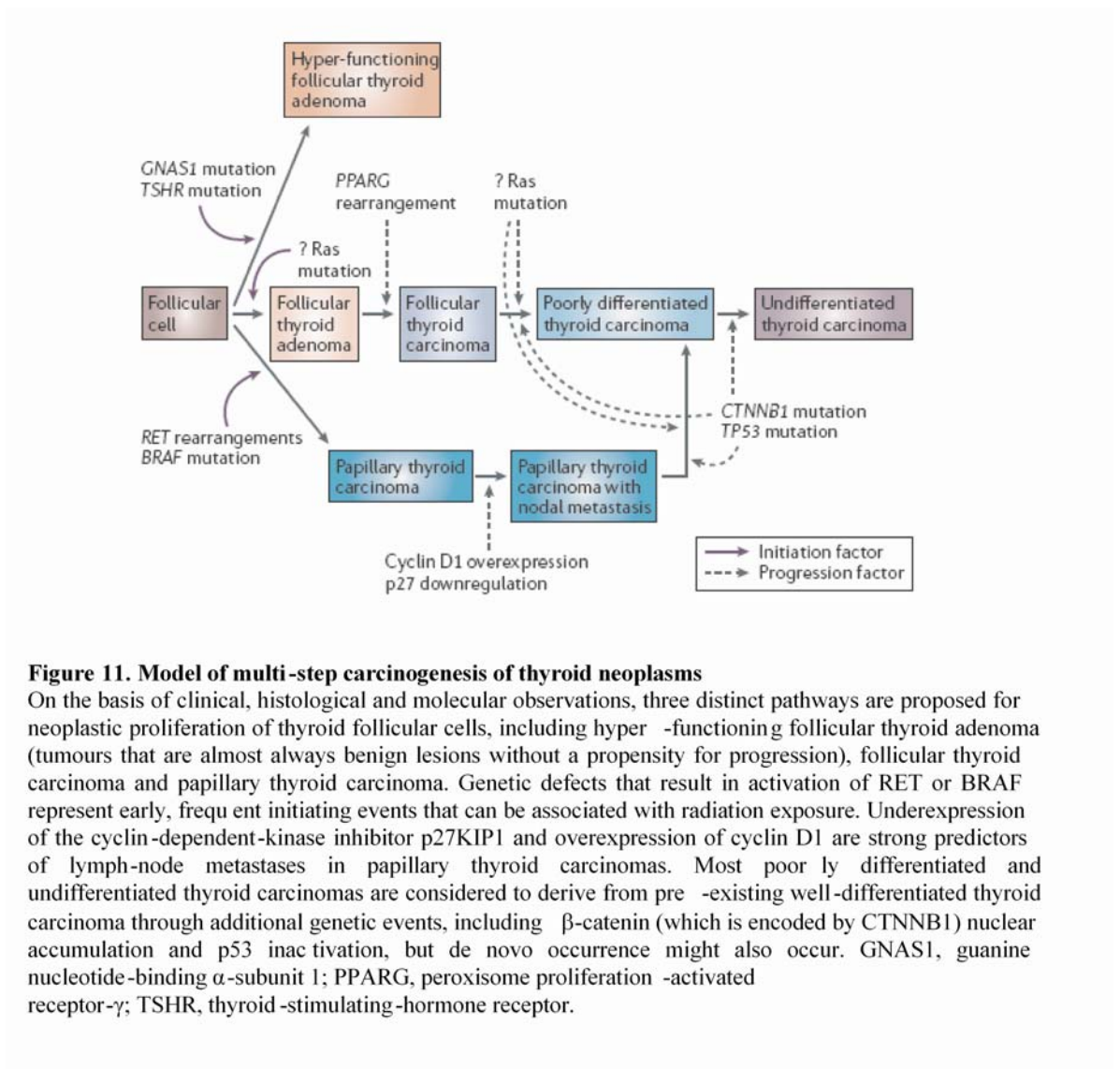


Figure 11. Model of multi-step carcinogenesis of thyroid neoplasms

On the basis of clinical, histological and molecular observations, three distinct pathways are proposed for neoplastic proliferation of thyroid follicular cells, including hyper-functioning follicular thyroid adenoma (tumours that are almost always benign lesions without a propensity for progression), follicular thyroid carcinoma and papillary thyroid carcinoma. Genetic defects that result in activation of RET or BRAF represent early, frequent initiating events that can be associated with radiation exposure. Underexpression of the cyclin-dependent-kinase inhibitor p27KIP1 and overexpression of cyclin D1 are strong predictors of lymph-node metastases in papillary thyroid carcinomas. Most poorly differentiated and undifferentiated thyroid carcinomas are considered to derive from pre-existing well-differentiated thyroid carcinoma through additional genetic events, including β -catenin (which is encoded by CTNNB1) nuclear accumulation and p53 inactivation, but de novo occurrence might also occur. GNAS1, guanine nucleotide-binding α -subunit 1; PPARG, peroxisome proliferation-activated receptor- γ ; TSHR, thyroid-stimulating-hormone receptor.

The genetic events that have been identified in the different types of thyroid cancers indicate a pattern of cumulative alterations that have a role in initiation, progression and de-differentiation (Fig. 12)

(142). From this analysis it appears that while mutations in the RAS/RAF /MAPK pathway are associated with well differentiated carcinoma and thus probably represents tumor initiating events, additional mutations of oncogenes and tumor suppressor genes, such as TP53, are necessary in order to allow progression to dedifferentiated anaplastic carcinoma.

Genetic alteration	Well-differentiated thyroid carcinoma		Poorly differentiated thyroid carcinoma	Undifferentiated thyroid carcinoma
	Papillary thyroid carcinoma	Follicular thyroid carcinoma		
RET rearrangement	13–43%	0%	0–13%	0%
BRAF mutation	29–69%	0%	0–13%	10–35%
BRAF rearrangement	1%	Unknown	Unknown	Unknown
NTRK1 rearrangement	5–13%	Unknown	Unknown	Unknown
Ras mutation	0–21%	40–53%	18–27%	20–60%
PPARG rearrangement	0%	25–63%	0%	0%
CTNNB1 mutation	0%	0%	0–25%	66%
TP53 mutation	0–5%	0–9%	17–38%	67–88%

Figure 12. Genetic defects in thyroid cancer (Kondo et al 2006)

3.3.Genetic alterations

The most commonly involved pathway in thyroid tumorigenesis is the RTK/RAS/BRAF/MAP kinase pathway, which seems to be required for thyroid transformation in well-differentiated carcinoma. Indeed exclusive non-overlapping activating events that involve the genes RET, NTRK1 (neurotrophic tyrosine kinase receptor 1), BRAF or Ras are detectable in nearly 70% of all cases (151). Mutations in this pathway are believed to be initiating events (152). Aberrant activation of PI3K/Akt pathway has also been found in thyroid cancers but its role in thyroid tumorigenesis, particularly needs to be further clarified but presently it is suggested that this pathway could be involved in the initiation of FTC and progression to ATC (153). PAX8/PPAR γ (Peroxisome proliferator-activator receptor- γ) rearrangement has been identified prevalently in FTC (36–45%) and follicular adenoma (4–33%), however the mechanism of transformation are still unclear and could not only be dependent upon inactivation of PPAR γ function (154). Inactivating point mutations of the p53 tumour suppressor gene are highly prevalent in anaplastic and poorly differentiated thyroid tumours, but not in well-

differentiated papillary or follicular carcinoma (155, 156) implying p53 inactivation as an important step in late stage progression of thyroid cancer.

Interestingly, despite TSHr stimulation induces thyrocytes proliferation, constitutive activating mutations of the main G-protein-coupled receptor of the thyroid, the TSHr or its G α subunit GNAS1, both of which activate cAMP, are very rare in thyroid malignancies and are found only in toxic benign nodules (157). It is indeed believed that activation of the TSH pathway may serve as a protective mechanism for tumour initiation in the thyroid (158).

The RTK/RAS/RAF /MAPK pathway

The RET gene encodes a transmembrane tyrosine kinase (TK) receptor whose expression and function is normally restricted to a subset of cells derived from the neural crest. In thyroid follicular cells, RET activation occurs through chromosomal recombination resulting in expression of a fusion protein consisting of the intracellular TK domain of RET coupled to the N-terminal fragment of a heterologous gene. Several forms have been identified that differ according to the partner gene involved in the rearrangement (159-161). The fusion proteins dimerise in a ligand independent manner resulting in constitutive activation of the downstream RAS/BRAF/MAP kinase pathway. Thyroid-specific overexpression of either RET/PTC1 (162, 163) or RET/PTC3 (164) in transgenic mice leads to development of tumours with histological features consistent with PTC.

The neurotrophic receptor-tyrosine kinase NTRK1 (also known as TRK and TRKA) was the second identified subject of chromosomal rearrangement in thyroid tumorigenesis. The NTRK1 proto-encodes the transmembrane tyrosine-kinase receptor for nerve growth factor. NTRK1 expression is typically restricted to neurons. . NTRK1 rearrangements — which show ectopic expression and constitutive activation of the tyrosine kinase that are analogous to RET rearrangements — have been noted in 5–13% of sporadic papillary thyroid carcinomas. The activated receptor initiates several signal- transduction cascades, including ERK, PI3K and the phospholipase-C pathway (142).

The BRAFV600E mutation is the most common genetic change in PTC, present in about 29–83% of cases(151) .The majority of the oncogenic mutations of BRAF destabilise the inactive BRAF structure, thereby promoting an active conformation and leading to a constitutive catalytic activation

(165, 166). The V600E mutant of BRAF is one of the most prevalent somatic genetic events in human cancer and possesses the hallmarks of a conventional oncogene (26). The kinase activity of this mutant protein is greatly elevated resulting in constitutive stimulation of ERK activity independently of RAS. Undifferentiated or anaplastic carcinomas arising from pre-existing papillary thyroid cancers also have a significant prevalence of BRAF mutations, whereas those arising from pre-existing follicular carcinoma do not (167-171). Thyroid-specific overexpression of the mutant BRAF in transgenic mice leads to development of tumours with histological features consistent with invasive PTC, which exhibit foci of classic features, foci of TC features and foci of poorly differentiated carcinomas. These mice had a 30% decrease in survival at 5 months (172).

Mutations of all three RAS genes are found in benign and malignant follicular neoplasms and in follicular variant PTC. The role of Ras oncogenes in thyroid cancerogenesis will be discussed in greater detail in paragraph 3.4.

The phosphatidylinositol 3-kinase (PI3K)/Akt pathway

It has been reported that alterations to the PI3K/Akt signalling pathway are frequent in human cancer. Constitutive activation of the PI3K/Akt pathway occurs due to mutations or amplification of the PIK3CA gene encoding PI3K or the Akt gene, or as a result of inactivating mutations in components of the pathway, for example PTEN (phosphatase and tensin homologue), which inhibit the activation of Akt.

In sporadic thyroid neoplasm loss of heterozygosity (LOH) at the pTEN locus was found in 27% of follicular carcinomas and 7% of follicular adenomas (173), and loss or reduction of PTEN expression as well as inappropriate subcellular compartmentalisation has been reported in thyroid tumours (143, 174, 175). Additionally, PTEN loss in transgenic mice causes goitre and follicular adenomas even though is not sufficient for malignant transformation of thyroid cells (176). Somatic mutations within the PI3K catalytic subunit, PIK3CA, is present in 23% of anaplastic carcinomas and in 8% of FTC and is likely to function as an oncogene in anaplastic thyroid cancer (ATC) and less frequently in well-differentiated thyroid carcinomas (177). The occurrence of any genetic alterations at the level of PIK3CA, RAS and PTEN were found to be mutually exclusive in well-differentiated

carcinomas, most frequently FTC, and adenomas but not in anaplastic carcinoma suggesting that accumulation of mutations in this pathway may be involved in the progression of FTC to ATC(153) .

The p53 pathway

p53 inactivation is an important step in late stage progression of thyroid cancer. Thyroid cells carrying a mutated p53 gene did not form colonies in soft agar or tumours in athymic mice, suggesting that a mutation of the p53 gene is not sufficient for the induction of the malignant phenotype, and probably cooperation with other oncogenes is necessary to accomplish full malignancy. However, a mutated p53 gene results in a marked loss of the differentiated phenotype in the rat thyroid cell line PCC13, including inhibition of the expression of the thyroid-specific transcription factor PAX8 (178). Conversely, re-expression of wt-p53 activity in undifferentiated thyroid carcinoma cell lines inhibits cell proliferation and restores differentiation (179, 180).

The PAX8/PPAR γ rearrangement

PPAR γ is a member of the steroid nuclear-hormone receptor superfamily. PAX8/PPAR γ rearrangement, which consists in fusion of the thyroid-specific transcription factor PAX8 gene with the PPAR γ gene. It involves a chromosome 3p25 and 2q13 translocation creating a fusion gene, encompassing the promoter and proximal 50 coding sequence of the thyroid-specific transcription factor PAX8 gene and most of the coding sequence of the PPAR γ gene. The fusion product functions through a dominant negative effect on the transcriptional activity of wild-type PPAR γ (181). These rearrangements seems to be restricted to Follicular thyroid adenoma (0-31%) and carcinoma (25-63%) (181-184).

The mechanism of transformation induced by PAX8/PPAR γ is still unclear as well is unclear whether the transforming properties of PAX8/PPAR γ can be attributed only to inhibition of PPAR γ function(154).

3.4.Role of Ras oncogenes

Constitutive activation of all three Ras oncogenes (H-, K- and N-Ras) is known to occur among tumors that originated from the thyroid follicular epithelium of the thyroid gland (185). However, there

are significant discrepancies related to the overall frequency of ras mutations (ranging from 7% to 62%) and their prevalence in specific thyroid tumors (186, 187). Although it is difficult to explain this lack of consistency, the mutation screening methods, the selection of patients, and the design of individual studies are critical to identify specific association between mutational status and clinical or pathological parameters. However in one of these studies involving highly specific analysis and performed on a large number of patients harboring tumors that included the full spectrum of differentiation observed in thyroid cancer of follicular cell derivation, Ras mutations were found to be associated with aggressive cancer behaviour, loss of differentiated phenotype and with the presence of distant metastasis (188).

The presence of Ras mutations in benign tumours suggested that this could have been an early event in thyroid tumorigenesis. However, besides the considerable variability in the prevalence of Ras mutations in different series of thyroid cancers as mentioned above, the high degree of observer variation in the diagnosis of follicular adenoma and follicular-variant papillary thyroid carcinoma might also explain this finding (189, 190). It should be considered then that highly specific analysis indicates that Ras mutations are more common in poorly differentiated and undifferentiated thyroid carcinoma, implicating this phenomenon in tumour progression rather than in tumor initiation(142).

Studies in vivo with transgenic mice have also given valuable information. A transgenic mouse line in which a human N-RAS (Gln61Lys) oncogene was expressed in thyroid follicular cells under control of the Tg promoter (Tg-N-RAS) was developed by Santoro's group. Significantly, Tg-N-RAS mice developed thyroid follicular neoplasms; 11% developed follicular adenomas and 40% developed invasive follicular carcinomas, in some cases with a mixed papillary/follicular morphology. About 25% of the Tg-N-RAS carcinomas displayed large, poorly differentiated areas, featuring vascular invasion and forming distant metastases in lung, bone or liver (191). Ras oncogene in this mouse model appears to contribute both to tumor initiation and progression. However level of expression of Ras oncogene should be taken into account. It was indeed demonstrated in immortalized rat follicular thyroid cells that RAS oncogene induces de-differentiation in a dose-dependent manner, although TSH-independent growth appears to be induced in the presence of both low and high levels of

oncogenic RAS expression(4). Thus a reasonable explanation to fit the data would be that low levels of Ras oncogene would allow thyroid tumor initiation while higher levels of expression or higher activity through additional mutation on the same pathway would allow tumor progression.

3.5. Thyroid cancer therapy

In the case of Differentiated Thyroid carcinomas, both diagnosis and treatment of both tumor remnants or distant metastasis with radioiodine is possible due to the ability of tumor cells to accumulate iodine (192). The higher tumor recurrence rate in patients treated only with surgery and TSH suppression than in those who also received radioiodine therapy shows the importance of thyroid remnant ablation by radioiodine (193). Well differentiated thyroid tumors show indeed good long-term survival (194, 195).

However, the effectiveness of radioiodine therapy depends on the effective radiation dose delivered to the tumor tissue, which depends on the iodine concentrating ability of the cells. Thus poorly differentiated histotypes and in particular ATC have a very poor prognosis (194, 195). Furthermore during tumor progression, up to 30% of patients with persistent/metastatic thyroid carcinoma show cellular de-differentiation, characterized by more aggressive growth, loss of iodide uptake ability and other markers of thyroid cell differentiation. These patients with de-differentiated thyroid carcinoma represent a therapeutic challenge, since treatment options are limited, and usually not efficient (196).

Since thyroid follicular cancer conserves a certain degree of differentiation, one logical therapeutic approach is to redifferentiate the cells and reinduce endogenous NIS expression so that radioiodine treatment can be performed. Many groups focused on this strategy and several compounds, also known to have tumour-inhibitory effects, have partially succeeded in reaching this goal. Among them, the most well known has been retinoic acid (RA). Several clinical trials have been done using RA in order to increase radioiodide uptake and improve clinical outcome of patients with recurrent thyroid cancer (70). In general terms, radioiodide uptake was improved in 20–42% of the cases, but tumour shrinkage was observed in very few cases after ¹³¹I treatment. The largest study was done on 50 iodide scan-negative patients: 26% had a significant increase in radioiodide uptake, but only 16% had

reduced tumour volume (197). Other compounds such as Troglitazone, HDAC inhibitors and demethylating agents are currently being tested with promising results (198).

The MAPK pathway is particularly important in thyroid cancer because it harbors several activating mutations in this pathway with a high prevalence, including *BRAF* mutation, *RAS* mutation, and *RET/PTC* rearrangement. Thus, as for other cancers (199, 200), targeted inhibition of the MAPK pathway is potentially an effective therapy for thyroid cancer.

Given the prominence of this ‘oncogene addiction’ phenotype involving the MAP kinase pathway in thyroid and other cancer types, several small molecules that target this pathway are currently being tested *in vitro* and *in vivo*. In thyroid cancer, this interest is further heightened by new information on the role of activated *BRAF* and MAPK pathway activation in disrupting iodine transport and thyroid hormonogenesis(172).

Inhibitors of MEK1/2 were evaluated with promising results. The potent MEK inhibitor, CI-1040 (201), entered phase I and II clinical trials on several human cancers, which have recently been completed (202, 203). It was recently demonstrated that *BRAF* mutation was a prerequisite for the sensitivity to MEK inhibitors in many cancer cell lines(204). Accordingly preclinical studies on the effects of this compound on thyroid cancer cells both *in vitro* and *in vivo* demonstrated its selective inhibition of proliferation and tumor growth of cells harboring *BRAF* or *RAS* mutations but not cells harboring *RET/PTC1* rearrangement or wild-type alleles encouraging a clinical trial on CI-1040, particularly in patients with conventionally incurable thyroid cancer that harbors *BRAF* or *RAS* mutations (205). Analogously the efficacy of the MEK1/2 inhibitor AZD6244 was proven in a panel of PTC and ATC cell lines and xenografts. Supporting the selection of AZD6244 for phase II clinical trials for this types of thyroid tumors (206).

Additional inhibitors under evaluation include Raf-Inhibitors. For example Sorafenib (BAY 43-9006) was one of the first compounds to be evaluated in clinical trials (207). Sorafenib is a multikinase inhibitor that inhibits *BRAF*, *CRAF* and *VEGFR3* at low concentrations *in vitro*. Despite its promising preclinical properties (208, 209), the preliminary efficacy data for sorafenib in patients with thyroid cancer appear modest(207). Other *RAF* inhibitors have been tested for thyroid cancer, yet they did not

show better in vitro potencies than sorafenib. For example, AAL881 and LBT613 (Novartis, Cambridge, MA, USA) both compounds were effective growth inhibitors of poorly differentiated thyroid cancer cell lines with either RET or RAF mutations(210). Presumably, other emerging RAF inhibitors may provide a more robust effect against MAP kinase activity in clinical trials.

Inhibitors of RTKs such as quinazolines are also promising (211). For instance, ZD1839 (Iressa) is a potent and selective inhibitor of the EGFR and is currently in advanced clinical development (Ciardiello et al. 2001). Another anilinoquinazoline, ZD6474, has been shown to be a selective inhibitor of the VEGF receptor-2 (flk-1/KDR) tyrosine kinase (212). Interestingly, this last compound has also been shown to inhibit the enzymatic and transforming activity of RET oncoproteins and arrests the development of RET/PTC3-induced tumours in nude mice. This compound also prevented the growth of two human PTC cell lines that carry spontaneous RET/PTC1 rearrangements. Thus targeting RET oncogenes with ZD6474 might offer a potential treatment strategy for carcinomas sustaining oncogenic activation of RET such as PTC thyroid carcinomas(213).

Whereas it is tempting to invoke the concept of oncogene addiction(214) in interpreting the apparently selective efficacy of MAPK pathway inhibitors for cancerous cells, it is important to consider that resistance could emerge relatively promptly with chronic single-agent cytostatic therapy. MEK inhibitors have been shown to sensitize cancer cells to a number of other agents including radiation(215, 216). AZD6244 has been shown to enhance the efficacy of cytotoxic chemotherapy agents in preclinical colon cancer studies (217). A key challenge in thyroid cancer systemic therapy will be the identification of effective combinations, potentially combining targeted inhibition of BRAF signaling with other targeted or cytotoxic agents.

4. The FRTL-5 thyroid cell line

The availability of cultured, differentiated thyroid cell lines offers an amenable system to study the action of activated Ras proteins on the differentiated phenotype of an epithelial cell type.

4.1.FRTL-5 cells

The FRTL5 cell line derive from spontaneous immortalization of a 3 weeks old rat epithelial follicular thyroid cells (218). These cells retains in culture the expression of all known thyroid differentiation markers such as Tg, NIS, TPO and TSHr as well as the the thyroid specific combination of transcriptiona factors Titf-1, Foxe1, Hhex and Pax8. Despite showing some thyroid functional properties such as the ability of concentrate iodide and to secrete thyroglobulin, these cells do nor show the charctaristic polarization observed in the TFCs and in the standard culture condition do not organize into follicular structures. FRTL5 cells rapidly proliferates (duplication time about 36h) and their proliferation as well as their differentiation is dependent upon TSH presence in the culture medium (5)

4.2.Transformation of FRTL-5 cells by Ras oncogene

It was previously shown that Ras oncogene expression in FRTL5 cells determines neoplastic transformation. Such transformation involve the acquiring of the following properties: TSH-independent growth, anchorage-independent growth, morphological alterations and the ability of giving rise to tumors when injected in nude mice. Ras oncogene mediated transformation of FRTL5 cells is associated with the silencing of thyroid-specific genes such as Tg, TPO and NIS (5, 219).

Studies aimed to characterized the pathways through which Ras oncogene induces transformation and dedifferentiation of FRTL-5 cells have highlighted that, though in fibroblasts constitutive activation of MEK (downstream of Raf) and Rac (downstream of PI3K and Tiam1) is sufficient to recapitulate Ras effects, in FRTL-5 cells these pathways can reproduce only the oncogenic Ras-induced proliferative phenotype but do not have consequences on FRTL5 differentiation (220). It was indeed demonstrated through the use of Ras effector domain mutants that Ras oncogene induced dedifferentiation requires activation of the Raf/MEK/ERK pathway plus an additional uncharacterized pathway (221). Furthermore It was shown that loss of differentiation is an early event, , thus not the result of chronic exposure to the activated oncogene, induced exclusively by high levels of Ras oncogene (4).

4.3. An inducible system of Ras mediated transformation of FRTL5 cells

In this study the relation between ras oncogene and thyroid differentiation was investigated by using a stable thyroid cell line (FRTL-5) which constitutively express a conditional ras oncoprotein called ER-Ras^{V12} activable by Tamoxifen. In this system ER-Ras^{V12} activation induces de-differentiation of FRTL-5 cells (4).

I could thus analyze the kinetics of Ras oncogene action on thyroid-specific gene expression in order to define a molecular hierarchy of events. I demonstrate that Ras oncoprotein inactivates Pax8 transcriptional activity early on in the transformation process and induces inhibition of the TSHr pathway through a double mechanism which involves both downregulation of TSHr expression itself plus an additional interference with the TSHr signalling, the latter located downstream of cAMP production. I demonstrate that such effects are reversible and induced by Ras through the MAPK pathway. I also demonstrate that cAMP pathway inhibition is the cause of Pax8 inactivation and that by restoring a functional cAMP pathway we can restore both Pax8 activity and thyroid-specific gene expression

MATERIALS AND METHODS

1.N-terminal Multiple-Tags (TTN, DTN, MTN) gene synthesis and cloning in pCEFL expression vector

1.1.TTN Tag

The TTN tag (Triple Tag N-terminal) DNA sequence was designed in order to codify the following peptide:MGLNDIFEAQKIEWHEHLEVLFOGPGDYKDDDDKGGKPIPPLLGLDSTGGPGGENLYFOGG. Underlined are the functional sites within the peptide: AVI sequence (GLNDIFEAQKIEWHE), Prescission protease cleavage site (EVLFOGPG), Flag epitope (DYKDDDDK), V5 epitope (KPIPPLLGLDST), TEV protease cleavage site (ENLYFQ). DNA sequence was projected accordingly and is, from 5' to 3', the following: agggcaagcttatgggcctgaacgacatcttcgaggccagaagatcgagtggcacgaacacctggaggtcctgttccaggacctggcgactac aaggatgacgatgacaaaggcggcaagcctatccctaaccctctgctgggcctggactccacaggcggccccggcgcgagaacctgtactcca ggcgatccggcgaattctaaatctagagccaag. Underlined are additional restriction sites required for cloning.

In order to synthesize such DNA sequence (225 bp long) a previously described PCR-based gene synthesis approach was adopted (222). Briefly 6 oligonucleotides (*TTN1-6*) about 40nt in length were designed in order to cover the whole desired DNA sequence with about 10 nt overlaps at both 5' and 3' ends between adjacent oligonucleotides. Two additional primers (*TNF* and *TNR*) were designed in order to amplify the obtained final DNA product (Fig.1). *TNF* primer (5'end) carrying the HindIII restriction site for subsequent cloning into pCEFL recipient vector and the *TNR* primer (3'end) carrying the XbaI restriction site for subsequent cloning into pCEFL recipient vector preceded by two additional restriction site (EcoRI and BamHI) to allow following cloning of a desired gene sequence in frame with the Tag.

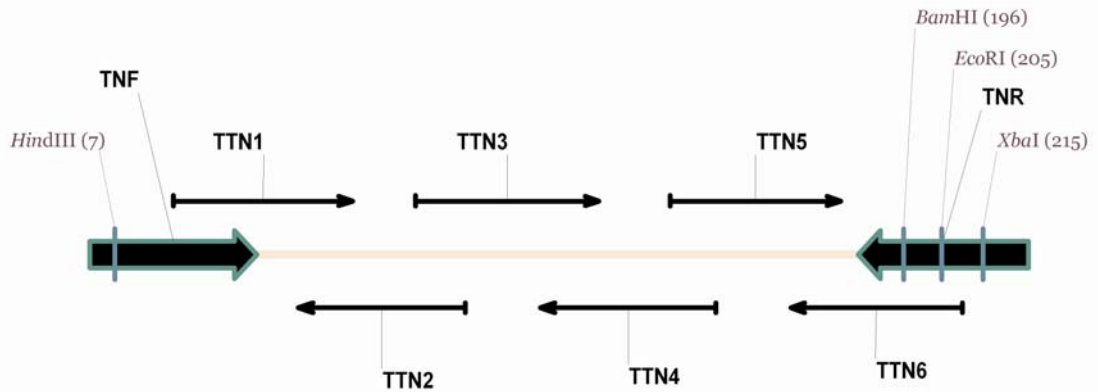


Figure 1. Schematic diagram of designed oligonucleotides for TTN Tag synthesis

TTN DNA sequence was dissected into oligos of about 40nt length with 10-15 nt overlaps at both 5' and 3' end.

Sequences of used oligonucleotides, from 5' to 3', were respectively the following:

TNF (agggcaagcttatgggcctgaacgacatcttcgaggccca),

TNR (cttgctctagatttagaattcggcgatccgccctggaag),

TTN1 (aacgacatcttcgaggccagaagatcgagtggcacgaacacc),

TTN2 (cgccaggtccctggaacaggacctccaggtgttcgtgccca),

TTN3 (agggacctggcgactacaaggatgacgatgacaaaggcggaag),

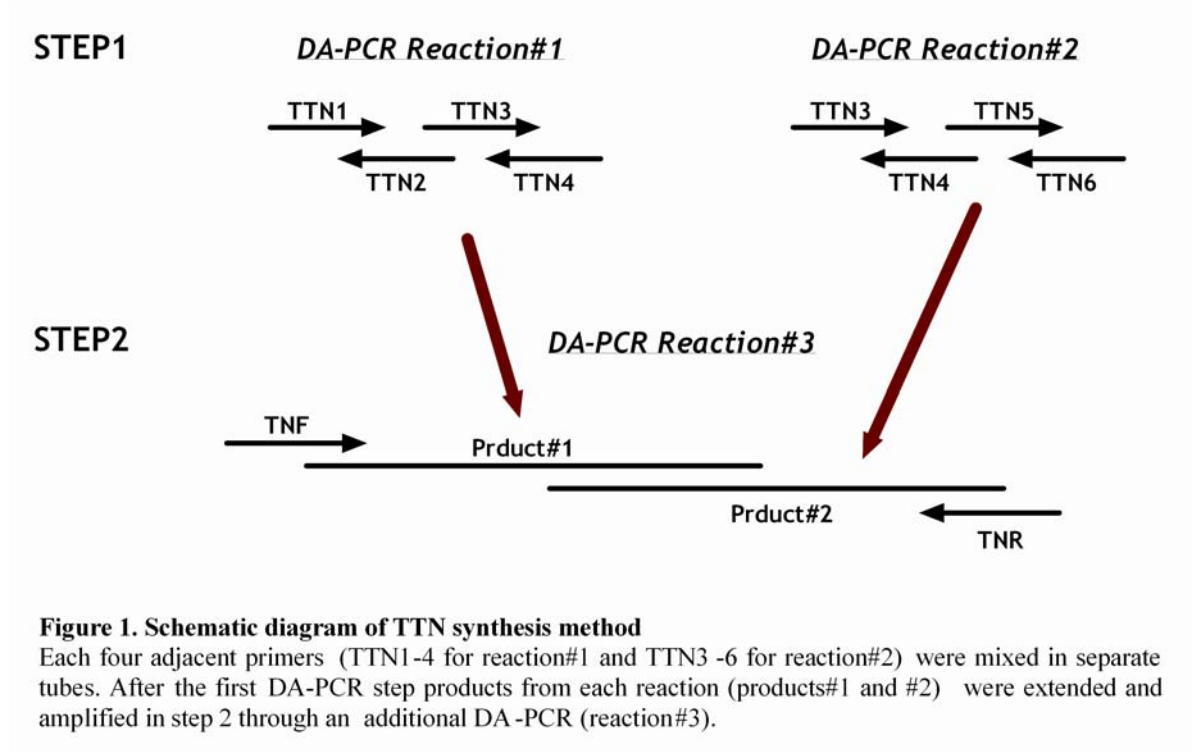
TTN4 (ccaggcccagcagagggttagggataggcttgccgctttgt),

TTN5 (gctgggcctggactccacaggcgccccggcgcgagaacc),

TTN6 (gaattcggcgatccgccctggaagtacaggttctcgccgc).

TTN tag synthesis strategy is schematized in Figure 2. In step1, A PCR reaction (DA-PCR) was carried out for every four consecutive oligonucleotides (reaction#1:*TTN1-4*, reaction#2:*TTN3-6*) that were mixed together in a 50 μ L reaction with the outer two oligonucleotides (*TTN1* and *TTN4* for reaction#1, *TTN3* and *TTN6* for reaction#3) at five times molar excess (400nM) to the inner ones (80nM) in the presence of 200nM dNTP and 2U *Pfu* polymerase (BioGem). The PCR profile 94° for 20s, 45° for 15s and 72° for 30s was repeated for 20 cycles. In step2, the products obtained from each of the first DA-PCR reactions (each about 130nt long and overlapping for about 80 nt) were gel extracted and used basically as inner oligonucleotides in an additional DA-PCR reaction (Reaction#3) in which the outer primers (*TNF* and *TNR*) were used to further amplify the PCR extended inner

product. The obtained product of 225bp was purified by phenol-chloroform extraction and ethanol precipitation, digested and cloned into HindIII/XbaI sites of pCEFL expression vector and sequence verified.



1.2.DTN Tag

The DTN tag (Triple Tag N-terminal) DNA sequence was designed in order to codify the following peptide: MDYKDDDDKGGKPIPNPLLGLDSTGGPGGENLYFQGG. Underlined are the functional sites within the peptide: Flag epitope (DYKDDDDK), V5 epitope (KPIPNPLLGLDST), TEV protease cleavage site (ENLYFQ). DNA sequence was projected accordingly and is, from 5' to 3', the following:

agggcaagcttatggactacaaggatgacgatgacaaaggcggcaagcctatccctaaccctctgctgggcctggactccacaggcg
gccccggcggcgagaacctgtactccaggcggatccggcgaattctaaatctagagccaag. Underlined are additional restriction sites required for cloning.

In order to synthesize such DNA sequence (150 bp long) a previously described PCR-based gene synthesis approach was adopted (222). As already described above for TTN tag synthesis

oligonucleotides about 40nt in length were designed in order to cover the whole desired DNA sequence with about 10 nt overlaps at both 5' and 3' ends between adjacent oligonucleotides (Fig.3).

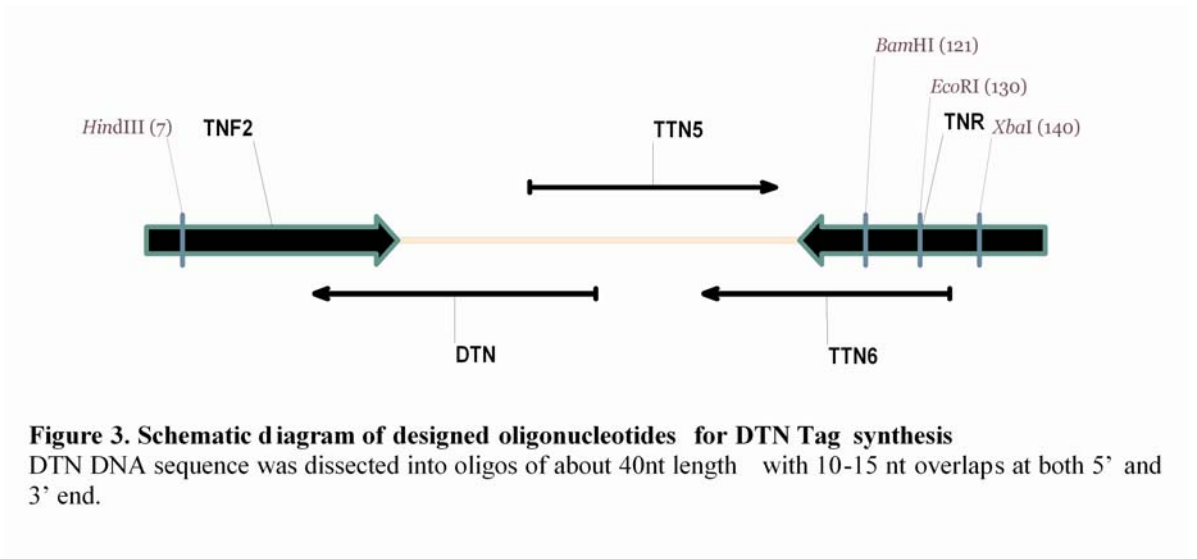


Figure 3. Schematic diagram of designed oligonucleotides for DTN Tag synthesis
DTN DNA sequence was dissected into oligos of about 40nt length with 10-15 nt overlaps at both 5' and 3' end.

Sequences of used oligonucleotides, from 5' to 3', were respectively the following:

TNF2 (agggcaagcttatggactacaaggatgacgatgacaaaggcg),

TNR (as for TTN tag synthesis),

DTN (ccaggcccagcagagggttagggataggctgcccgttgcctcatcg),

TTN5 (as for TTN tag synthesis),

TTN6 (as for TTN tag synthesis).

DTN tag synthesis strategy is schematized in Figure 4. In step1, A DA-PCR reaction was carried out for the first four consecutive oligonucleotides (reaction#1:*TNF2*, *DTN*, *TTN5*, *TTN6*) as described in the TTN tag paragraph. In step2, the product obtained from the DA-PCR reaction (about 130bp) was gel extracted and used as template (20ng/50µL) in a canonical PCR reaction (Reaction#2) using *TNF2* and *TNR* as primers (500nM each). PCR reaction profile 94° for 20s, 55° for 30s and 72° for 30s was repeated for 25 cycles The obtained product of 150bp was purified by phenol-chloroform extraction and ethanol precipitation, digested and cloned into HindIII/XbaI sites of pCEFL expression vector and sequence verified.

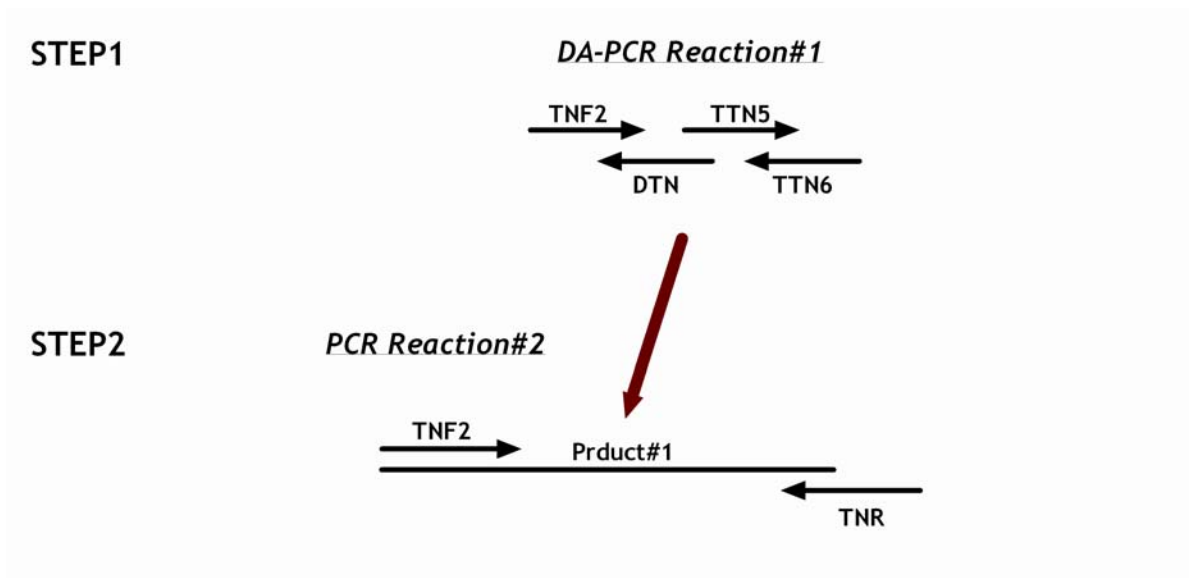


Figure 4. Schematic diagram of DTN synthesis method
 Four adjacent primers were processed by DA-PCR reaction (step1) in order to generate the DNA template that is amplified in step2 through a PCR reaction.

1.3.MTN Tag

The MTN tag (Triple Tag N-terminal) DNA sequence was designed in order to codify the following peptide: MGLNDIFEAQKIEWHEHLEVLFQGPGGPGGENLYFQGG. Underlined are the functional sites within the peptide: AVI sequence (GLNDIFEAQKIEWHE), Precision protease cleavage site (EVLFQGP) and TEV protease cleavage site (ENLYFQ). DNA sequence was projected accordingly and is, from 5' to 3', the following:

aggccaagccttatgggcctgaacgacatctcgaggccagaagatcgagtggcacgaacacctggaggtcctgtccaggacctggcgcccc
ggcggcgagaacctgtactccaggcgatccggcgaattctaaatctagagccaag. Underlined are additional restriction sites required for cloning.

In order to synthesize such DNA sequence (153 bp long) a previously described PCR-based gene synthesis approach was adopted (222). As already described above for TTN tag synthesis oligonucleotides about 40nt in length were designed in order to cover the whole desired DNA sequence with about 10 nt overlaps at both 5' and 3' ends between adjacent oligonucleotides (Fig.5).

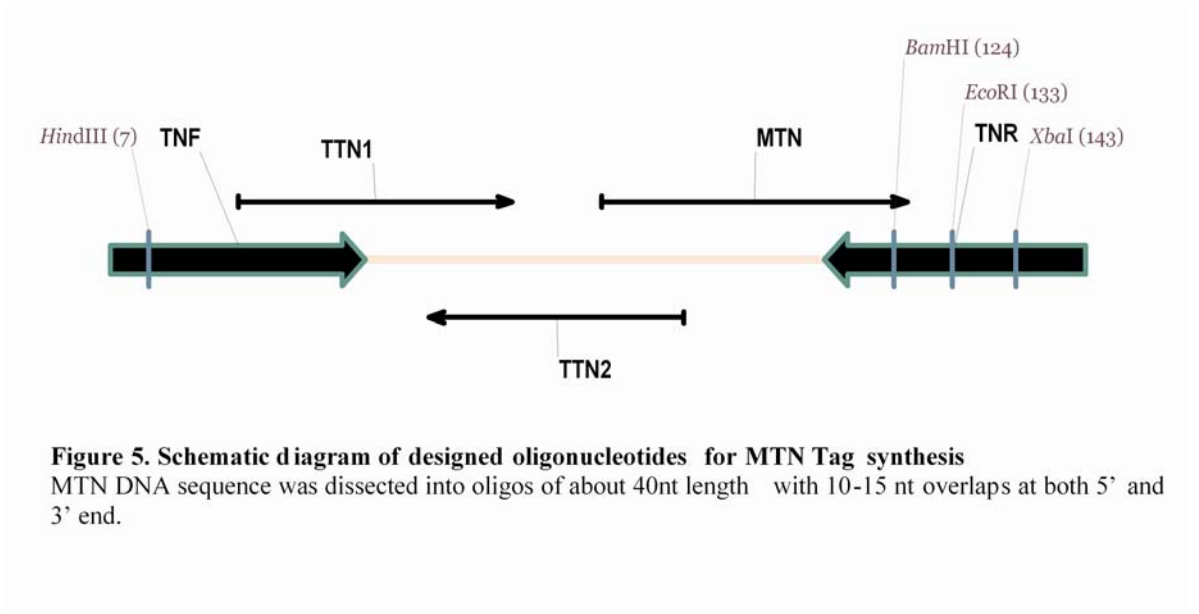


Figure 5. Schematic diagram of designed oligonucleotides for MTN Tag synthesis

MTN DNA sequence was dissected into oligos of about 40nt length with 10-15 nt overlaps at both 5' and 3' end.

Sequences of used oligonucleotides, from 5' to 3', were respectively the following:

TNF (as for TTN tag synthesis),

TNR (as for TTN tag synthesis),

MTN (cagggacctggcggccccggcggcgagaacctgtacttccagggcgga),

TTN1 (as for TTN tag synthesis),

TTN2 (as for TTN tag synthesis).

MTN tag synthesis strategy is schematized in Figure 6. In step1, A DA-PCR reaction was carried out for the first four consecutive oligonucleotides (reaction#1:*TTN1*, *MTN*, *TTN2*, *TNR*) as described in the TTN tag paragraph. In step2, the product obtained from the DA-PCR reaction (about 130bp) was gel extracted and used as template (20ng/50µL) in a canonical PCR reaction (Reaction#2) using *TNF* and *TNR* as primers (500nM each). PCR reaction profile 94° for 20s, 55° for 30s and 72° for 30s was repeated for 25 cycles The obtained product of 153bp was purified by phenol-chloroform extraction and ethanol precipitation, digested and cloned into HindIII/XbaI sites of pCEFL expression vector and sequence verified.

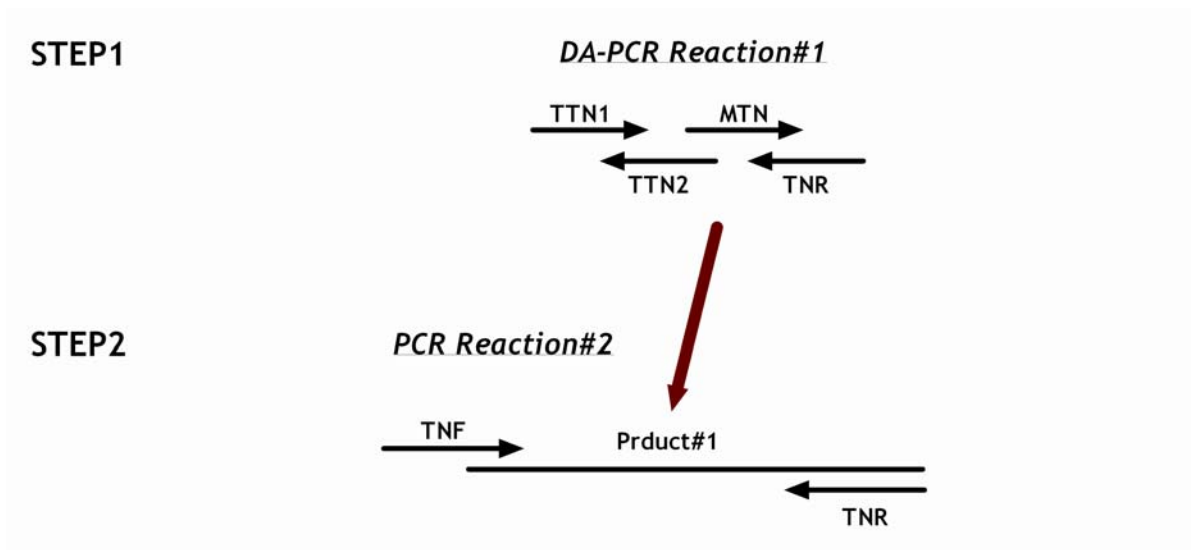


Figure 6. Schematic diagram of MTN synthesis method
 Four adjacent primers were processed by DA -PCR reaction (step1) in order to generate the DNA template that is amplified in step2 through a PCR reaction

2.C-terminal Multiple-Tags (TTC, DTC, MTC) cloning in pCEFL expression vector

2.1.TTC Tag

The TTC tag (Triple Tag C-terminal) encoding vector (pGEM-TAG) was provided from Stunnenberg H.G. Laboratory. TTC tag codify the following peptide: **FGPAGAIAG****ENLYFQ****GGGGPGGG****KPIP****NPLLGLDST****GDYKDDDDK****GLEVL****FQGP****HGLNDIFE****AQKIEWHE**. Underlined are the functional sites within the peptide: TEV protease cleavage site (**ENLYFQ**), V5 epitope (**KPIP****NPLLGLDST**), Flag epitope (**DYKDDDDK**), Precision protease cleavage site (**EVL****FQGP**), AVI sequence (**GLNDIFE****AQKIEWHE**).

DNA sequence of the provided Tag was, from 5' to 3', the following:

gggccggccggcgcgatcggcggcgaacgtacttccagggcggcggccccggcggcgaagcctatccctaaccctctgctgggctg
 gactccacaggagactacaaggatgacgatgacaaaggcctggaggctctgtccagggacctcagggcctgaacgacatcttcgagggccagaa
 gatcgagtggcacaatgatga. Underlined are the two terminal stop codons.

TTC tag was PCR amplified from the original vector with the following primers: The Forward *TCF* primer (5'- ctaggaattcgggccggccggcgcg-3') carrying the EcoRI restriction site for cloning into

pCEFL recipient vector and subsequent upstream in frame cloning of desired gene sequence. The Reverse *TCR* primer (5'-ggctctagattattcgtgccactcgatcttctgggc-3') carrying the XbaI restriction site for cloning into pCEFL recipient vector preceded by a STOP codon. PCR reaction was carried out in 50µL including template DNA (100ng/50µL), dNTP(200nM), primers pair (500nM each) and 2U Pfu (biogem). PCR profile 94° for 20s, 55° for 30s and 72° for 30s was repeated for 25 cycles. The obtained product of 225bp was purified by phenol-chloroform extraction and ethanol precipitation, digested and cloned into EcoRI/XbaI sites of pCEFL expression vector and sequence verified.

2.2.DTC Tag

The DTC tag (Triple Tag C-terminal) was obtained by PCR amplification of the first 150bp of the provided TTC tag template (pGEM-TAG) in order to obtain a DNA sequence encoding the following peptide: FGPAGAIAGENLYFQGGGPGGGKPIPNLLGLDSTGDYKDDDDK. Underlined are the functional sites within the peptide: TEV protease cleavage site (ENLYFQ), V5 epitope (KPIPNLLGLDST), Flag epitope (DYKDDDDK).

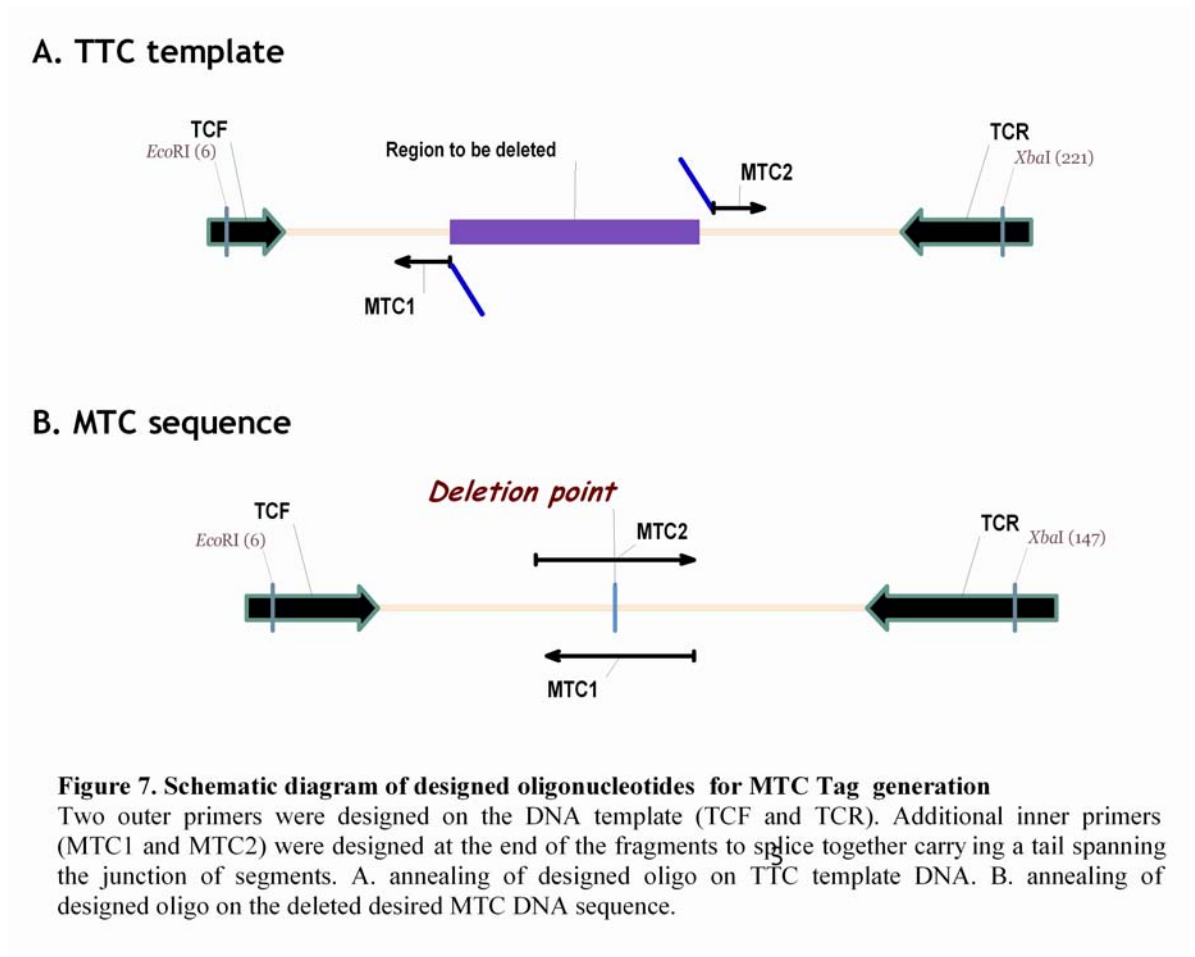
DTC tag was PCR amplified from the original TTC containing vector with the following primers: The Forward *TCF* primer (5'- cttagaattcgggccgcccggcgcg-3'), the same used for TTC amplification, carrying the EcoRI restriction site for cloning into pCEFL recipient vector and subsequent upstream in frame cloning of desired gene sequence . The Reverse *TCR2* primer (5'- ggctctagattattgtcatcgtcatcctttagtctcc-3'), annealing almost at the center of the TTC sequence, carrying the XbaI restriction site, preceded by a STOP codon, in its tail for cloning into pCEFL recipient vector. PCR reaction was carried out as described for TTC tag in chapter 2.1. The obtained product of 151bp was purified by phenol-chloroform extraction and ethanol precipitation, digested and cloned into EcoRI/XbaI sites of pCEFL expression vector and sequence verified.

2.3.MTC Tag

The MTC tag DNA encode the following peptide: FGPAGAIAGENLYFQGGGPGGGLEEVLFQPHGLNDIFEAQKIEWHE. Underlined are the

functional sites within the peptide: TEV protease cleavage site (ENLYFQ), Precision protease cleavage site (EVLFOGP), AVI sequence (GLNDIFEAQKIEWHE).

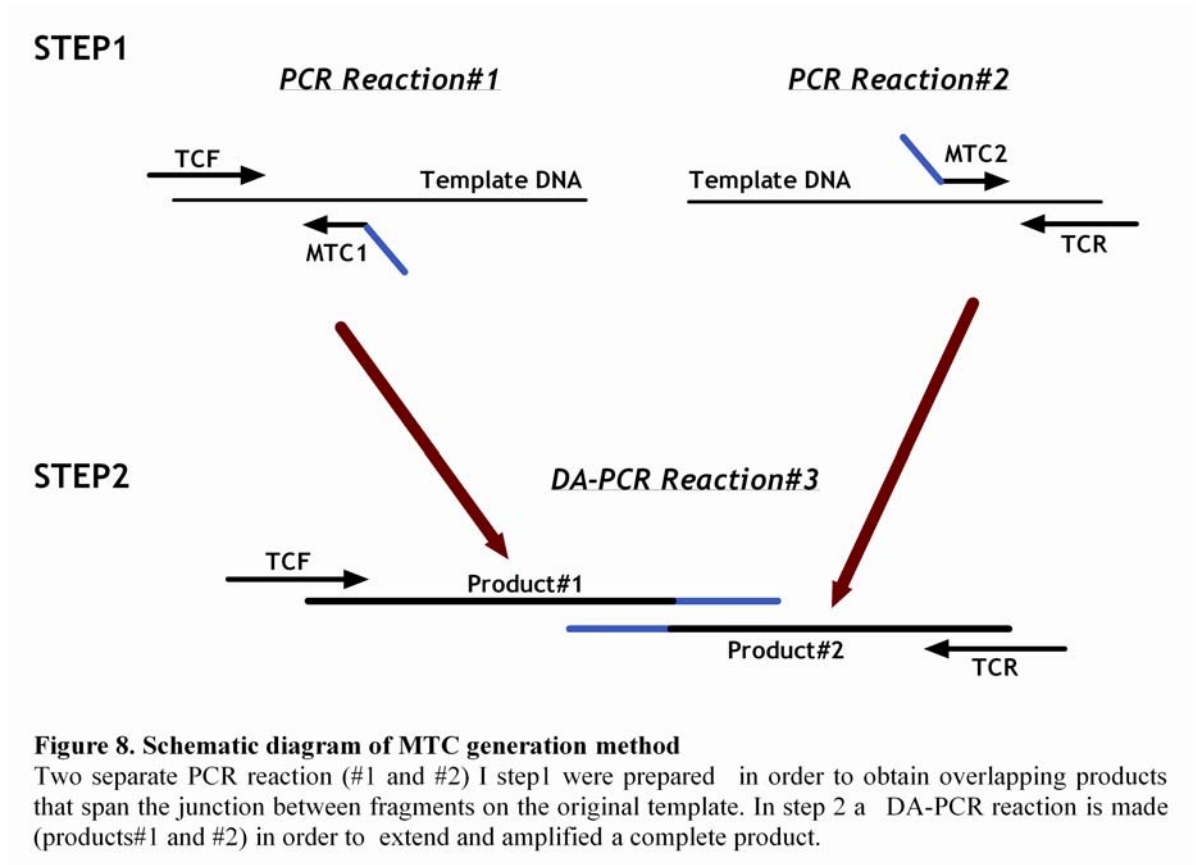
The MTC tag (Triple Tag C-terminal) was obtained by generating an internal central deletion in the TTC tag template through a PCR-driven overlap extension approach previously described (223). Briefly, to generate a product carrying a central deletion, the target gene is amplified from the template DNA using two external primers that anneals to the ends of the template (*TCF* and *TCR* primers in Fig.7 that are the same used for TTC amplification) plus two internal primers (*MTC1* and *MTC2* in Fig.7), each annealing at the end of the DNA fragments that have to be spliced together, and designed in order to generate overlapping sequences by including nucleotide in their tail that span the junction of the DNA segments to merge (Fig. 7).



MTC tag amplification strategy is schematized in Figure 8. In step1, two separate PCR reaction were carried out. In Reaction#1 template was amplified with *TNF* and *MTC1* (5'-

gaacaggacctccaggccgccggggccg-3') primers while in reaction#2: *MTC2* (5'-ggcgccccggcgccctggaggtctgttc-3') and *TNR* primers were used. In this way overlapping products spanning the junction of the deletion point were generated. PCR reactions were carried out as described in chapter 2.1.

In Step2, products from the first reactions (product#1 85bp, product#2 100bp) were gel extracted, purified and mixed together (7nM final concentration for each) with the outer two oligonucleotides *TCF* and *TCR* (500nM final concentration each) in a 50 μ L DA-PCR reaction (as described in chapter1.1).The obtained product of 154bp was purified by phenol-chloroform extraction and ethanol precipitation, digested and cloned into *EcoRI/XbaI* sites of pCEFL expression vector and sequence verified.



3. Expression and reporter constructs

3.1. Reporter constructs

Reporter vectors pNIS-Luc1, NIS-Luc9 and pNIS-Luc5 were previously reported (64). The pE1B-luc construct was obtained by cloning a chemical synthesized oligonucleotide (5'-ctcgagtctagagggtatataatggatcc-3') containing the E1B TATAbox flanked by XhoI site at 5' and BamHI site at 3' into an XhoI/BamHI cleaved pGL3 basic luciferase reporter vector (Promega corporation). pNUE-Luc (NUE reporter) construct was obtained by excising with KpnI and XhoI the NUE sequence from the previously reported pNISTKluc3 construct (64) and cloning it into KpnI/XhoI sites of pE1B-luc construct. The pCp5-E1B-Luc (Cp5 reporter) construct was obtained by excising with PvuII and BamHI the Cp5E1b cassette from the previously reported Cp5CAT vector(4) and cloning it into SmaI/BglII cleaved pGL3 basic luciferase reporter vector (Promega corporation). The pG5-E1B-Luc (G5 reporter) construct was obtained by excising with PvuII and BamHI the G5-E1b cassette from the previously reported G5CAT vector (224) and cloning it into SmaI/BglII cleaved pGL3 basic luciferase reporter vector (Promega corporation). The 5xCRE-luc (CRE reporter) was previously described (225). The pGL3/eGFP basic vector was obtained by substituting the luciferase gene of the pGL3 luciferase basic reporter vector (Promega corporation) with the eGFP gene. The eGFP gene was excised with NcoI and XbaI enzymes from the pEGFP n1 vector (clontech) and cloned into the NcoI/XbaI sites of pGL3 vector. The pNUE-GFP expression vector was obtained by excising with NcoI and BamHI the NUE-E1B cassette from the pNUE-luc vector and cloning it into NcoI/BamHI sites of pGL3/eGFP basic vector. The TK-renilla reporter vector was purchased from Promega Corporation (phRL-TK).

3.2. N-terminal (TTN, DTN, MTN) tagged-Pax8 expression vectors

Mouse Pax8 gene sequence was amplified by PCR from the previously described pCEFL-3xFlagPax8 vector (107). Forward primer (*Pd*F* 5'- agggcggatcccctcacaactcgatcagatccggc -3') was designed in order to delete the ATG start codon and create an EcoRI restriction site to allow in frame cloning downstream of the N-terminal Tags in the pCEFL expression vectors described in chapter1. Reverse primer (*PRL* 5'- ccacagccttgaccatctgtagtatatctagagcc -3') was flanked by an XbaI restriction

site. Amplified Pax8 was purified by phenol-chloroform extraction and ethanol precipitation, digested and cloned into EcoRI/XbaI sites respectively downstream of the TTN, DTN and MTN tags in the relative pCEFL expression vectors (chapter1). Amplified Pax8 was sequence verified.

3.3.C-terminal (TTC, DTC, MTC) tagged-Pax8 expression vectors

Mouse Pax8 gene sequence was amplified by PCR from the previously described pCEFL-3xFlagPax8 vector (107). Forward primer (*PCF* 5'- agggcaagcttatgcctcacaactcgatcatgaccc -3') was flanked by a HindIII restriction site. Reverse primer (*PCR* 5'- ccacagccttgaccatctggaattctaattagagcc -3') was designed in order to delete the stop codon and create an EcoRI restriction site to allow in frame cloning upstream of the C-terminal Tags in the pCEFL expression vectors described in chapter2. Amplified Pax8 was purified by phenol-chloroform extraction and ethanol precipitation, digested and cloned into HindIII/EcoRI sites respectively upstream of the TTC, DTC and MTC tags in the relative pCEFL expression vectors (chapter2). Amplified Pax8 was sequence verified.

3.4.GAL-Pax8 deletion derivatives expression vectors

The pCEFL-GAL expression vector was obtained by excising the GAL4-DBD (DNA binding Domain corresponding to aa 1-146 from yeast GAL4) with BglII and EcoRI from the pM vector (clontech) and cloned into BamHI/EcoRI sites of pCEFL expression vector. All transactivation domains that were fused to GAL4-DBD were amplified by PCR (25 cycles using 100ng plasmid DNA as template and 2U Pfu per 50µL reaction) with primers flanked by tails introducing respectively, a EcoRI site at the 5' end of the amplicon to allow in frame cloning downstream of the GAL4-DBD and, a XbaI site at the 3' end of the amplicon. All transactivation domains PCR products were purified by phenol-chloroform extraction and ethanol precipitation, digested and cloned into EcoRI/XbaI site of pCEFL-GAL expression vector and sequence verified.

pCEFL-GalVp16. Vp16 transactivation domain (aa 416-490 from vmw65 hHSV1) was amplified from a previously reported FlagHDVp16 construct (4) with the following primers pair: *VF* 5'-ggcgcaattcgccccccgaccgacgtcagcctggggg -3'/*VR* 5'- gcattgacgactttgggggtgagatatctagagcc-3'.

All Pax8 transactivation deletion derivatives domains were amplified from the previously reported pCEFL3xFlagPax8 vector (107).

pCEFL-GP. Contains the whole Pax8 transactivation domain (aa 134-457 in mouse Pax8A protein) amplified with the following primers pair: *PFL* 5'- ggccaattcaccaagtcagcagccattcaacc - 3'/*PRL* 5'- ccacagccttgaccatctgtagttagatctagagcc -3'

pCEFL-GP1. Contains the whole Pax8 transactivation domain depleted of the putative inhibitory region (226) localized at its C-terminal end (aa 134-425 in mouse Pax8A protein) amplified with the following primers pair: *PFL* 5'- ggccaattcaccaagtcagcagccattcaacc -3'/*PRS* 5'- tcctctacagtgaggcctggcgctagatctagagcc-3'

pCEFL-GP2. Contains the Pax8 transactivation domain depleted of the Homeodomain homology region (aa 219-457 in mouse Pax8A protein) amplified with the following primers pair: *PFS* 5'- ggccaattcggctcctcgaaagcaccttcgtacg -3'/*PRL* 5'- ccacagccttgaccatctgtagttagatctagagcc -3'

pCEFL-GP3. Contains the Pax8 transactivation domain depleted of the Homeodomain homology region and the putative inhibitory region (226) localized at its C-terminal end (aa 219-425 in mouse Pax8A protein) amplified with the following primers pair: *PFS* 5'- ggccaattcggctcctcgaaagcaccttcgtacg -3'/*PRS* 5'- tcctctacagtgaggcctggcgctagatctagagcc -3'

pCEFL-GP4. Contains the putative minimal Pax8 transactivation domain (226) (aa 370-457 in mouse Pax8A protein) amplified with the following primers pair: *PFSS* 5'- ggccaattcggcgagagatggtgggg -3'/*PRL* 5'- ccacagccttgaccatctgtagttagatctagagcc -3'

pCEFL-GP5. Contains the putative minimal Pax8 transactivation domain depleted of the putative inhibitory region (226) localized at its C-terminal end (aa 370-425 in mouse Pax8A protein) amplified with the following primers pair: *PFSS* 5'- ggccaattcggcgagagatggtgggg -3'/*PRS* 5'- tcctctacagtgaggcctggcgctagatctagagcc -3'

3.5. Pax8 deletion derivatives expression vectors

The Paired DNA binding Domain (Pd) of Pax8 (aa 1-133 of mouse Pax8A protein) was amplified from the previously described pCEFL3xFlagPax8 vector (107) and cloned into HindIII/XbaI

site of 3xFlag-CMV10 (Sigma). Amplification was carried out with primers (*PdF* 5'-agggcaagcttctcacaactcgatcagatccggc -3'/*PdR* 5'-ggctctagatttagaattcccggatgattctgttgatggagc -3') flanked by tails introducing respectively, a HindIII site at the 5' end of the amplicon projected to allow in frame cloning downstream of the 3xFlag tag and, a XbaI site at the 3' end of the amplicon preceded by an EcoRI site to allow in frame cloning downstream of the Pd domain. Paired domain sequence was verified. 3xFlag-Pd cassette was then excised with HindIII and XbaI from the pCMV-3xFlag-Pd vector and cloned in the pCEFL expression vector (pCEFL-Pd).

All transactivation domains used were obtained respectively by excision with EcoRI and XbaI from the corresponding pCEFL-GAL containing vector (see chapter 3.4) and subcloned in the EcoRI/XbaI sites of the pCEFL-Pd expression vector.

pCEFL-PdVp16. Vp16 transactivation domain (aa 416-490 from vmw65 hHSV1) from pCEFL-GalVp16.

pCEFL-Pax8. Pax8 transactivation domain (aa 134-457 in mouse Pax8A protein) from pCEFL-GP.

pCEFL-P1. Pax8 transactivation domain depleted of the putative inhibitory region (226) (aa 134-425 in mouse Pax8A protein) from pCEFL-GP1.

pCEFL-P2. Pax8 transactivation domain depleted of the Homeodomain homology region (aa 219-457 in mouse Pax8A protein) from pCEFL-GP2.

pCEFL-P3. Pax8 transactivation domain depleted of the Homeodomain homology region and the putative inhibitory region (226) (aa 219-425 in mouse Pax8A protein) from pCEFL-GP3.

pCEFL-P4. Pax8 minimal transactivation domain (226) (aa 370-457 in mouse Pax8A protein) from pCEFL-GP4.

3.6. Other Expression constructs

The pCEFL-3xFlagPax8 and pCMV-cPKA expression vectors have been previously described (107, 225). The SpRT TSHr coding sequence (Rho-Tagged human-TSHr)(227) was excised by cleavage with KpnI and XbaI from the original pcDNAIII vector, blunted and cloned into BamHI blunted sites of pBABEpuro vector. BirA gene was amplified by RT-PCR from previously described ES cells

clones stably expressing BirA (228) with a forward primer (BrF 5' agggcaagcttatgaaggataacaccgtgcca3') flanked by a HindIII restriction site in its 5' end and a reverse primer (BrR 5' ggtctagatttttctgcactacgcagg3') flanked by a XbaI restriction sites in its tail. The amplified BirA product was purified by phenol-chloroform extraction and ethanol precipitation, digested and cloned into HindIII/XbaI sites of a pCEFL expression vector carrying Puromycine resistance gene instead of Neomicine, and sequence verified.

4. Cell culture

Rat thyroid follicular FRTL-5-derived cell lines were maintained in Coon's modified F12 medium (EuroClone, Milano, Italy) supplemented with 5% newborn bovine serum (HyClone, Logan, UT) and six growth factors (6H), including bovine TSH 1 mU/ml (Sigma-Aldrich), and insulin 10 µg/ml (Sigma-Aldrich) as previously described (218) (6H medium). Tamoxifen treatment, where indicated, was performed by addition of 100 nM 4-hydroxytamoxifen (Sigma-Aldrich) to the culture medium. Stimulation of the cAMP pathway, where indicated, was performed by adding to the culture medium, respectively Forskolin 10µM (Sigma-Aldrich) to stimulate adenylate cyclase, 8-CPT 100µM (Sigma-Aldrich) as cAMP analogue or IBX 100µM (Sigma-Aldrich) to inhibits phosphodiesterases or combination of them as indicated in the text. Inhibition of PKA activity was obtained by adding to the culture medium H-89 (Biomol) 12µM. Inhibition of MAPK pathway was obtained by adding to the culture medium 50µM U-0126 (Biomol) or 50µM PD (Biomol).

Hela cells and NIH 3T3 mouse fibroblasts were grown as previously described (105, 229).

5. Transfections

All transfections were carried out by the use of FuGene 6 (Roche Molecular Biochemicals, Indianapolis, IN) following the manufacturer's instructions. For stable transfection experiments, 2×10^6 cells were seeded on 100-mm dishes 24 hours prior to transfection and transfected with 4 µg/dish of the indicated expression vector. Forty-eight hours later, transfected cells were selected in the presence of 1

$\mu\text{g/ml}$ of puromycin (Sigma-Aldrich). After 3 weeks of continuous selection single clones were picked, screened for expression of the transgene and amplified individually.

For transient transfections 4×10^5 cells were seeded on 60-mm dishes 24 hours prior to transfection. Transfections were performed with 3 $\mu\text{g/dish}$ of Total DNA consisting of 1 μg of reporter vector encoding Firefly Luciferase (FF luc), 0.5 μg of TK-Renilla vector to follow transfection efficiency, cotransfecting vectors or empty vector up to 3 μg . Transfection medium was replaced 15 hours later with standard culture medium, supplemented or not with additional drugs as indicated in the text, and cells cultured for additional 48 hours.

Cells were lysed in 100 $\mu\text{L/dish}$ PLB buffer 1x (Promega Corporation) and Firefly and Renilla Luciferase activity were assayed respectively on 20 μL of each sample with the “luciferase Assay system” (Promega Corporation) and the “Renilla assay system” (Promega Corporation) following manufacturer’s instructions. Luminescence was measured with LUMAT LB 9507 luminometer (Berthold technologies). Firefly Luciferase activity was normalized on the activity of TK-renilla vector in order to correct each sample for transfection efficiency. Data were obtained from at least two independent experiments with triplicate samples.

6. cAMP Enzyme Immunometric assay

Cells were seeded on 60-mm dishes and cultured either in 4H or 6H medium as indicated in the text for 72h. Following treatments described in the text, cells (about 2×10^6) were lysed in 1 mL of 0.1M HCl/0.5% Triton. cAMP was quantitatively determined on 100 μL of cell lysate using the “cAMP EIA kit” (stressgen) following manufacturer’s instruction. Briefly, samples were added to wells containing antibodies to cAMP together with a cAMP conjugate to alkaline phosphatase that works as a cAMP competitor in binding the antibody. Alkaline phosphatase activity bound to the antibody is detected and considered inversely proportional to the amount of cAMP in the sample. A standard curve of cAMP was run in the assay in order to determine cAMP (pmol/mL) in each sample. These values were then normalized on total protein present in each sample in order to obtain pmol of cAMP produced per mg of Protein.

7. PKA kinase activity assay

5×10^6 cells were seeded on 100-mm dishes and cultured 72h in 4H medium. Following treatments indicated in the text, cells were lysed in 100 μ L of lysis buffer (50mM TRIS, 0.5%Np40,150mM NaCl, 1mM Na₃VO₄, 50mM NaF, 5mM EGTA, 2mM EDTA,1mM DTT, 1mM PMSF and protease inhibitor cocktail (Sigma)). PKA activity was assayed on 0.5 μ g of extracted proteins using an ELISA-based commercially available assay kit (“PKA kinase activity assay kit (non radioactive) ”from Stressgen) and following manufacturer’s instructions. Briefly, samples were incubated with ATP, 60 min at 30°C, in the substrate-coated microtiter plate. Phosphorylation of the peptide substrate is then detected through the use of a specific antibody. A standard curve was run in the assay in order to determine ng of active PKA in each sample. These values were then normalized on total protein present in each sample in order to obtain ng of PKA produce per μ g of Protein.

8. Proteins extraction

For total protein extracts 2×10^6 cells were seeded on 60-mm dishes and cultured 48hours with or without additional drugs for the time indicated in the text. Cells were washed in cold PBS and lysed, except where indicated differently, in Tissue Lysis Buffer (50mM TRIS pH8, 5mMgCl₂, 150mM NaCl, 1%Triton, 0.1%SDS, 0.5%deoxycholic acid) supplemented with NaF 10mM, Na₃VO₄ 1mM, PMSF 1mM, and protease inhibitor cocktail (Sigma-Aldrich). Lysis was allowed to continue for 15 min on ice, samples were centrifuged at full speed at 4°C for 25 min. Protein concentration was measured by the BCA protein assay reagent (Pierce, Rockford, IL), following the manufacturer's instructions. For monodimensional Western blot analysis 30 μ g were loaded on SDS-PAGE.

Fractionated protein extraction was performed using the “Proteoextract™ Subcellulare proteome extraction kit” (Calbiochem) and following manufacturer instruction. For monodimensional Western blot analysis 1/20 of each fraction volume was loaded on SDS-PAGE.

Protein extracts, where indicated, were precipitated using a methanol-chloroform protocol (230). Briefly, proteins (150-300 μ g) solved in 150 μ l of extraction buffer were progressively mixed with 600 μ l of methanol, 150 μ l of chloroform and 450 μ l of water. Samples were centrifuged for 5 min at

12000 rpm. The upper phase was removed and 450 μ l of methanol were added; after vortexing, samples were centrifuged for 5 min. All the liquid phase was removed and samples were dried in a chemical hood for 30 min.

9. Flag-Pax8 Immunoprecipitation (IP)

9.1. Nuclear proteins extraction

For Flag-Pax8 IP the 5x10⁶ cells of Px31 clone were seeded on 100-mm dishes and cultured 24 hours with or without Tamoxifen. At the end of the treatment cells were washed in cold PBS and collected in buffer A (85 mM KCl, 0.5% NP40, 5 mM HEPES pH 8.0) (1.5mL /dish) supplemented with protease inhibitor cocktail (sigma) and PMSF 1mM, homogenized by Dounce, incubated on ice for 15 min and centrifuged at 3500 g for 5 min to pellet the nuclei.

The nuclei pellet was resuspended in Lysis Buffer (50mM TRIS pH7.4, 1mM EDTA, 150mM NaCl) supplemented with NaF 10mM, Na₃VO₄ 1mM, PMSF 1mM, and protease inhibitor cocktail (Sigma-Aldrich) and lysis was proceeded as described in previous chapter8.

9.2. Immunoprecipitation

Anti-Flag M2 affinity gel beads (sigma A 2220) were washed as suggested by manufacturers using nuclear lysis bufer. Nuclear lysates (300 μ g in 1mL of nuclear lysis buffer) were then added to the beads (50 μ L of packed gel) and incubated o.n. under rotation at 4°C. An aliquote of unprocessed Nuclear lysate (10 μ L corresponding to 1% of total Input proteins) was stored as INPUT control for subsequent analysis.

After o.n. incubation beads were pellet and supernatant containing unbound proteins discarded. An aliquote of the supernatant (10 μ L corresponding to 1% of total unbound proteins) was stored as UNBOUND control for subsequent Western Blot analysis. Beads were then extensively washed in lysis buffer as suggested by manufacturer.

9.3. Elution with 3xFLAG peptide

Elution of the bait from washed beads was performed by competition with the 3xFLAG peptide (sigma F 4799). Beads (50 μ L) were incubated with 80 μ L Elution buffer (TRIS Hcl 150mM, EDTA 1mM, Glycerol 10%, 3xFlag peptide 500 μ g/mL, NaF 10mM, Na₃VO₄ 1mM, PMSF 1mM, protease inhibitor cocktail) for 30 min under rotation at 4°C. Elution step was performed twice and supernatant from the two elution steps combined together (about 160 μ L).

An aliquote of the eluted material (5 μ L corresponding to 3% of Immunoprecipitated proteins) was stored as IP control for subsequent Western Blot analysis. Residual eluted material (150 μ L) were precipitated using a methanol-chloroform protocol (described in chapter8) and 10% of it was processed by Bidimensional electrophoresis.

10. Multiple Tagged-Pax8 Affinity purification TESTs

10.1. Protein extracts preparation

Protein extracts were obtained by lysing cells with 100 μ L/100mm dish Co-IP lysis buffer (20mM TRIS-HCL pH 7.9, 120mM KCl, 5mM MgCl₂, 5mM EDTA, 0.3% nonidet 40) supplemented with inhibitors as described in chapter8.

Protein extracts were then pre-cleared with 200 μ L/2mL of Mouse IgG-Agarose (Sigma). Cleared lysates were quantified and protein concentration, within different lysates, normalized by adding lysis buffer to the lower concentrated one. Protein concentration in the lysates was kept to 5 μ g/ μ L for all the following experiments. An aliquote of each cleared protein extract was stored as control for INPUT fraction.

10.2. Streptavidin-binding affinity purification

Paramagnetic streptavidin beads (Dynabeads M280 streptavidin, Invitrogen, DYNAL) were washed twice with lysis buffer following manufacturer's instructions. The beads were immobilized using a magnetic particle concentrator (DYNAL MPCTM-S, Invitrogen, DYNAL) rack. Washed beads

were blocked 1h at 4°C under rotation with Co-IP lysis buffer supplemented with BSA 200ng/mL. After incubation blocking buffer was removed and 600µL protein extract (3mg of total proteins) added to each IP (20µL of Streptavidin beads for IP reaction). Binding was allowed 2h at 4°C under rotation. After binding. Beads were immobilized on the magnetic rack and the supernatant containing unbound material was discarded. An aliquote of the supernatant was stored as control for UNBOUND fraction. Beads were then washed as suggested by manufacturer in co-IP lysis buffer. Methods for elution of bound material from the beads are described in the following paragraphs. Chosen elution method is indicated time by time in the results section text.

10.3.V5-IP

Anti-V5 affinity gel beads (clone V5-10, sigma A 7345) were washed with lysis buffer following manufacturer's instructions. Beads were pellet by 1 min centrifugation at 3000g. Washed beads were blocked 1h at 4°C under rotation with Co-IP lysis buffer supplemented with BSA 200ng/mL. After incubation blocking buffer was removed and 600µL protein extract (3mg of total proteins) added to each IP (60µL of Anti-V5 resin for IP reaction). Binding was allowed 2h at 4°C under rotation. After binding beads were pellet and the supernatant containing unbound material was discarded. An aliquote of the supernatant was stored as control for UNBOUND fraction. Beads were then washed as suggested by manufacturer in co-IP lysis buffer. Elution of bound material from the beads can be made through SDS boiling or TEV protease cleavage as described in the following paragraphs. Chosen elution method is indicated time by time in the results section text.

10.4.Flag-IP

Anti-Flag M2 affinity gel beads (sigma A 2220) were washed with lysis buffer following manufacturer's instructions. Beads were pellet by 1 min centrifugation at 3000g. Washed beads were blocked 1h at 4°C under rotation with Co-IP lysis buffer supplemented with BSA 200ng/mL. After incubation blocking buffer was removed and 600µL protein extract (3mg of total proteins) added to each IP (60µL of Anti-Flag resin for IP reaction). Binding was allowed 2h at 4°C under rotation. After binding beads were pellet and the supernatant containing unbound material was discarded. An

aliquote of the supernatant was stored as control for UNBOUND fraction. Beads were then washed as suggested by manufacturer in co-IP lysis buffer. Elution of bound material from the beads can be made through SDS boiling or TEV protease cleavage as described in the following paragraphs or by competition with the 3xFlag peptide as described in paragraph 9.3. Chosen elution method is indicated time by time in the results section text.

10.5.Flag/V5 double IP

Anti-Flag M2 affinity gel beads (sigma A 2220) were washed and blocked as described above. 1200 μ L protein extract (6mg of total proteins) was added to 120 μ L of Anti-Flag resin. Binding was allowed 2h at 4°C under rotation. After binding beads were pellet and the supernatant containing unbound material was discarded. An aliquote of the supernatant was stored as control for UNBOUND FLAG fraction. Beads were then washed as described above and elution was performed with 300 μ L of 3xFLAG peptide elution buffer as described in paragraph 9.3. Half of eluted proteins (150 μ L) were precipitated by using a methanol-chloroform protocol (described in chapter8) and stored as the IP FLAG fraction.

Residual eluted proteins (150 μ L) were furtherly processed through a V5-IP. Flag-eluted proteins were diluted in 1mL of co-IP lysis buffer and V5-IP was performed on this purified lysate exactly as described above in the relative V5-IP paragraph.

10.6.Aspecific elution through boiling in SDS

Washed beads were incubated 5 minutes at 99°C. with 30 μ L (volume ratio Beads/Elution buffer 1:1) of LDS loading buffer 2x (Invitrogen) in order to elute bound material. Beads (Streptavidin, Flag or V5 conjugated) were then respectively pellet as suggested by manufacturers and supernatant (about 30 μ L) stored as IP fraction.

10.7.TEV cleavage mediated elution

Washed beads were incubated in 160 μ L of TEV reaction buffer (500mM TRIS-HCl pH8, 0.5mM EDTA, 10mM DTT) supplemented with 10U AcTEVTM Protease (Invitrogen). Reaction was

incubated 16h at 4°C. Beads (Streptavidin, Flag or V5 conjugated) were then respectively pellett as suggested by manufacturers and supernatant (150µL) stored as IP fraction. Proteins of the IP fraction were precipitated using a methanol-chloroform protocol (described in chapter8) and resuspended in 30µL of LDS loading buffer (Invitrogen). Residual proteins still bound to the TEV-treated beads were then eluted through boiling (as described above) and the supernatant stored as UNELUTED fraction.

10.8.Prescission cleavage mediated elution

Washed beads were incubated in 160µL of Prescission reaction buffer (50mM TRIS-HCl pH7, 150mM NaCl, 1mM EDTA, 10mM DTT) supplemented with 10U Prescission™ Protease (GE healthcare). Reaction was incubated 16h at 4°C. Beads (Streptavidin, Flag or V5 conjugated) were then respectively pellet as suggested by manufacturers and supernatant (150µL) stored as IP fraction. Proteins of the IP fraction were precipitated using a methanol-chloroform protocol (described in chapter8) and resuspended in 30µL of LDS loading buffer (Invitrogen). Residual proteins still bound to the Prescission-treated beads were then eluted through SDS boiling (as described above) and the supernatant stored as UNELUTED fraction.

11. Monodimensional SDS-PAGE and Bidimensional electrophoresis

Protein extracts or immunoprecipitated proteins were resolved by Monodimensional SDS-Page or small-format 2-DE and further analyzed by coomassie staining or Immunoblotting as indicated in the text. .

Monodimensional SDS-PAGE separations were performed using precasted NuPAGE 4-12% Bis-Tris gels (Invitrogen, Carlsbad, CA). Separation conditions were set following the manufacturer's instructions.

For small-format 2-DE, samples were precipitated and resuspended in 100 µl DeStreak Rehydration Buffer with 0.5% (v/v) of 3-11NL IPG Buffer (Amersham Bioscience). Samples were applied by passive rehydratation on a 3-11NL 7 cm IPGstrip (Amersham Bioscience). Focusing condition was set following the manufacturer's instructions. After focusing IPGstrip were equilibrated.

The first step of equilibration (reduction) was carried out with 2% (w/v) DTT; the second one (alkylation) was carried out with 2.5% (w/v) iodoacetamide and 0.03% Coomassie Brilliant Blue R-250. Both steps were performed for 15 min each at room temperature. As described above, the second-dimension SDS-PAGE separations were performed using precasted NuPAGE 4-12% Bis-Tris ZOOM gels (Invitrogen, Carlsbad, CA). Separation conditions were set following the manufacturer's instructions.

Gels were fixed with 50% (v/v) methanol, 10% (v/v) acetic acid aqueous solution for 30 min, extensively washed with water, and stained with a colloidal Coomassie solution (Pierce). Stain and destain was performed according to the manufacturer's instructions.

12. Western Blot

Gels were electroblotted on PVDF membranes (Immobilon-P, Millipore, Bedford, ME) and screened for different antibodies. Rabbit polyclonal antibodies against Pax8 and NIS were previously produced in our laboratory were used respectively at 0.5 µg/ml and 0.2µg/ml (219). Mouse monoclonal antibody against Rho-Tag and mouse monoclonal antibody against TSHr (mAb 103) were previously described (227) and were used both at 1:50 dilution. CREB (48H2) Rabbit mAb, Phospho-CREB (Ser133) Mouse mAb, PKA C-α (Cell signalling Technologies), PKAβ cat(C-20) (Santa Cruz biotechnology), PKA RIIβ, PKA RIIα, PKA RIα (BD Transduction Laboratories), Histone H3 antibody -ChiP grade (ab1791, Abcam), GAPDH (clone 6C5) (ImmunoChemical), Chicken polyclonal anti-BirA (Novus Biologicals), anti-Flag M2 monoclonal (sigma). and RAS (clone Ras10) (Upstate) antibodies were used as suggested by the manufacturers. Secondary antibodies Mouse IgG Horseradish peroxidase linked whole antibody (Amersham Biosciences), Rabbit IgG Horseradish peroxidase linked whole antibody (Amersham Biosciences) and chicken Ig Horseradish peroxidase conjugate (Novus biologicals NB7289) were used as suggested by manufacturers. Immune complexes were detected by enhanced chemiluminescence as instructed by manufacturer (Amersham Biosciences, Arlington Heights, IL). Quantitative analysis (QWB), where indicated, was performed on at least three independent experiment by capturing and analyzing

chemiluminescence with Chemidoc XRS instrument (Bio-Rad, Hercules, CA) supported by the Quantity One 4.6.5 software (Bio-Rad).

13. RNA extraction and Real-Time RT-PCR

1.5×10^6 cells were seeded on 60-mm dishes and cultured 48 hours with or without additional drugs for the time indicated in the text. Total RNA was isolated with RNeasyTM mini kit (Quiagen) following manufacturer's instructions. Four micrograms of total RNA from each cell line were used as a template for the synthesis of the first strand cDNA, starting from random hexamers, using the Superscript II Reverse Transcriptase kit (Invitrogen Life Technologies, Carlsbad, CA) according to manufacturer's instructions. Real-Time RT-PCR was conducted using an ABI Prism 7700 sequence detection system and SYBR Green chemistry (Applied Biosystems, Foster City, CA). Each reaction was carried out in triplicate, on duplicate biological samples, using cDNA obtained from 150 ng of total RNA per reaction as template. Specific primers pair for each gene analysed were previously described and used at 130nM (4). Results were analysed using α -1 tubulin mRNA (4) as reference gene. Analysis of results was performed following Real-Time relative-quantitation guidelines through the relative Standard curve method as suggested by Applied Biosystem. Briefly, amplification efficiency was calculated from triplicates relative standard curves for each primer pairs and then used to convert Ct values obtained from each reaction into relative-expression units (231). Data obtained in this way were then normalized on the relative-expression of reference gene. Statistical analysis was performed on normalized relative-expression values of each gene.

14. Chromatin-IP

14.1. Crosslinked chromatin preparation

Briefly 4×10^6 cells were seeded on 100-mm dishes and cultured 24 hours with or without additional drugs for the time indicated in the text. At the end of the treatment formaldehyde was added to the cells to final 1% for 10 min to crosslink the chromatin and the reaction was stopped by adding glycine to a final concentration of 0.125 M. Cells were washed twice with PBS, and collected in cell lysis buffer

(85 mM KCl, 0.5% NP40, 5 mM HEPES pH 8.0) (1.5mL /dish) supplemented with a protease inhibitor cocktail (sigma) , homogenized by Dounce, incubated on ice for 15 min and centrifuged at 3500 g for 5 min to pellet the nuclei. The pellet was resuspended in nuclear lysis buffer (10 mM EDTA, 1% SDS, 50 mM Tris-HCl, pH 8.1) in a ratio 400 μ L/10⁷cells. Crosslinked chromatin aliquots were stored at -80°C or either processed directly.

14.2. Transcription rate measurement

Transcription rate measurement was performed through an RNA-polymeraseII-based Chromatin-IP as previously described(232). Crosslinked chromatin (400 μ L aliquotes) was sonicated on ice with 8 pulses of 30% amplitude in a BRANSON 250 sonicator . The average chromatin size of the fragments obtained was about 300 bp. The sonified chromatin was centrifuged at 14,000 g for 10 min and the supernatants, containing soluble chromatin fragments, were diluted 10-fold with dilution buffer (165 mM NaCl, 0.01% SDS, 1.1% Triton X, 1.2 mM EDTA, 16.7 mM Tris-HCl, pH 8.0) supplemented with protease inhibitor cocktail (Sigma-Aldrich). Diluted samples were precleared with 50 μ L/mL of Salmon sperm DNA/proteinA agarose (Upstate) and left 1h under rotation at 4°C. After centrifuging 1 min at 3000g at 4°C aliquots from the supernatant of each sample (1mL each) were incubated with 2.5 μ g of RNA pol II antibody (Santa Cruz, sc-899), or as negative controls with 2.5 μ g of Normal Rabbitt IgG (Upstate) or in the absence of any antibody and left to stay overnight at 4°C under rotation (An aliquote of the supernatant was stored at 4°C to evaluate INPUT DNA for each sample). The samples were then incubated with 30 μ l of Salmon sperm DNA/proteinA agarose (Upstate) under rotation for an additional period of 1h. Immunocomplex were then recovered and washed as suggested by Upstate. Elution was performed with 2x100 μ l of elution buffer (1% SDS, 100 mM NaHSO₃). Both Immunoprecipitated Chromatin and Input Chromatin were incubated at 65°C overnight to reverse formaldehyde crosslinks. DNA purification was performed as suggested by Upstate and resuspended in 100 μ L TE buffer. The entire chromatin-IP procedure has been repeated on independent tweek samples. All obtained DNA samples have been analysed in triplicates by Real-Time PCR. Real-time PCR was performed and analysed as described in the previous paragraph using 5 μ L of DNA as

template for each reaction. Primer pairs were designed with the Primer express^R software (Applied Biosystem) to amplify a region of 135 bp in length, corresponding to NIS coding region and located about 2kb downstream of Transcription start site (NisF 5'-cccctcaccctgtetaacc-3'/NisR 5'-gctgaagagtgaccccagct-3'). For Pax8 gene primers were designed exactly with the same criteria (PaxF 5'-atgagtgagaaatgatcgcg-3'/PaxR 5'-ggaaggacggagagacaggtt-3'). For each sample immunoprecipitated DNA levels have been reported as percent of Total INPUT DNA and the average value has been calculated on the two independent chromatin IP.

14.3. Pax8 binding measurement

Pax8 Chromatin binding measurement was performed exactly as described above but using 1µg of Pax8 antibody for each ChIP instead of the RNA polymerase one. Real-time PCR was performed on triplicate samples and analysed as described in the previous paragraph using 5µL of immunoprecipitated DNA as template for each reaction. Primer pairs were designed with the Primer express^R software (Applied Biosystem) to amplify a DNA region of about 200bp including the putative Pax8 binding site (Di gennaro A, De feliceM. And Di LauroR. unpublished) on Pax8 gene promoter (PP2F 5'- atgtgtctggtgaggctctcag-3'/PP2R 5'- agccttcactctccactccc-3') . For each sample, immunoprecipitated DNA levels have been reported as percent of Total INPUT DNA and the average value has been calculated on two independent chromatin IP.

15. Gel mobility shift

4×10^6 cells were seeded on 100-mm dishes and cultured 48hours with or without additional drugs for the time indicated in the text. Nuclear extracts were prepared from FRTL-5 cells according to the previously described method (233). The Pax8 probe is the previously reported oligoC π (5'-TCAGTCACGCGTGA CTGGGCAGTG-3')(108). The Sp1 probe (5'-ATTCGATCGGGGCGGGGCGAG-3') used to check nuclear extract quality was previously reported (225). The chemically synthesized oligonucleotides were labeled with ³²P using polynucleotide kinase and annealed to the antisense complementary sequences. The end-labeled double-strand oligonucleotide probes (80,000 cpm) were mixed with FRTL-5 cell extract (4 µg) in 20 µl of reaction

buffer [reaction buffer: 20mM Tris (pH 7.5), 75mM KCl, 5mM MgCl₂, 1mM dithiothreitol, 1 mM EDTA, 3µg/20µL poly(deoxyinosine-deoxycytosine), 1mg/ml BSA, 10% glycerol] and incubated at room temperature for 30 min before loading on the 5% polyacrylamide gel in 0.5x TBE buffer at 200 V. After electrophoresis in a cold room, gels were dried and processed for autoradiography on Kodak (Rochester, NY) OMAX films for 24 h.

16.EMBL Compounds library

The Chemical Biology Core Facility screening library used was composed of 50,000 compounds arrayed in 96well or 384well plates format. The selected compounds of the EMBL library were checked for drug-likeness, structural and shape diversity, novelty and compliance with medicinal chemistry requirements. At the time at which the screening was performed all the compounds of the EMBL library were bought from TRIPOS inc. Compounds were stored in DMSO at 10mM concentration. All compounds used for the library screening were diluted at 1mM concentration with water (final DMSO 20%) and arrayed in barcoded 96well plates.

17.GFP assay for High-throughput screening (HTS-GFP assay)

17.1.Cell culturing

NG6 cells (C111-derived cell line stably expressing NUC-GFP) were amplified in complete 6H medium to confluency. On day 0 cells were split 1:4 in 100mm dishes. On day1 Tamoxifen treatment was started and kept up to the end of procedure.

17.2.Cell plating on 96well assay plates

On day6 cells were harvested, counted and diluted in Tamoxifen containing medium in order to obtain a 20000cells/100µL cell concentration. Cells were then plated on CulturePlate 96 F (Black, 96well,TC, sterile, with lids) from PerkinElmer. Manual plating, for test experiments, was performed with ePET multichannel pipettator (8 channel / 50-1200uL) from BioHit. In the automated setup,

plating was performed through FlexDrop automated dispenser equipped with stacker (PerkinElmer) on barcoded plates.

17.3. Compounds addition

On Day 7 compounds were added to the assay plates and cells were then cultured for additional 48 hours.

Compound vehicle was DMSO for all the tested compounds and final DMSO concentration (0.5%) was kept the same for all compounds tested within an experiment. Cells DMSO tolerance was verified prior to the start of the experiment.

Assay Plate layout was kept the same for all the experiment performed: on the whole column 1 DMSO vehicle was added to each well (negative control) while on the whole column 12 the known MAPK inhibitor U-0126 was added to each well (positive control). Compounds were added respectively in the wells from column 2-11 (Fig.9).

	1	2	3	4	5	6	7	8	9	10	11	12
A	DMSO											UO
B	DMSO											UO
C	DMSO											UO
D	DMSO											UO
E	DMSO											UO
F	DMSO											UO
G	DMSO											UO
H	DMSO											UO

Figure 9. HTS 96well Assay plate layout

Layout of 96well plate was kept the same for each experiment performed. DMSO was added to column 1 wells as negative control at a final concentration depending on the amount of compounds used as described in the text (between 0.5-1%). The MAPK inhibitor U-0126 was added to column 12 wells to a final 10 μ M concentration as positive control. Compounds under testing were added respectively in the central wells.

For Pilot screen (PS) 1 μ L of DMSO 20%, 1 μ L of 1mM U-0126/DMSO 20% or 1 μ L of each of the 1mM compounds/DMSO 20% solutions arrayed in the PS compounds library were added respectively to each well (following the layout indicated in Fig.9) through an automated robotic setup (EP3 Robot from PerkinElmer) available at the Chemical core facility of EMBL-Heidelberg.

For Lead screen (LS) 2.5 μ L of DMSO 20%, 2.5 μ L of 400 μ M U-0126/DMSO 20% or 2.5 μ L of each of the 1mM compounds/DMSO 20% solutions arrayed in the LS compounds library were added

respectively to each well (following the layout indicated in Fig.9) through an automated robotic setup (EP3 Robot from PerkinElmer) available at the Chemical core facility of EMBL-Heidelberg.

Dose-response curves were performed by creating a source plate containing, on each row, a two-fold factor serial dilution of each compound under testing. Starting solution in well 2 was 550 μ M compound/ DMSO 5.5% and was serially diluted up to well 11 with cell culture medium/DMSO 5.5%. On column1 of the source plate was dispensed the cell culture medium/DMSO 5.5% while on column2 cell culture medium/110 μ M U-0126/DMSO 5.5% was dispensed. Once the source plate was created, 10 μ L from each source-plate well were transferred in triplicate assay plates through the automated robotic setup or, where indicated for test experiments, manually with ePET multichannel pipettator (8 channel / 5-100 μ L) from BioHit. Final layout on Dose-response assay plates is described in Fig.10.

	1	2	3	4	5	6	7	8	9	10	11	12
compound A	DMSO	50 μ M	25 μ M	12.5 μ M	6.2 μ M	3.1 μ M	1.6 μ M	0.8 μ M	0.4 μ M	0.2 μ M	0.1 μ M	UO
compound B	DMSO	50 μ M	25 μ M	12.5 μ M	6.2 μ M	3.1 μ M	1.6 μ M	0.8 μ M	0.4 μ M	0.2 μ M	0.1 μ M	UO
compound C	DMSO	50 μ M	25 μ M	12.5 μ M	6.2 μ M	3.1 μ M	1.6 μ M	0.8 μ M	0.4 μ M	0.2 μ M	0.1 μ M	UO
compound D	DMSO	50 μ M	25 μ M	12.5 μ M	6.2 μ M	3.1 μ M	1.6 μ M	0.8 μ M	0.4 μ M	0.2 μ M	0.1 μ M	UO
compound E	DMSO	50 μ M	25 μ M	12.5 μ M	6.2 μ M	3.1 μ M	1.6 μ M	0.8 μ M	0.4 μ M	0.2 μ M	0.1 μ M	UO
compound F	DMSO	50 μ M	25 μ M	12.5 μ M	6.2 μ M	3.1 μ M	1.6 μ M	0.8 μ M	0.4 μ M	0.2 μ M	0.1 μ M	UO
compound G	DMSO	50 μ M	25 μ M	12.5 μ M	6.2 μ M	3.1 μ M	1.6 μ M	0.8 μ M	0.4 μ M	0.2 μ M	0.1 μ M	UO
compound H	DMSO	50 μ M	25 μ M	12.5 μ M	6.2 μ M	3.1 μ M	1.6 μ M	0.8 μ M	0.4 μ M	0.2 μ M	0.1 μ M	UO

Figure 10. Dose-response 96well Assay plate final layout

From the Dose-response source plate described in the text 10 μ L of each well solution were serially transferred to the assay plate generating the following compounds final concentrations. 10 μ L of 5.5% DMSO solution (0.5% DMSO final concentration) and 10 μ L of 5.5% DMSO/110 μ M U-0126 (0.5% DMSO/10 μ M U-0126 final concentration) culture medium were added respectively to column1 and column12.

17.4. Plate washing

At the end of the 48hours culturing in the presence of the compounds, , on day 9, assay plates were extensively washed with PBS (supplemented with calcium and magnesium) in order to completely remove from the wells the culture medium that give high-background on green fluorescence read-out. As control of culture medium fluorescence background a 96well culture plate containing only 100 μ L medium/well, and no cells, was washed along with the assay plates.

Automated washing was performed with PlateWasher instrument, supplied with stacker, from perkinElmer. The protocol necessary to abolish background without provoking cell detachment was determined as the following:

PlateWasher Protocol
Pressure
Dispensing Default Pressure = 1.6 psi
Vacuum
Minimum vacuum required = 3.4
Plates coordinates
Clearance: 17.0 mm
Height= Low: 7.5 mm / High: 12.5mm
X0 = 4.3
Y0 = 4.4
Program
1.6 psi pressure
SEG1: Aspiration/ height LOW / 3 sec
SEG2: Dispense/ height HIGH / 150uL
SEG3: loop 6 time from 1
SEG4: Aspiration/ height LOW / 3 sec

Manual washing, where indicated for test experiments, was performed with ePET multichannel pipettator (8 channel / 50-1200uL). As initial step, culture medium was removed by inverting assay plate on absorbent paper and tapping plate on it repeatedly to remove medium completely. Subsequently, wells were washed by adding 200uL/well of PBS and removing it by inversion as described above. Washing step was repeated twice. PBS (100uL/well), which does not affect background, was then added to wells only to allow waiting before read-out.

17.5. GFP fluorescence read-out

Washed plates fluorescence was read-out on an EnVision plate reader supplied with stacker (PerkinElmer). EnVision parameters for eGFP fluorescence reading in living cells cultured in black 96well culture plate (perkinElmer) were evaluated on the basis of settings giving the higher ratio between positive control plate (containing GFP expressing cells) and background plate (empty wells as described in paragraph 17.4). EnVision definitive parameters were established as the following:

EnVision GFP read-out protocol	
Labels:	
Mirror.....	FITC
Exc. filter.....	FITC 485
Using of excitation filter.....	Top
Ems. filter.....	FITC 535
Measurement height.....	2.4 mm
Number of flashes.....	10
Number of flashes integrated.....	1
PMT gain.....	167
Limits of excitation light.....	79%
Range of excitation light.....	100%
scan number	4 x4
scanning measures	0.8 mm

For each well, as indicated in the protocol, fluorescence measurement was performed 16 times in different positions inside the well (scan 4x4). Fluorescence read-out, for each well, was considered as the average value among the 16 measurements obtained by scanning of the well. EnVision plate reader was set in order to produce directly averaged fluorescence values.

17.6. Results analysis (fold activation and determination of hits frequency)

For each row of each plate fluorescence values were converted into fold activation values by normalizing each compound-treated well fluorescence value on the DMSO-treated one lying on the same row. The Reason of such conversion is due, for the GFP-assay, mainly to issues relative to the adopted technical procedure of plating cells through FlexDrop automated dispenser 1) each plate can contain a different number of cells 2) cells on different rows are plated through different pins of the FlexDrop instrument thus even on the same plate different rows can contain different number of cells.

All statistical analysis were performed on fold activation values.

18. Luciferase assay for High-throughput screening (HTS-Luc assay)

18.1. Cell culturing

Cl11 cells were amplified in complete 6H medium to confluency. On day 0 cells were splitted 1:8 in 100mm dishes. On day1 Tamoxifen treatment was started and kept up to the end of procedure.

18.2. Cell plating

On day6 cells were harvested, counted and diluted in Tamoxifen containing medium in order to obtain a 30000cells/90 μ L cell concentration. Cell suspension (90 μ L/well) was then plated on CulturePlate-96 (White opaque, 96well,TC, sterile, with lids) from PerkinElmer. Manual and automated plating was performed as described in the GFP assay.

18.3. Transfection

Transfection was performed on day7 using as transfection reagent PEI (Polyethylenimine,linear, MW~250000 from Polysciences inc.). PEI was dissolved at 1mg/mL in tissue culture grade water and pH adjusted to 7.0 with 1N HCl. Transfection conditions for 96well plates were optimized by testing different amount of DNA/well and, for each DNA amount, different ratios between PEI (μ g) and DNA (ng) amount. Optimized conditions (highest transfection efficiency) were set on 100ngDNA/well and a 4:1 ratio PEI (μ g)/ DNA (ng).

Definitive transfection mix for each 96well plate was prepared as follow: 10 μ g of plasmid DNA (pNUE-luc) were added to 1mL of 0.15M NaCl and mixed for 5 seconds. PEI (40 μ L) was then added and mixed 10 seconds. Transfection mix was incubated 10 min at Room Temperature and then added to assay plates (10 μ L /well) through the EP3 robotic automated procedure or, where indicated for test experiments, with ePET multichannel pipettator (8 channel / 5-100uL). Transfected cells were rested for about 3h in the cells incubator.

18.4. Compound addition

After this short 3h incubation of transfected cells, compounds were added to the assay plates and cells cultured for additional 48 hours. Compounds addition procedure and assay plate layout was exactly the same described for the GFP assay.

18.5. Luciferase luminescence read-out

Luciferase read-out was performed on day9. BriteLight (PerkinElemer) solution (100µL/well) was added to assay plates through FlexDrop automated dispenser. Each plate was then read at the EnVision plate reader 10 minutes after Britelight solution dispensation.

EnVision readout was performed with default parameters for enhanced luminescence detection. but measurement time was set to 0.5sec per well and an additional 1 minute of orbital shaking was added prior to read-out.

18.6. Results analysis

Luminescence read-out results were converted into Fold Activation values as described for the GFP-assay. All statistical analysis were performed as described for the GFP-assay on Fold Activation values.

19. ERK phosphorylation assay

C111 cells were cultured 5 days in the presence of Tamoxifen and then 20000 cells/well of Tamoxifen treated C111 cells were plated on 96well plates on day 1. On day 2, the MAPK inhibitor U-0126, the unknown selected compounds, or the DMSO vehicle were respectively added to the cells, each at the final concentration indicated in the Results section text, and cells were cultured additional 24 hours. The activity of each compound was tested on triplicate wells. The entire experiment was performed on twin 96well plates.

Inhibitory activity of compounds on ERK phosphorylation was assayed through the FACE™ ERK1/2-in cell Western analysis for phospho ERK1/2- kit (active motif) following manufacturer's instruction. Briefly, at the end of the treatments cells were fixed in a 4% formaldeyde PBS solution. After inactivation of endogenous peroxidases, washing and blocking, cells were incubated 3 hours at 25°C with primary antibodies (phospho-ERK antibody on one 96-well plate and Total ERK antibody on the tween 96-well plate), washed and subsequently incubated with HRP-conjugate secondary antibody. Developing solution was then added to washed cells and developing reaction was allowed for 10 minutes. Colorimetric read-out was performed by reading absorbance at 450nm in EnVision plate

reader (perkin Elmer). Background absorbance was determined by incubating cells with the secondary antibody in the absence of any primary antibody. Each absorbance value was subtracted of the average background absorbance obtained in the plate. Each phospho-ERK absorbance value was normalized on the corresponding total-ERK signal in the twin plate. Triplicates results expressed as a ratio of phosphoERK/Total ERK signal were then averaged.

RESULTS

1. ER-Ras^{V12} activation induces a rapid downregulation of thyroid-specific gene expression

I analyzed, by Real-Time-PCR, the kinetics of Ras-induced down-regulation of thyroid-specific gene expression in a rat thyroid cell line, called C111, expressing an inducible H-Ras^{V12} oncoprotein (ER-Ras^{V12}) (4). Shortly after ER-Ras^{V12} activation by tamoxifen (4OHT) there is a simultaneous decrease of the mRNAs encoding several thyroid differentiation markers, except for the Tg and Nkx2-1/Titf1 mRNAs that show, at least in the time window used, a small or no decrease, respectively (C111 in Fig. 1). The simultaneous down-regulation of several differentiation markers suggests that Ras oncogene might interfere with a regulatory target common to many thyroid-enriched genes. No inhibition of gene expression was detected when wild type cells (FRTL-5 in Fig.1) were treated with tamoxifen, thus demonstrating the role of oncogenic Ras in the observed loss of differentiation..

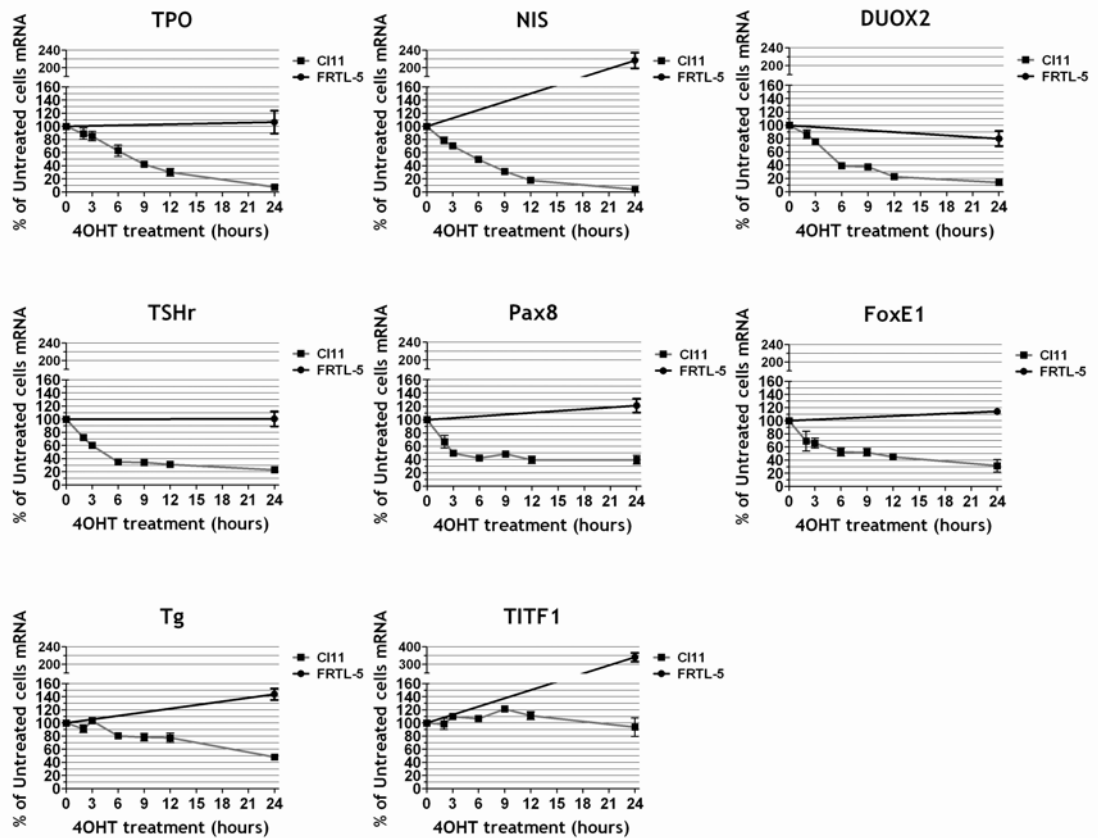


Figure 1. Kinetic of Ras oncogene induced dedifferentiation of FRTL5 cells.

CI11 cells were treated with Tamoxifen (4OHT) for increasing times as indicated. For each time point mRNA was extracted from triplicate plates of CI11 or FRTL-5 cell lines and analyzed by Real-Time RT-PCR for each of the genes indicated.

2. NIS downregulation is achieved through an ER-RAS^{V12} mediated impairment of NUE (NIS Upstream enhancer) transcriptional activity

In order to approach the mechanisms responsible for the oncogenic Ras induced down-regulation of thyroid-specific gene expression, we focused our attention on the gene encoding the sodium-iodide symporter (NIS), whose regulatory elements have been extensively studied. First, to test whether the decrease in NIS mRNA levels resulted from decreased transcription we measured, by chromatin immunoprecipitation, RNA polymerase II occupancy of the NIS gene coding sequence in C111 cells after activation of Ras oncoprotein. This assay shows that the amount of RNA polymerase II bound to NIS gene is already reduced 6 hours after Ras oncogene activation and almost completely abolished at 24 hours. These results are consistent with the observed mRNA decrease and indicate that Ras activation rapidly inhibits NIS gene transcription (Fig. 2).

The NIS gene regulatory elements affected by Ras oncoprotein were investigated using previously described chimeric constructs (64) in which either the entire upstream region of the rNIS gene or deletion derivatives are fused to the LUC reporter gene (Fig. 3). Each construct was transiently transfected into C111 either in the presence or absence of Tamoxifen (4OHT). The 2.9-kb DNA fragment from the rNIS regulatory region (pNIS-Luc1) is significantly down regulated by Ras activation. The same extent of inhibition is also seen with the pNIS-Luc9 construct in which the sequence located between positions -2495 and -2264, corresponding to the NIS Upstream Enhancer (NUE) (64) is fused to the proximal NIS promoter (between positions -564 and +1). In contrast, no Ras induced inhibition is observed on the activity of the proximal NIS promoter (pNIS-Luc5). I conclude that Ras oncoprotein reduces NIS expression mainly through inhibition of NUE activity.

To further assess the ability of oncogenic Ras to inhibit NUE activity independently from other surrounding NIS gene sequences we cloned the NUE sequence upstream of the E1B TATA box in pGL3-basic and tested its transcriptional activity in C111 either in the presence or absence of 4OHT (Fig. 4). Again, a severe impairment of transcriptional activity is observed following Ras activation. No impairment of NUE transcriptional activity was detected if wild type cells were used (FRTL-5 in Fig.4)

Taken together, these data demonstrate that Ras oncogenic activity inhibits NIS gene expression at the transcriptional level and that such inhibition is mediated, at least in part, by interference with the stimulatory activity of the NUE regulatory element.

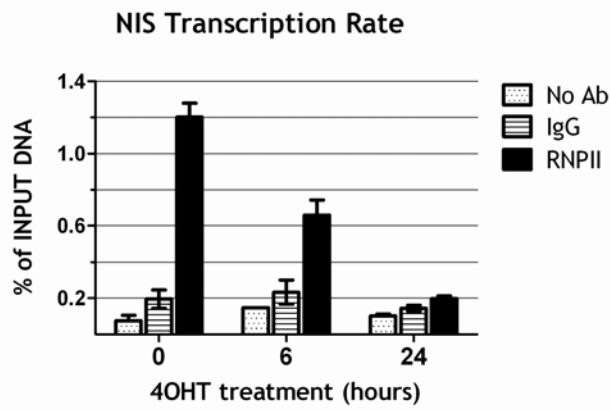


Figure 2. Oncogenic Ras downregulates NIS transcription

C111 cells were treated with Tamoxifen for the indicated times (0, 6h, 24h). For each time point NIS transcription was measured by performing a Chromatin -IP with RNA polymerase II Antibody (RNPII) as described in materials and methods. For each time point a Chromatin IP was performed also, as negative controls, with non -specific Rabbit IgG (IgG) or in the absence of any Antibody (no Ab). Immunoprecipitated DNA was measured by Real-Time PCR and is reported as percentage of Input DNA for each time point.

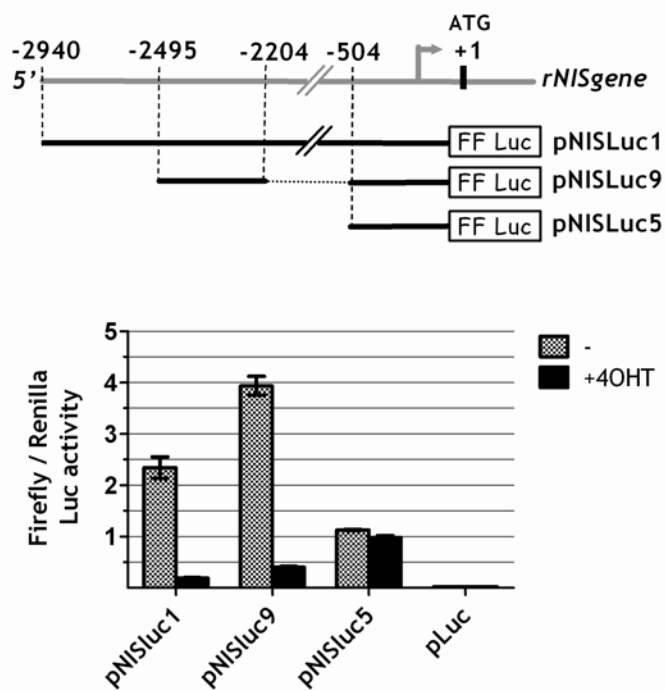


Figure 3. Oncogenic Ras inactivates NUE (NIS Upstream Enhancer).

Transient transfection assays of luciferase reporter constructs containing NIS regulatory regions in C111 cells treated or not 48h with Tamoxifen (4OHT). pLuc is the empty vector.

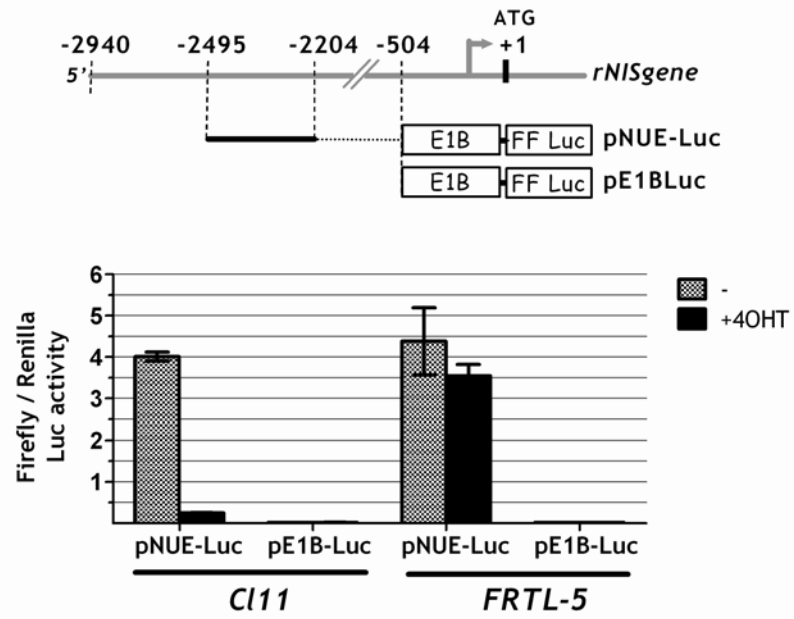


Figure 4. Oncogenic Ras inactivates NUE (NIS Upstream Enhancer) independently from the surrounding regulatory regions .

Transient transfection assays of luciferase reporter constructs containing NUE enhancer upstream of the E1B TATA box in CI11 cells and FRTL-5 cells treated or not 48h with Tamoxifen (4OHT).

3.Activation of Ras reduces both the amount and the activity of Pax8

The NIS enhancer NUE contains at least three functionally relevant protein binding sites: a central CRE-like element called NUC surrounded by two Pax8 binding sites ((64), Fig. 5). The two Pax8 binding sites have been shown to be necessary for NUE activity (225). In C111 cells Ras activation induces an early and significant down regulation of Pax8 protein levels (Fig. 6).

In order to analyze the role of Pax8 down regulation in Ras oncoprotein induced de-differentiation we stably transfected into C111 cells a Pax8 expression vector that encodes a flagged Pax-8 protein (Flag-Pax8) under the control of a Ras independent promoter (Fig. 7). I selected 3 stable clones (Px31, Px33 and Px37 in Fig. 8) in which the Pax8 protein levels are unaffected by Ras activation, since the transfected, flagged protein maintains its expression while the endogenous protein is down-regulated (Fig. 7, 8). However, irrespective of Pax8 protein levels, expression of the endogenous NIS gene was still down regulated by Ras activation as in the parental cell line (Fig. 8). Consistently, also the activity of a transfected NUE enhancer was down regulated by oncogenic Ras, both in the presence or in the absence of the Pax8 protein (compare results in C111 with those obtained in cell lines Px31, Px33 and Px37, Fig. 9). These results suggest that the Ras oncoprotein interferes with transcriptional activity of Pax8, besides the observed negative effect on Pax8 protein levels.

To further test this hypothesis, we used a reporter construct driving the expression of Luciferase under the control of an artificial promoter made by a pentamer of Pax8 binding sites (Cp5, (4)) located upstream of the E1B TATA box (Fig. 10). Cp5 is stimulated by both wild type and flagged-Pax8 in non-thyroid cells, demonstrating that the addition of the flag does not have any adverse effect on Pax8 transcriptional activity (Fig. 11). However, data in Fig. 12 show that Cp5 activity is equally down regulated by the activated Ras both in the absence (C111) and in the presence of Pax8 (Px31, Px33, Px37).

Furthermore, given that there is no interference by the activation of Ras on the DNA binding activity of Pax8 (Fig. 13), we conclude that the inhibition of NIS expression by oncogenic Ras is

mediated by an interference with Pax8 transcriptional activity. Such an inhibition presumably precedes the observed decrease in Pax8 protein levels.

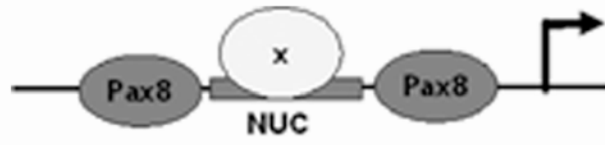


Figure 5. Schematic representation of NIS enhancer NUC .

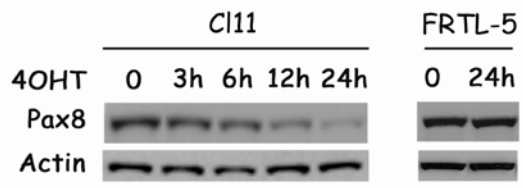


Figure 6. Kinetic of Ras oncogene induced Pax8 protein downregulation.

Western blot analysis of Pax8 protein levels in CI11 and FRTL-5 cells treated with Tamoxifen (4OHT) for the reported increasing time. Levels of Actin are used to normalize for protein loading.

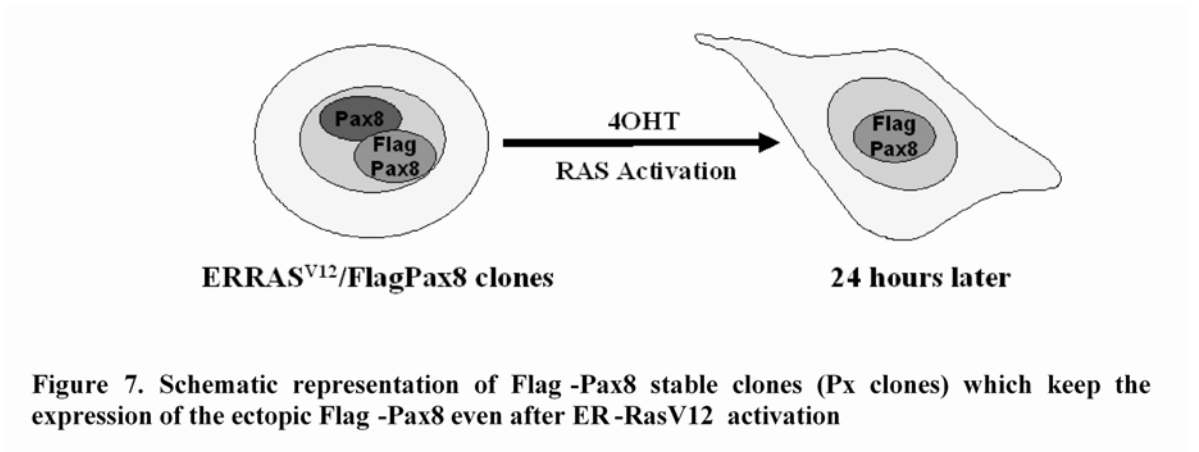


Figure 7. Schematic representation of Flag -Pax8 stable clones (Px clones) which keep the expression of the ectopic Flag -Pax8 even after ER -RasV12 activation

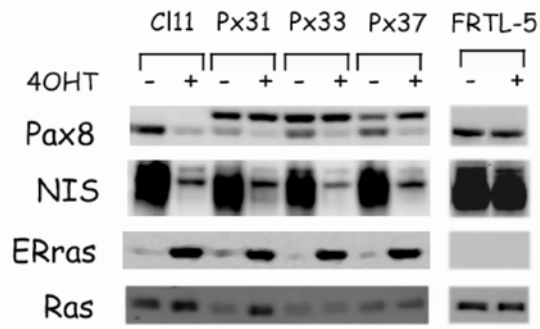


Figure 8. Ras oncogene downregulates NIS expression even if Pax8 protein is expressed to wild-type levels.

C111, three representative Flag-Pax8 clones (Px31, Px33 and Px37) and FRTL5 cells were treated 24 hours with or without Tamoxifen and analyzed by Western Blot for several genes as indicated. In Px clones the ectopic Flag-Pax8 is identified by the band migrating above the endogenous Pax8 protein visible in C111.

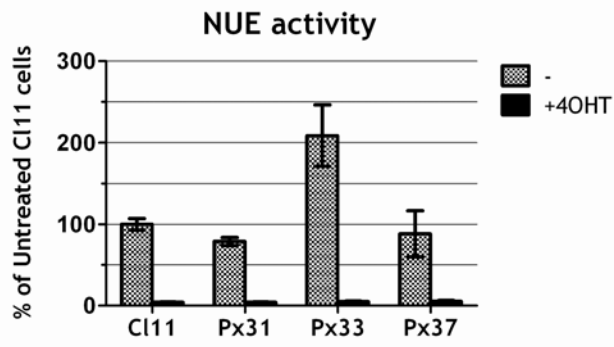


Figure 9. Ras oncogene downregulates NUE activity even if Pax8 protein is expressed to wild-type levels.

Transient transfection assay of NUE reporter activity in C111 cells and in Px clones (Px31, 33 and 37) with or without Tamoxifen (4OHT). NUE activity (normalized for transfection efficiency) is expressed as percent of activity obtained in untreated C111 cells.

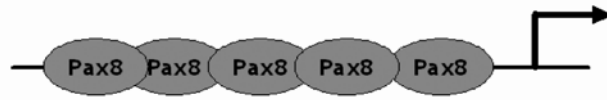


Figure 10. Schematic representation of Cp5 artificial promoter Oncogenic

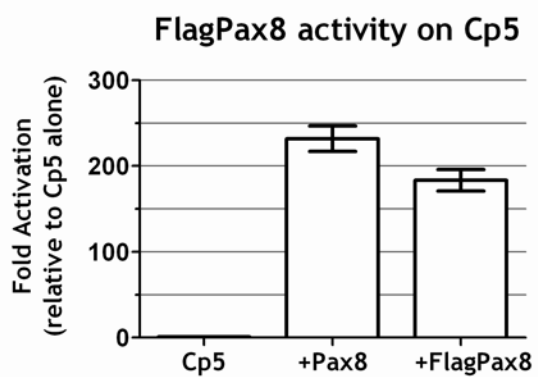


Figure 11. Functional test of Flag-Pax8 protein

Transient transfection assay of Cp5 reporter activity in HeLa cells cotransfected respectively with an empty vector (Cp5), with 100ng of Pax8 (+Pax8) or with 100ng of the flagged Pax8 (+FlagPax8)

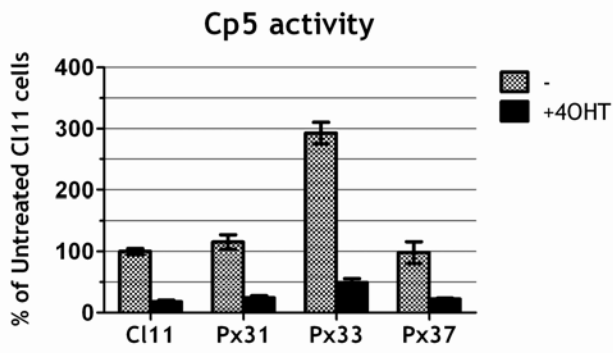


Figure 12. Oncogenic Ras impairs Pax8 transcriptional activity.

Transient transfection assay of Cp5 reporter activity in C111 and Flag Pax8 expressing clones (Px31, Px33 and Px37) performed in the absence or presence of Tamoxifen (4OHT). Cp5 reporter activity (normalized for transfection efficiency), is expressed as percentage of activity obtained in untreated C111 cells.

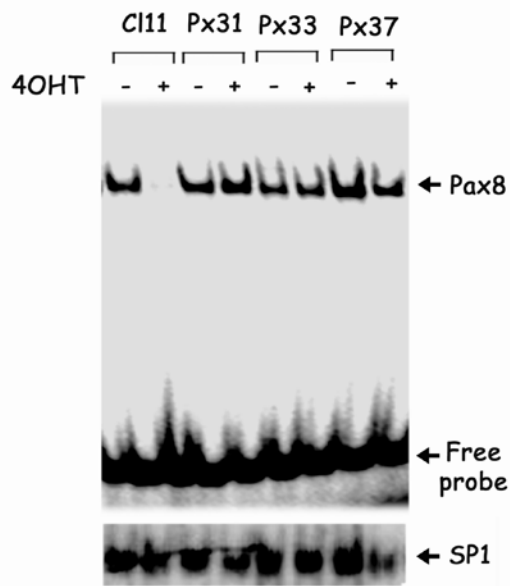


Figure 13. Oncogenic Ras does not affect Pax8 DNA binding activity.
 Bandshift analysis of nuclear Pax8 DNA - binding activity in Cl11 and Flag Pax8 expressing clones (Px31,Px33 and Px37). In the lower panel is reported binding of nuclear extract to the unrelated SP1 binding sequence.

4.Role of the TSHr/cAMP pathway in ER-RAS^{V12} induced dedifferentiation

Pax8 transcriptional activity has been suggested to be dependent upon TSH stimulation of the cAMP pathway (86, 234). TSHr mRNA is rapidly reduced after Ras activation (Fig. 1). Such a decrease is immediately reflected in a reduction in TSHr protein level (Fig. 14A) and in a functional impairment of the cAMP pathway, as demonstrated by a significant decrease in the levels of phosphorylated CREB protein (Fig. 14B). Again, none of these effects could be observed in FRTL-5 cells treated with tamoxifen, thus demonstrating that they are truly a consequence of Ras activation (Fig. 14A and B, FRTL-5). In addition, TSH has been previously established to be necessary for maintaining thyroid differentiation (235, 236) and in particular for NIS expression (99, 237). I thus hypothesized that inhibition of the TSHr/cAMP pathway could be a crucial event in Ras oncoprotein induced NIS down regulation .

4.1.TSHr downregulation is not the master event in oncogenic Ras induced de-differentiation

In order to test if oncogenic Ras was down regulating NIS through inhibition of TSHr expression we used an approach similar to the one illustrated above for Pax8. Thus, I stably transfected into C111 an expression vector encoding the human TSHr (227) under the control of a Ras independent promoter (Fig. 15). In the stable hTSHr expressing clones (T4 and T17 in Fig. 16), expression of the ectopic TSHr is maintained after Ras activation. However, irregardless of TSHr protein levels, the expression of the endogenous NIS gene was still down regulated by Ras activation as in the parental cell line (Fig. 16). I conclude that TSHr expression down regulation is not the crucial event in oncogenic Ras induced de-differentiation of FRTL5 cells.

4.2. The reduction of cAMP intracellular levels induced by oncogenic Ras is not the cause of the dedifferentiated phenotype

Measurements of intracellular cAMP demonstrates that while in the parental cell line Ras activation decreases cAMP levels, in clones T4 and T17 such a decrease is not observed. This evidence is in support of the persistent expression of a functional TSHr in clones T4 and T17 (Fig. 17). In keeping with these observations, addition of the cAMP analogue 8-CPT to C111 was ineffective in contrasting the inhibitory effect of activated Ras on the endogenous NIS expression (Fig. 18). As well as for endogenous NIS expression, reagents capable of increasing cAMP levels, such as Forskolin, 8-CPT and the phosphodiesterase inhibitor IBX, were ineffective in contrasting the inhibitory effect of activated Ras on NIS transcriptional activity (Fig. 19). I conclude that Ras oncoprotein induced NIS down regulation is not due either to the decreased levels of TSH receptor or to a reduced production of cAMP, since restoring either of them does not prevent the negative effect exerted by activated Ras.

4.3. Oncogenic Ras inhibits the TSHr/cAMP pathway by acting also downstream of cAMP production

Even though in T4 and T17 clones TSHr expression and cAMP levels are maintained (fig. 16 and 17), CREB phosphorylation in these clones is still impaired by Ras activation, as in the parental cell line C111 (Fig. 20). This observation suggests that oncogenic Ras acts downstream of TSHr. Given also that either Forskolin/IBX and 8-CPT could not rescue CREB phosphorylation in the presence of activated Ras (Fig. 21), I conclude that Ras oncogene also inactivates the cAMP pathway through a mechanism downstream of those regulating intracellular cAMP levels. Interestingly, using cells stably transfected with a constitutively active Ras oncoprotein, I demonstrate that the observed down regulation of phosphorylated CREB is a persistent effect of oncogenic Ras (Fig. 22).

4.4. Oncogenic Ras Inhibits PKA activity

Ras oncoprotein in our cells inhibits CREB phosphorylation at Ser133. However, many signaling pathways and several different kinases converge on CREB Ser133 (89). Given the specific stimulation

of PKA, via cAMP, by forskolin, I tested whether oncogenic Ras interferes with forskolin induced CREB phosphorylation. To this end, I acutely stimulated C111 cells with Forskolin, in the absence or in the presence of oncogenic Ras and measured phosphorylated CREB by quantitative WB (QWB). The results of such an experiment show that Ras significantly reduces Forskolin induced CREB phosphorylation, (Fig. 23) even though cAMP levels are equally stimulated both in the presence or in the absence of the oncoprotein (Fig. 24), strongly suggesting that Ras interferes with PKA activity. In support of this conclusion, I show a reduced PKA activation by forskolin in the presence of oncogenic Ras (Fig.25). Such a reduction is not due to alterations in levels or subcellular localization of PKA regulatory and/or catalytic subunits (Fig. 26 and 27). I conclude that oncogenic Ras in thyroid cells interferes with PKA activity. The mechanism of such interference remains to be elucidated.

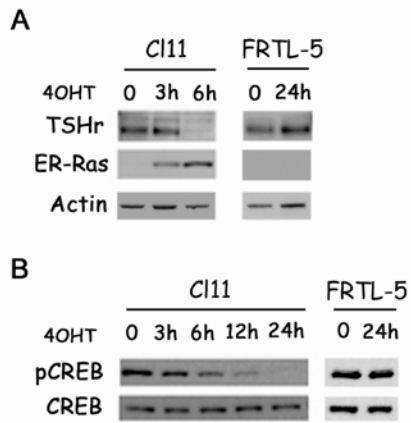


Figure 14. Oncogenic Ras early inhibits TSHr pathway.

A&B.C111 and FRTL5 cells were treated with Tamoxifen (4OHT) for the reported time and analysed by Western Blot. A. TSHr expression analysis; ERRAS shows accumulation of the inducible oncoprotein. Actin is used to normalize for protein loading B. total CREB and phosphoCREB Ser133 (pCREB) analysis.

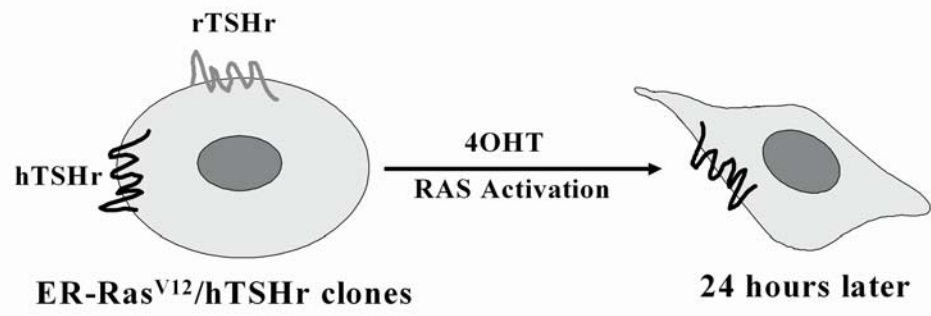


Figure 15. Schematic representation of SPRT-TSHr expressing clones which keep the expression of the ectopic TSHr (hTSHr) even after ER-Ras^{V12} activation

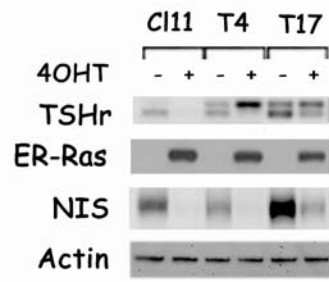


Figure 16. TSHr downregulation is not the crucial event in Ras oncogene induced dedifferentiation.

C111 and SPRT-TSHr expressing clones were treated 24 hours with or without Tamoxifen. Total proteins were analyzed by Western Blot for the reported genes. In T4 and T17 clones the ectopic hTSHr is identified by the band migrating above the endogenous rTSHr visible in the untreated C111.

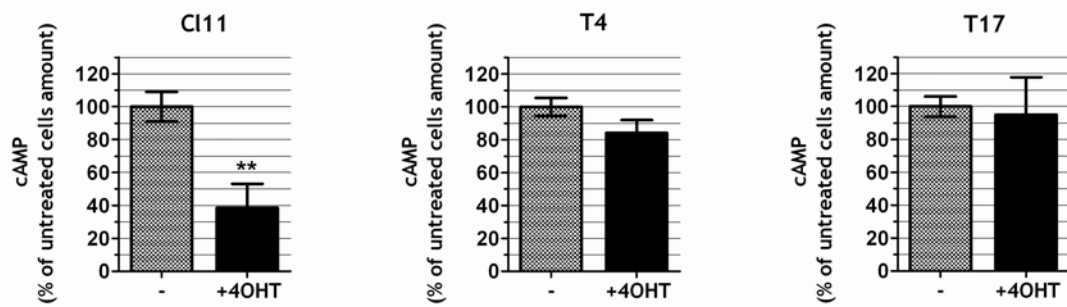


Figure 17. cAMP intracellular levels are unmodified by Ras activation in clones which keep the expression of the ectopic TSHr (hTSHr)

CI11 and SPRT-TSHr expressing clones were treated 24 hours with or without Tamoxifen. cAMP was quantitatively measured in each clone before and after the Tamoxifen treatment. **p< 0.01

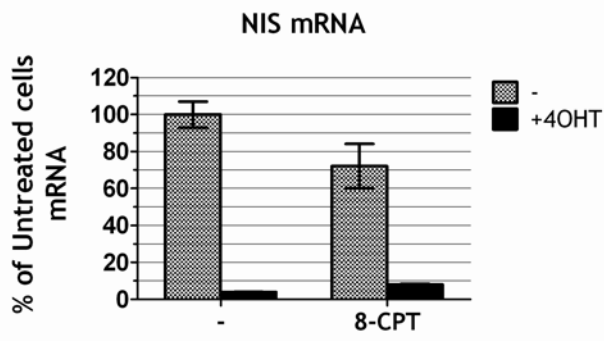


Figure 18. Intracellular cAMP can only weakly counteract oncogenic Ras action on NIS expression.

Real-time RT-PCR analysis of NIS expression in C111 cells treated 24 hours with or without Tamoxifen either in the presence or in the absence of 8-CPT. NIS gene expression is reported as percent age of levels observed in C111 untreated cells.

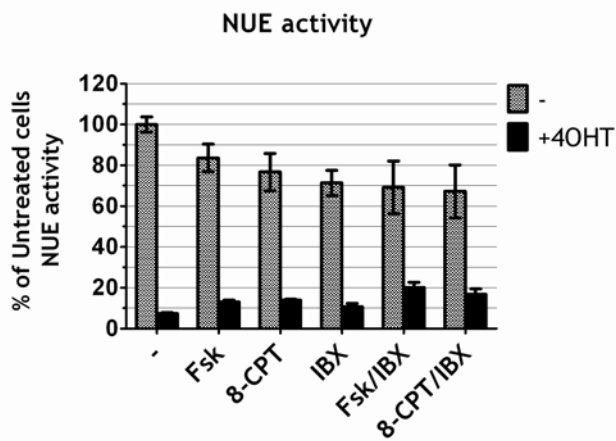


Figure 19. Intracellular cAMP can only weakly counteract oncogenic Ras action NUE activity.

Transient transfection assay of NUE reporter activity in C111 cells treated or not with Tamoxifen (4OHT) either in the absence or in the presence of FSK, 8-CPT, IBX or a combination of them for 48h as reported in the picture. NUE activity is expressed as percentage of the activity obtained in untreated cells.

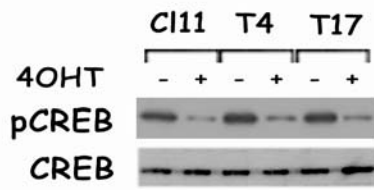


Figure 20. Ras oncogene impairs CREB phosphorylation in SPRT-TSHr expressing clones.

Western blot analysis of CREB phosphorylation at Ser133 in C111 and SPRT-TSHr expressing clones (T4 and T17) treated 24 hours with or without Tamoxifen .

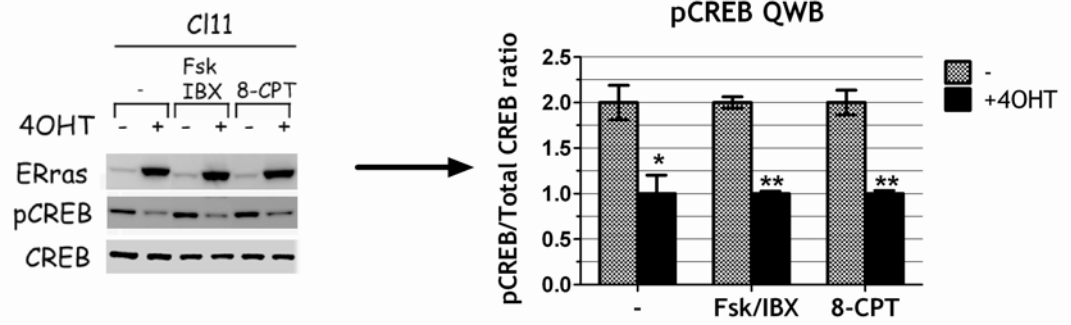


Figure 21. Ras oncogene impairs CREB phosphorylation independently from cAMP .
 Quantitative Western blot (QWB) analysis of CREB phosphorylation at Ser133 in C111 cells treated 24 hours with or without Tamoxifen either in the presence or absence of Fsk/IBX and 8-CPT. pCREB signal quantitation for three independent experiments is reported on the right side. **p<<0.01

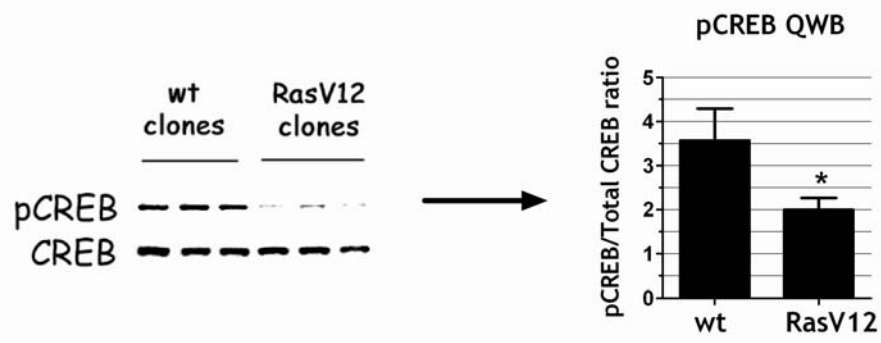


Figure 22. CREB phosphorylation is persistently impaired by oncogenic Ras .

Quantitative Western blot (QWB) analysis of CREB phosphorylation at Ser133 in three wildtype FRTL-5 stable clones expressing only the resistance gene (wt clones) and three FRTL-5 stable clones expressing oncogenic RasV12 (RasV12 clones). pCREB signal quantitation for three independent experiments is reported on the right side. * $p \leq 0.03$

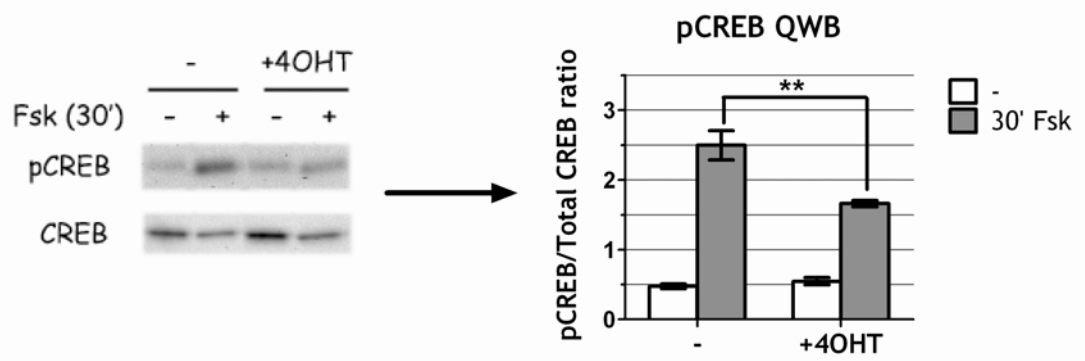


Figure 23. Ras oncogene impairs Forskolin induced acute CREB phosphorylation .

C111 cells were starved 48h in 4H medium (0.2%serum, no TSH, no Insulin), cultured additional 24h in 4H medium either with or without Tamoxifen and then stimulated with Forskol in (10 μ M) for 30'. Quantitative Western blot (QWB) analysis of CREB phosphorylation at Ser133 shows an impairment of CREB phosphorylation in the presence of ras oncogene. **p<0.01

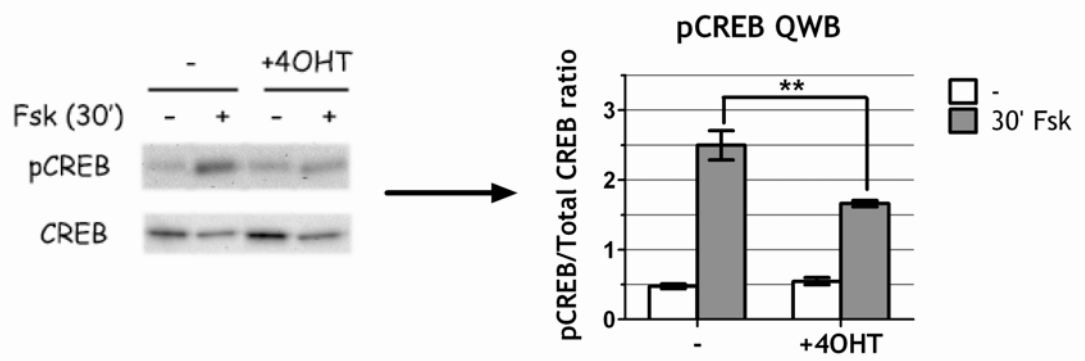


Figure 23. Ras oncogene impairs Forskolin induced acute CREB phosphorylation .
 C111 cells were starved 48h in 4H medium (0.2%serum, no TSH, no Insulin), cultured additional 24h in 4H medium either with or without Tamoxifen and then stimulated with Forskol in (10 μ M) for 30'. Quantitative Western blot (QWB) analysis of CREB phosphorylation at Ser133 shows an impairment of CREB phosphorylation in the presence of ras oncogene. **p<0.01

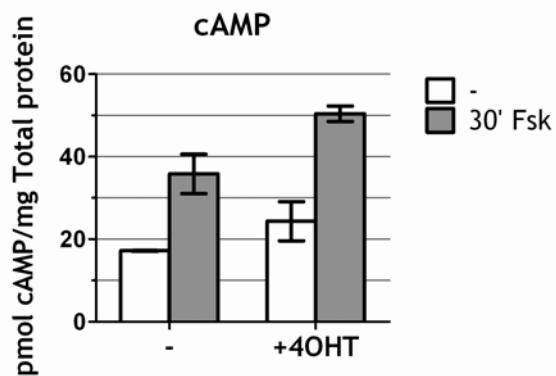


Figure 24. Ras oncogene does not impair Forskolin induced acute cAMP production.

C111 cells were starved 48h in 4H medium (0.2%serum, no TSH, no Insulin), cultured additional 24h in 4H medium either with or without Tamoxifen and then stimulated with Forskolin (10 μ M) for 30'. cAMP measurement shows equal production of cAMP in both condition.

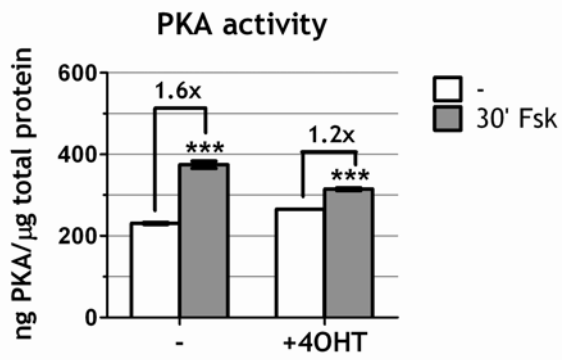


Figure 25. Ras oncogene impairs PKA activity.

CI11 cells were starved 48h in 4H medium (0.2%serum, no TSH, no Insulin), cultured additional 24h in 4H medium either with or without Tamoxifen and then stimulated with Forskolin (10μM) for 30'. PKA activity assay shows reduced PKA activity in Ras oncogene activated cells. ***p ≅0.002

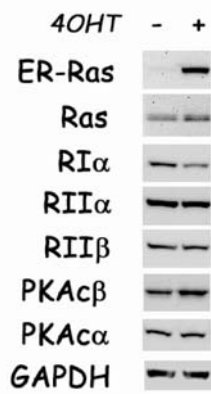


Figure 26. Ras oncogene does not impair PKA expression.

C111 cells were treated 24 hours with or without Tamoxifen in 6H medium. Catalytic (PKAc α , PKAc β) and regulatory (RI α , RII α , RII β) PKA subunit expression was analysed by Western Blot in total cellular extracts. ERRas was also measured to verify Ras oncogene activation by 4OHT.

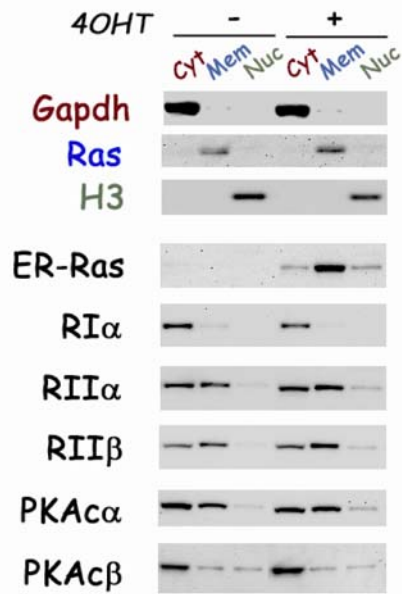


Figure 27. Ras oncogene does not impair PKA localization .

C111 cells were treated 24 hours with or without Tamoxifen in 6H medium. Catalytic (PKA α , PKA β) and regulatory (RI α , RII α , RII β) PKA subunit expression was analysed by Western Blot in fractionated cellular extracts. Cyt=Cytosolic protein fraction, Mem=Membrane/organelle protein fraction, Nuc=Nuclear protein fraction. GAPDH (cytosolic), endogenous Ras (membranes) and Histone H3 (nuclear) were used to monitor efficacy of the fractionating procedure.

5. Pax8 activity is impaired by Ras oncogene through inhibition of the cAMP/PKA pathway

Given that oncogenic Ras negatively interferes with PKA, we wondered whether such interference could explain the observed reduction in Pax8-dependent transcription.

5.1. Pax8 activity is regulated by PKA

First, to test if PKA regulates Pax8 activity, I measured the stimulation of the Cp5 reporter by Pax8 in the NIH 3T3 cell line either in the presence or absence of a PKA catalytic subunit alpha (cPKA) expression vector. I found indeed that Pax8 transcriptional activity is strongly enhanced (approx. 30 fold) by PKA over-expression, without a significant effect on the levels of Pax8 protein (Fig28).

5.2. PKA catalytic subunit over-expression restore Ras oncogene induced Pax8 inactivation and NUE activity

I next tested whether PKA could rescue the inhibition exerted by oncogenic Ras on Pax8-dependent NIS transcription. Even though I have shown that in our cells Ras does not impact on the amount of intracellular PKA (Fig. 26), I reasoned that PKA over expression might counteract Ras inhibition, whatever the nature of the inhibitory mechanism is. I therefore measured the effect of cPKA over-expression on Ras oncogene induced inhibition of Cp5 transcription. These experiments were carried out in both C111 and Px31 cells since these two cell lines express, after Ras activation, very little (C111) or normal levels (Px31) of the Pax8 protein (Fig.8). I observed that cPKA greatly stimulates Cp5 activity in the presence of activated Ras and such an effect is even more pronounced in Px31 cells, where the levels of Pax8 are close to normal (Fig. 29A and B). As predicted, the PKA specific inhibitor H89 completely blocks the observed stimulation of Cp5 transcription, thus demonstrating that the observed effect is PKA dependent (Fig. 29B). Finally, I could demonstrate that

also the activity of NUE is rescued by transfection of PKA, again with a better efficiency in Px31 (Fig. 30B) than in C111 (Fig. 30A) cells.

Taken together, these data strongly suggest that the negative interference exerted by oncogenic Ras on PKA causes a reduction of Pax8 transcriptional activity that, in turn, provokes a diminished transcription of NIS. It remains to be ascertained what mechanism Ras uses to reduce Pax8 protein levels. Recent data (A. Di Gennaro, M. De Felice and R.D.L., unpublished results) suggesting that transcription of the Pax8 is auto-regulated, might provide an unifying view of these events, and would highlight the block of PKA as the highest in the hierarchy of events leading to Ras-induced de-differentiation of thyroid cells in culture.

In support of this hypothesis I found that oncogenic Ras turns down very early Pax8 gene transcription (Fig. 31) and that this effect is associated with a decreased binding of Pax8 protein itself to its own gene promoter (Fig. 32).

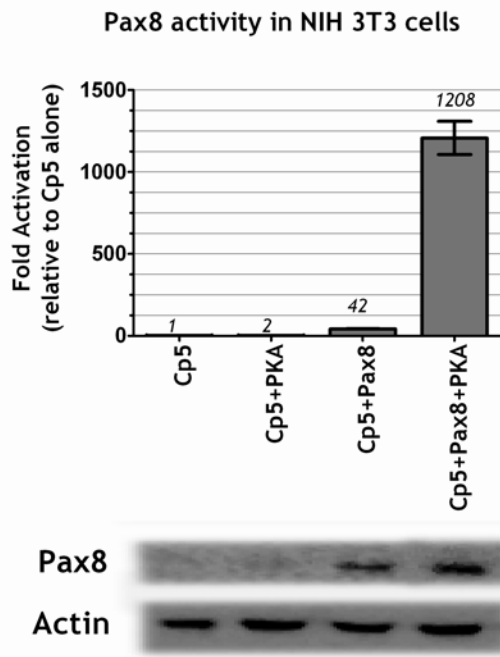


Figure 28. PKA regulates Pax8 activity.

Transient transfection assay of Cp5 reporter activity in NIH 3T3 cells cotransfected respectively with an empty vector (Cp5), with 1 μ g of cPKA (Cp5+PKA), with 250ng of Pax8 (Cp5+Pax8) or with 250ng of Pax8 and 1 μ g of cPKA (Cp5+Pax8+PKA). Western Blot analysis of Pax8 expression in the lysates is also shown.

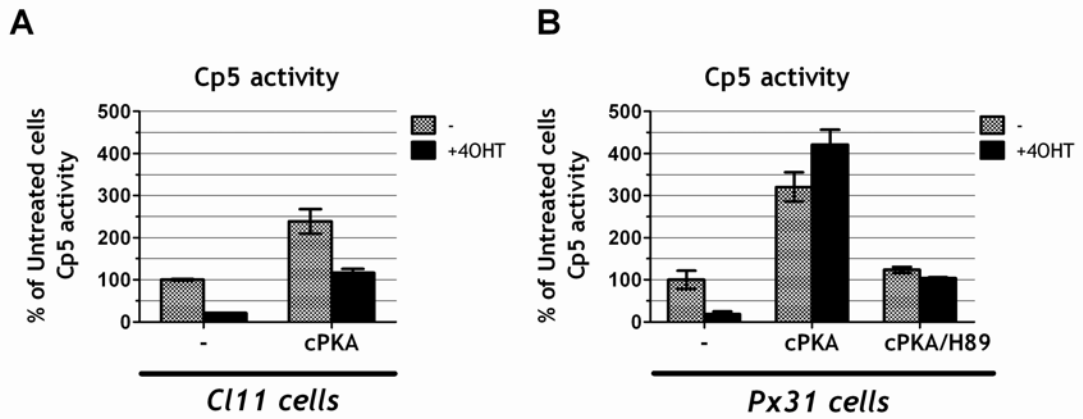


Figure 29. PKA activity restore oncogenic Ras mediated impairment of Pax8 activity .

Transient transfection assay of Cp5 reporter activity in CI11 (little Pax8 expression after 4OHT treatment) (A) or Px31 cells (Pax8 expressed as wildtype levels after 4OHT treatment) (B). Reporters activity was tested with or without Tamoxifen (4OHT) in the absence of further treatment (-) or with 1 μ g of cPKA cotransfecting vector (cPKA) as indicated. The activity of Cp5 is reported, as percentage of activity obtained respectively in untreated cells. A. Transient transfection assay of Cp5 reporter activity in CI11 cells. B. Transient transfection assay of Cp5 reporter activity in Px31 cells. cPKA effects were tested also in the presence (48h) of PKA inhibitor H -89 12 μ M (cPKA/H-89) as indicated

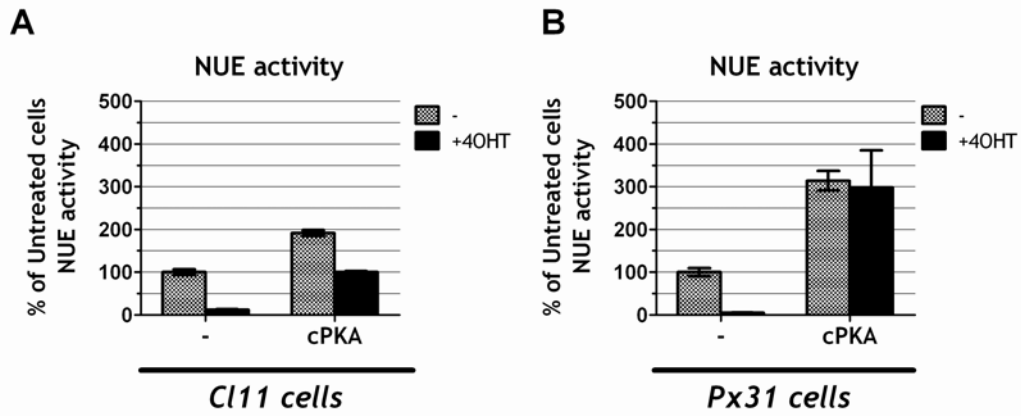


Figure 30. PKA activity restore oncogenic Ras mediated impairment of NUE.

Transient transfection assay of NUE reporter activity in C111 (little Pax8 expression after 4OHT treatment) (A) or Px31 cells (Pax8 expressed as wildtype levels after 4OHT treatment) (B). Reporters activity was tested with or without Tamoxifen (4OHT) in the absence of further treatment (-) or with 1 μ g of cPKA cotransfecting vector (cPKA) as indicated. The activity of NUE is reported, as percentage of activity obtained respectively in untreated cells. A. Transient transfection assay of NUE reporter activity in C111 cells. B. Transient transfection assay of NUE reporter activity in Px31 cells.

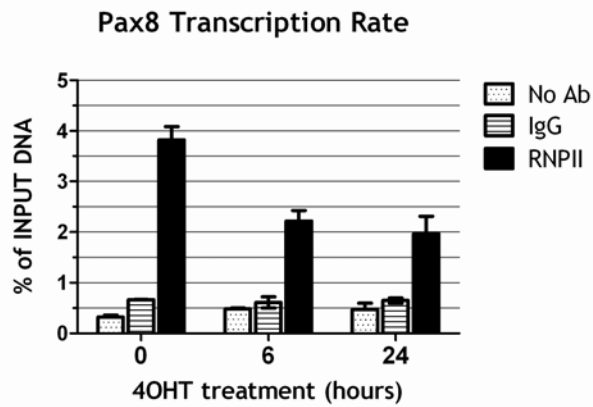


Figure 31. Oncogenic Ras downregulates Pax8 transcription

C111 cells were treated with Tamoxifen for the indicated times (0, 6h, 24h). For each time point Pax8 transcription was measured by performing a Chromatin -IP with RNA polymerase II Antibody (RNPII) as described in materials and methods. For each time point a Chromatin IP was performed also, as negative controls, with non-specific Rabbit IgG (IgG) or in the absence of any Antibody (no Ab). Immunoprecipitated DNA was measured by Real-Time PCR and is reported as percentage of Input DNA for each time point.

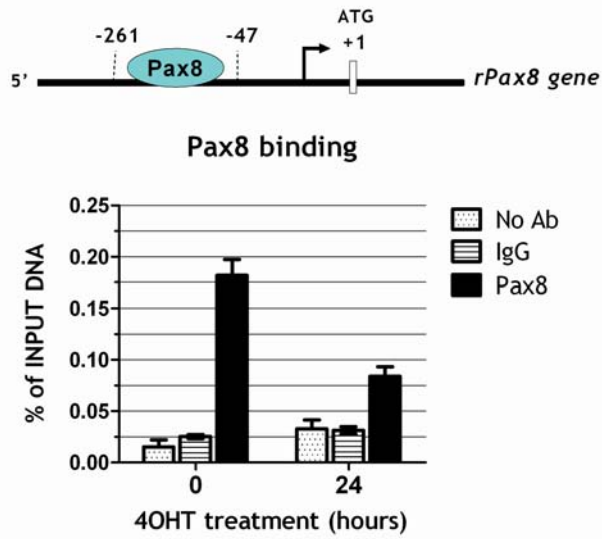


Figure 32. Pax8 binds its own promoter and its binding is downregulated by Ras oncogene

CI11 cells were treated with Tamoxifen for the indicated times (0, 24h). For each time point Pax8 binding was measured by performing a Chromatin-IP with Pax8 antibody (Pax8) as described in materials and methods. For each time point a Chromatin IP was performed also, as negative controls, with non-specific Rabbit IgG (IgG) or in the absence of any Antibody (no Ab). Immunoprecipitated DNA was measured by Real-Time PCR and is reported as percentage of Input DNA for each time point.

6.A minimal Pax8 transactivation domain is required to confer PKA responsiveness

6.1.Oncogenic Ras does not induce major post-translational modification on Pax8

In order to test whether oncogenic Ras and the subsequent impairment of PKA kinase activity was acting by modifying Pax8 protein itself I decided to analyse its migration on a bidimensional gel before and after activation of oncogenic Ras. To this aim I immunoprecipitated the flagged-Pax8 protein from the Px31 clone (described at page 21) in which Flag-Pax8 expression is kept constant also after Ras oncogene activation. Immunoprecipitated Flag-Pax8, from untreated and Tamoxifen-treated cells, were loaded on a bidimensional gel and analysed by Western Blot (Fig 33). This analysis showed that there are no macroscopic modifications induced by oncogenic Ras on Pax8 protein. Indeed its migration pattern appeared to be unmodified by oncogenic Ras. However this negative result could be due to technical limits. For example, Pax8 protein is known to be highly phosphorylated (234), it is reasonable to think that remotion of a single phosphate on a highly phosphorylated substrate would not produce a clear migration variation still being functionally extremely relevant. In order to refine the analysis and reduce the background I decided to identify a minimal Pax8 domain required for oncogenic Ras regulation.

6.2.Identification of Pax8 transactivation domain minimal regions responsive to ERRAS^{V12}

In order to investigate the Pax8 protein region necessary to confer oncogenic Ras responsiveness I engineered a series of Pax8 transactivation domain deletion derivatives and fused each of them to the GAL4 DNA binding domain (Fig. 34). In this way I could have compared Pax8 transactivation domains activity in C111 before and after activation of Ras oncogene in transient transfection assays using an artificial GAL4 responsive reporter vector (G5 reporter vector: it contains 5 binding sites for

GAL4) thus avoiding interference of the endogenous Pax8 protein activity on my analysis. Unluckily the Pax8-GAL4 derivatives had very poor, if no activity in our cells (Fig.35) and this was unlikely to be dependent upon technical issues since the GalVp16 control fusion protein (GAL4 DNA binding domain fused to the Vp16 transactivation domain) worked as expected in the assay. I reasoned that the poor activity of the Pax8-GAL4 derivatives could have been due to an incompatibility of the DNA binding properties of the GAL4 domain and the ability of the Pax8 transactivation domain to promote transcription. I thus decided to pursue an alternative strategy in which I could keep using the Pax8 paired DNA binding domain. However, to do so I could not use our C111 cells anymore since endogenous Pax8 in untreated cells would have covered the activity of the deletion derivatives on Cp5 reporter vector. I thus decided to use an NIH-derived stable cell line expressing the ERRAS^{V12} oncogene (De vita G., unpublished data) which does not express Pax8.

6.3.Oncogenic Ras action is FRTL-5 specific

I tested whether oncogenic Ras could regulate Pax8 activity in the NIH-derived stable cell line expressing the ERRAS^{V12} oncogene (NIH-ERRAS). I transiently transfected Pax8 together with the Cp5 reporter vector in these cells and tested its activity with or without Tamoxifen (Fig. 36). Surprisingly, I found that in these cells oncogenic Ras activation increases Pax8 activity, rather than decreasing it, and that this increase was not due to the Tamoxifen treatment itself (Fig. 37). I wondered what were the effects of Ras oncogene on the PKA pathway in these cells and so I tested CREB activity by using an artificial CREB-responsive reporter vector containing 5xCREB binding sites (CRE reporter vector) (Fig. 38). I found that in NIH cells oncogenic Ras upregulates CREB activity rather than decreasing it thus having an opposite effect with respect to the FRTL-5 derived cells.

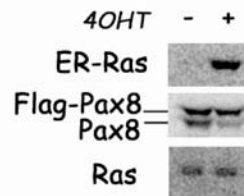
6.4.Identification of Pax8 transactivation domain minimal regions responsive to PKA

In NIH cells we could not analyse oncogenic Ras mediated inhibition of Pax8 activity since this effect appears to be FRTL-5 specific. However we could test PKA mediated regulation of Pax8 activity. I reasoned that since oncogenic Ras action on Pax8 is mediated by PKA, identification of the

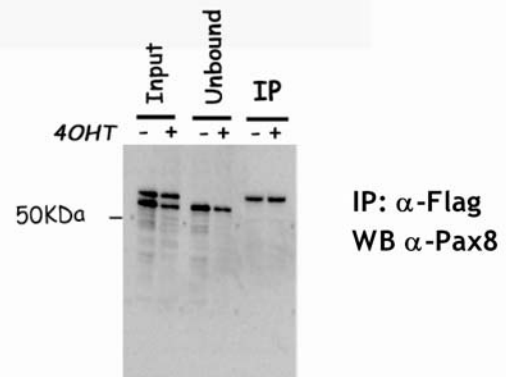
PKA responsive minimal Pax8 domain should have coincided with the oncogenic Ras responsive domain. I thus fused Pax8 transactivation domain deletion derivatives to the Pax8 paired DNA-binding domain (Fig.39). I tested the activity of the Pax8 deletion derivatives in NIH cells by cotransfecting them with the Cp5 reporter vector (Fig. 40). I found that Pax8 deletion derivatives had an activity comparable to the endogenous Pax8 with the only exception of deletion P4 which showed a reduced activity. I next tested their regulation by PKA in NIH cells (Fig. 41). I found that all Pax8 transactivation domain deletion derivatives were responsive to PKA. This PKA responsiveness was not mediated by the Paired DNA binding domain since the Pd-Vp16 fusion protein (Vp16 transactivation domain fused to the Pax8 paired DNA binding domain) was not regulated by PKA.

I conclude that a minimal transactivation domain (aminoacid 370-454 in the mouse Pax8 protein) is required to confer PKA responsiveness. This minimal domain is the region to which the majority of cofactor have been identified to interact with, strongly suggesting that PKA acts by modifying Pax8-cofactors interactions.

A



B



C

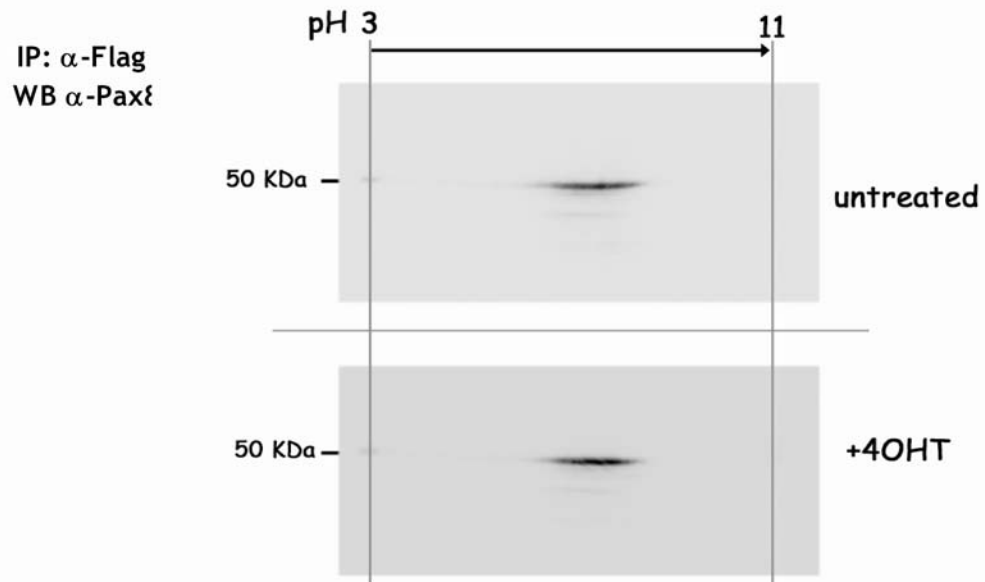


Figure 33. Oncogenic Ras does not modify Pax8 migration pattern

Pdx31 cells were treated or not with Tamoxifen for 24h. Extracted proteins were immunoprecipitated with the α -Flag antibody. Immunoprecipitates were analysed on monodimensional SDS -PAGE (B) or bidimensional electrophoresis (isoelectrophocusing+SDS -PAGE) and analysed by Western Blot with the α -Pax8 antibody. A. Western Blot analysis of total extracts to check ER -Ras activation and Pax8 expression. Endogenous Ras is used to normalize for protein loading. B. Western Blot analysis of immunoprecipitates run on monodimensional SDS-PAGE. C. Western Blot analysis of immunoprecipitates run on a bidimensional electrophoresis.

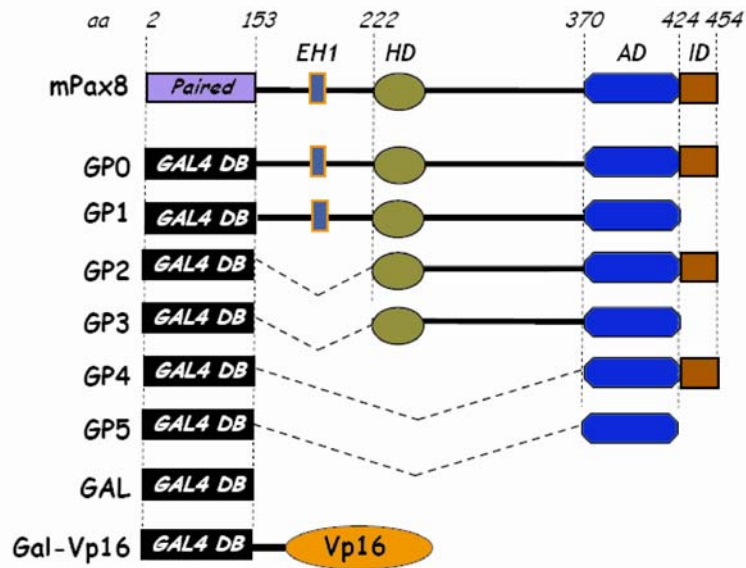


Figure 34. Schematic representation of GAL4-Pax8 fusion proteins

mPax8: mouse Pax8 protein with previously characterized functional domains (Paired: DNA binding domain, EH1: engrailed homology region 1, HD: Homodomain homology region, AD: activation domain, ID: Inhibitory domain). Dotted lines indicate deletion extremes positions along the mPax8 protein. In all Pax8 deletion derivatives the Paired domain (aa 1-153) has been substituted with the GAL4 DNA binding domain (aa 1-147). Further details are reported in Materials and methods section.

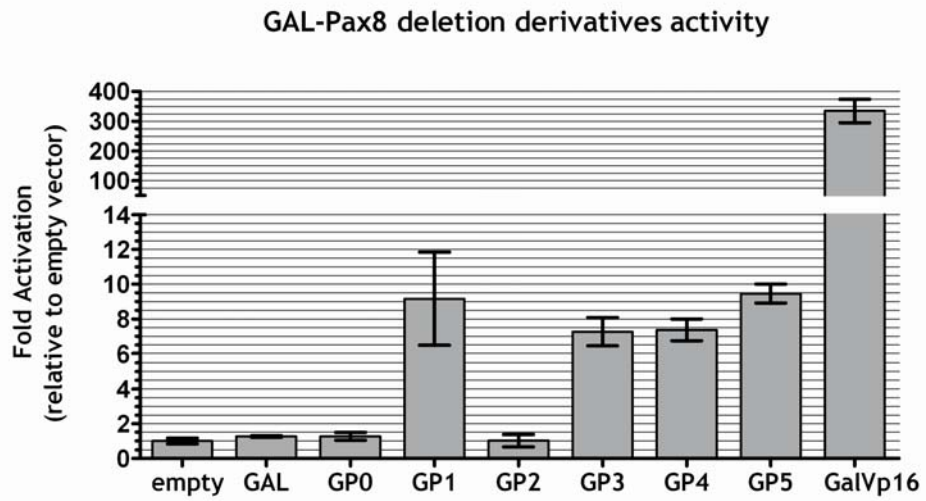


Figure 35. Gal-Pax8 fusion proteins activity in CH11 cells

Transient transfection assay of G5 reporter activity in CH11 cells. Reporter vector (1 μ g) was transfected either with 500ng of empty vector (-) or 500ng of vectors encoding respectively the fusion proteins indicated in Fig. 34.

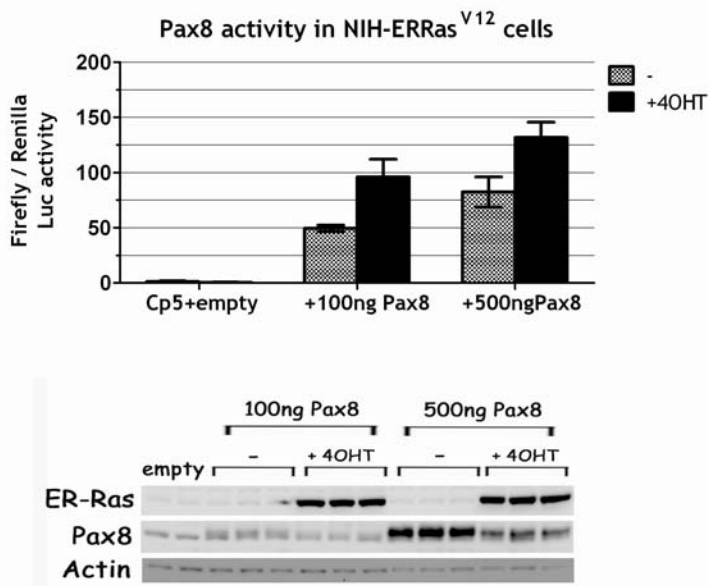


Figure 36. Oncogenic Ras upregulates Pax8 activity in NIH cells.

Transient transfection assay of Cp5 reporter activity in NIH 3T3 derived cell line expressing ER-Ras^{V12} either in the absence or in the presence of Tamoxifen (4OHT). Cells were cotransfected respectively with an empty vector (Cp5+empty), with 100ng of Pax8 (+100ng Pax8), or with 500ng of Pax8 (+500ng Pax8). Western Blot analysis of ERRAS activation and Pax8 expression in the lysates is also shown below.

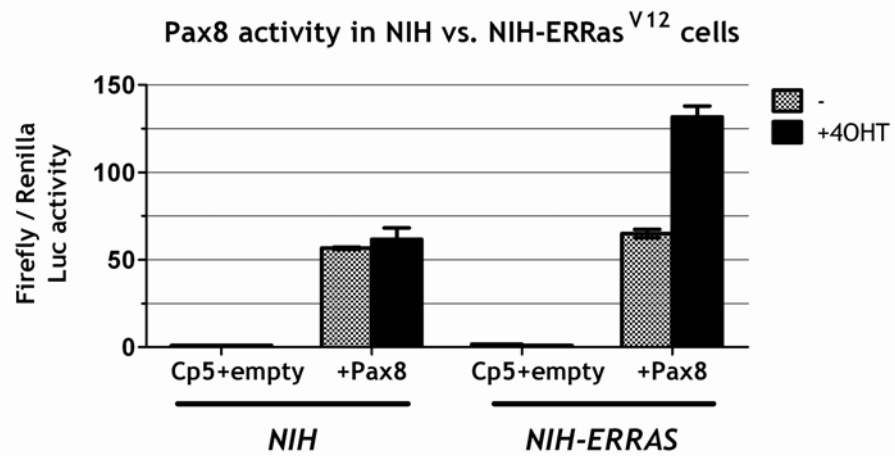


Figure 37. Tamoxifen has no effects on Pax8 activity in NIH cells

Transient transfection assay of Cp5 reporter activity in NIH 3T3 cells (NIH) and NIH 3T3 derived cell line expressing ER-Ras^{V12} (NIH-ERRas) either in the absence or in the presence of Tamoxifen (4OHT). Cells were cotransfected respectively with an empty vector (Cp5+empty) or with 100ng of Pax8.

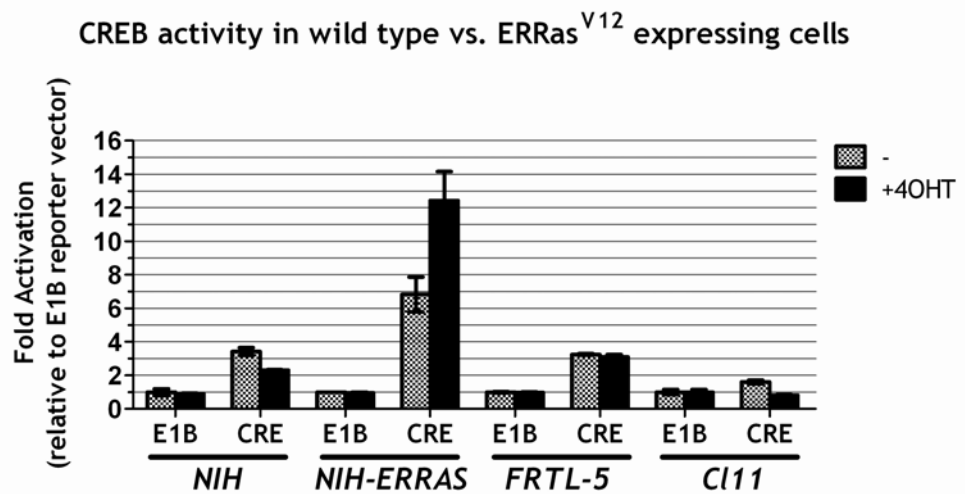


Figure 37. Ras oncogene has opposite effect on CREB activity in NIH and FRTL-5 cells

Transient transfection assay of CRE reporter activity in NIH 3T3 cells (NIH), NIH 3T3 derived cell line expressing ER-Ras^{V12} (NIH-ERRas), FRTL-5 cells (FRTL-5) and NIH 3T3 derived cell line expressing ER-Ras^{V12} (C111) either in the absence or in the presence of Tamoxifen (4OHT). Each cell line was transfected alternatively with a reporter vector containing 5x CREB responsive element upstream of the E1B TATA box (CRE) or with the reporter vector containing only the E1B TATA box (E1B). For each reporter vector luciferase activity was normalized on Renilla activity in order to correct for transfection efficiency. CRE activity was then expressed for each cell line as fold of activation over the activity of the E1B reporter vector.

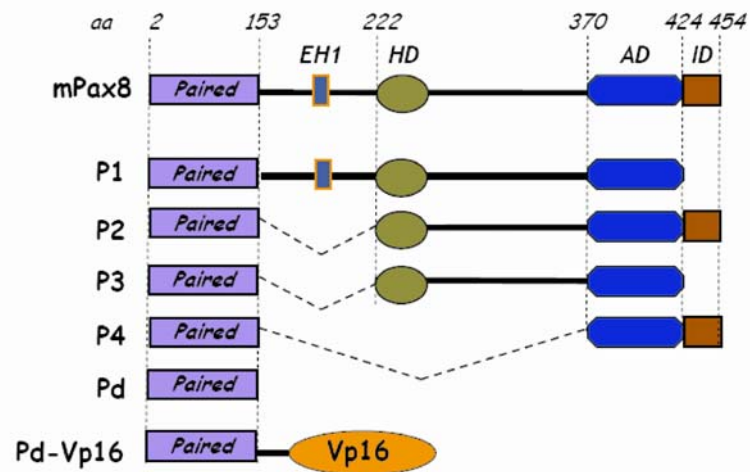


Figure 39. Schematic representation of Pax8 deletion derivatives proteins

mPax8: mouse Pax8 protein with previously characterized functional domains (Paired: DNA binding domain, EH1: engrailed homology region 1, HD: Homodomain homology region, AD: activation domain, ID: Inhibitory domain). Dotted lines indicate deletion extremes positions along the mPax8 protein. Further details are reported in Materials and methods section.

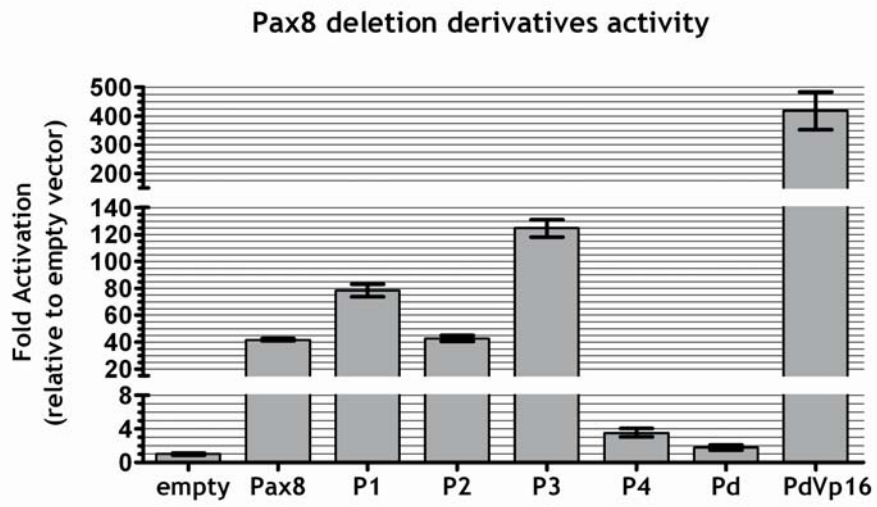


Figure 40. Pax8 deletion derivatives proteins activity in NIH cells

Transient transfection assay of Cp5 reporter activity in NIH cells. Reporter vector (1 μ g) was transfected either with 250ng of empty vector (-) or 250ng of vectors encoding respectively the fusion proteins indicated in Fig. 39.

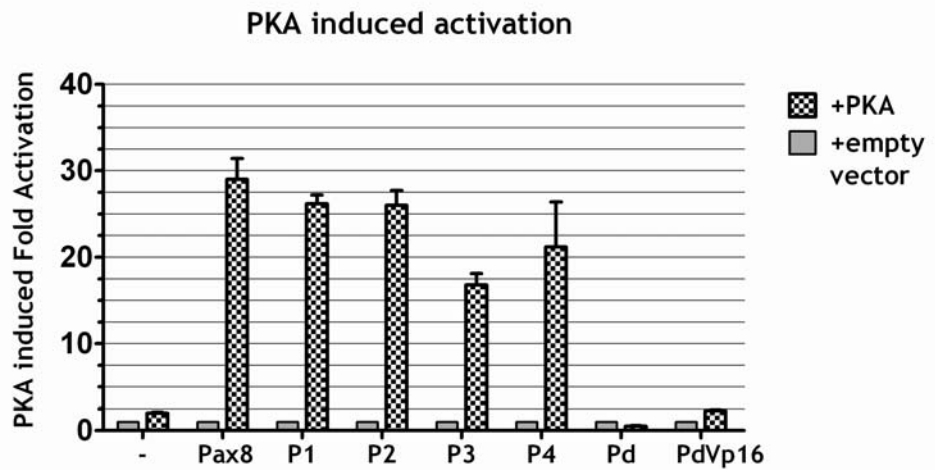


Figure 41. Pax8 deletion derivatives responsiveness to PKA in NIH cells

Transient transfection assay of Cp5 reporter activity in NIH cells. Reporter vector (1 μ g) was transfected with 250ng of empty vector (-) or 250ng of vectors encoding respectively the deletion derivatives proteins indicated in Fig. 39. For each deletion derivative tested, transfection was performed with 1.25 μ g of PKA encoding expression vector (PKA) or with the empty vector (empty vector). Luciferase activity, normalized on renilla activity to correct for transfection efficiency, is expressed, for each deletion derivative tested, as a ratio on the value obtained by cotransfecting the empty vector.

7.Characterization of oncogenic Ras induced modifications of Pax8 transcriptional complexes

7.1.Gel filtration analysis of Pax8 transcriptional complex

In order to gain clues about eventual variations in Pax8 transcriptional complexes I performed a gel filtration analysis. Through this analysis is possible to sort proteins by molecular weight. A linear relationship exist between the logarithm of Molecular Weight and the volume (each collected fraction is 0.5mL) at which the protein is eluted (Fig.42A). If gel filtration is performed on a cellular extract whose conditions are appropriate (protein interactions are kept) is possible to understand distribution of a given protein in macromolecular complexes. Indeed I performed a gel filtration test run on C111 cells in order to analyze whether or not Pax8 was partner of a macromolecular complex. In Fig42B is shown the total proteins elution profile along the collected fractions. Proteins from each fraction were precipitated, resuspended in an appropriate volume and analysed by Western Blot to check Pax8 distribution (Fig. 42C). Results showed that Pax8 (~50KDa) is eluted, as expected, in fractions corresponding to low molecular weight (fractions 14-17 should contains proteins ranging from 80KDa to 40 KDa as determined from the standard curve) but also in fractions corresponding to high molecular weight (fractions 9-11 that correspond to proteins ranging from 330 KDa to 160 KDa) suggesting Pax8 it is partner of a macromolecular complex. Furthermore TTF1 which is a known Pax8 cofactor is eluted within the same High Molecular Weight fractions strengthening the result. This distribution along the fractions it is not random since GAPDH, a cytosolic protein of about 42 KDa, is eluted exclusively in low molecular weight fractions.

I thus analysed by gel filtration extracts of C111 cells treated or not with Tamoxifen. Results obtained with this analysis showed very similar profiles of Pax8 distribution in Tamoxifen treated and untreated cells (Fig.43) . I thus conclude that through this technique is not possible to detect any macroscopic alterations of the multimolecular Pax8 complex induced by oncogenic Ras.

7.2. Generation of multiple Tags to isolate Pax8 cofactors

I thus decided to isolate Pax8 cofactors in order to analyze them qualitatively before and after Ras oncogene activation. To this end I generated a series of different multiple Tags (Fig. 44) that should have allowed a very efficient tandem IP procedure for cofactor isolation.

The starting point was a triple-tag, obtained from Stunnenberg H.G. Laboratory, that I called TTC (Triple Tag C-terminal). This TTC tag was projected to be fused to the C-terminal end of the protein of interest and consisted of three different kind of peptide tags 1) the V5 epitope tag (V5) (238) 2) the Flag epitope tag (Flag TM) (239, 240) and 3) The Biotin acceptor peptide tag (AVI) that is the minimal target peptide recognized by the bacterial biotin ligase BirA (241), separated by two proteases cleavage sites (respectively the Tobacco etch virus protease TEV (242) and the Human Rhinovirus 3C protease (243) Prescission) as illustrated in Figure 44. Since Pax8 was never tagged at the C-terminal I synthesized through appropriate PCR reactions (see materials and methods for details) a specular triple-tag in order to fuse it at the Pax8 N-terminal end (TTN in Fig. 44). Furthermore since the triple tags are both 68 aminoacid long I decided to synthesize two shorter kind of tags. The double-tag, both for the N-terminal (DTN) and C-terminal (DTC) fusion, is basically like the triple-tag but it miss the Prescission cleavage site and the AVI sequence. On the other hand since it was demonstrated that the BirA/AVI biotinylation system allowed a very efficient isolation of transcription cofactors in a single step IP procedure (244, 245), I also synthesized a mono-tag, again both for the N-terminal (MTN) and C-terminal (MTC) fusion, consisting of only the Prescission cleavage site and the AVI sequence.

7.3. Evaluation of Tagged-Pax8 chimaeric proteins activity

I fused each of the generated Tag to Pax8 protein and tested the activity of these chimaeric proteins by evaluating their ability to transactivate the Cp5 artificial promoter (5x Pax8 binding sites) in NIH cells (Fig. 45). Results showed that DTN-Pax8 is the only protein that keep an activity and an expression very similar to the already characterized FlagPax8. The other tagged Pax8 proteins shows

very modest expression when compared with FlagPax8 and, though being functional, an increased activity with respect to FlagPax8.

Since from data presented up to here it appears that PKA induced regulation of Pax8 protein is connected to Ras oncogenic action I also tested whether these tagged Pax8 were still responsive to PKA in order to choose an appropriate Tag (Fig. 46). The analysis showed that all the chimaeras were equally responsive to PKA as the wild-type Pax8.

I thus selected two Pax8 tagged versions for different reasons. The DTN-Pax8 (Double Tag fused to Pax8 N-terminal end as described in Fig.44) since it presents a very good expression level and an activity very similar to the wild-type control. I also selected the TTN-Pax8 (Triple Tag fused to Pax8 N-terminal end as described in Fig.44) since even though not express at optimal levels in transient transfections it is the best tag among the ones carrying the AVI sequence.

7.4.Generation of stable cell lines expressing different multitag-Pax8

In order to obtain a suitable system to isolate and compare Pax8 cofactors before and after Ras oncogene activation I generated several stable cell lines starting from C111 cells.

I stably transfected in C111 cells the DTN-Pax8 protein. Among the clones obtained (Fig. 47) the F16 clone was selected since it expressed the greater amount of DTN-Pax8 and a comparable amount of endogenous Pax8 and ER-Ras^{V12} with respect to the parental C111 cell line.

Since the AVI tag requires the biotinylating bacterial BirA enzyme I generated a cell line which express both the TTN-Pax8 and the BirA biotin ligase (Fig. 48) and an additional control cell line that express only the BirA enzyme (Fig. 49). As expected and shown in Figure 48 none of the obtained TTN-Pax8 expressing clones (E clones) had an expression of the ectopic Pax8 comparable to the endogenous one. This represent an issue since the endogenous Pax8 can compete with the bait for cofactors. However I choose the best TTN-Pax8/BirA expressing clone (E15) and a comparable BirA expressing control cell line (D16) in order to analyse, within the same cellular extract, different IP procedures and establish whether use the DTN-Pax8 system or either project additional kind of tags.

7.5. Testing of BirA/Avi biotinylation system and elution procedures

I used the E15 clone expressing TTN-Pax8 and BirA (Fig. 48) in order to compare different immunoprecipitation procedures. As first I decided to test in our E15 clone 1) Working of BirA biotinylation of the AVI Tag on TTN-Pax8 by purifying TTN-Pax8 with streptavidin conjugated beads 2) Efficiency of eluting the bait (TTN-Pax8) by TEV or Prescission protease cleavage. The experimental scheme is illustrated in figure 50A Results, illustrated in figure 50C, showed that effectively in our system BirA biotynalates TTNPax8. Infact TTNPax8 is found in the streptavidin bound fraction (clone E15, IP#1 in Fig50C) while the endogenous untagged Pax8 is exclusively in the Unbound fraction (clone E15, UnBound#1 in Fig50C). Analogously in the BirA only expressing clone D6 no signal for Pax8 is detected in the streptavidin bound fraction (clone D6, IP#1 in Fig.50C). Concerning Elution procedures results showed that boiling streptavidin beads in SDS to recover the bait is an efficient procedure (compare IP#1,2,3 in Fig.50C). However if looking at the Coomassie staining in Figure 50B it is clear that it is also the procedure with the higher background. Infact a lot more of aspecific protein bands are visible by coomassie staining (compare IP#1 in E15 clone with IP#2 and IP#3 and with IP#1 in clone D6 in Figure 50B). On the other hand both TEV and Prescission protease cleavage-based elution greatly reduce the background when looking at the coomassie staining (compare IP#1 with IP#2 and #3 in Figure 50B). Furtermore both TEV and Prescission protease mediated cleavage of TTN-Pax8 bait is almost complete. Infact cut by TEV should produce a Pax8 migrating band at the same height of the endogenous pax8 since it removes completely the Tag (see TTN tag in Fig44). My results shows that TEV cut all the TTN-Pax8 has been cut, even though strangely not all the cut TTN-Pax8 is eluted from the beads since it can be recovered only by boiling the TEV treated beads (look Pax8 band height in IP#2 and Uneluted #2 in Fig. 50C). Prescission protease, on the other hand should remove only the AVI tag (see TTN tag in Fig 44) generating a DTNpax8 like band migrating slightly belove the TTN-Pax8 band. I detected an aspecific cut of Prescission protease on the TEV cleavage site. Infact in IP#3 in Figure 50C is clearly visible the presence of two bands one migrating as expected like a DTNPax8 and the other one migrating like the endogenous Pax8. However with prescission protease the bait can be completely eluted from the beads

since no Pax8 is visible when Prescission treated beads are boiled in SDS (see uneluted #1 clone E15 in Fig 50C).

I conclude that Protease-based elution greatly reduces the background and that Prescission protease, as previously suggested, is the best cleavage-based elution system since it allows an almost complete recovery of the bait but can't be used on baits that carry a TEV cleavage site for subsequent purification procedures.

7.6. Comparison of Biotin-based purification system versus V5 and Flag epitopes based immunoprecipitations

The advantage of using a the TTN tagged Pax8 expressing clone (Fig. 44 and 48) is that is possible to apply different purification procedures on the same cell lysate thus easily comparing different purification protocols. I decided to compare the single-step biotinylation-based purification of TTN-Pax8 versus respectively V5 and Flag immunopurification procedures. I used again the E15 clone expressing TTN-Pax8 and BirA and the negative control cell line D6, expressing only BirA, in order to discriminate between specific bands and background. In order to apply the same protease-based elution procedure to all the purification systems in testing I had to use TEV protease (see TTN tag structure in Fig. 44).

The experimental scheme is illustrated in figure 51A Results, illustrated in figure 51, showed that first of all when looking at the background (see Coomassie staining in Fig. 51B) the three purification procedures are not that different between each other. It is in fact almost impossible to establish a difference within the coomassie staining lanes relative to three protocols (compare IP#1, #2 and #3 in Fig. 51B). Furthermore there is no advantage neither in bait recovery. In fact Pax8 Western Blot analysis in Figure 51C clearly shows that the amount of recovered bait is almost the same for the three procedures.

I conclude that the biotin-based purification system does not produce results which are significant better than the ones that can be obtained by using the standard V5 or Flag epitopes based purifications neither in terms of background nor in terms of bait recovery. Furthermore, since as previously shown (see Fig. 45 and Fig. 48) the presence of the Avi tag apparently impairs a proper

expression of the tagged protein and, as explained above, does not give any evident advantage I decided to move on the DTN tag (see Fig.44 for structure and Fig. 45 and 47 for expression of DTNPax8).

7.7. Comparison of V5 and Flag single-step IPs versus double-step IP

Established that the Avi Tag did not confer any advantage with respect to V5 and Flag epitopes I decided to test whether I could improve the IP procedure by combining the V5 and Flag immunoprecipitation procedures in a tandem purification protocol. In order to do that I used the F16 cell line (Fig.47) expressing DTNPax8 (see fig.44 for DTN tag structure).

I compared, on the same cell lysate, the following purification protocols: 1) Immunoprecipitation through V5-antibody conjugated beads and TEV-mediated elution of the bait 2) Immunoprecipitation through Flag-antibody conjugated beads and elution of the bait by competition with a 3xFlag peptide 3) Immunoprecipitation through Flag-antibody conjugated beads, elution of the bait by competition with a 3xFlag peptide, re-immunoprecipitation of recovered material with V5-antibody conjugated beads and elution through TEV-mediated cleavage of the bait. The experimental scheme is illustrated in figure 52A.

Coomassie staining analysis showed that V5-based purification clearly reduces the background with respect to the Flag-based one (compare lanes IP#1 and #2 in Fig. 52B). However bait recovery is poor in V5 immunoprecipitation when compared to the Flag one (compare lanes IP#1 and #2 Fig. 52C). This poor recovery in the single step V5-based IP is based in part on the inefficient TEV protease elution (see Uneluted#1 in Fig. 52C), but maybe could be improved also by testing different kind of commercially available antibodies against V5 epitope. What I found relevant is that background of V5-based IP can be further reduced by combining the two V5 and Flag procedures without significantly affecting Pax8 bait recovery amount (compare lanes IP#1 and #3 Fig. 52B and Fig 53B).

I conclude that the double Flag/V5 tandem purification protocol is potentially a very good system that has its major drawback at present in bait recovery. The first modification that should be made to the DTN tag in order to improve bait recovery is the substitution of the TEV cleavage site with

the Prescission protease one in order to avoid the almost 50% loss of the bait during protease-based elution (see previously discussed Fig. 50 for comparison of elution procedure). Additionally new V5 antibodies should be tested in order to obtain a purification system suitable for unbiased cofactor isolation and identification through mass spectrometry.

7.8. Analysis of Pax8 cofactors differentially regulated by ERRAS^{V12}

Eventhough at present not suitable for mass spectrometry analysis of Pax8 cofactors the DTNPax8 expressing clone F16 and the double Flag/V5 tandem purification protocol can be used to analyse through WesternBlot analysis interaction of Pax8 with known cofactors before and after Ras activation. I'm planning to use the system in order to analyse Pax8 interaction with the following known cofactors either in the absence or in the presence of Tamoxifen: 1) TTF1 (107, 128), 2) p300 (129-131), 3) Rb (132), 4)PARP (133), 5)Taz (134), 6) WBP-2 (135). As control, obviously, the same procedure will be performed on C111 as negative control cell line in order to check specificity of the observed results.

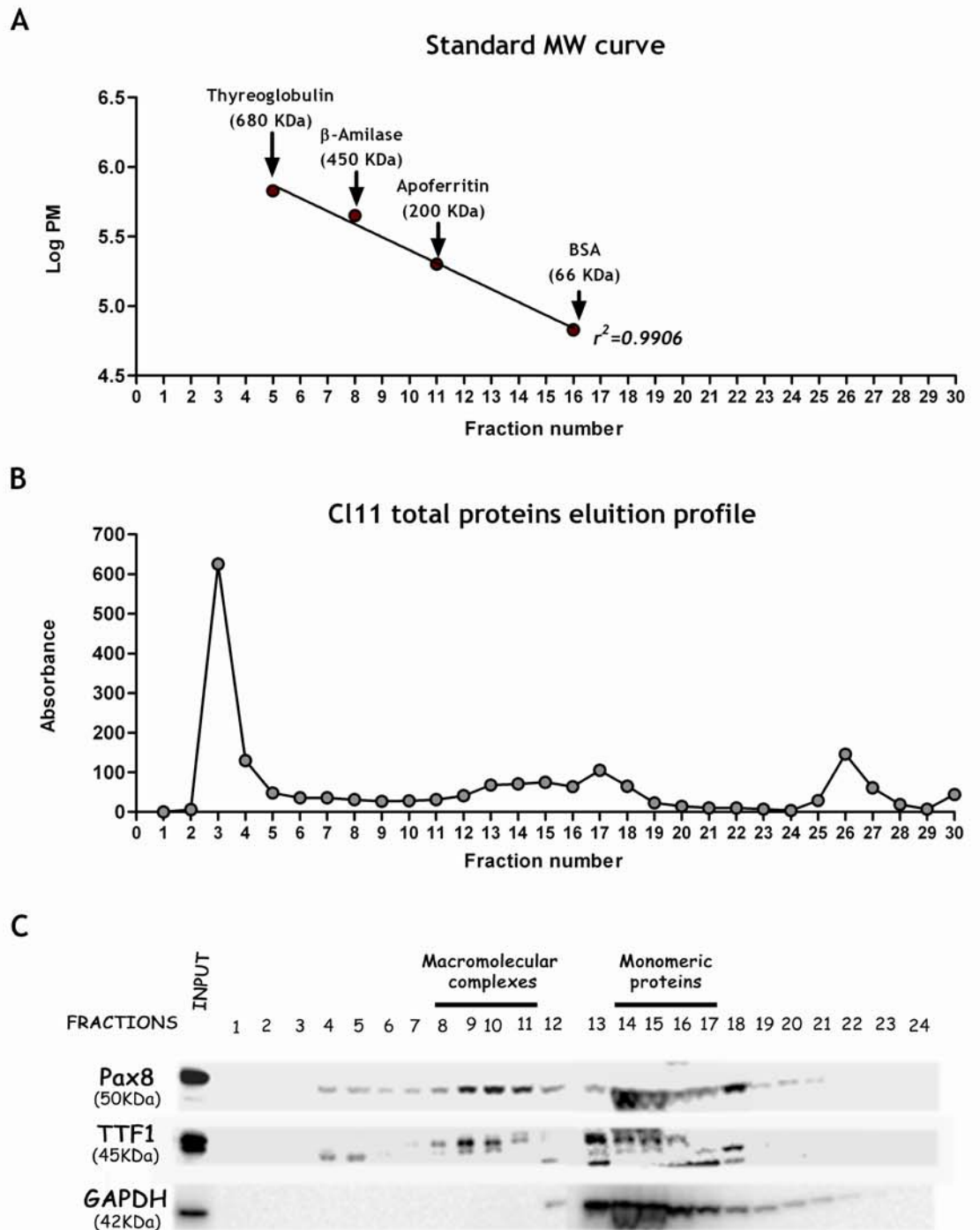


Figure 42. Pax8 protein is part of a macromolecular complex

Gel filtration analysis. A. Standard curve performed by analyzing the elution profiles of molecular weight markers. In the graph is reported the logarithm of markers molecular weight versus the volume at which those markers are eluted. Each fraction is 0.5mL. B&C. Cl11 cells extract was loaded on the gel filtration column. B. Total protein elution profile obtained by reading absorbance at 280nm of the flowthrough. C. Proteins from each fraction were precipitated and analyzed by Western Blot for each of the indicated gene.

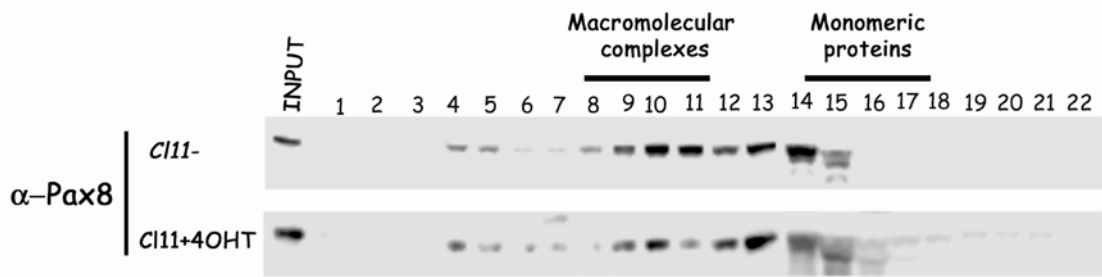


Figure 43. Gel filtration analysis of Ras oncogene induced modifications of Pax8 macromolecular complexes

C111 cells were treated or not with Tamoxifen for 24h and cell extract were analysed by gel filtration . Proteins eluted in each of the indicated frac tion were precipitatd and analysed by Western Blot in order to detect Pax8 distribution along the fractions.

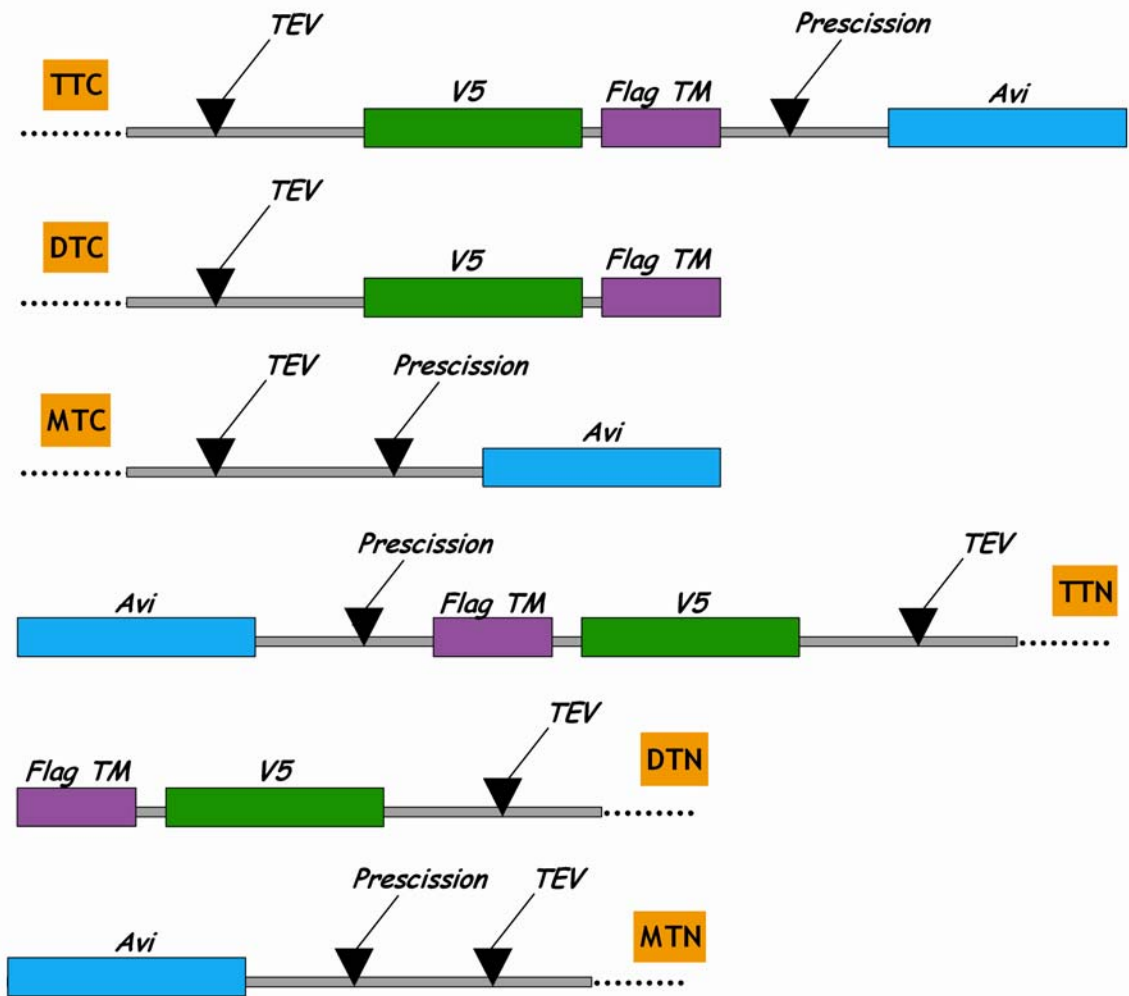


Figure 44. Schematic representation of generated multiple Tags

In the figure are schematically represented the six multiple tags (TTC, DTC, MTC, TTN, DTN, MTN) that were fused to Pax8 protein. TTC, DTC and MTC tags were projected in order to be fused to Pax8 C-terminal end. TTN, DTN and MTN were projected to be fused to Pax8 N-terminal end. Both Triple Tags (TTC and TTN) include the TEV protease cleavage site (TEV), V5 epitope, Flag TM epitope, the Prescission protease cleavage site (Prescission) and the Biotinylation tag (Avi). Double tags (DTC and DTN) only include the TEV site followed by the V5 and Flag epitope. The Mono Tags (MTC and MTN) consist in the two proteases cleavage sites followed by the Avi Tag.

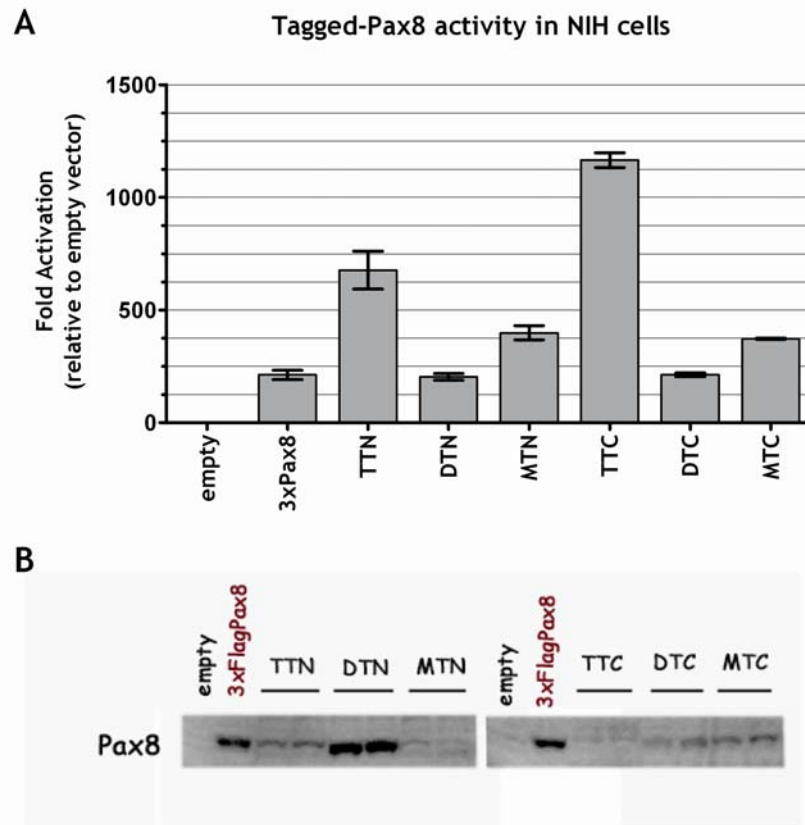


Figure 45. Tagged-Pax8 activity and expression in NIH cells

Transient transfection assay of Cp5 reporter activity in NIH cells. Reporter vector (1 μ g) was transfected either with 250ng of empty vector (-) or 250ng of vectors encoding respectively the Pax8 protein fused to each of the Tag indicated in Fig. 44. A. Activity of Tagged-Pax8 reported as fold induction over the value obtained by co-transfecting the Cp5 reporter vector with an empty vector B. Western Blot analysis of tagged-Pax8 expression. 3xFlagPax8 (3xPax8) was used as a positive control for activity and expression of the tagged -Pax8.

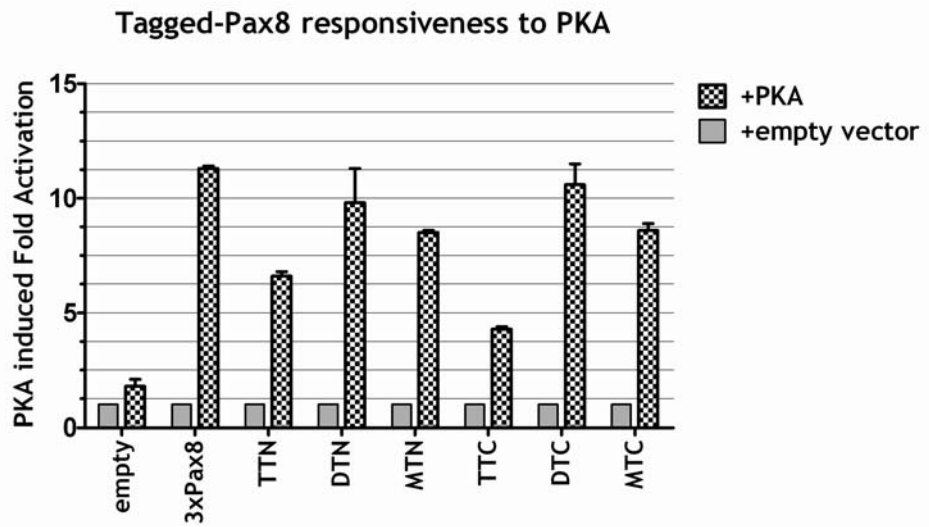


Figure 46. Tagged-Pax8 responsiveness to PKA in NIH cells

Transient transfection assay of Cp5 reporter activity in NIH cells. Reporter vector (1 μ g) was transfected with 250ng of empty vector (-) or 250ng of vectors encoding respectively the Pax8 protein fused to each of the Tags indicated in Fig. 44. For each tagged-Pax8 tested, transfection was performed with 1.25 μ g of PKA encoding expression vector (PKA) or with the empty vector (empty vector). Luciferase activity, normalized on renilla activity to correct for transfection efficiency, is expressed, for each construct tested, as a ratio on the value obtained by cotransfecting the empty vector.

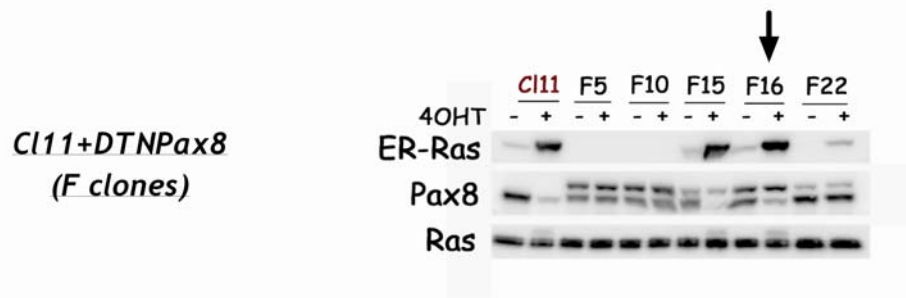


Figure 47. C111 derived stable clones expressing DTN -Pax8

C111 cells were stably transfected with the DTN -Pax8 encoding vector plus a puromycin resistance encoding vector in a 10:1 ratio. Stable clones were selected after culturing cells three weeks in puromycin (1 µg/mL) selection. In the figure is shown a Western Blot analysis of some positive clones. DTN-Pax8 protein positive clones were screened by looking at DTN -Pax8 expression which is the C111 and positive DTN-Pax8 expressing clones (F5, F10, F15, F16, F22) were treated 24 hours with or without Tamoxifen and analyzed by Western Blot for the genes indicated. In F clones the ectopic DTN-Pax8 is identified by the band migrating above the endogenous Pax8 protein visible in C111.



Figure 48. CI11 cells derived stable clones expressing TTN -Pax8 and BirA

CI11 cells were stably transfected with the DTN -Pax8 encoding vector plus the BirA encoding vector carrying the puromycin resistance in a 10:1 ratio. Stable clones were selected after culturing cells three weeks in puromycin (1 µg/mL) selection. In the figure is shown a Western Blot analysis of some positives clones. CI11 and positives TTN-Pax8 expressing clones (E10, E13, E15, E18, E24) were treated 24 hours with or without Tamoxifen and analyzed by Western Blot for the genes indicated. In E clones the ectopic TTN-Pax8 is identified by the band migrating above the endogenous Pax8 protein visible in CI11.



Figure 49. Cl11 cells derived stable clones expressing BirA

Cl11 cells were stably transfected with the BirA encoding vector carrying the puromycin resistance. Stable clones were selected after culturing cells three weeks in puromycin (1µg/mL) selection. In the figure is shown a Western Blot analysis of some positives clones. Cl11, clone E15 and positives BirA expressing clones (D6, D12, D13, D16, D17) were treated 24 hours with or without Tamoxifen and analyzed by Western Blot for the genes indicated.

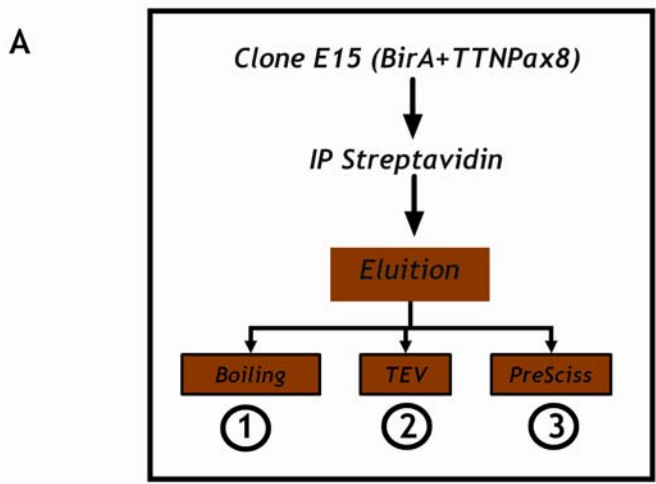
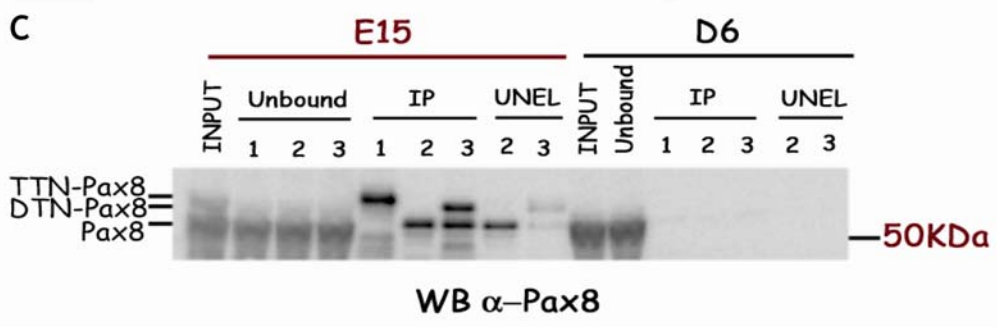
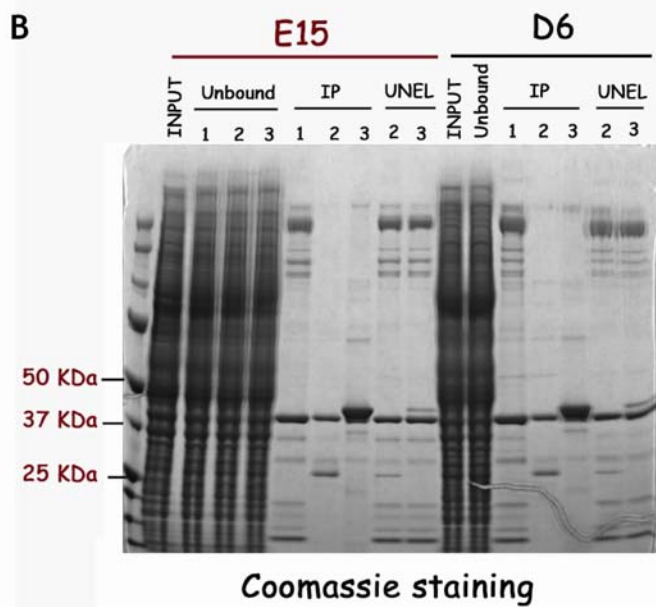


Figure 50. comparison of elution protocols

A. synthetic representation of the experimental scheme. About 4.5 mg of total proteins from respectively E15 clone (TTNPax8+BirA) were affinity purified through streptavidin conjugated beads. At the end of the procedure the streptavidin bound material was aliquoted in three fractions which were respectively eluted through the following different procedures : 1)boiling in SDS 2)Cleavage with 10U TEV 16h at 4°C 3)Cleavage with 10U precession 16h at 4°C. The same procedure was applied to the control D6 clone expressing only BirA in order to discriminate between specific bands and background of the procedure. Proteins were then loaded on SDS page and analysed by Coomassie staining (B) or Western Blot analysis (C). INPUT fraction (3.2% of total INPUT proteins), UNBOUND fractions (3.2% of total Unbound material), IP fraction (30% of eluted material) and UNELUTED fraction (30% of material obtained by boiling beads after protease elution). B) Coomassie staining C) Western Blot analysis of Pax8 Bait recovery.



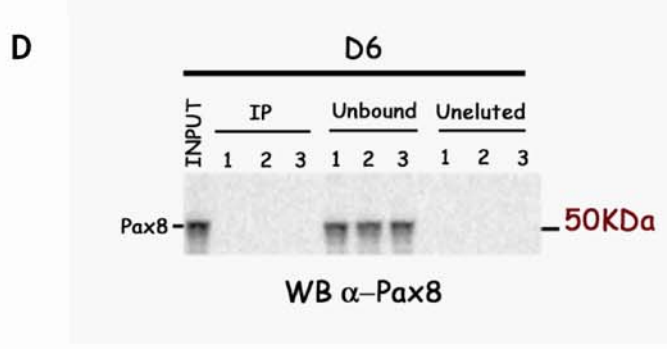
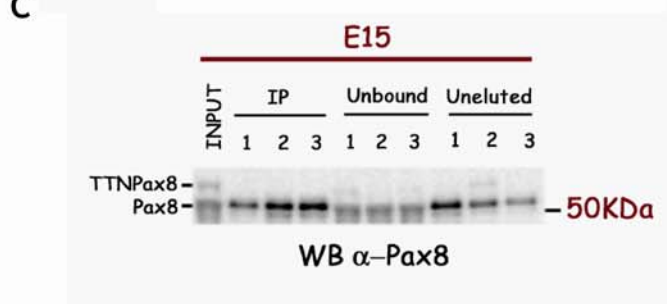
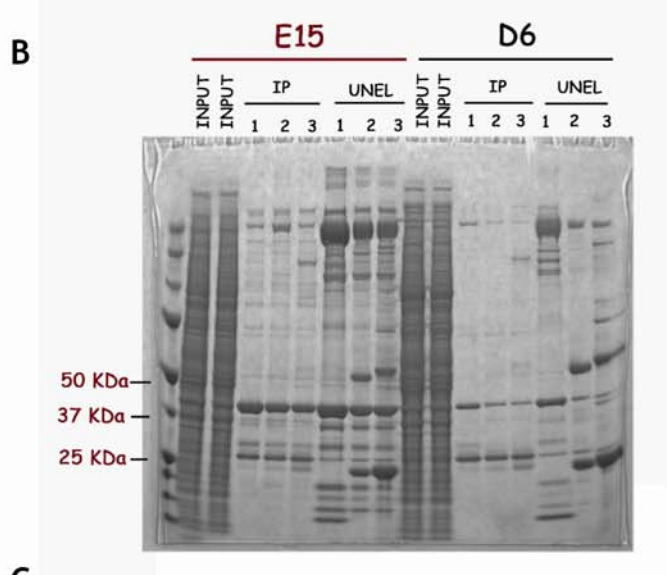
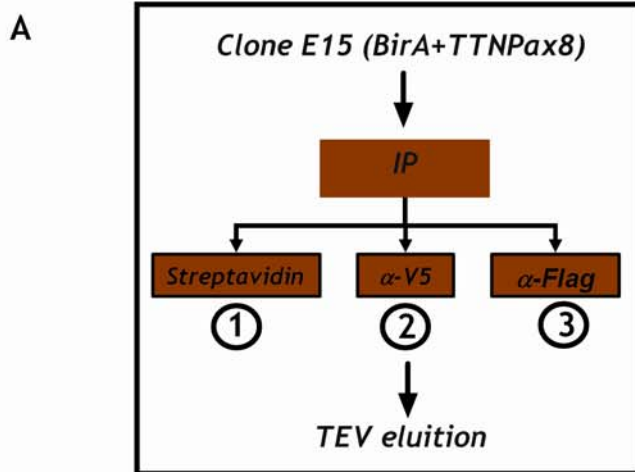


Figure 51. Comparison of Biotin-based versus Flag and V5 epitopes - based purification systems

A. synthetic representation of the experimental scheme. About 1.5 mg of total proteins from E15 clone (TTNPax8+BirA) were respectively purified through 1)streptavidin conjugated beads 2)V5 antibody conjugated beads or 3)Flag Antibody conjugated beads. At the end of all the three procedures the bait was eluted through cleavage with 10U TEV 16h at 4°C. The same procedure was applied to the control D6 clone expressing only BirA in order to discriminate between specific bands and background of the procedures.

Proteins were then loaded on SDS page and analysed by Coomassie staining (B) or Western Blot analysis (C&D). INPUT fraction (3.2% of total INPUT proteins), UNBOUND fractions (3.2% of total Unbound material), IP fraction (30% of eluted material) and UNELUTED fraction (30% of material obtained by boiling beads after protease elution). B. Coomassie staining C. Western Blot analysis of Pax8 Bait recovery in clone E15. D. Western Blot analysis of Pax8 Bait recovery in control clone D6.

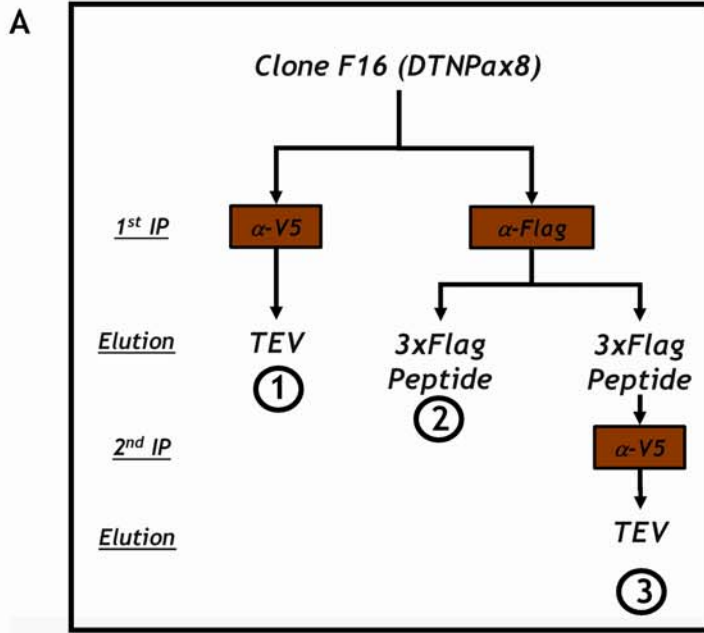
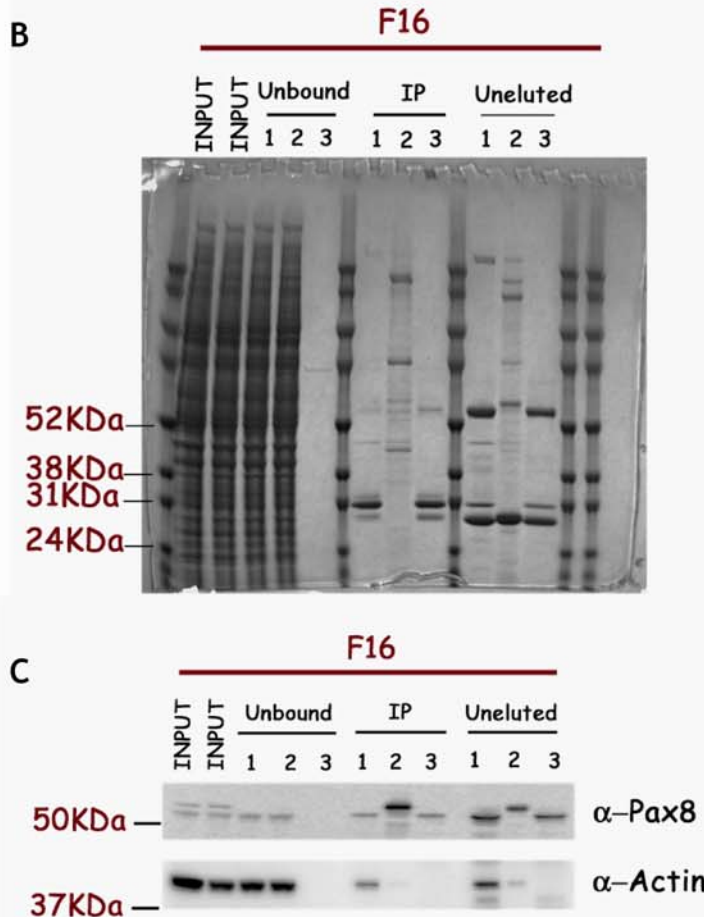


Figure 52. Comparison of double Flag-V5 IP versus single ones

A. synthetic representation of the experimental scheme. About 1.5 mg of total proteins from F16 clone (DTNPax8) were respectively purified through 1) V5 antibody conjugated beads and eluted through TEV protease cleavage 2)Flag Antibody conjugated beads and eluted by competition with 3xFlag Peptide 3)Flag Antibody conjugated beads, eluted by competition with 3xFlag Peptide, diluted in lysis buffer and re-purified through V5 antibody conjugated beads and eluted through TEV protease cleavage.

Proteins were then loaded on SDS page and analysed by Coomassie staining (B) or Western Blot (C). INPUT fraction (3.2% of total INPUT proteins), UNBOUND fractions (3.2% of total Unbound material), IP fraction (30 % of eluted material) and UNELUTED fraction (30% of material obtained by boiling beads after protease elution). B. Coomassie staining C. Western Blot analysis of Pax8 Bait recovery and Actin contamination as representative of Background.



8. Oncogenic Ras induced de-differentiation is a reversible phenotype

Oncogene addiction is today a very known phenomenon that can be used as a weapon against cancer cells (214, 246-248). In FRTL-5 cells previous data obtained by using a Temperature-sensitive Ras oncogene suggested that once Ras oncogene is activated, thyroid differentiated phenotype can't be restored by simply inactivating Ras oncogene (249-251). However, in those cells, Ras oncogene inactivation required a temperature shift which could have made the results artificial.

I thus decided to investigate whether our cells are Ras oncogene addicted. I used the possibility of simply inactivating Ras oncogene by removal of Tamoxifen from the culture medium in order to analyse the reversibility of oncogenic Ras induced de-differentiation. I treated C111 cells 5 weeks with Tamoxifen. After these 5 weeks of Tamoxifen treatment I cultured cells for an additional week either in the presence or in the absence of Tamoxifen and I analysed their differentiation by looking at the expression of several differentiation markers (Fig. 53). I found that even after 5 weeks of oncogenic Ras activity the differentiated phenotype can be restored by suppressing Ras oncogene activity through removal of Tamoxifen from the culture medium thus demonstrating the relevance of finding ways to inactivate Ras oncogene in order to restore a normal phenotype.

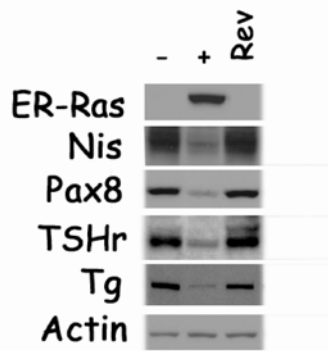


Figure 53. Ras oncogene induced de-differentiation can be reversed by inactivating the oncogene.

Western Blot analysis of several thyroid differentiation markers in C111 cells treated 5 weeks with Tamoxifen (+) and then cultured for an additional week in the absence of Tamoxifen (REV). Untreated C111 cells (-) kept in culture for the same amount of time were also analysed. Actin has been used to normalize for protein loading.

9. Oncogenic Ras de-differentiates FRTL-5 cells through the MAPK pathway

I next wondered which was the pathway through which Ras oncogene was inducing de-differentiation. Previous studies, performed in a different experimental system, aimed to the identification of signalling cascades involved in oncogenic Ras-mediated dedifferentiation of FRTL5 cells suggested the involvement of the MAPK (Mitogen Activated Protein Kinase) pathway plus an uncharacterized Ras effector pathway (220, 221).

I thus tested the effect of MAPK pathway inhibition on oncogenic Ras induced phenotype. I analysed in first the role of the MAPK pathway in ERRas^{V12} induced NUE activity impairment through the use of known inhibitors of MAPK pathway such as U-0126 and PD-98059 (Fig. 54). I found that MAPK inhibition, strongly impairs ERRas^{V12} ability to downregulate NUE activity.

I tested next whether MAPK inhibition could also restore endogenous NIS gene expression. Real-time RT-PCR results showed that MAPK inhibition substantially restore NIS expression very close to wild-type levels and almost completely restore also Pax8 and TSHr expression (Fig. 55). The same result was observed by looking at NIS protein levels (Fig. 56). Furthermore and very interestingly I found that MAPK inhibition also blocks oncogenic Ras mediated impairment of CREB phosphorylation (Fig. 56) highlighting the existence of a previously unreported crosstalk between the MAPK pathway and the cAMP/PKA pathway (89).

I conclude that oncogenic Ras induced de-differentiation is mainly achieved through the MAPK pathway. Complete abrogation of NIS expression however could still require the activation of an additional and unidentified pathway.

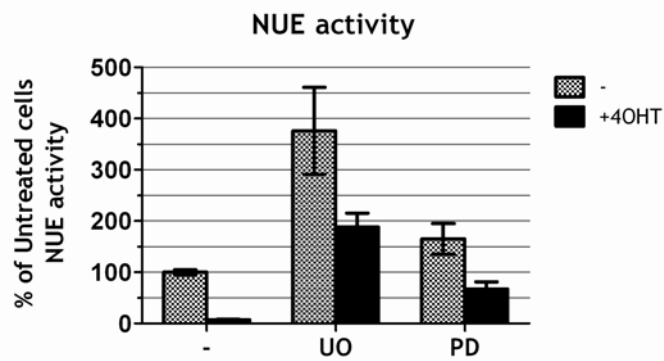


Figure 54 . MAPK inhibition restore NUE activity

NUE reporter vector was transiently transfected in C111 cells. Reporter activity was tested after 48h of culturing with or without Tamoxifen (4OHT) in the absence of further treatment (-) or with respectively MAPK inhibitors U-0126 50 μ M (UO) and PD-98059 50 μ M (PD). The activity of NUE is reported, as percentage of activity obtained respectively in untreated cells (in the absence of 4OHT and any further treatment) .

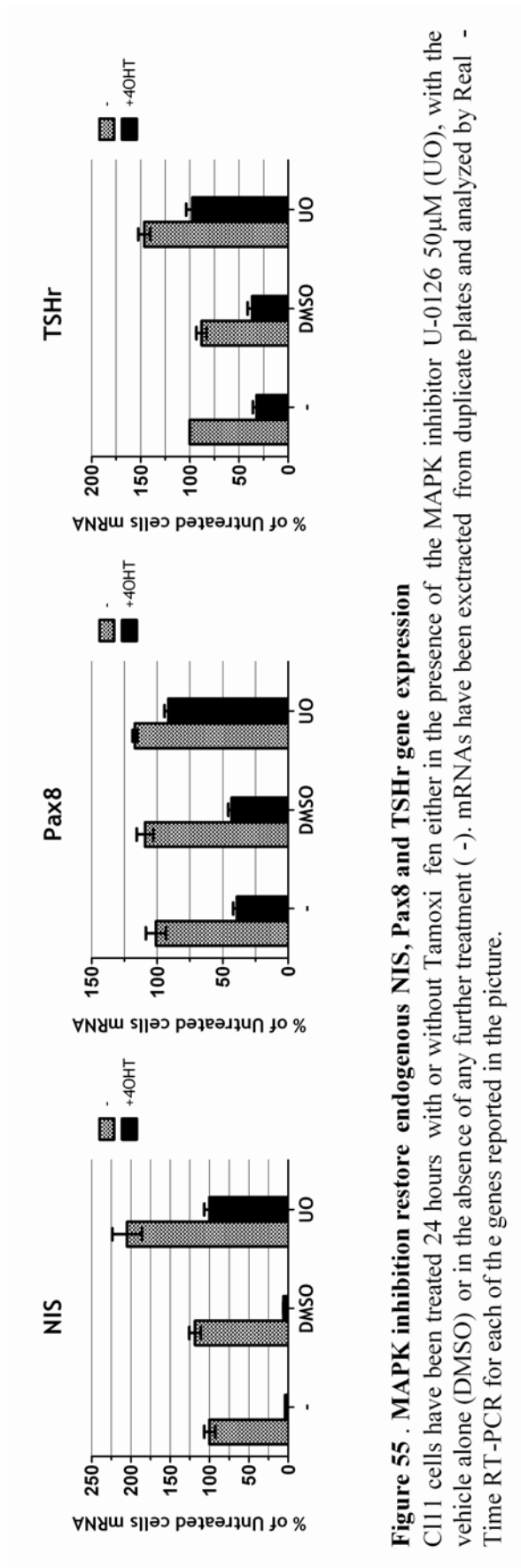


Figure 55 . MAPK inhibition restore endogenous NIS, Pax8 and TSHr gene expression
 C111 cells have been treated 24 hours with or without Tamoxifen either in the presence of the MAPK inhibitor U-0126 50µM (UO), with the vehicle alone (DMSO) or in the absence of any further treatment (-). mRNAs have been extracted from duplicate plates and analyzed by Real - Time RT-PCR for each of the genes reported in the picture.

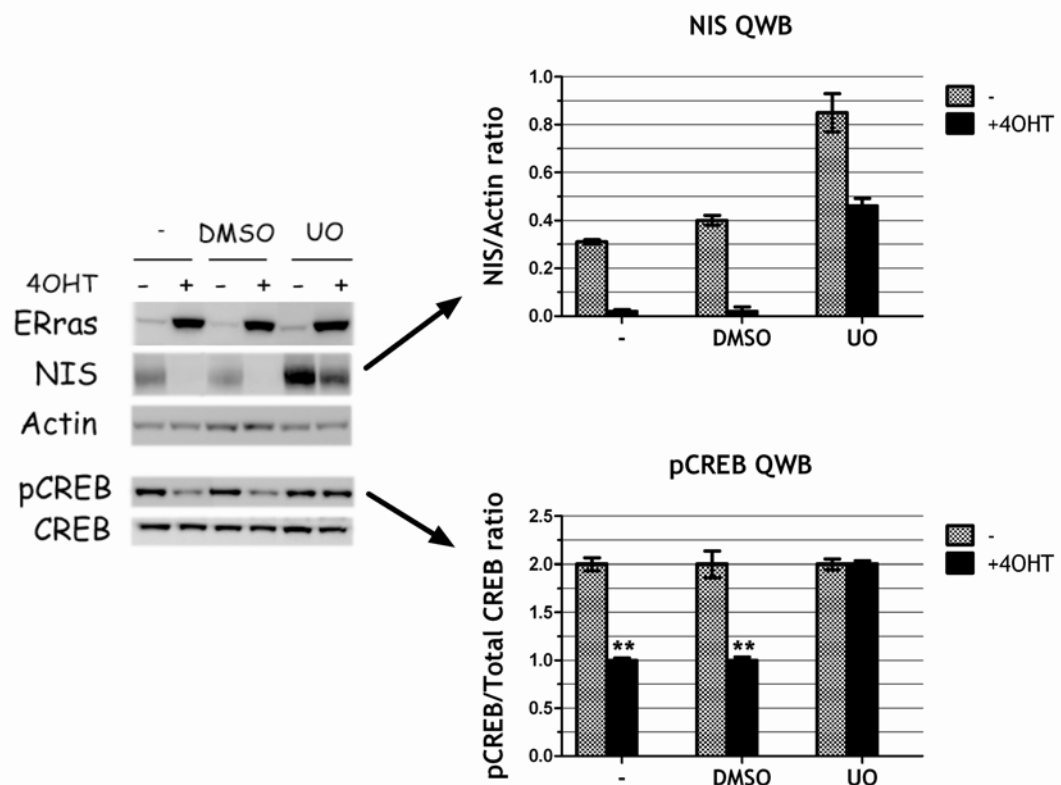


Figure 56 . MAPK inhibition restore both NIS protein expression and CREB phosphorylation at Ser133.

Quantitative Western blot (QWB) analysis of NIS expression and CREB phosphorylation at Ser133 in C111 cells treated 24 hours with or without Tamoxifen either in the presence of U-0126 (UO), with the vehicle alone (DMSO) or in the absence of any further treatment (-). NIS and pCREB signal quantitation for three independent experiments is reported on the right side. **p<0.01

10. Identification of chemical inhibitors of the MAPK pathway through a cell-based HTS assay

Since Ras/Raf/MAPK inhibition is relevant for many cancer types therapies (37-39, 252). I planned to use this cellular system to set up a cell-based assay in order to screen the inhibitory activity of a 50000 compound library towards this pathway .

10.1. GFP expression, driven by the NIS gene enhancer, is sensitive to oncogenic Ras activation

I engineered a C111-derived cell line which stably express GFP under the control of the NIS gene enhancer NUE which we know to be regulated by oncogenic Ras in our cells (Fig.4). Thus GFP expression, driven by the NUE enhancer, should be sensitive to ERKs^{V12} activation by Tamoxifen (Fig.57). Indeed, in this C111-derived cell line called NG6, GFP expression is turned off by addition of Tamoxifen and can be restored by removal of Tamoxifen (Fig. 58), exactly in the same way we observed for endogenous NIS gene (Fig. 53).

10.2. Set-up of cell-based HTS assays

I set up two different automatable assay formats aimed to detect MAPK inhibitory activity of compounds in 96-well plates. (Fig. 59). The first assay, GFP-based, involves the use of the NG6 cell line which stably express GFP under the control of NIS enhancer NUE. The second assay, Luciferase based, involves transient transfection of a NUE-driven luciferase reporter vector in C111 cells. In both assays, cells are treated with Tamoxifen for 5days in order to allow oncogenic Ras to completely inhibit NUE activity. In this way the activity of NUE and thus the expression of the reporter gene, GFP or Luciferase depending on the protocol, is abolished. At this point cells are treated 48h additional hours with Tamoxifen plus the compound that is to be tested.

In order to validate such assays I tested them with increasing doses of the known inhibitor of MAPK pathway U-0126 (Fig. 60). Results indicate that in the definitive automated setup (see “materials and method” section) both assays were quantitatively sensitive to MAPK inhibition in a comparable and reproducible way.

I conclude that these cellular assays are suitable to test the inhibitory activity of lead compounds toward the MAPK pathway.

10.3.Pilot Screen

In order to evaluate suitability of the assays to screen the entire library of compounds I performed an initial Pilot Screen (PS) by using a small pool of compounds (3000). Aim of the pilot screen is 1) to evaluate the frequency of compounds that show activity in the assay (Hits) 2) evaluate reproducibility of obtained results.

For each kind of cell-based assay I performed the PS twice using a starting compound concentration of 10 μ M. Compounds activity was expressed as fold activation (reporter gene activity induced by the compound over reporter gene activity obtained in untreated cells). Fold activations obtained, respectively for each kind of assay, from duplicate PS were then plotted against each other (scatter plot) in order to understand reproducibility of results (Fig. 61). In the scatter plot reproducibility of results can be immediately visualized. Infact non-reproducible result tend to spread in the graph away from the bisector line while reproducible results tends to be concentrated on the bisector line. Furthermore the scatter plot also allow to visually appreciate standard deviation of results distribution by looking at the length of the bisector line covered by results. The scatter plots obtained respectively for the Luciferase-based and for the GFP-based assay clearly showed that the GFP assay was much more reproducible. This conclusion is mathematically and quantitatively demonstrated by looking at the R squared values obtained for each assay as indicated in Fig. 61.

Frequency of Hits for the GFP assay was determined by evaluating 1) parameters (average value μ and standard deviation σ) of the Gaussian distribution of obtained “fold activation” (Fig.62) 2) number of compounds whose “fold activation” were greater than the average plus three standard deviations ($p < 0.03$) (Fig. 62). The frequency of hits obtained from the GFP-based assay was 13 out of 3000 which is an acceptable frequency. I thus decided to keep compounds concentration at 10 μ M for the 50k library screening (Lead Screen).

10.4. Lead Screen

Since reproducibility of the GFP based assay, as seen in the pilot screen, was largely better than that of the Luciferase-based assay we screened the 50K compound library with the GFP-based assay. The screening of the library resulted in 312 compounds (Hits) which induced a significant ($p < 0.03$) increase of GFP expression (Fig. 63) over the value obtained in untreated cells.

10.5. Hits confirmation and specificity screen

The activity of the Hits obtained from the lead screen have been confirmed within the same GFP assay format by re-testing the activity of hits in triplicates (Fig. 64). I confirmed 244 out of 312 hits. I next tested the specificity of these hits by testing their autonomous fluorescence in a GFP negative cell line. I confirmed the specificity of 182 out of 244 hits (Fig. 65).

10.6. EC50 determination and confirmatory screening

For each of the specific Hits (182) I performed dose-response curves in order to determine 1) EC50 concentration and 2) the maximal response (TOP) obtainable with each compound (Fig. 66). Compounds were ranked and selected on the basis of these parameters.

In Figure 67 are shown dose-response curves relative to selected best hit compounds (29) and their relative structures and where applicable their EC50 and TOP values. Results were confirmed by testing their action in dose-response curves within the technically unrelated luciferase based-assay (confirmatory screening).

Unfortunately all the tested hits gave a fold activation at saturation lower than the one obtained with the known MAPK inhibitor U-0126 (compare Fig. 60 with Fig. 67). Furthermore, most of the hits had very high EC50 values (25-50 μ M).

10.7.Hits activity on MAPK pathway and endogenous NIS gene expression

For each of the selected 29 Hit compounds I choose the working concentration on the basis of the dose-response curves shown in Figure 67. The concentration used are reported in Figure 68 and represents the lowest concentration that determines the mximal effect. I analysed the effect of each the Hits on the MAPK pathway by evaluating their ability to inhibit oncogenic Ras induced ERK1/2 phosphorylation (Fig. 69) and their ability to restore transcription of the NIS gene by Real-Time RT-PCR (Fig. 70). Infact I wish that selected compounds counteract Ras oncogene induced repression of NIS gene since NIS gene expression in thyroid cancers is required for the success of anti-cancer therapy(253). My results shows that only 2 of the hits (F and Y) can modestly inhibit ERK phosphorylation, even though not extensively, and that this modest inhibition is indeed associated for both compounds with a 2 fold increase of NIS gene expression. Furthermore I found 4 additional compounds (G, K, Z1 and Z3) that can stimulate NIS expression (over 2 fold) apparently without affecting ERK phosphorylation. Since I'm interested in the pathways which regulate NIS expression these chemicals could be used as a ligand in affinity chromatography to identify new genes relevant to NIS regulation.

Even though the effects of the found compounds are not large and the effective concentration very high, their structures (Fig. 71) can be optimized in order to ameliorate these parameters and test their effectiveness on humans thyroid cancers cell lines.

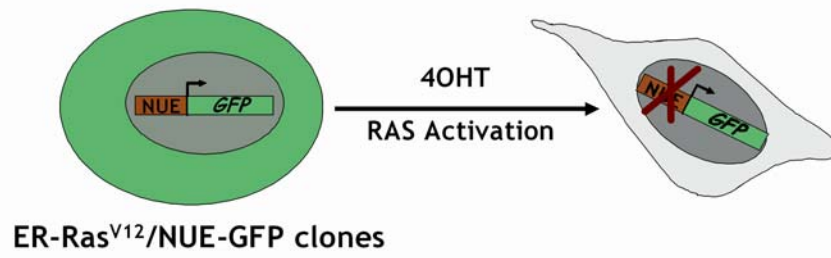


Figure 57. Schematic representation of NG6 stable cell line

NG6 cell line express GFP and ERRAS^{V12}. This cell line is normally fluorescent due to GFP expression driven by the NIS gene enhancer NUE. After Ras oncogene activation, through addition of Tamoxifen, the cells loose their fluorescence since NUE activity is inhibited and so is GFP expression.

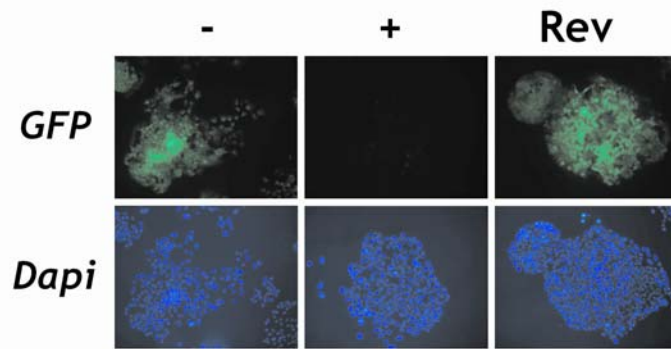


Figure 58. NG6 fluorescence is regulated by oncogenic Ras as well as the endogenous NIS gene.

C111 cells were treated 5 weeks with Tamoxifen (+) and then cultured for an additional week in the absence of Tamoxifen (REV). Untreated C111 cells (-) kept in culture for the same amount of time were also analysed. Cells were fixed, colored with the nuclear staining (DAPI) and analysed through microscopy to detect green fluorescence (GFP). Shown are representative images of these cells at 20x magnitude.

The HTS cell-based assay formats

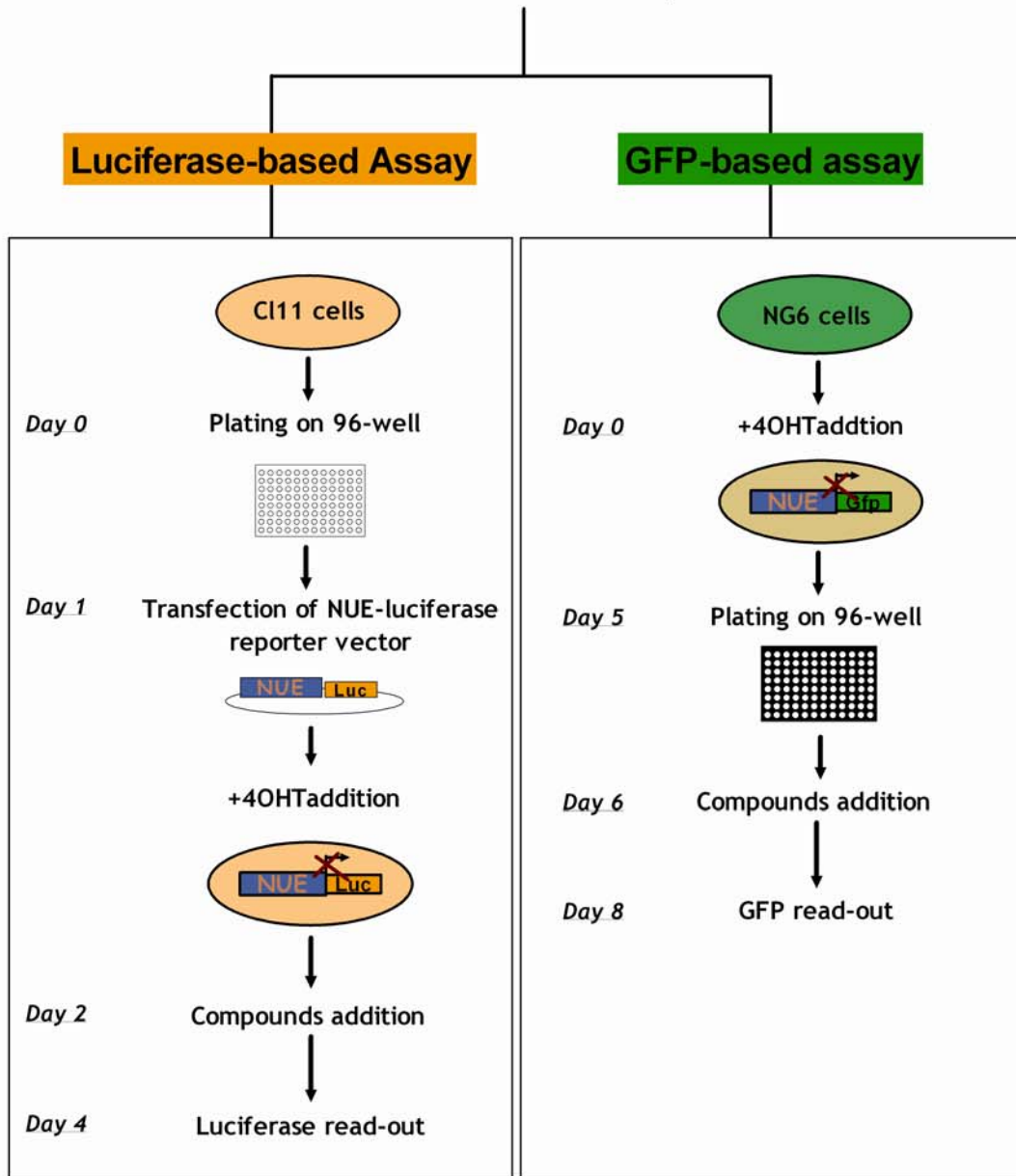


Figure 59. The HTS assay formats scheme .

Luciferase-based assay. C111 cells (FRTL-5 derived cell line stably expressing the conditional oncoprotein ERRas^{V12}) were plated on 96-well plates on day 0. NUC-luciferase reporter vector was transfected on day 1. Tamoxifen (4OHT) 100nM was added 3 hours after transfection in order to allow oncogenic Ras to turn off NUC activity and thus Luciferase transcription. On Day 2 compounds were added to the cells in order to test their ability to restore NUC activity. Read -out was performed 48hours after compound addition on Day4. GFP-based assay. NG6 cells (C111 derived cell line stably expressing both GFP under NUC control and the conditional oncoprotein ERRas^{V12}) were treated with Tamoxifen (4OHT) 100nM on Day 0 and kept under Tamoxifen treatment for 5 days in order to allow oncogenic Ras to turn off NUC activity and degradation of pre -existing GFP protein. On Day 5 cells were plated on 96-well plates still in the presence of Tamoxifen . On Day 6 compounds were added to the cells in order to test their ability to restore NUC activity. Read -out was performed 48hours after compound addition on Day8.

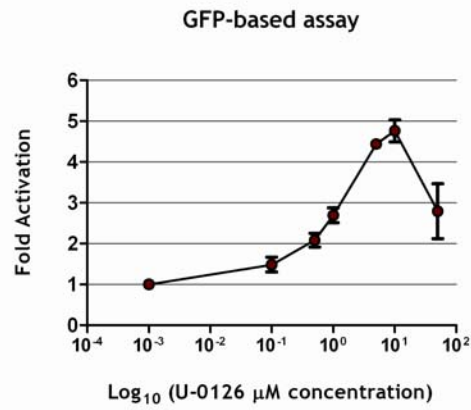
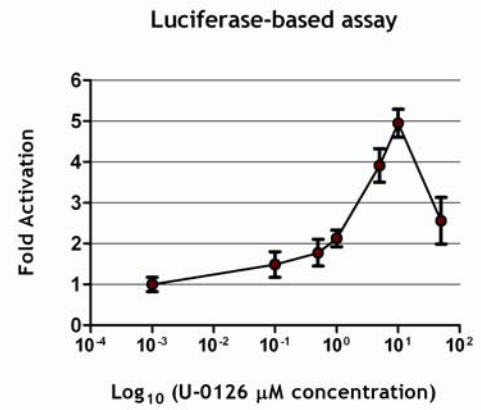
A**B**

Figure 60. Dose-response curves to MAPK inhibitor U-0126.

Dose-response curves were performed for each assay as described in materials and methods. Assay formats are schematized in Fig x. Reporter gene activity obtained for each point was converted in Fold activation over the activity observed in the untreated cells. For each assay format Fold activation was plotted versus the Logarithm of U-0126 concentration as indicated A. GFP-based assay format. B. Luciferase-based assay format

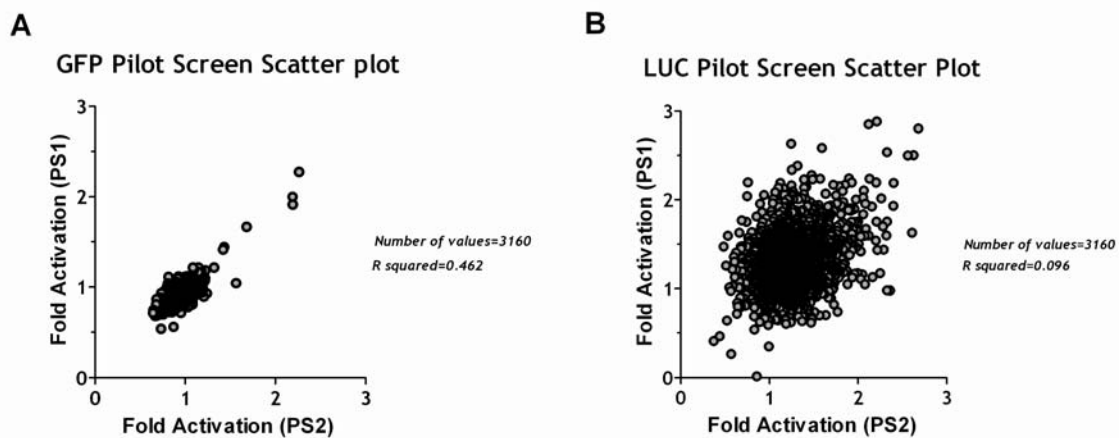


Figure 61. GFP-based assay format is much more reproducible than the Luciferase -based one Scatter plots of Pilot screens. Pilot screens were performed as described in materials and methods and schematized in Fig x. Reporters gene activity obtained for each tested compound were converted in Fold activation over the activity of the untreated cells. For each assay format, Fold activation obtained in the first Pilot Screen (PS1) were plotted versus Fold Activation obtained in the second Pilot Screen (PS2) A. GFP-based assay format. B. Luciferase -based assay format.

GFP Pilot Screen Results Distribution

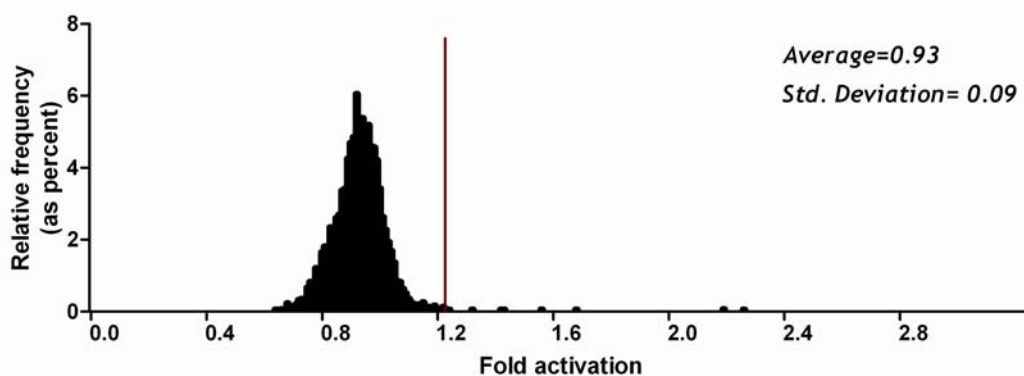


Figure 62. Analysis of Pilot Screen results obtained with the GFP-based assay format

Reporters gene activity obtained for each tested compound were converted in Fold activation over the activity of the untreated cells. Distribution of obtained Fold activations is shown in the figure. Average and standard deviation of the distribution have been determined. The Red line represents the threshold (average fold activation + 3x standard deviations) over which Fold activations value are not considered random anymore but determined by the compound action. Compounds, whose resulting Fold activation fall on the right side of the red line were considered active (hits).

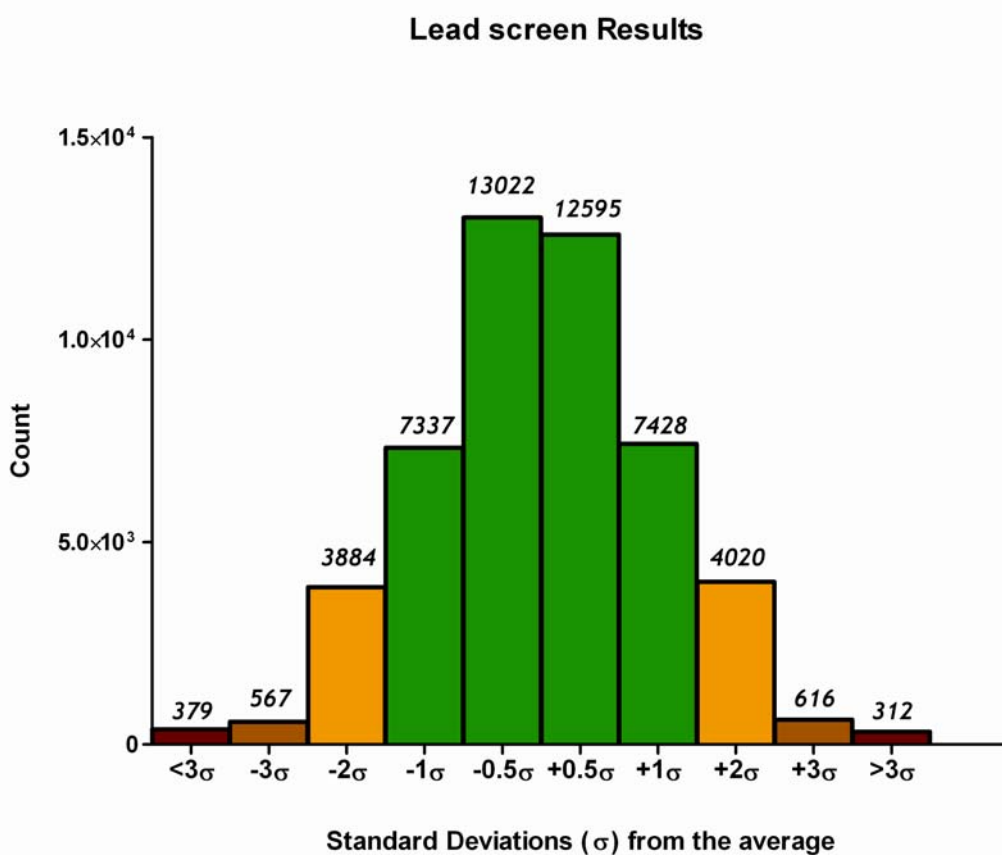
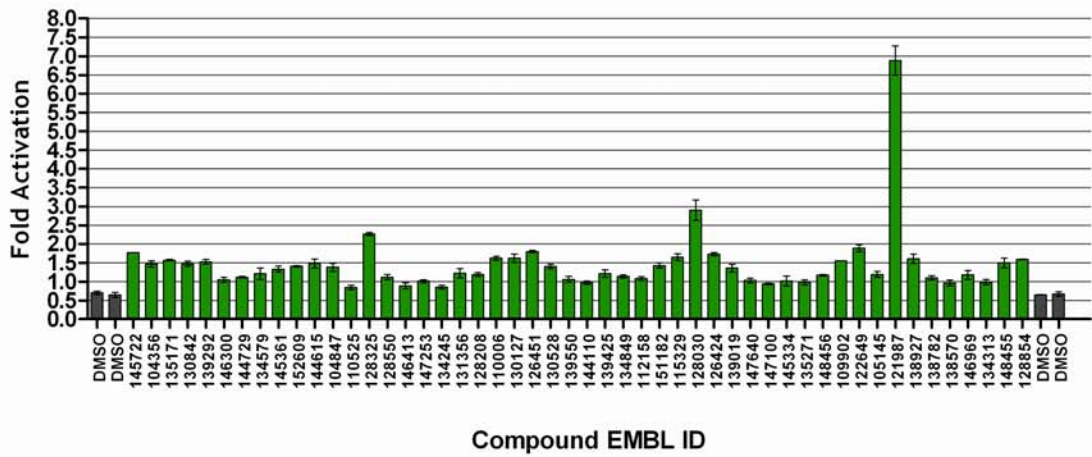


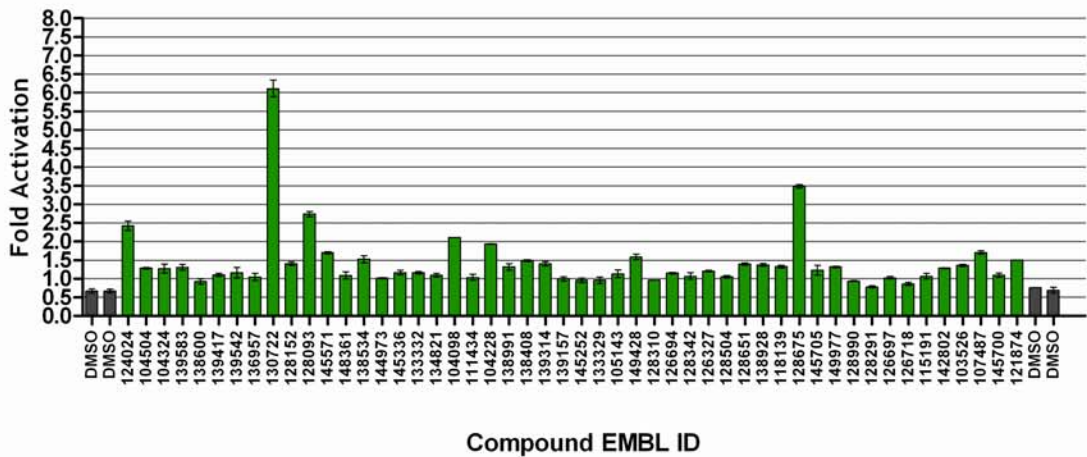
Figure 63. Lead screen results .

Results distribution has been characterized in terms of average and standard deviation (σ). Results have been binned considering their distance from the average in terms of multiples of standard deviations (σ). Compounds have been considered hits when their resulting fold activation was greater than the average $+3\sigma$.

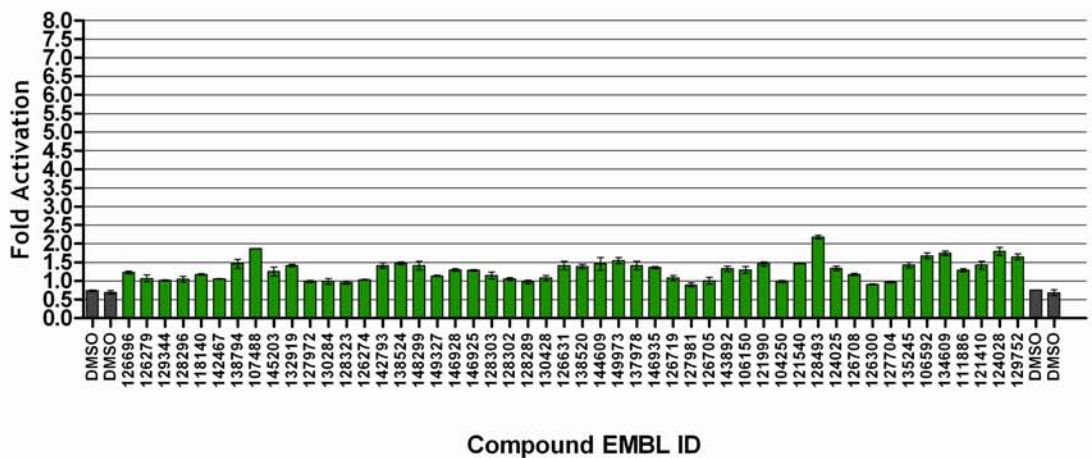
Hits confirmation



Compound EMBL ID



Compound EMBL ID



Compound EMBL ID

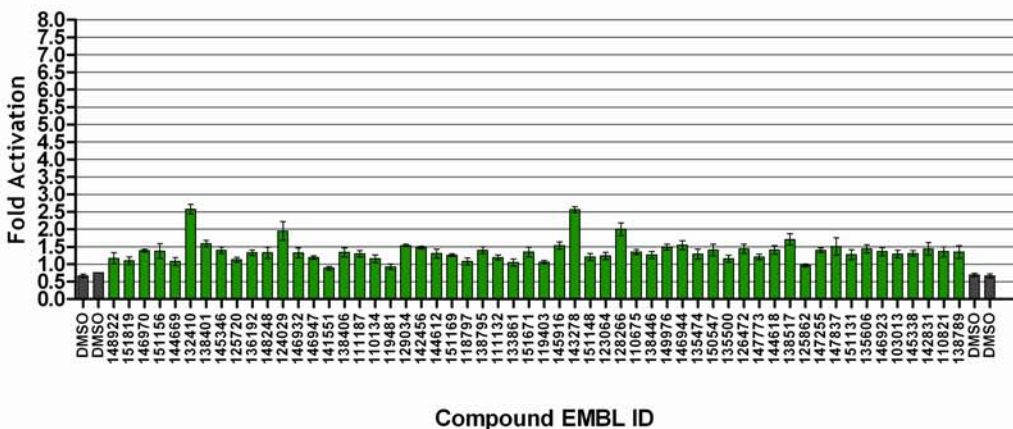
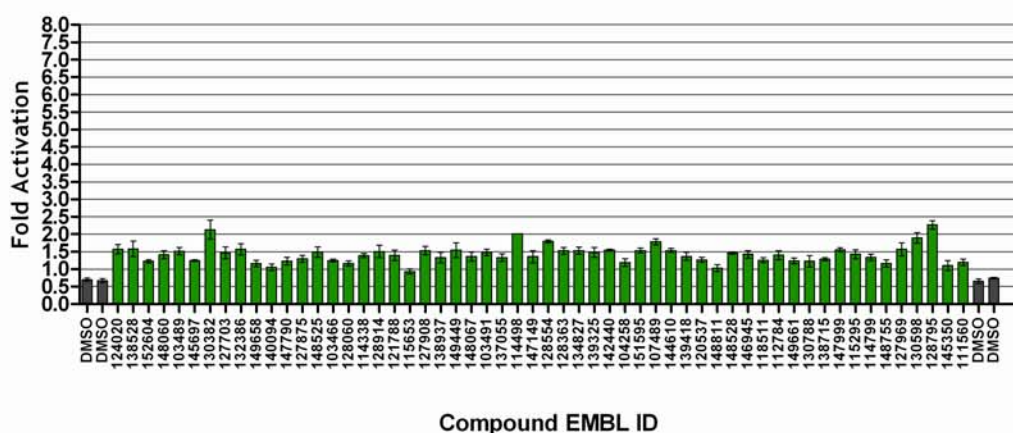
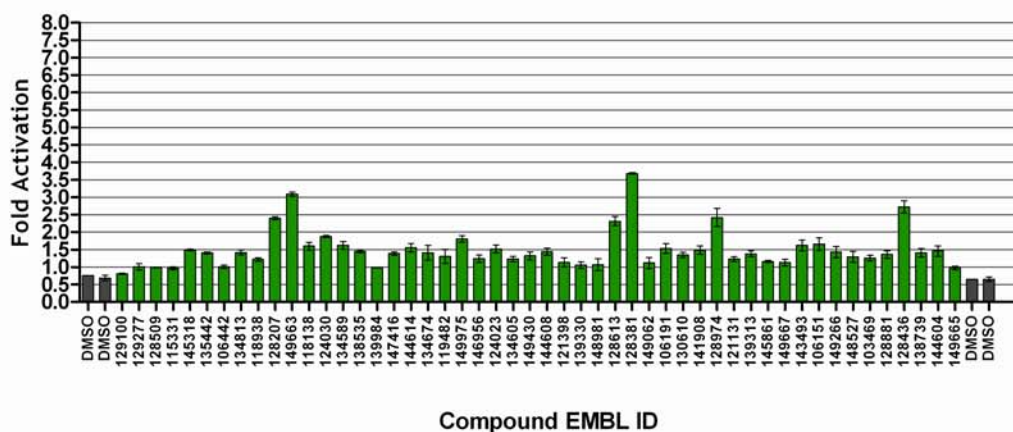
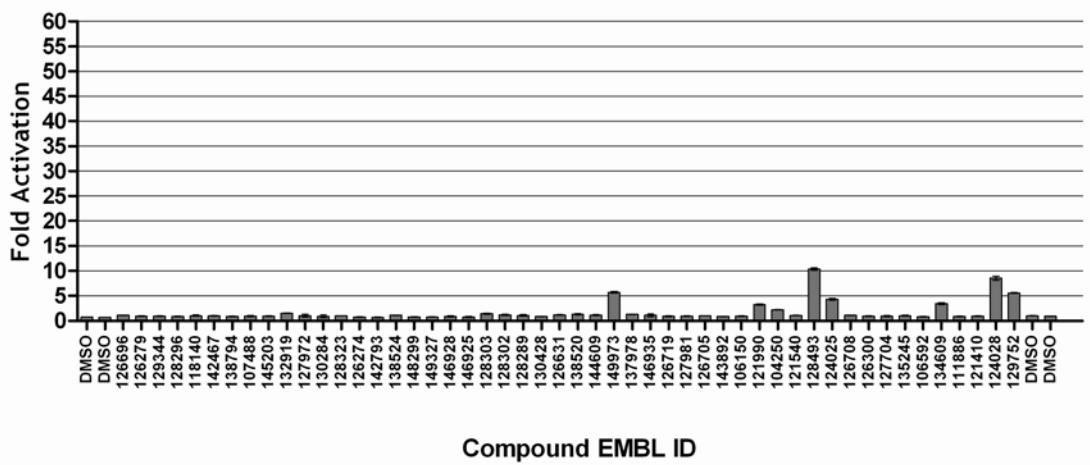
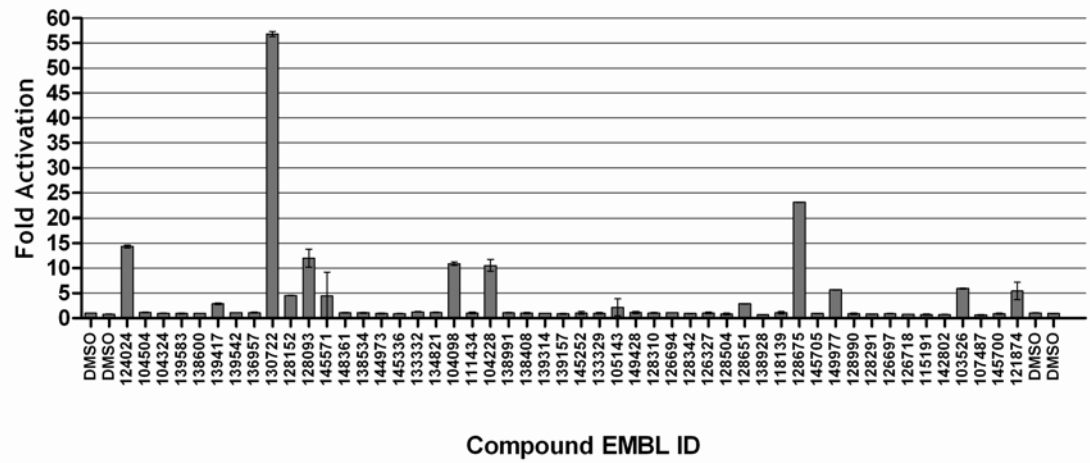
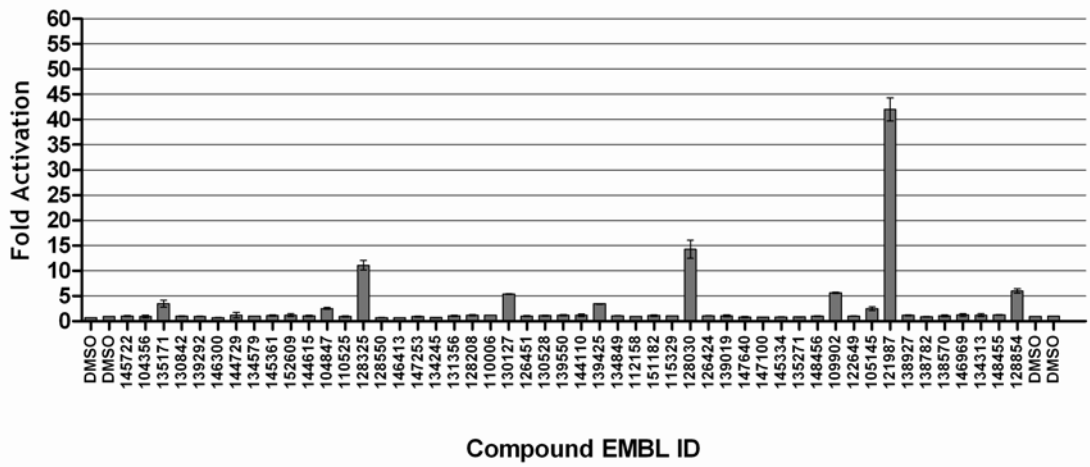


Figure 64. Hits confirmation

The activity of each of the Hit compounds identified through the lead screen was re -tested within the GFP-assay in triplicate to confirm their ability to increase fluorescence. Activity of the compound is expressed as fold activation over the fluorescence observed in Tamoxifen -only treated cells. DMSO (compounds vehicle) has been used in order to determine the threshold over which compounds should have been called active. We have considered active all compounds whose fold activation was significantly ($p < 0.01$) higher than the DMSO treated cells.

Hits specificity



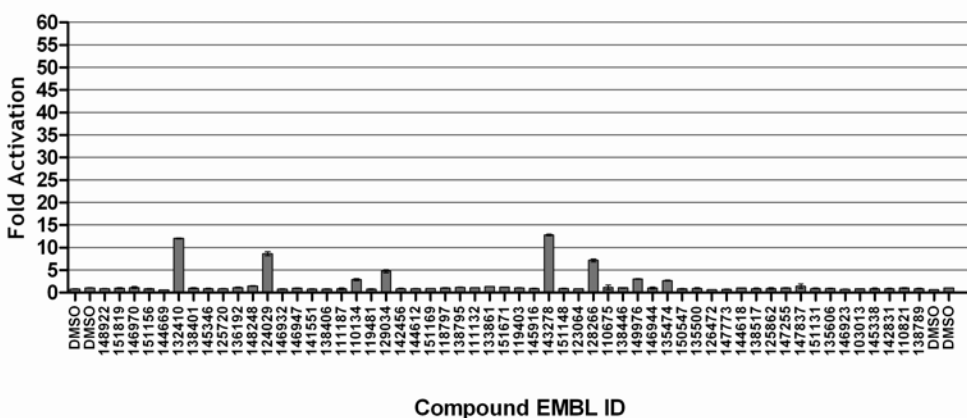
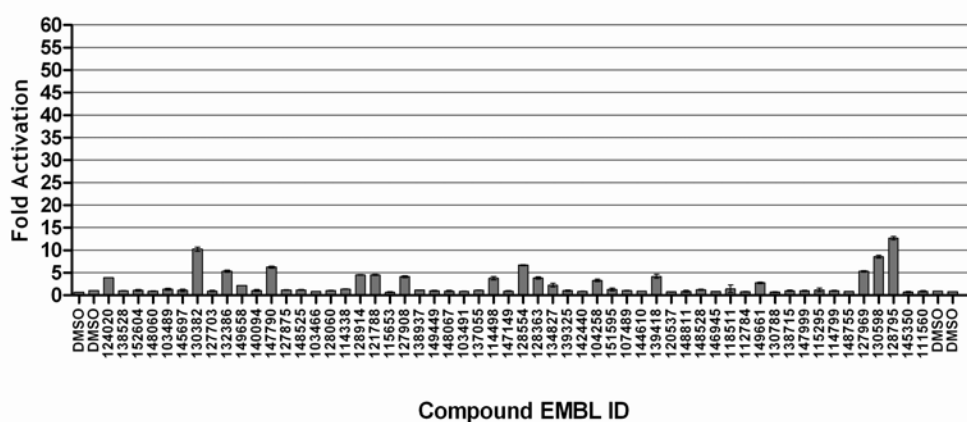
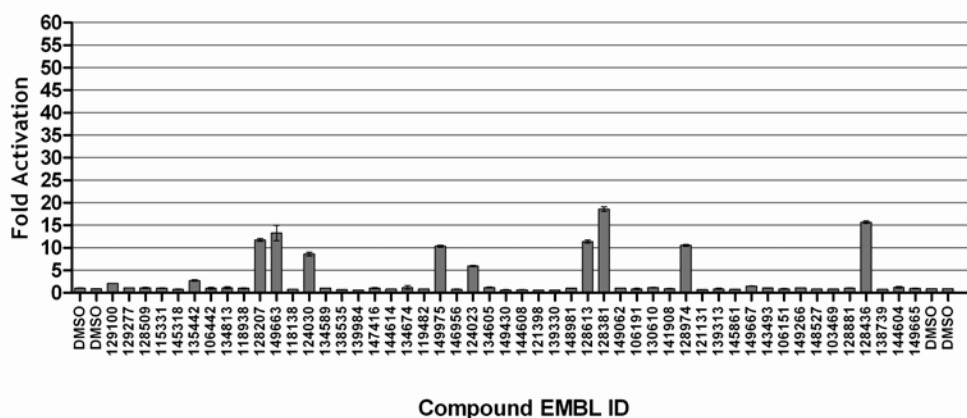


Figure 65. Hits specificity determination

In order to determine whether positivity of confirmed Hit compounds was due to autonomous fluorescence properties of the molecules I performed the same GFP -assay format but using a negative GFP cell line (CH1). Activity of the compound is expressed as fold activation over the fluorescence observed in Tamoxifen-only treated cells. DMSO (compounds vehicle) has been used in order to determine the threshold over which compounds should have been called active. We have considered false-positives all compounds whose fold activation was at least 5fold the value obtained in DMSO treated cells.

The shape of Dose-response curves

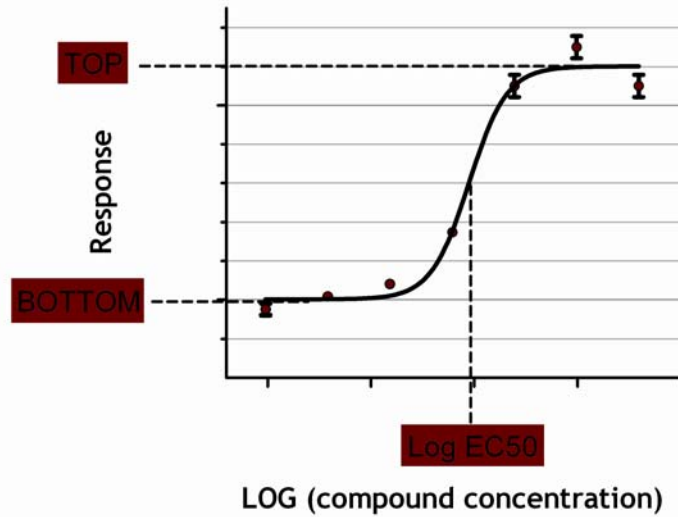
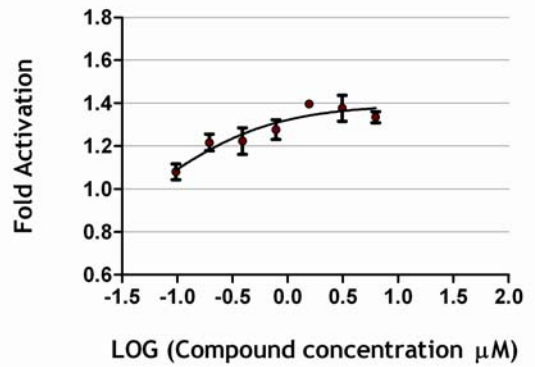
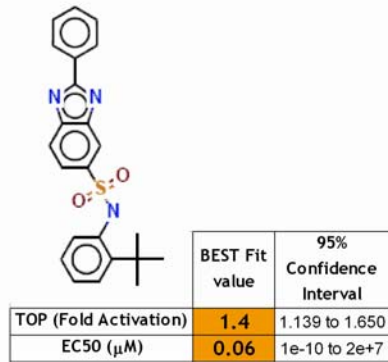


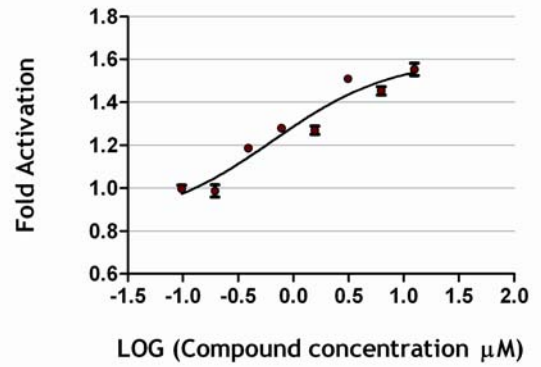
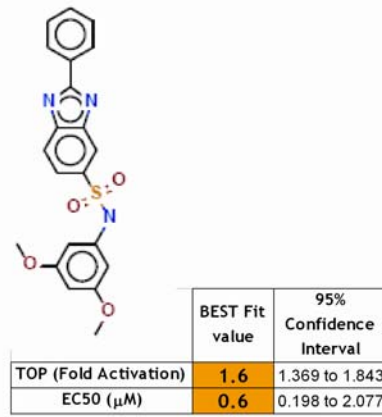
Figure 66. Dose-response curves

A standard dose response curve is defined by four parameters: the baseline response (bottom), the maximum response (Top), the slope (Hill slope), and the drug concentration that provokes a response halfway between baseline and maximum (EC50). Non-linear regression for sigmoidal dose-response curves was performed through the use of Graphpad prism software.

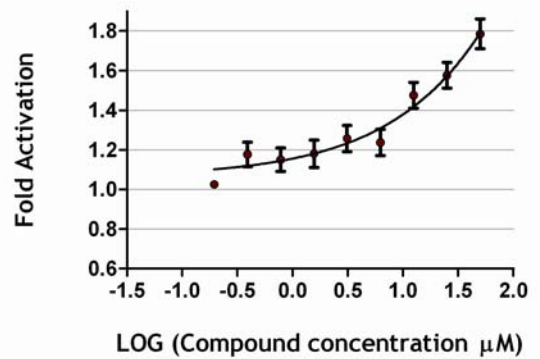
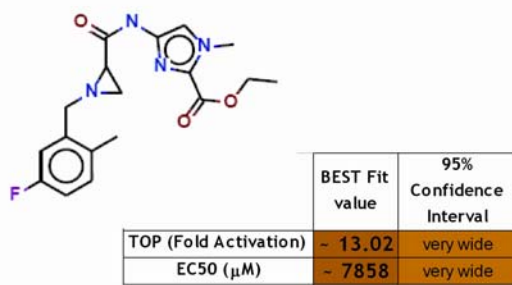
A



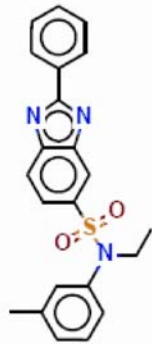
B



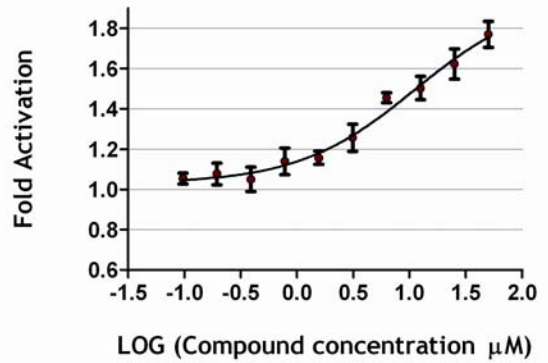
C



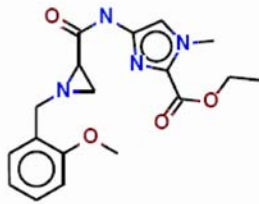
D



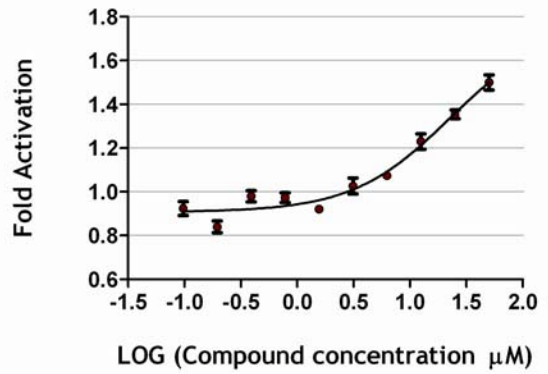
	BEST Fit value	95% Confidence Interval
TOP (Fold Activation)	2.0	1.372 to 2.550
EC50 (μM)	11.1	2.215 to 55.94



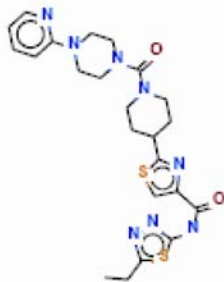
E



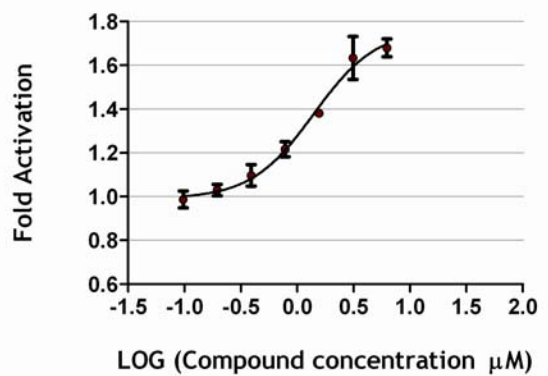
	BEST Fit value	95% Confidence Interval
TOP (Fold Activation)	1.8	1.197 to 2.322
EC50 (μM)	22.2	5.41 to 90.98



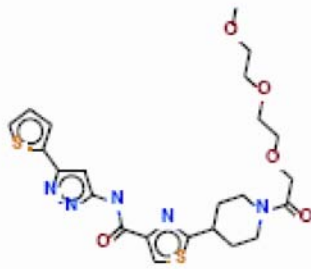
F



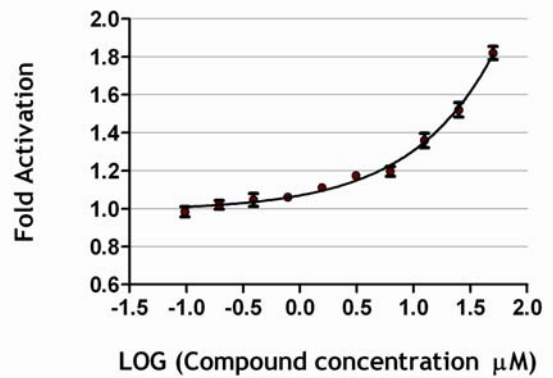
	BEST Fit value	95% Confidence Interval
TOP (Fold Activation)	1.8	1.536 to 1.996
EC50 (μM)	1.4	0.852 to 2.297



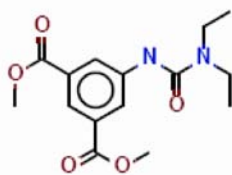
G



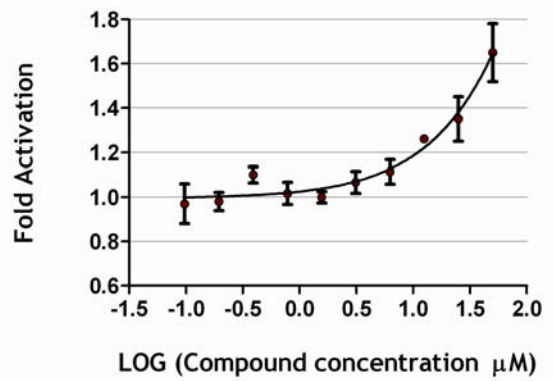
	BEST Fit value	95% Confidence Interval
EC50 (μM)	- 821.9	very wide
	- 5e+06	very wide



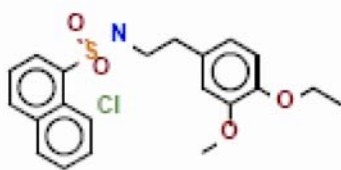
H



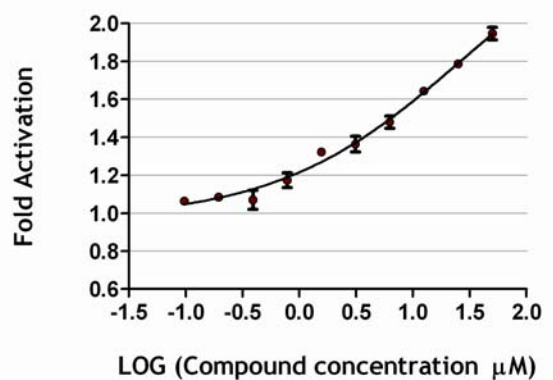
	BEST Fit value	95% Confidence Interval
TOP (Fold Activation)	- 9.654	very wide
EC50 (μM)	- 1164	very wide



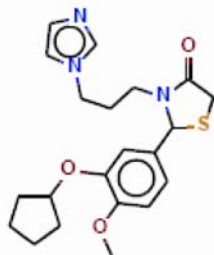
I



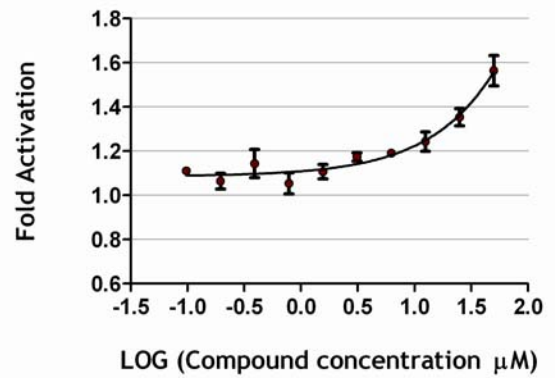
	BEST Fit value	95% Confidence Interval
TOP (Fold Activation)	2.7	1.3 to 4.0
EC50 (μM)	28.0	1.7 to 449



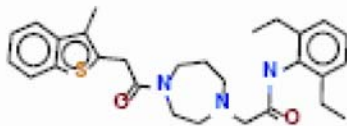
J



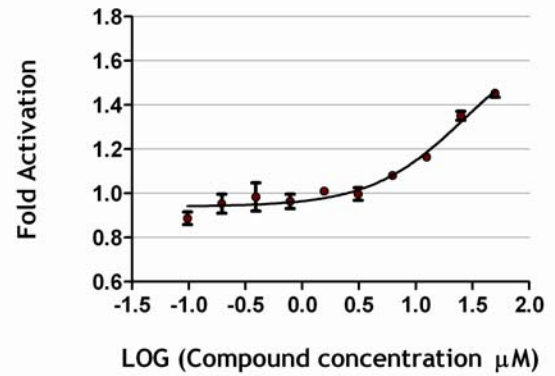
	BEST Fit value	95% Confidence Interval
TOP (Fold Activation)	- 55.60	very wide
EC50 (μM)	- 23408	very wide



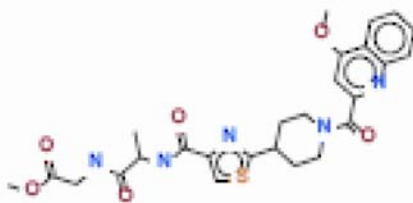
K



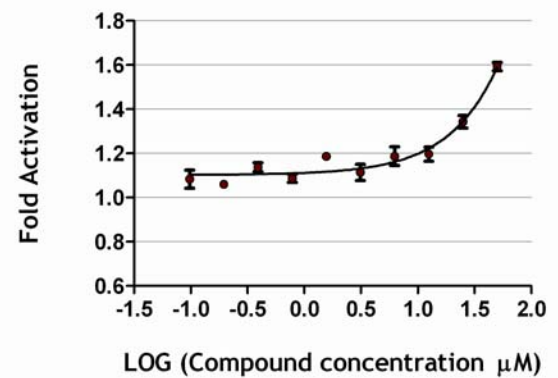
	BEST Fit value	95% Confidence Interval
TOP (Fold Activation)	1.7	1.047 to 2.432
EC50 (μM)	27.2	4.679 to 157.8



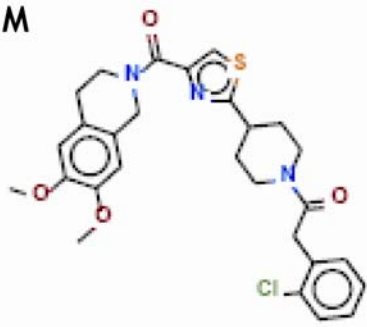
L



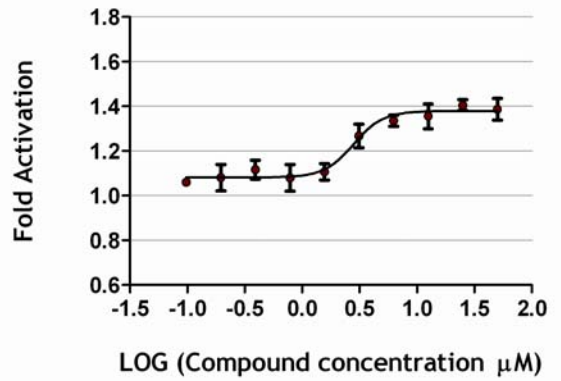
	BEST Fit value	95% Confidence Interval
TOP (Fold Activation)	- 147.6	very wide
EC50 (μM)	- 14239	very wide



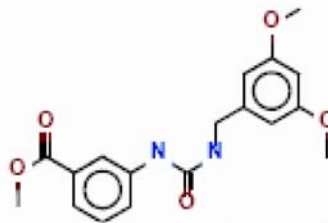
M



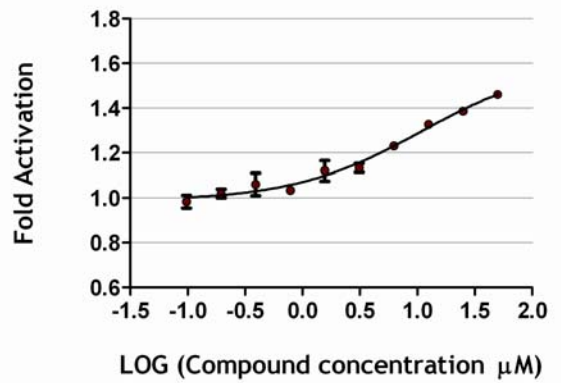
	BEST Fit value	95% Confidence Interval
TOP (Fold Activation)	1.4	1.328 to 1.429
EC50 (μM)	2.8	1.991 to 3.937



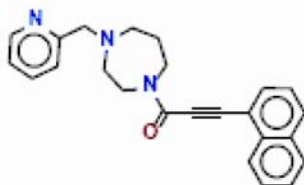
N



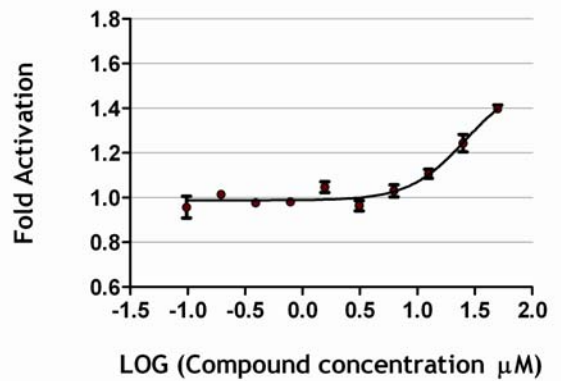
	BEST Fit value	95% Confidence Interval
TOP (Fold Activation)	1.6	1.235 to 1.980
EC50 (μM)	11.0	2.236 to 54.11



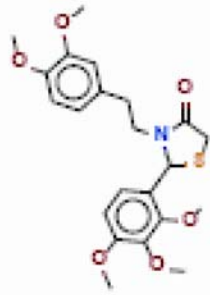
O



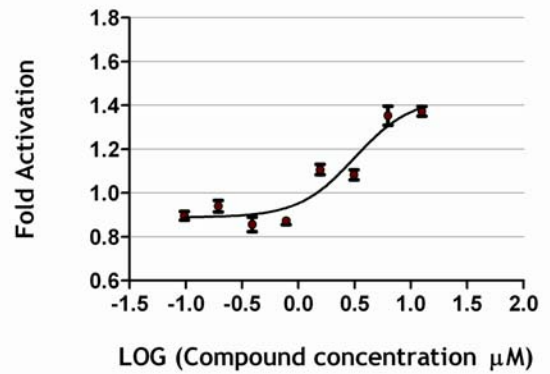
	BEST Fit value	95% Confidence Interval
TOP (Fold Activation)	1.5	1.192 to 1.860
EC50 (μM)	26.2	11.14 to 61.58



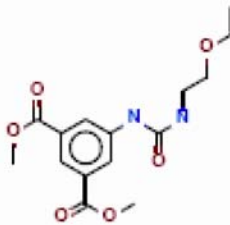
P



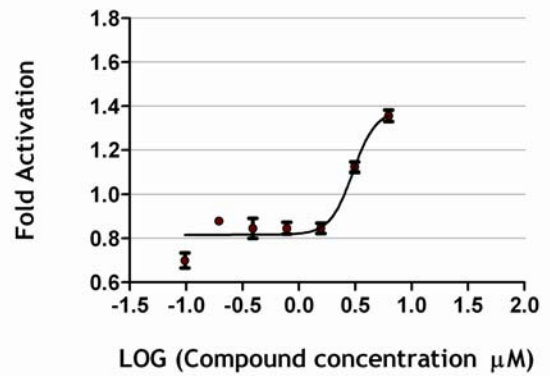
	BEST Fit value	95% Confidence Interval
TOP (Fold Activation)	1.4	1.242 to 1.631
EC50 (μM)	3.3	1.779 to 5.714



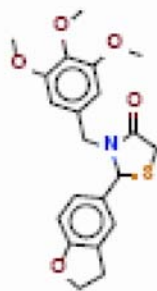
Q



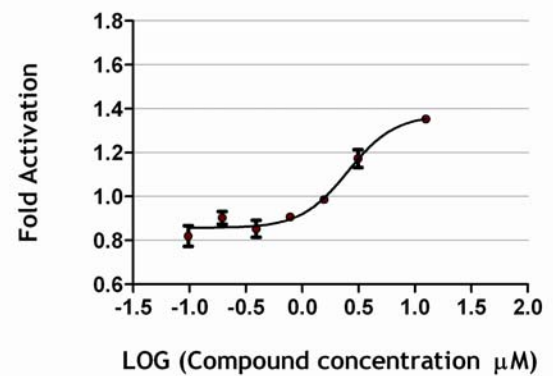
	BEST Fit value	95% Confidence Interval
TOP (Fold Activation)	1.4	1.234 to 1.528
EC50 (μM)	3.0	2.445 to 3.689



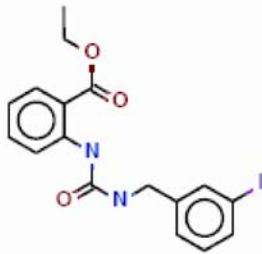
R



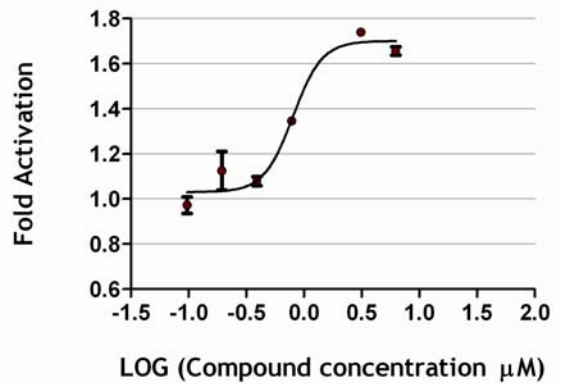
	BEST Fit value	95% Confidence Interval
TOP (Fold Activation)	1.4	1.281 to 1.462
EC50 (μM)	2.5	1.875 to 3.414



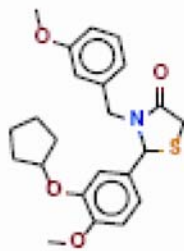
S



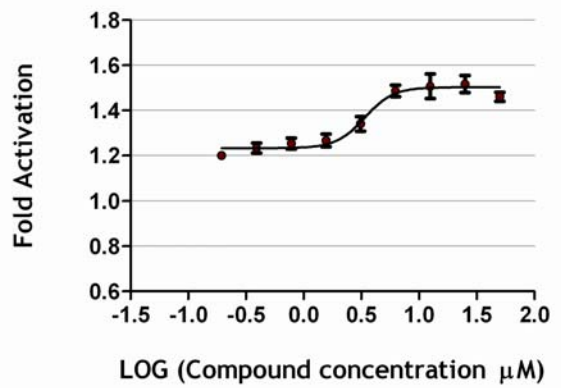
	BEST Fit value	95% Confidence Interval
TOP (Fold Activation)	1.7	1.631 to 1.770
EC50 (μM)	0.8	0.666 to 0.968



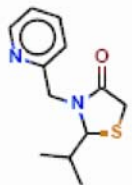
T



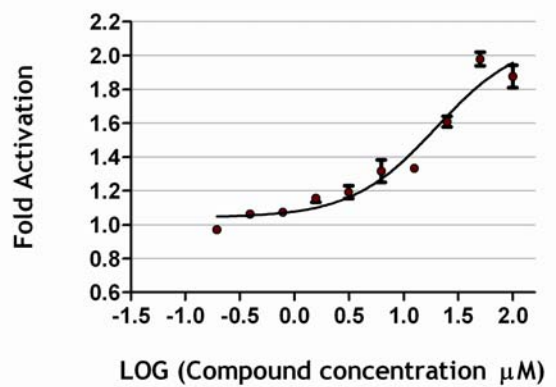
	BEST Fit value	95% Confidence Interval
TOP (Fold Activation)	1.5	1.462 to 1.543
EC50 (μM)	3.4	2.522 to 4.518



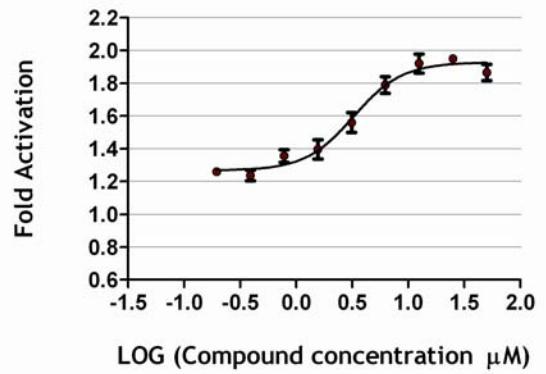
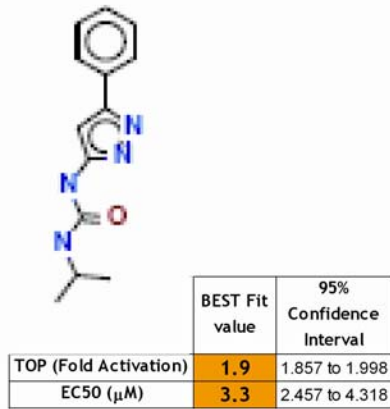
U



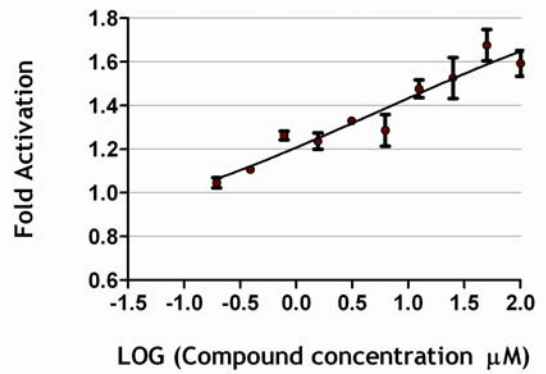
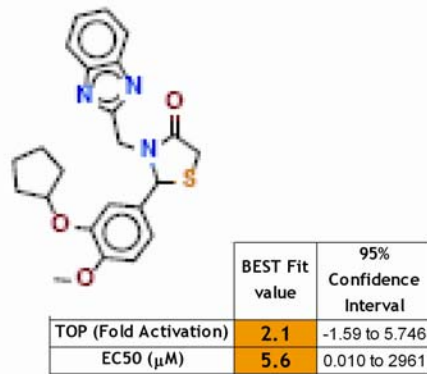
	BEST Fit value	95% Confidence Interval
TOP (Fold Activation)	2.1	0.956 to 1.126
EC50 (μM)	19.8	9.530 to 41.26



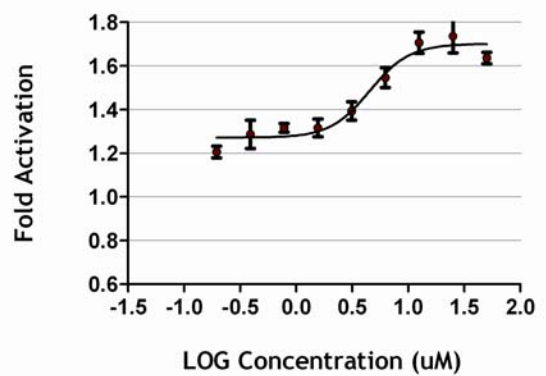
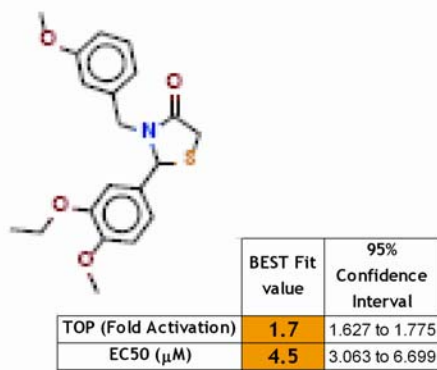
V



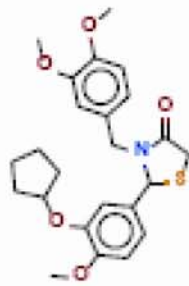
W



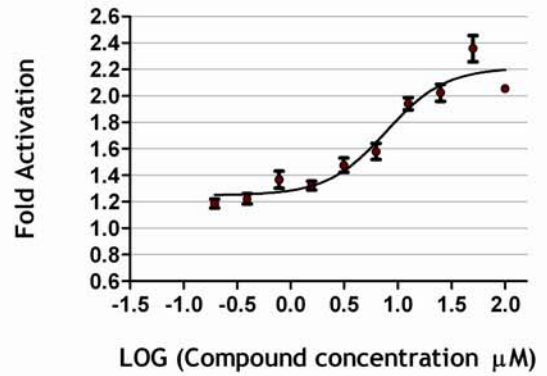
X



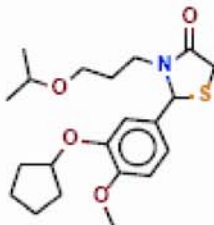
Y



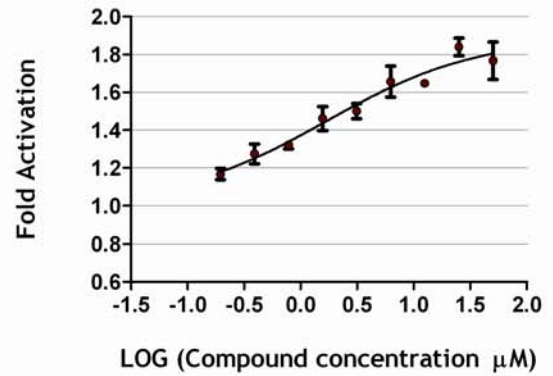
	BEST Fit value	95% Confidence Interval
TOP (Fold Activation)	2.2	2.061 to 2.362
EC50 (μM)	7.8	5.237 to 11.54



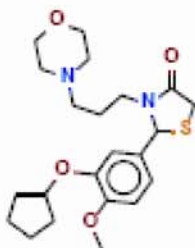
Z



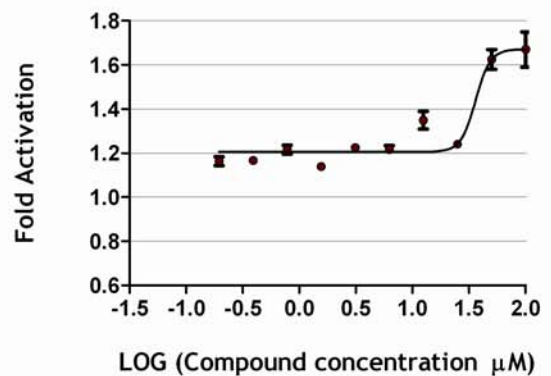
	BEST Fit value	95% Confidence Interval
TOP (Fold Activation)	1.9	1.487 to 2.298
EC50 (μM)	1.7	0.242 to 11.95



Z1

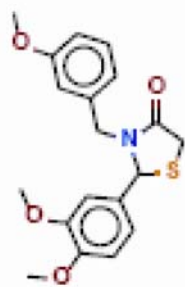


	BEST Fit value	95% Confidence Interval
TOP (Fold Activation)	1.7	1.580 to 1.762
EC50 (μM)	36.1	25.27 to 51.54

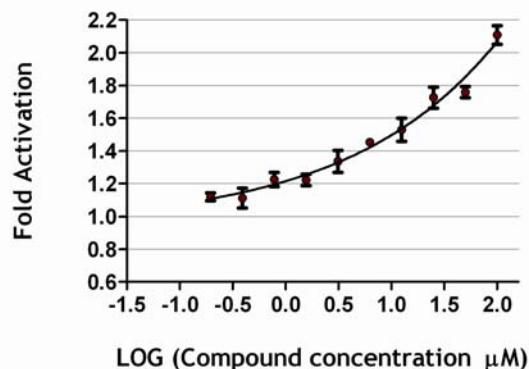


1539-01546

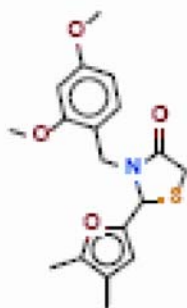
Z2



	BEST Fit value	95% Confidence Interval
TOP (Fold Activation)	~ 303,4	very wide
EC50 (μM)	~ 7e+09	very wide



Z3



	BEST Fit value	95% Confidence Interval
TOP (Fold Activation)	1.4	1.302 to 1.468
EC50 (μM)	0.8	0.179 to 3.909

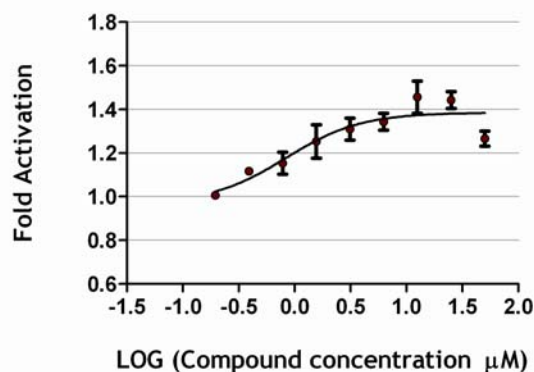


Figure 67. Selected Hits Dose-response curves

For each compound (identified by the correspondent letter in the figure) is reported 1) its structure 2) the dose response curve obtained within the GFP based assay as described in the “materials and methods” section. In the graph each dot represent the experimental values while the curve describing the experimental values was calculated through a non-linear regression analysis as described in the “materials and methods” section 3) a tab reporting the best-fitting values calculated from the dose-response curve for the maximum response (Top) and the drug concentration that provokes a response halfway between baseline and maximum (EC50). Also reported is the 95% confidence interval for those values.

compound	concentration (μM)
DMSO	0.5%
U-0126	10
A	6
B	12
C	50
D	50
E	50
F	6
G	50
H	50
I	50
J	50
K	50
L	50
M	12
N	50
O	50
P	12
Q	6
R	12
S	3
T	12
U	50
V	25
W	50
X	25
Y	50
Z	50
Z1	100
Z2	100
Z3	25

Figure 68. Selected Hit Compounds chosen working concentration.

On the basis of the dose-response curves shown in Fig. 67 I selected for each compound the appropriate concentration as the lower one that produce the maximal effect.. Each compound has been indicated with the letter reported in Fig. 67.

ERK phosphorylation inhibition

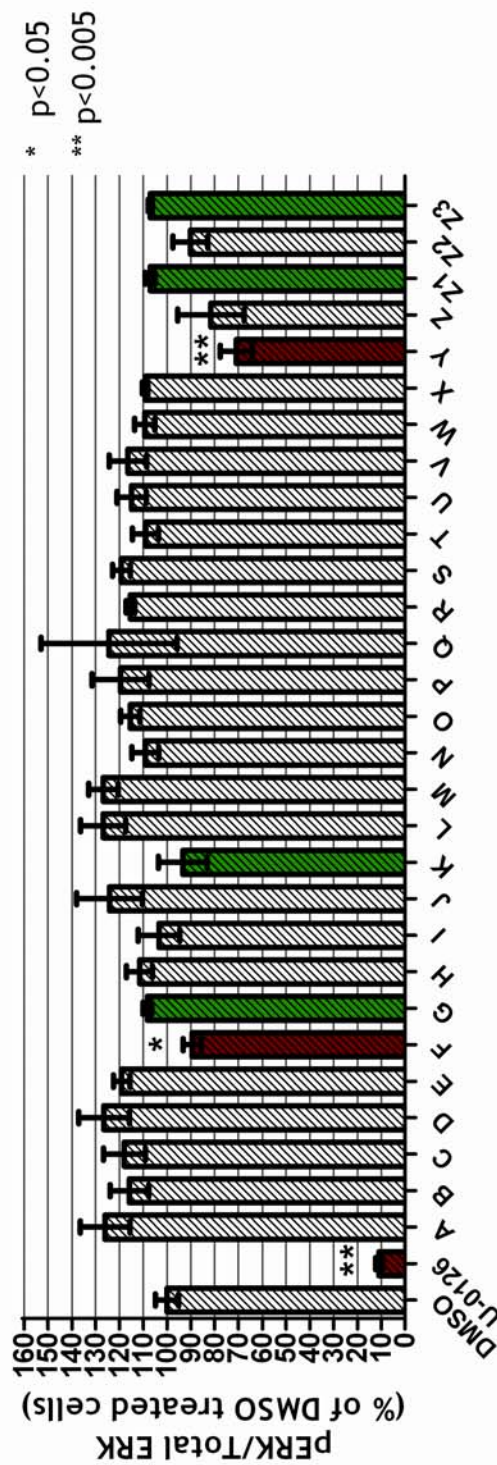


Figure 69. Selected Hit Compounds inhibitory activity of ERK phosphorylation

C111 cells were treated with Tamoxifen for 24h either in the presence of the vehicle (DMSO 0.5%) or respectively with the Hit compounds at the concentrations indicated in Fig. 68. For each treatment ERK phosphorylation was analyzed from triplicate plates through an ELISA -based assay. In red (F, Y) are highlighted compounds that significantly reduce ERK phosphorylation. In green (G, K,Z1,Z3) are highlighted compounds that act on NIS expression (see Figure 70) without affecting ERK phosphorylation. U -0126 is a known MAPK pathway inhibitor that is used as a positive control.

NIS mRNA induction

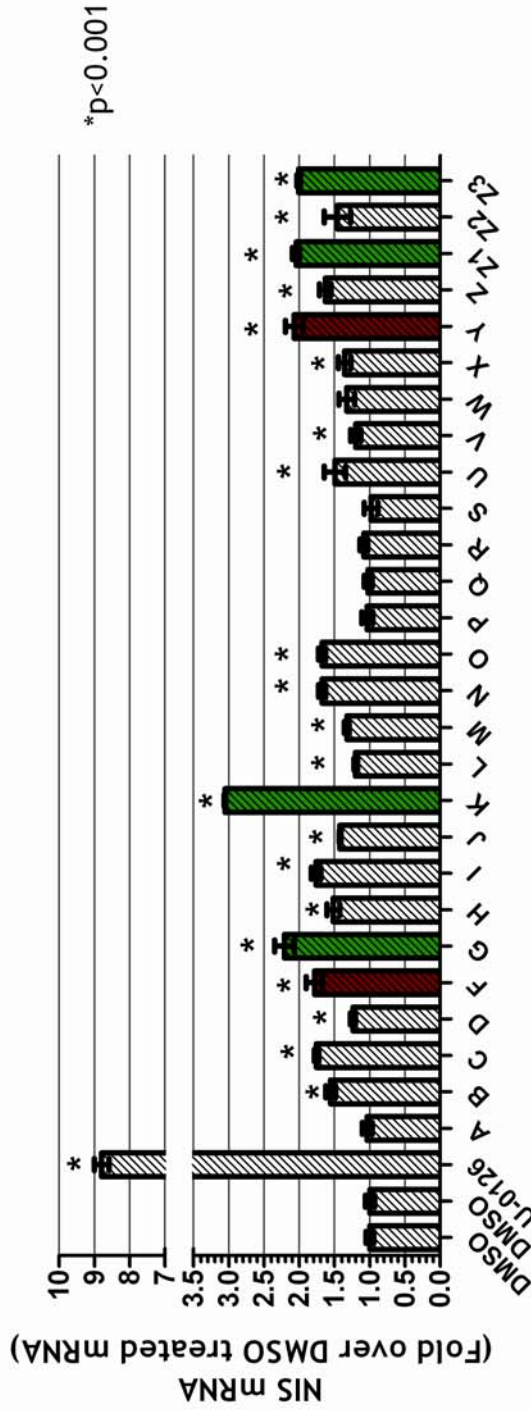


Figure 70. Selected Hit Compounds activity on endogenous NIS gene expression

C111 cells were treated with Tamoxifen for 24h either in the presence of the vehicle (DMSO 0.5%) or respectively with the Hit compounds at the concentrations indicated in Fig. 68. For each treatment mRNA was extracted from triplicate plates and NIS mRNA quantitized by Real -Time RT-PCR., In red (F, Y) are highlighted compounds that significantly increase NIS gene expression and also showed inhibitory activity toward the MAPK pathway (see figure 69). In green (G, K,Z1,Z3) are highlighted compounds that significantly increase NIS expression over 2 -fold with respect to the DMSO treated point. U-0126 is a known MAPK pathway inhibitor that is used as a positive control.

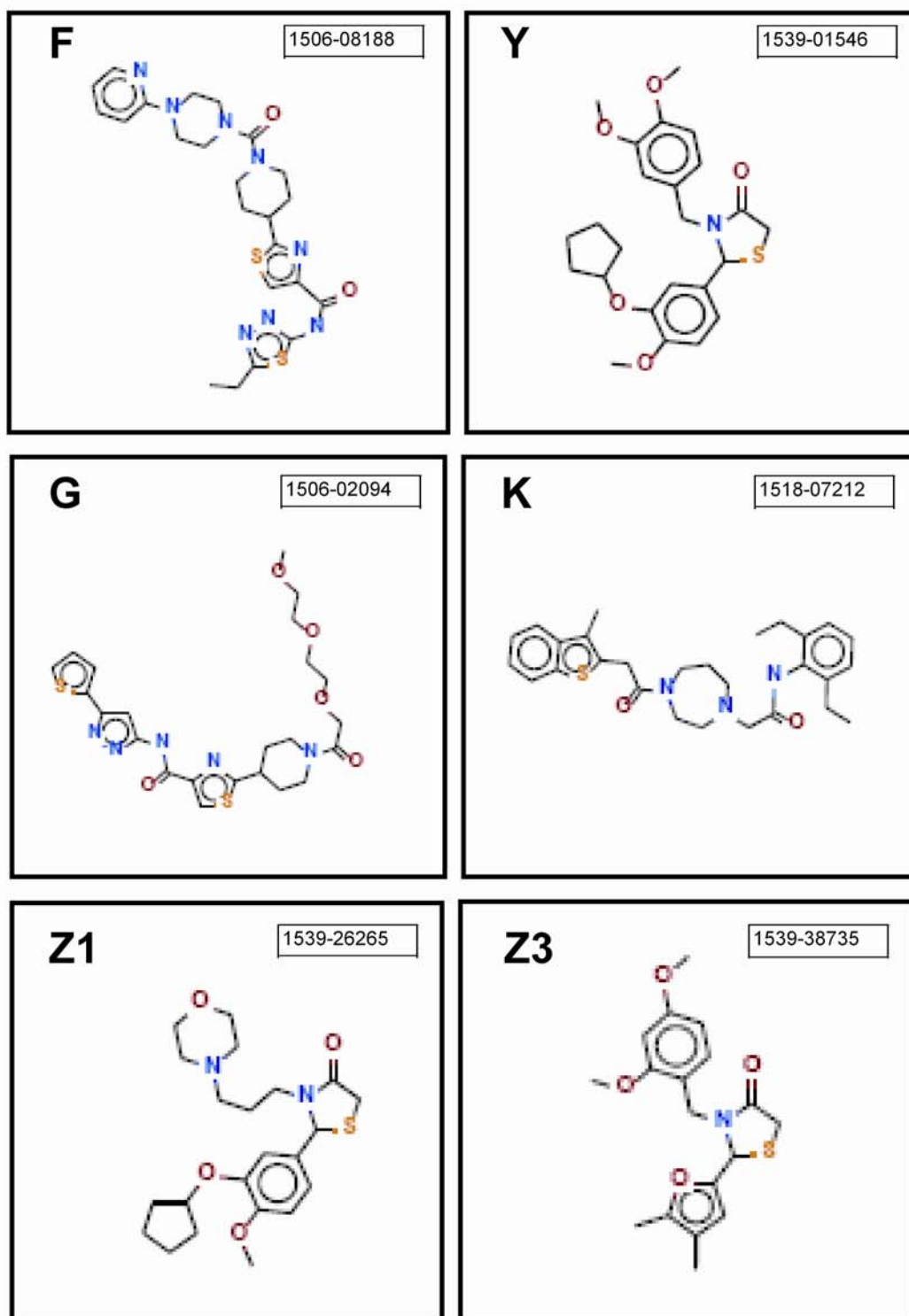


Figure 71. Structures of Compounds that counteract Ras oncogene mediated inhibition of NIS gene expression

Shown in the figure are the structures of the compounds that show an activity in restoring NIS gene expression. For each of them is indicated on the upper left side the letter with which compounds have been dubbed in this chapter and on the upper right side the code that identifies them at the selling company (TRIPOS).

DISCUSSION

Ras proteins play important roles in growth and differentiation of several cell types . However, when de-regulated by certain mutations, Ras proteins constitutively activate diverse downstream pathways and can elicit both tumoral transformation and a deranged differentiation phenotype (9, 254). Recent results obtained in animal models indicate cell type specific mechanisms involved in oncogenic Ras action and suggest that molecular events initiated by Ras activation could either be different or have divergent consequences in diverse cell types (45, 46, 255). Oncogenic Ras proteins have been shown to play important roles in epithelial cell transformation and are indeed associated with 35% of human cancers (9). In particular, mutations on genes encoding Ras proteins have been associated with all types of thyroid malignancies, including anaplastic thyroid cancers, thus suggesting that Ras oncoproteins might have a role in the suppression of thyroid differentiated phenotype (142). Consistently, experiments performed in immortalized thyroid cell lines showed that transformation by Ras oncogenes inhibits differentiation through still unknown mechanisms (219, 256, 257).

In this study I demonstrate that activation of Ras oncogene in thyroid cells causes loss of activity of the transcription factor Pax8 that can be rescued by over- expression of the PKA catalytic subunit. In keeping with this observation, we show a reduced PKA activity and a significant decrease of phosphorylated CREB in cells expressing oncogenic Ras. These data indicate novel biochemical actions of Ras oncogene that might play important roles in the Ras induced transformed phenotype.

It was previously demonstrated that such inhibition of differentiation is not an artifact of the chimeric Ras molecule used since stable transfectants expressing oncogenic Ras show a similar phenotype (4). The global downregulation of thyroid specific gene expression greatly resembles the effect of TSH starvation on thyroid follicular cells (86, 99, 258). The observations reported here show that among the earliest events following Ras activation are a decrease of TSHr protein and of cAMP

signalling, as indicated by a reduced CREB phosphorylation, suggesting that the effects of Ras could be mediated by reduced TSHr signalling.

I tested such a hypothesis by generating a stable cell line which expressed an ectopic TSHr (hTSHr) under the control of a promoter not influenced by Ras activation. I demonstrate that in these cells TSHr expression, even though effectively rescued in the presence of activated Ras, is not sufficient to restore a differentiated phenotype. In addition, in hTSHr expressing cells oncogenic Ras still impairs CREB phosphorylation and such an effect cannot be rescued by the cAMP elevating agent forskolin. Furthermore, I demonstrate a clear reduction of PKA activity in cells expressing oncogenic Ras. I conclude that activated Ras inhibits the TSHr pathway at two major levels, one of which is the downregulation of TSHr expression and a further level which is located downstream of cAMP production and results in reduction of PKA activity, with a consequent block in the transduction of the cAMP signal to the nucleus.

This latter effect by oncogenic Ras indicates the presence of an unusual inhibitory interference exerted by oncogenic Ras on the cAMP signalling pathway. While it is well established that cAMP signalling can interfere with Ras action (89, 259), the data presented in this paper represent a strong indication of a block exerted by Ras on cAMP signalling. These data support the notion that the Ras oncoprotein inactivates the cAMP pathway through a mechanism that is acting downstream of cAMP production and converges on PKA. I propose that in thyroid cells these events lead to the observed global down regulation of thyroid differentiation

Previous data on dedifferentiated thyroid transformed cell lines such as PCpY cells (rat thyroid cell line transformed with polyoma virus middle T antigen) and ARO cells (human anaplastic thyroid carcinoma derived cell line) have shown that re-activation of Pax8 expression can restore a differentiated thyroid phenotype and in particular can upregulate NIS expression (102, 260).

I thus tested whether Pax8 down regulation had a key role in oncogenic Ras induced NIS downregulation, by generating a stable cell line expressing an ectopic Pax8 under the control of a Ras independent promoter. However, persistent Pax8 expression does not affect the ability of oncogenic Ras to down regulate NIS expression. I provide evidence that Ras activation inhibits Pax8

transcriptional activity and that such inhibition is achieved through the inhibition of the TSHr pathway. In fact, I found that Pax8 activity is dependent upon the TSHr/PKA pathway as previously suggested (86, 234) and that PKA over-expression rescues oncogenic Ras induced Pax8 inhibition. Consistently, I found that PKA over-expression also restores the ability of Pax8 to stimulate NIS transcription mediated by the NUE enhancer.

I thus envision a mechanism in which the initial event following Ras activation is a block of PKA activity. As a consequence, Pax8 activity is impaired, resulting in a decrease of thyroid-specific gene expression. Interestingly, Pax8 transcription itself is under cAMP control (86). Furthermore, preliminary evidence suggest that Pax8 transcription is auto-regulated (Di gennaro, A, De Felice M and Di Lauro, R, unpublished). Thus, the reduced cAMP signalling induced by oncogenic Ras would interfere both with the activity and synthesis of Pax8, resulting in an amplification of the de-differentiating effect. This effect apperas to be thyroid specfic since neither the inhibition of the cAMP pathway nor inhibition of Pax8 activity could be detected in fibroblasts upon Ras oncogene activation.

Published data support the notion that in thyroid cells oncogenic Ras inhibits cAMP signalling. However, the mechanisms proposed envisage both a de-localization of the PKA catalytic subunit and a down-regulation of the PKA regulative subunit RIIbeta (261-264). In our system we did not detect either of these effects, since we found no effects of oncogenic Ras on either the intracellular distribution or protein levels for both regulatory and catalytic PKA subunits. However, we demonstrate for the first time a clear Ras-induced downregulation of CREB phosphorylation at Ser133 concomitant with a decreased PKA activity.

Even though CREB Ser133 is the target not only of PKA but also of many other kinases (89, 265), I clearly show that oncogenic Ras blocks forskolin induced CREB phosphorylation in thyroid cells, indicating that PKA is a bona fide target of Ras action. Along the same lines, I show that the stimulation of Pax8 activity by PKA over expression, in cells expressing oncogenic Ras, is blocked by the PKA specific inhibitor H89.

I have not identified the mechanism responsible for PKA inhibition by Ras. Since this effect is relieved by PKA overexpression, I hypotesize that we might be titrating out an inhibitory mechanism,

whose nature is at present unknown. Previous data have shown, for example, that upregulation of PP1 phosphatase activity can downregulate thyroid differentiation (266). However further studies are required in order to define the mechanisms underpinning this Ras-oncogene promoted PKA inhibition.

It should also be noted that, in addition to a potential general inhibition of cAMP pathway induced by Ras oncogene and the consequential effect on Pax8 activity, CREB compromised function itself could be relevant to thyroid function. It has been reported that CREB activity is required for differentiation of FRTL5 cells (225, 267) and that mice expressing a dominant negative CREB transgene show impairment in thyroid differentiation (268).

The ability of Ras oncoprotein to negatively regulate differentiation in thyroid cells is of utmost importance in therapy. Cancerous thyroid cells can be killed with radioactive iodide, since they have an exquisite capacity, mediated by the NIS protein, to accumulate this element that is physiologically used for thyroid hormone biosynthesis (269). However for anaplastic cancer, the most aggressive and inevitably fatal thyroid cancer, the radioactive iodide-based therapy is ineffective since the expression of NIS gene is suppressed in these cells. The understanding of the events causative of loss of thyroid differentiation induced by Ras oncogene in cultured cells might give clues on the genes that could be targeted in human anaplastic thyroid cancers in order interest to design new, highly required, therapeutic strategies aimed at re-expression of the differentiated phenotype in cancer cells that will allow the ablation of cancerous cells through the well-established therapy protocol based on radioactive iodide.(270, 271)

Oncogene addiction is today a very known phenomenon that can be used as a weapon against cancer cells (214, 246-248). In FRTL-5 cells previous data obtained by using a Temperature-sensitive Ras oncogene suggested that once Ras oncogene is activated, thyroid differentiated phenotype can't be restored by simply inactivating Ras oncogene (249-251). However, in those cells, Ras oncogene inactivation required a temperature shift which could have made the results artificial. On the contrary, in the cellular system I used in this work, Ras oncogene can be inactivated by simply removing Tamoxifen from the culture medium. I found that thyroid differentiated phenotype can be restored by suppressing Ras oncogene activity thus demonstrating the relevance of finding ways to inactivate Ras

oncogene in order to restore a normal phenotype. I obtained the same result by inhibiting the MAPK pathway with the MEK1/2 inhibitors U-0126 and PD-98059 accordingly to the increasing number of data that highlighting the relevance of the MAPK pathway for thyroid cancer initiation and progression toward full malignancy (142, 151, 272, 273).

I developed a thyroid cell-based assay system which can sense MAPK pathway activation and I screened the inhibitory activity of a compound library consisting of 50.000 molecules. The system I set up also allow identification of compounds capable of restoring NIS gene expression independently from MAPK inhibition. From the screening I identified two new compounds that can inhibit MEK activity and that consequently increase NIS expression in FRTL5 cells dedifferentiated by Ras oncogene. These compound may represent lead structures to optimize in order to obtain new classes of MAPK pathway inhibitors. In addition I identified four compounds that could increase NIS expression without apparently affecting the MAPK pathway. These latter compounds, besides confirming the potential involvement of additional Ras oncogene activated pathways in the observed NIS downregulation, offer the possibility to further characterize such pathways by using the chemicals as ligands in affinity chromatography.

There are increasing evidences suggesting that targeted inhibition of the MAPK pathway is an effective therapy for thyroid cancer such as advanced papillary and anaplastic thyroid cancers that have escaped radioiodine sensitivity (172, 205, 206). The inhibition of Ras/Raf/MAPK pathway is indeed relevant for many cancer types therapies, especially when used in combination with conventional cytotoxic agents (39). Currently inhibitors of the kinase function of Raf and MEK represent the most studied and advanced approaches for blocking ERK signalling, with several inhibitors under evaluation in clinical trials and additional ones in pre-clinical analysis. Considering the ability of cancer cells to escape inhibition, the availability of alternative compounds which trigger the same pathway through different mechanisms could represents a great resource (252).

Bibliography

1. Malumbres M, Barbacid M 2003 RAS oncogenes: the first 30 years. *Nature reviews* 3:459-465
2. Campbell PM, Der CJ 2004 Oncogenic Ras and its role in tumor cell invasion and metastasis. *Seminars in cancer biology* 14:105-114
3. Pardal R, Clarke MF, Morrison SJ 2003 Applying the principles of stem-cell biology to cancer. *Nature reviews* 3:895-902
4. De Vita G, Bauer L, da Costa VM, De Felice M, Baratta MG, De Menna M, Di Lauro R 2005 Dose-dependent inhibition of thyroid differentiation by RAS oncogenes. *Molecular endocrinology (Baltimore, Md)* 19:76-89
5. Fusco A, Berlingieri MT, Di Fiore PP, Portella G, Grieco M, Vecchio G 1987 One- and two-step transformations of rat thyroid epithelial cells by retroviral oncogenes. *Molecular and cellular biology* 7:3365-3370
6. Tallini G 2002 Molecular pathobiology of thyroid neoplasms. *Endocrine pathology* 13:271-288
7. Krauss G ed. 2001 *Biochemistry of signal transduction and regulation*: Wiley vch
8. Prior IA, Hancock JF 2001 Compartmentalization of Ras proteins. *Journal of cell science* 114:1603-1608
9. Karnoub AE, Weinberg RA 2008 Ras oncogenes: split personalities. *Nature reviews* 9:517-531
10. Schubert S, Shannon K, Bollag G 2007 Hyperactive Ras in developmental disorders and cancer. *Nature reviews* 7:295-308
11. Downward J 2003 Targeting RAS signalling pathways in cancer therapy. *Nature reviews* 3:11-22
12. Schreck R, Rapp UR 2006 Raf kinases: oncogenesis and drug discovery. *International journal of cancer* 119:2261-2271
13. Wellbrock C, Karasarides M, Marais R 2004 The RAF proteins take centre stage. *Nature reviews* 5:875-885
14. Mercer KE, Pritchard CA 2003 Raf proteins and cancer: B-Raf is identified as a mutational target. *Biochimica et biophysica acta* 1653:25-40
15. Zuber J, Tchernitsa OI, Hinzmann B, Schmitz AC, Grips M, Hellriegel M, Sers C, Rosenthal A, Schafer R 2000 A genome-wide survey of RAS transformation targets. *Nature genetics* 24:144-152
16. Schulze A, Lehmann K, Jefferies HB, McMahon M, Downward J 2001 Analysis of the transcriptional program induced by Raf in epithelial cells. *Genes & development* 15:981-994
17. Yoon S, Seger R 2006 The extracellular signal-regulated kinase: multiple substrates regulate diverse cellular functions. *Growth factors (Chur, Switzerland)* 24:21-44
18. Repasky GA, Chenette EJ, Der CJ 2004 Renewing the conspiracy theory debate: does Raf function alone to mediate Ras oncogenesis? *Trends in cell biology* 14:639-647
19. Emuss V, Garnett M, Mason C, Marais R 2005 Mutations of C-RAF are rare in human cancer because C-RAF has a low basal kinase activity compared with B-RAF. *Cancer research* 65:9719-9726
20. Marais R, Light Y, Paterson HF, Mason CS, Marshall CJ 1997 Differential regulation of Raf-1, A-Raf, and B-Raf by oncogenic ras and tyrosine kinases. *The Journal of biological chemistry* 272:4378-4383

21. Papin C, Denouel A, Calothy G, Eychene A 1996 Identification of signalling proteins interacting with B-Raf in the yeast two-hybrid system. *Oncogene* 12:2213-2221
22. Huser M, Luckett J, Chiloeches A, Mercer K, Iwobi M, Giblett S, Sun XM, Brown J, Marais R, Pritchard C 2001 MEK kinase activity is not necessary for Raf-1 function. *The EMBO journal* 20:1940-1951
23. Mikula M, Schreiber M, Husak Z, Kucerova L, Ruth J, Wieser R, Zatloukal K, Beug H, Wagner EF, Baccarini M 2001 Embryonic lethality and fetal liver apoptosis in mice lacking the c-raf-1 gene. *The EMBO journal* 20:1952-1962
24. Pritchard CA, Bolin L, Slattery R, Murray R, McMahon M 1996 Post-natal lethality and neurological and gastrointestinal defects in mice with targeted disruption of the A-Raf protein kinase gene. *Curr Biol* 6:614-617
25. Pritchard CA, Hayes L, Wojnowski L, Zimmer A, Marais RM, Norman JC 2004 B-Raf acts via the ROCKII/LIMK/cofilin pathway to maintain actin stress fibers in fibroblasts. *Molecular and cellular biology* 24:5937-5952
26. Davies H, Bignell GR, Cox C, Stephens P, Edkins S, Clegg S, Teague J, Woffendin H, Garnett MJ, Bottomley W, Davis N, Dicks E, Ewing R, Floyd Y, Gray K, Hall S, Hawes R, Hughes J, Kosmidou V, Menzies A, Mould C, Parker A, Stevens C, Watt S, Hooper S, Wilson R, Jayatilake H, Gusterson BA, Cooper C, Shipley J, Hargrave D, Pritchard-Jones K, Maitland N, Chenevix-Trench G, Riggins GJ, Bigner DD, Palmieri G, Cossu A, Flanagan A, Nicholson A, Ho JW, Leung SY, Yuen ST, Weber BL, Seigler HF, Darrow TL, Paterson H, Marais R, Marshall CJ, Wooster R, Stratton MR, Futreal PA 2002 Mutations of the BRAF gene in human cancer. *Nature* 417:949-954
27. Shaw RJ, Cantley LC 2006 Ras, PI(3)K and mTOR signalling controls tumour cell growth. *Nature* 441:424-430
28. Cully M, You H, Levine AJ, Mak TW 2006 Beyond PTEN mutations: the PI3K pathway as an integrator of multiple inputs during tumorigenesis. *Nature reviews* 6:184-192
29. Mao JH, To MD, Perez-Losada J, Wu D, Del Rosario R, Balmain A 2004 Mutually exclusive mutations of the Pten and ras pathways in skin tumor progression. *Genes & development* 18:1800-1805
30. Malliri A, van der Kammen RA, Clark K, van der Valk M, Michiels F, Collard JG 2002 Mice deficient in the Rac activator Tiam1 are resistant to Ras-induced skin tumours. *Nature* 417:867-871
31. Bai Y, Edamatsu H, Maeda S, Saito H, Suzuki N, Satoh T, Kataoka T 2004 Crucial role of phospholipase Cepsilon in chemical carcinogen-induced skin tumor development. *Cancer research* 64:8808-8810
32. Gonzalez-Garcia A, Pritchard CA, Paterson HF, Mavria G, Stamp G, Marshall CJ 2005 RalGDS is required for tumor formation in a model of skin carcinogenesis. *Cancer cell* 7:219-226
33. Dasgupta B, Gutmann DH 2003 Neurofibromatosis 1: closing the GAP between mice and men. *Current opinion in genetics & development* 13:20-27
34. Zandi R, Larsen AB, Andersen P, Stockhausen MT, Poulsen HS 2007 Mechanisms for oncogenic activation of the epidermal growth factor receptor. *Cellular signalling* 19:2013-2023
35. Moasser MM 2007 The oncogene HER2: its signaling and transforming functions and its role in human cancer pathogenesis. *Oncogene* 26:6469-6487
36. Roberts PJ, Der CJ 2007 Targeting the Raf-MEK-ERK mitogen-activated protein kinase cascade for the treatment of cancer. *Oncogene* 26:3291-3310
37. Sridhar SS, Hedley D, Siu LL 2005 Raf kinase as a target for anticancer therapeutics. *Molecular cancer therapeutics* 4:677-685

38. Thompson N, Lyons J 2005 Recent progress in targeting the Raf/MEK/ERK pathway with inhibitors in cancer drug discovery. *Current opinion in pharmacology* 5:350-356
39. Kohno M, Pouyssegur J 2006 Targeting the ERK signaling pathway in cancer therapy. *Annals of medicine* 38:200-211
40. Rajagopalan H, Bardelli A, Lengauer C, Kinzler KW, Vogelstein B, Velculescu VE 2002 Tumorigenesis: RAF/RAS oncogenes and mismatch-repair status. *Nature* 418:934
41. Singer G, Oldt R, 3rd, Cohen Y, Wang BG, Sidransky D, Kurman RJ, Shih Ie M 2003 Mutations in BRAF and KRAS characterize the development of low-grade ovarian serous carcinoma. *Journal of the National Cancer Institute* 95:484-486
42. Sieben NL, Macropoulos P, Roemen GM, Kolkman-Uljee SM, Jan Fleuren G, Houmadi R, Diss T, Warren B, Al Adnani M, De Goeij AP, Krausz T, Flanagan AM 2004 In ovarian neoplasms, BRAF, but not KRAS, mutations are restricted to low-grade serous tumours. *The Journal of pathology* 202:336-340
43. Vos MD, Ellis CA, Elam C, Ulku AS, Taylor BJ, Clark GJ 2003 RASSF2 is a novel K-Ras-specific effector and potential tumor suppressor. *The Journal of biological chemistry* 278:28045-28051
44. Bos JL 1989 ras oncogenes in human cancer: a review. *Cancer research* 49:4682-4689
45. Johnson L, Mercer K, Greenbaum D, Bronson RT, Crowley D, Tuveson DA, Jacks T 2001 Somatic activation of the K-ras oncogene causes early onset lung cancer in mice. *Nature* 410:1111-1116
46. Guerra C, Mijimolle N, Dhawahir A, Dubus P, Barradas M, Serrano M, Campuzano V, Barbacid M 2003 Tumor induction by an endogenous K-ras oncogene is highly dependent on cellular context. *Cancer cell* 4:111-120
47. Jackson EL, Willis N, Mercer K, Bronson RT, Crowley D, Montoya R, Jacks T, Tuveson DA 2001 Analysis of lung tumor initiation and progression using conditional expression of oncogenic K-ras. *Genes & development* 15:3243-3248
48. Tuveson DA, Shaw AT, Willis NA, Silver DP, Jackson EL, Chang S, Mercer KL, Grochow R, Hock H, Crowley D, Hingorani SR, Zaks T, King C, Jacobetz MA, Wang L, Bronson RT, Orkin SH, DePinho RA, Jacks T 2004 Endogenous oncogenic K-ras(G12D) stimulates proliferation and widespread neoplastic and developmental defects. *Cancer cell* 5:375-387
49. Rangarajan A, Hong SJ, Gifford A, Weinberg RA 2004 Species- and cell type-specific requirements for cellular transformation. *Cancer cell* 6:171-183
50. Rangarajan A, Weinberg RA 2003 Opinion: Comparative biology of mouse versus human cells: modelling human cancer in mice. *Nature reviews* 3:952-959
51. Hamad NM, Elconin JH, Karnoub AE, Bai W, Rich JN, Abraham RT, Der CJ, Counter CM 2002 Distinct requirements for Ras oncogenesis in human versus mouse cells. *Genes & development* 16:2045-2057
52. Kaufman MH, Bard J 1999 The thyroid. In: Kaufman MH, Bard J eds. *The anatomic basis of mouse development*. San Diego: Academic Press; 165-166
53. Di Lauro R, De Felice M 2003 Factors in differentiation and morphogenesis of the thyroid gland. *Topical Endocrinology* 21:13-17
54. Thomas PQ, Brown A, Beddington R 1998 Hex: a homeobox gene revealing peri-implantation asymmetry in the mouse embryo and an early transient marker of endothelial cell precursors. *Development* 125:85-95
55. Lazzaro D, Price M, De Felice M, Di Lauro R 1991 The transcription factor TTF-1 is expressed at the onset of thyroid and lung morphogenesis and in restricted regions of the foetal brain. *Development* 113:1093-1104

56. Zannini M, Avantaggiato V, Biffali E, Arnone M, Sato K, Pischetola M, Taylor BA, Phillips SJ, Simeone A, Di Lauro R 1997 TTF-2, a new forkhead protein, shows a temporal expression in the developing thyroid which is consistent with a role in controlling the onset of differentiation. *EMBO J* 16:3185-3197
57. Damante G, Tell G, Di Lauro R 2001 A unique combination of transcription factors controls differentiation of thyroid cells. *Prog Nucleic Acid Res Mol Biol* 66:307-356
58. Fontaine J 1979 Multistep migration of calcitonine cell precursors during ontogeny of the mouse pharynx. *Gen Comp Endocrinol* 37:81-92
59. Le Douarin N, Fontaine J, LeLievre C 1974 New studies on the neural crest origin of the avian ultimobranchial glandular cells. Interspecific combinations and cytochemical characterization of C cells based on the uptake of biogenic amine precursors. *Histochemie* 38:297-305
60. Fagman H, Liao J, Westerlund J, Andersson L, Morrow BE, Nilsson M 2006 The 22q11 deletion syndrome candidate gene *Tbx1* determines thyroid size and positioning. *Hum Mol Genet*
61. Meunier D, Aubin J, Jeannotte L 2003 Perturbed thyroid morphology and transient hypothyroidism symptoms in *Hoxa5* mutant mice. *Dev Dyn* 227:367-378
62. Riedel C, Levy O, Carrasco N 2001 Post-transcriptional regulation of the sodium/iodide symporter by thyrotropin. *The Journal of biological chemistry* 276:21458-21463
63. Kaminsky SM, Levy O, Salvador C, Dai G, Carrasco N 1994 Na(+)-I- symport activity is present in membrane vesicles from thyrotropin-deprived non-I(-)-transporting cultured thyroid cells. *Proceedings of the National Academy of Sciences of the United States of America* 91:3789-3793
64. Ohno M, Zannini M, Levy O, Carrasco N, di Lauro R 1999 The paired-domain transcription factor *Pax8* binds to the upstream enhancer of the rat sodium/iodide symporter gene and participates in both thyroid-specific and cyclic-AMP-dependent transcription. *Molecular and cellular biology* 19:2051-2060
65. Smanik PA, Liu Q, Furminger TL, Ryu K, Xing S, Mazzaferri EL, Jhiang SM 1996 Cloning of the human sodium iodide symporter. *Biochemical and biophysical research communications* 226:339-345
66. Smanik PA, Ryu KY, Theil KS, Mazzaferri EL, Jhiang SM 1997 Expression, exon-intron organization, and chromosome mapping of the human sodium iodide symporter. *Endocrinology* 138:3555-3558
67. Levy O, Dai G, Riedel C, Ginter CS, Paul EM, Lebowitz AN, Carrasco N 1997 Characterization of the thyroid Na⁺/I⁻ symporter with an anti-COOH terminus antibody. *Proceedings of the National Academy of Sciences of the United States of America* 94:5568-5573
68. Levy O, De la Vieja A, Ginter CS, Riedel C, Dai G, Carrasco N 1998 N-linked glycosylation of the thyroid Na⁺/I⁻ symporter (NIS). Implications for its secondary structure model. *The Journal of biological chemistry* 273:22657-22663
69. Dohan O, Carrasco N 2003 Advances in Na⁺/I⁻ symporter (NIS) research in the thyroid and beyond. *Molecular and cellular endocrinology* 213:59-70
70. Dohan O, De la Vieja A, Paroder V, Riedel C, Artani M, Reed M, Ginter CS, Carrasco N 2003 The sodium/iodide Symporter (NIS): characterization, regulation, and medical significance. *Endocrine reviews* 24:48-77
71. Eskandari S, Loo DD, Dai G, Levy O, Wright EM, Carrasco N 1997 Thyroid Na⁺/I⁻ symporter. Mechanism, stoichiometry, and specificity. *The Journal of biological chemistry* 272:27230-27238

72. Scott DA, Wang R, Kreman TM, Sheffield VC, Karniski LP 1999 The Pendred syndrome gene encodes a chloride-iodide transport protein. *Nature genetics* 21:440-443
73. Tatsumi K, Miyai K, Amino N 1998 Genetic basis of congenital hypothyroidism: abnormalities in the TSHbeta gene, the PIT1 gene, and the NIS gene. *Clin Chem Lab Med* 36:659-662
74. Dohan O, Gavrielides MV, Ginter C, Amzel LM, Carrasco N 2002 Na(+)/I(-) symporter activity requires a small and uncharged amino acid residue at position 395. *Molecular endocrinology (Baltimore, Md)* 16:1893-1902
75. Davies TF, Ando T, Lin RY, Tomer Y, Latif R 2005 Thyrotropin receptor-associated diseases: from adenomata to Graves disease. *The Journal of clinical investigation* 115:1972-1983
76. Brown RS, Shalhoub V, Coulter S, Alex S, Joris I, De Vito W, Lian J, Stein GS 2000 Developmental regulation of thyrotropin receptor gene expression in the fetal and neonatal rat thyroid: relation to thyroid morphology and to thyroid-specific gene expression. *Endocrinology* 141:340-345
77. Abe E, Marians RC, Yu W, Wu XB, Ando T, Li Y, Iqbal J, Eldeiry L, Rajendren G, Blair HC, Davies TF, Zaidi M 2003 TSH is a negative regulator of skeletal remodeling. *Cell* 115:151-162
78. Yokomori N, Tawata M, Saito T, Shimura H, Onaya T 1998 Regulation of the rat thyrotropin receptor gene by the methylation-sensitive transcription factor GA-binding protein. *Molecular endocrinology (Baltimore, Md)* 12:1241-1249
79. Ohe K, Ikuyama S, Takayanagi R, Kohn LD, Nawata H 1996 Interferon-gamma suppresses thyrotropin receptor promoter activity by reducing thyroid transcription factor-1 (TTF-1) binding to its recognition site. *Molecular endocrinology (Baltimore, Md)* 10:826-836
80. Chen ST, Lin JD, Lin KH 2002 Characterization of a thyroid hormone-mediated short-loop feedback control of TSH receptor gene in an anaplastic human thyroid cancer cell line. *The Journal of endocrinology* 175:459-465
81. Uyttersprot N, Costagliola S, Dumont JE, Miot F 1999 Requirement for cAMP-response element (CRE) binding protein/CRE modulator transcription factors in thyrotropin-induced proliferation of dog thyroid cells in primary culture. *European journal of biochemistry / FEBS* 259:370-378
82. Seetharamaiah GS, Dallas JS, Prabhakar BS 1999 Glycosylated ectodomain of the human thyrotropin receptor induces antibodies capable of reacting with multiple blocking antibody epitopes. *Autoimmunity* 29:21-31
83. Parmentier M, Libert F, Maenhaut C, Lefort A, Gerard C, Perret J, Van Sande J, Dumont JE, Vassart G 1989 Molecular cloning of the thyrotropin receptor. *Science* 246:1620-1622
84. Vassart G, Pardo L, Costagliola S 2004 A molecular dissection of the glycoprotein hormone receptors. *Trends Biochem Sc* 29:119-126
85. Loosfelt H, Pichon C, Jolivet A, Misrahi M, Caillou B, Jamous M, Vannier B, Milgrom E 1992 Two-subunit structure of the human thyrotropin receptor. *Proc Natl Acad Sci U S A* 89:3765-3769
86. Mascia A, Nitsch L, Di Lauro R, Zannini M 2002 Hormonal control of the transcription factor Pax8 and its role in the regulation of thyroglobulin gene expression in thyroid cells. *The Journal of endocrinology* 172:163-176
87. Vassart G, Dumont JE 1992 The thyrotropin receptor and the regulation of thyrocyte function and growth. *Endocrine reviews* 13:596-611

88. Ludgate M, Gire V, Crisp M, Ajjan R, Weetman A, Ivan M, Wynford-Thomas D 1999 Contrasting effects of activating mutations of GalphaS and the thyrotropin receptor on proliferation and differentiation of thyroid follicular cells. *Oncogene* 18:4798-4807
89. Johannessen M, Delghandi MP, Moens U 2004 What turns CREB on? *Cellular signalling* 16:1211-1227
90. Garcia-Jimenez C, Santisteban P 2007 TSH signalling and cancer. *Arquivos brasileiros de endocrinologia e metabologia* 51:654-671
91. Avvedimento VE, Tramontano D, Ursini MV, Monticelli A, Di Lauro R 1984 The level of thyroglobulin mRNA is regulated by TSH both in vitro and in vivo. *Biochemical and biophysical research communications* 122:472-477
92. Santisteban P, Kohn LD, Di Lauro R 1987 Thyroglobulin gene expression is regulated by insulin and insulin-like growth factor I, as well as thyrotropin, in FRTL-5 thyroid cells. *The Journal of biological chemistry* 262:4048-4052
93. Chazenbalk G, Magnusson RP, Rapoport B 1987 Thyrotropin stimulation of cultured thyroid cells increases steady state levels of the messenger ribonucleic acid for thyroid peroxidase. *Molecular endocrinology (Baltimore, Md)* 1:913-917
94. Zarrilli R, Formisano S, Di Jeso B 1990 Hormonal regulation of thyroid peroxidase in normal and transformed rat thyroid cells. *Molecular endocrinology (Baltimore, Md)* 4:39-45
95. Ortiz L, Zannini M, Di Lauro R, Santisteban P 1997 Transcriptional control of the forkhead thyroid transcription factor TTF-2 by thyrotropin, insulin, and insulin-like growth factor I. *The Journal of biological chemistry* 272:23334-23339
96. Van Renterghem P, Vassart G, Christophe D 1996 Pax 8 expression in primary cultured dog thyrocyte is increased by cyclic AMP. *Biochimica et biophysica acta* 1307:97-103
97. Marians RC, Ng L, Blair HC, Unger P, Graves PN, Davies TF 2002 Defining thyrotropin-dependent and -independent steps of thyroid hormone synthesis by using thyrotropin receptor-null mice. *Proc Natl Acad Sci U S A* 99:15776-15781
98. Stuart A, Oates E, Hall C, Grumbles R, Fernandez L, Taylor N, Puett D, Jin S 1994 Identification of a point mutation in the thyrotropin receptor of the *hyt/hyt* hypothyroid mouse. *Mol Endocrinol* 8:129-138
99. Postiglione MP, Parlato R, Rodriguez-Mallon A, Rosica A, Mithbaokar P, Maresca M, Marians RC, Davies TF, Zannini MS, De Felice M, Di Lauro R 2002 Role of the thyroid-stimulating hormone receptor signaling in development and differentiation of the thyroid gland. *Proceedings of the National Academy of Sciences of the United States of America* 99:15462-15467
100. Postiglione MP, Parlato R, Rodriguez-Mallon A, Rosica A, Mithbaokar P, Maresca M, Marians RC, Davies TF, Zannini MS, De Felice M, Di Lauro R 2002 Role of the thyroid-stimulating hormone receptor signaling in development and differentiation of the thyroid gland. *Proc Natl Acad Sci U S A* 99:15462-15467
101. Damante G, Tell G, Di Lauro R 2001 A unique combination of transcription factors controls differentiation of thyroid cells. *Progress in nucleic acid research and molecular biology* 66:307-356
102. Pasca di Magliano M, Di Lauro R, Zannini M 2000 Pax8 has a key role in thyroid cell differentiation. *Proceedings of the National Academy of Sciences of the United States of America* 97:13144-13149
103. Lang D, Powell SK, Plummer RS, Young KP, Ruggeri BA 2007 PAX genes: roles in development, pathophysiology, and cancer. *Biochemical pharmacology* 73:1-14
104. Amendola E, De Luca P, Macchia PE, Terracciano D, Rosica A, Chiappetta G, Kimura S, Mansouri A, Affuso A, Arra C, Macchia V, Di Lauro R, De Felice M 2005 A mouse

- model demonstrates a multigenic origin of congenital hypothyroidism. *Endocrinology* 146:5038-5047
105. Zannini M, Francis-Lang H, Plachov D, Di Lauro R 1992 Pax-8, a paired domain-containing protein, binds to a sequence overlapping the recognition site of a homeodomain and activates transcription from two thyroid-specific promoters. *Molecular and cellular biology* 12:4230-4241
 106. Parlato R, Rosica A, Rodriguez-Mallon A, Affuso A, Postiglione MP, Arra C, Mansouri A, Kimura S, Di Lauro R, De Felice M 2004 An integrated regulatory network controlling survival and migration in thyroid organogenesis. *Developmental biology* 276:464-475
 107. D'Andrea B, Iacone R, Di Palma T, Nitsch R, Baratta MG, Nitsch L, Di Lauro R, Zannini M 2006 Functional inactivation of the transcription factor Pax8 through oligomerization chain reaction. *Molecular endocrinology (Baltimore, Md)* 20:1810-1824
 108. Fabbro D, Pellizzari L, Mercuri F, Tell G, Damante G 1998 Pax-8 protein levels regulate thyroglobulin gene expression. *Journal of molecular endocrinology* 21:347-354
 109. Plachov D, Chowdhury K, Walther C, Simon D, Guenet JL, Gruss P 1990 Pax8, a murine paired box gene expressed in the developing excretory system and thyroid gland. *Development (Cambridge, England)* 110:643-651
 110. Kozmik Z, Kurzbauer R, Dorfler P, Busslinger M 1993 Alternative splicing of Pax-8 gene transcripts is developmentally regulated and generates isoforms with different transactivation properties. *Molecular and cellular biology* 13:6024-6035
 111. Plachov D, Chowdhury K, Walther C, Simon D, Guenet JL, Gruss P 1990 Pax8, a murine paired box gene expressed in the developing excretory system and thyroid gland. *Development* 110:643-651
 112. Poleev A, Wendler F, Fickenscher H, Zannini MS, Yaginuma K, Abbott C, Plachov D 1995 Distinct functional properties of three human paired-box-protein, PAX8, isoforms generated by alternative splicing in thyroid, kidney and Wilms' tumors. *Eur J Biochem* 228:899-911
 113. Fabbro D, Pellizzari L, Mercuri F, Tell G, Damante G 1998 Pax-8 protein levels regulate thyroglobulin gene expression. *J Mol Endocrinol* 21:347-354
 114. Van Renterghem P, Vassart G, Christophe D 1996 Pax 8 expression in primary cultured dog thyrocyte is increased by cyclic AMP. *Biochim Biophys Acta* 1307:97-103
 115. D'Andrea B, Di Palma T, Mascia A, Motti ML, Viglietto G, Nitsch L, Zannini M 2005 The transcriptional repressor DREAM is involved in thyroid gene expression. *Exp Cell Res* 305:166-178
 116. Stapleton P, Weith A, Urbanek P, Kozmik Z, Busslinger M 1993 Chromosomal localization of seven PAX genes and cloning of a novel family member, PAX-9. *Nature genetics* 3:292-298
 117. Walther C, Guenet JL, Simon D, Deutsch U, Jostes B, Goulding MD, Plachov D, Balling R, Gruss P 1991 Pax: a murine multigene family of paired box-containing genes. *Genomics* 11:424-434
 118. Balczarek KA, Lai ZC, Kumar S 1997 Evolution of functional diversification of the paired box (Pax) DNA-binding domains. *Molecular biology and evolution* 14:829-842
 119. Wilson D, Sheng G, Lecuit T, Dostatni N, Desplan C 1993 Cooperative dimerization of paired class homeo domains on DNA. *Genes & development* 7:2120-2134

120. Czerny T, Schaffner G, Busslinger M 1993 DNA sequence recognition by Pax proteins: bipartite structure of the paired domain and its binding site. *Genes & development* 7:2048-2061
121. Treisman J, Harris E, Desplan C 1991 The paired box encodes a second DNA-binding domain in the paired homeo domain protein. *Genes & development* 5:594-604
122. Xu W, Rould MA, Jun S, Desplan C, Pabo CO 1995 Crystal structure of a paired domain-DNA complex at 2.5 Å resolution reveals structural basis for Pax developmental mutations. *Cell* 80:639-650
123. Czerny T, Busslinger M 1995 DNA-binding and transactivation properties of Pax-6: three amino acids in the paired domain are responsible for the different sequence recognition of Pax-6 and BSAP (Pax-5). *Molecular and cellular biology* 15:2858-2871
124. Epstein J, Cai J, Glaser T, Jepeal L, Maas R 1994 Identification of a Pax paired domain recognition sequence and evidence for DNA-dependent conformational changes. *The Journal of biological chemistry* 269:8355-8361
125. Kozmik Z, Kurzbauer R, Dörfler P, Busslinger M 1993 Alternative splicing of Pax-8 gene transcripts is developmentally regulated and generates isoforms with different transactivation properties. *Mol Cell Biol* 13:6145-6149
126. Kambe F, Nomura Y, Okamoto T, Seo H 1996 Redox regulation of thyroid-transcription factors, Pax-8 and TTF-1, is involved in their increased DNA-binding activities by thyrotropin in rat thyroid FRTL-5 cells. *Mol Endocrinol* 10:801-812.
127. Tell G, Pellizzari L, Cimarosti D, Pucillo C, Damante G 1998 Redox potential controls the structure and DNA binding activity of the paired domain. *J Biol Chem* 273:25062-25072.
128. Di Palma T, Nitsch R, Mascia A, Nitsch L, Di Lauro R, Zannini M 2003 The paired domain-containing factor Pax8 and the homeodomain-containing factor TTF-1 directly interact and synergistically activate transcription. *The Journal of biological chemistry* 278:3395-3402
129. De Leo R, Miccadei S, Zammarchi E, Civitareale D 2000 Role for p300 in Pax 8 induction of thyroperoxidase gene expression. *The Journal of biological chemistry* 275:34100-34105
130. Grasberger H, Ringkananont U, Lefrancois P, Abramowicz M, Vassart G, Refetoff S 2005 Thyroid transcription factor 1 rescues PAX8/p300 synergism impaired by a natural PAX8 paired domain mutation with dominant negative activity. *Molecular endocrinology (Baltimore, Md)* 19:1779-1791
131. Puppin C, D'Aurizio F, D'Elia AV, Cesaratto L, Tell G, Russo D, Filetti S, Ferretti E, Tosi E, Mattei T, Pianta A, Pellizzari L, Damante G 2005 Effects of histone acetylation on sodium iodide symporter promoter and expression of thyroid-specific transcription factors. *Endocrinology* 146:3967-3974
132. Miccadei S, Provenzano C, Mojzisek M, Natali PG, Civitareale D 2005 Retinoblastoma protein acts as Pax 8 transcriptional coactivator. *Oncogene* 24:6993-7001
133. Di Palma T, de Cristofaro T, D'Ambrosio C, Del Prete D, Scaloni A, Zannini M 2008 Poly(ADP-ribose) polymerase 1 binds to Pax8 and inhibits its transcriptional activity. *Journal of molecular endocrinology* 41:379-388
134. Di Palma T, D'Andrea B, Liguori GL, Liguoro A, de Cristofaro T, Del Prete D, Pappalardo A, Mascia A, Zannini M 2009 TAZ is a coactivator for Pax8 and TTF-1, two transcription factors involved in thyroid differentiation. *Experimental cell research* 315:162-175

135. Nitsch R, Di Palma T, Mascia A, Zannini M 2004 WBP-2, a WW domain binding protein, interacts with the thyroid-specific transcription factor Pax8. *The Biochemical journal* 377:553-560
136. Congdon T, Nguyen LQ, Nogueira CR, Habiby RL, Medeiros-Neto G, Kopp P 2001 A novel mutation (Q40P) in PAX8 associated with congenital hypothyroidism and thyroid hypoplasia: evidence for phenotypic variability in mother and child. *J Clin Endocrinol Metab* 86:3962-3967
137. Komatsu M, Takahashi T, Takahashi I, Nakamura M, Takahashi I, Takada G 2001 Thyroid dysgenesis caused by PAX8 mutation: the hypermutability with CpG dinucleotides at codon 31. *J Pediatr* 139:597-599
138. Macchia PE, Lapi P, Krude H, Pirro MT, Missero C, Chiovato L, Souabni A, Baserga M, Tassi V, Pinchera A, Fenzi G, Gruters A, Busslinger M, Di Lauro R 1998 PAX8 mutations associated with congenital hypothyroidism caused by thyroid dysgenesis. *Nat Genet* 19:83-86
139. Meeus L, Gilbert B, Rydlewski C, Parma J, Roussie AL, Abramowicz M, Vilain C, Christophe D, Costagliola S, Vassart G 2004 Characterization of a novel loss of function mutation of PAX8 in a familial case of congenital hypothyroidism with in-place, normal-sized thyroid. *J Clin Endocrinol Metab* 89:4285-4291
140. Vilain C, Rydlewski C, Duprez L, Heinrichs C, Abramowicz M, Malvaux P, Renneboog B, Parma J, Costagliola S, Vassart G 2001 Autosomal dominant transmission of congenital thyroid hypoplasia due to loss-of-function mutation of PAX8. *J Clin Endocrinol Metab* 86:234-238
141. de Sanctis L, Corrias A, Romagnolo D, Di Palma T, Biava A, Borgarello G, Gianino P, Silvestro L, Zannini M, Dianzan I 2004 Familial PAX8 small deletion (c.989_992delACCC) associated with extreme phenotype variability. *J Clin Endocrinol Metab* 89:5669-5674
142. Kondo T, Ezzat S, Asa SL 2006 Pathogenetic mechanisms in thyroid follicular-cell neoplasia. *Nature reviews* 6:292-306
143. Gimm O 2001 Thyroid cancer. *Cancer letters* 163:143-156
144. Salajegheh A, Petcu EB, Smith RA, Lam AK 2008 Follicular variant of papillary thyroid carcinoma: a diagnostic challenge for clinicians and pathologists. *Postgraduate medical journal* 84:78-82
145. Michor F, Iwasa Y, Nowak MA 2004 Dynamics of cancer progression. *Nature reviews* 4:197-205
146. Greaves M 2002 Cancer causation: the Darwinian downside of past success? *The lancet oncology* 3:244-251
147. Ain KB 1998 Anaplastic thyroid carcinoma: behavior, biology, and therapeutic approaches. *Thyroid* 8:715-726
148. Aldinger KA, Samaan NA, Ibanez M, Hill CS, Jr. 1978 Anaplastic carcinoma of the thyroid: a review of 84 cases of spindle and giant cell carcinoma of the thyroid. *Cancer* 41:2267-2275
149. Nishiyama RH, Dunn EL, Thompson NW 1972 Anaplastic spindle-cell and giant-cell tumors of the thyroid gland. *Cancer* 30:113-127
150. Hunt JL, Tometsko M, LiVolsi VA, Swalsky P, Finkelstein SD, Barnes EL 2003 Molecular evidence of anaplastic transformation in coexisting well-differentiated and anaplastic carcinomas of the thyroid. *The American journal of surgical pathology* 27:1559-1564
151. Xing M 2005 BRAF mutation in thyroid cancer. *Endocrine-related cancer* 12:245-262

152. Fagin JA 2004 Challenging dogma in thyroid cancer molecular genetics--role of RET/PTC and BRAF in tumor initiation. *The Journal of clinical endocrinology and metabolism* 89:4264-4266
153. Hou P, Liu D, Shan Y, Hu S, Studeman K, Condouris S, Wang Y, Trink A, El-Naggar AK, Tallini G, Vasko V, Xing M 2007 Genetic alterations and their relationship in the phosphatidylinositol 3-kinase/Akt pathway in thyroid cancer. *Clin Cancer Res* 13:1161-1170
154. Au AY, McBride C, Wilhelm KG, Jr., Koenig RJ, Speller B, Cheung L, Messina M, Wentworth J, Tasevski V, Learoyd D, Robinson BG, Clifton-Bligh RJ 2006 PAX8-peroxisome proliferator-activated receptor gamma (PPARgamma) disrupts normal PAX8 or PPARgamma transcriptional function and stimulates follicular thyroid cell growth. *Endocrinology* 147:367-376
155. Ito T, Seyama T, Mizuno T, Tsuyama N, Hayashi T, Hayashi Y, Dohi K, Nakamura N, Akiyama M 1992 Unique association of p53 mutations with undifferentiated but not with differentiated carcinomas of the thyroid gland. *Cancer research* 52:1369-1371
156. Fagin JA, Matsuo K, Karmakar A, Chen DL, Tang SH, Koeffler HP 1993 High prevalence of mutations of the p53 gene in poorly differentiated human thyroid carcinomas. *The Journal of clinical investigation* 91:179-184
157. Krohn K, Fuhrer D, Bayer Y, Eszlinger M, Brauer V, Neumann S, Paschke R 2005 Molecular pathogenesis of euthyroid and toxic multinodular goiter. *Endocrine reviews* 26:504-524
158. Shirokawa JM, Elisei R, Knauf JA, Hara T, Wang J, Saavedra HI, Fagin JA 2000 Conditional apoptosis induced by oncogenic ras in thyroid cells. *Molecular endocrinology (Baltimore, Md)* 14:1725-1738
159. Bongarzone I, Monzini N, Borrello MG, Carcano C, Ferraresi G, Arighi E, Mondellini P, Della Porta G, Pierotti MA 1993 Molecular characterization of a thyroid tumor-specific transforming sequence formed by the fusion of ret tyrosine kinase and the regulatory subunit RI alpha of cyclic AMP-dependent protein kinase A. *Molecular and cellular biology* 13:358-366
160. Grieco M, Santoro M, Berlingieri MT, Melillo RM, Donghi R, Bongarzone I, Pierotti MA, Della Porta G, Fusco A, Vecchio G 1990 PTC is a novel rearranged form of the ret proto-oncogene and is frequently detected in vivo in human thyroid papillary carcinomas. *Cell* 60:557-563
161. Santoro M, Dathan NA, Berlingieri MT, Bongarzone I, Paulin C, Grieco M, Pierotti MA, Vecchio G, Fusco A 1994 Molecular characterization of RET/PTC3; a novel rearranged version of the RET proto-oncogene in a human thyroid papillary carcinoma. *Oncogene* 9:509-516
162. Jhiang SM, Sagartz JE, Tong Q, Parker-Thornburg J, Capen CC, Cho JY, Xing S, Ledent C 1996 Targeted expression of the ret/PTC1 oncogene induces papillary thyroid carcinomas. *Endocrinology* 137:375-378
163. Santoro M, Chiappetta G, Cerrato A, Salvatore D, Zhang L, Manzo G, Picone A, Portella G, Santelli G, Vecchio G, Fusco A 1996 Development of thyroid papillary carcinomas secondary to tissue-specific expression of the RET/PTC1 oncogene in transgenic mice. *Oncogene* 12:1821-1826
164. Powell DJ, Jr., Russell J, Nibu K, Li G, Rhee E, Liao M, Goldstein M, Keane WM, Santoro M, Fusco A, Rothstein JL 1998 The RET/PTC3 oncogene: metastatic solid-type papillary carcinomas in murine thyroids. *Cancer research* 58:5523-5528
165. Moretti S, Macchiarulo A, De Falco V, Avenia N, Barbi F, Carta C, Cavaliere A, Melillo RM, Passeri L, Santeusano F, Tartaglia M, Santoro M, Puxeddu E 2006

- Biochemical and molecular characterization of the novel BRAF(V599Ins) mutation detected in a classic papillary thyroid carcinoma. *Oncogene* 25:4235-4240
166. Wan PT, Garnett MJ, Roe SM, Lee S, Niculescu-Duvaz D, Good VM, Jones CM, Marshall CJ, Springer CJ, Barford D, Marais R 2004 Mechanism of activation of the RAF-ERK signaling pathway by oncogenic mutations of B-RAF. *Cell* 116:855-867
 167. Namba H, Nakashima M, Hayashi T, Hayashida N, Maeda S, Rogounovitch TI, Ohtsuru A, Saenko VA, Kanematsu T, Yamashita S 2003 Clinical implication of hot spot BRAF mutation, V599E, in papillary thyroid cancers. *The Journal of clinical endocrinology and metabolism* 88:4393-4397
 168. Nikiforova MN, Kimura ET, Gandhi M, Biddinger PW, Knauf JA, Basolo F, Zhu Z, Giannini R, Salvatore G, Fusco A, Santoro M, Fagin JA, Nikiforov YE 2003 BRAF mutations in thyroid tumors are restricted to papillary carcinomas and anaplastic or poorly differentiated carcinomas arising from papillary carcinomas. *The Journal of clinical endocrinology and metabolism* 88:5399-5404
 169. Begum S, Rosenbaum E, Henrique R, Cohen Y, Sidransky D, Westra WH 2004 BRAF mutations in anaplastic thyroid carcinoma: implications for tumor origin, diagnosis and treatment. *Mod Pathol* 17:1359-1363
 170. Soares P, Trovisco V, Rocha AS, Feijao T, Rebocho AP, Fonseca E, Vieira de Castro I, Cameselle-Teijeiro J, Cardoso-Oliveira M, Sobrinho-Simoes M 2004 BRAF mutations typical of papillary thyroid carcinoma are more frequently detected in undifferentiated than in insular and insular-like poorly differentiated carcinomas. *Virchows Arch* 444:572-576
 171. Quiros RM, Ding HG, Gattuso P, Prinz RA, Xu X 2005 Evidence that one subset of anaplastic thyroid carcinomas are derived from papillary carcinomas due to BRAF and p53 mutations. *Cancer* 103:2261-2268
 172. Knauf JA, Ma X, Smith EP, Zhang L, Mitsutake N, Liao XH, Refetoff S, Nikiforov YE, Fagin JA 2005 Targeted expression of BRAFV600E in thyroid cells of transgenic mice results in papillary thyroid cancers that undergo dedifferentiation. *Cancer research* 65:4238-4245
 173. Halachmi N, Halachmi S, Evron E, Cairns P, Okami K, Saji M, Westra WH, Zeiger MA, Jen J, Sidransky D 1998 Somatic mutations of the PTEN tumor suppressor gene in sporadic follicular thyroid tumors. *Genes, chromosomes & cancer* 23:239-243
 174. Bruni P, Boccia A, Baldassarre G, Trapasso F, Santoro M, Chiappetta G, Fusco A, Viglietto G 2000 PTEN expression is reduced in a subset of sporadic thyroid carcinomas: evidence that PTEN-growth suppressing activity in thyroid cancer cells mediated by p27kip1. *Oncogene* 19:3146-3155
 175. Vasko V, Saji M, Hardy E, Kruhlak M, Larin A, Savchenko V, Miyakawa M, Isozaki O, Murakami H, Tsushima T, Burman KD, De Micco C, Ringel MD 2004 Akt activation and localisation correlate with tumour invasion and oncogene expression in thyroid cancer. *Journal of medical genetics* 41:161-170
 176. Yeager N, Klein-Szanto A, Kimura S, Di Cristofano A 2007 Pten loss in the mouse thyroid causes goiter and follicular adenomas: insights into thyroid function and Cowden disease pathogenesis. *Cancer research* 67:959-966
 177. Garcia-Rostan G, Costa AM, Pereira-Castro I, Salvatore G, Hernandez R, Hermsem MJ, Herrero A, Fusco A, Cameselle-Teijeiro J, Santoro M 2005 Mutation of the PIK3CA gene in anaplastic thyroid cancer. *Cancer research* 65:10199-10207
 178. Battista S, Martelli ML, Fedele M, Chiappetta G, Trapasso F, De Vita G, Battaglia C, Santoro M, Viglietto G, Fagin JA, et al. 1995 A mutated p53 gene alters thyroid cell differentiation. *Oncogene* 11:2029-2037

179. Fagin JA, Tang SH, Zeki K, Di Lauro R, Fusco A, Gonsky R 1996 Reexpression of thyroid peroxidase in a derivative of an undifferentiated thyroid carcinoma cell line by introduction of wild-type p53. *Cancer research* 56:765-771
180. Moretti F, Farsetti A, Soddu S, Misiti S, Crescenzi M, Filetti S, Andreoli M, Sacchi A, Pontecorvi A 1997 p53 re-expression inhibits proliferation and restores differentiation of human thyroid anaplastic carcinoma cells. *Oncogene* 14:729-740
181. Kroll TG, Sarraf P, Pecciarini L, Chen CJ, Mueller E, Spiegelman BM, Fletcher JA 2000 PAX8-PPARgamma1 fusion oncogene in human thyroid carcinoma [corrected]. *Science (New York, NY)* 289:1357-1360
182. Marques AR, Espadinha C, Catarino AL, Moniz S, Pereira T, Sobrinho LG, Leite V 2002 Expression of PAX8-PPAR gamma 1 rearrangements in both follicular thyroid carcinomas and adenomas. *The Journal of clinical endocrinology and metabolism* 87:3947-3952
183. Nikiforova MN, Lynch RA, Biddinger PW, Alexander EK, Dorn GW, 2nd, Tallini G, Kroll TG, Nikiforov YE 2003 RAS point mutations and PAX8-PPAR gamma rearrangement in thyroid tumors: evidence for distinct molecular pathways in thyroid follicular carcinoma. *The Journal of clinical endocrinology and metabolism* 88:2318-2326
184. Nikiforova MN, Biddinger PW, Caudill CM, Kroll TG, Nikiforov YE 2002 PAX8-PPARgamma rearrangement in thyroid tumors: RT-PCR and immunohistochemical analyses. *The American journal of surgical pathology* 26:1016-1023
185. Lemoine NR, Mayall ES, Wyllie FS, Farr CJ, Hughes D, Padua RA, Thurston V, Williams ED, Wynford-Thomas D 1988 Activated ras oncogenes in human thyroid cancers. *Cancer research* 48:4459-4463
186. Horie H, Yokogoshi Y, Tsuyuguchi M, Saito S 1995 Point mutations of ras and Gs alpha subunit genes in thyroid tumors. *Jpn J Cancer Res* 86:737-742
187. Pilotti S, Collini P, Mariani L, Placucci M, Bongarzone I, Vigneri P, Cipriani S, Falchetta F, Miceli R, Pierotti MA, Rilke F 1997 Insular carcinoma: a distinct de novo entity among follicular carcinomas of the thyroid gland. *The American journal of surgical pathology* 21:1466-1473
188. Garcia-Rostan G, Zhao H, Camp RL, Pollan M, Herrero A, Pardo J, Wu R, Carcangiu ML, Costa J, Tallini G 2003 ras mutations are associated with aggressive tumor phenotypes and poor prognosis in thyroid cancer. *J Clin Oncol* 21:3226-3235
189. Hirokawa M, Carney JA, Goellner JR, DeLellis RA, Heffess CS, Katoh R, Tsujimoto M, Kakudo K 2002 Observer variation of encapsulated follicular lesions of the thyroid gland. *The American journal of surgical pathology* 26:1508-1514
190. Lloyd RV, Erickson LA, Casey MB, Lam KY, Lohse CM, Asa SL, Chan JK, DeLellis RA, Harach HR, Kakudo K, LiVolsi VA, Rosai J, Sebo TJ, Sobrinho-Simoes M, Wenig BM, Lae ME 2004 Observer variation in the diagnosis of follicular variant of papillary thyroid carcinoma. *The American journal of surgical pathology* 28:1336-1340
191. Vitagliano D, Portella G, Troncone G, Francione A, Rossi C, Bruno A, Giorgini A, Coluzzi S, Nappi TC, Rothstein JL, Pasquinelli R, Chiappetta G, Terracciano D, Macchia V, Melillo RM, Fusco A, Santoro M 2006 Thyroid targeting of the N-ras(Gln61Lys) oncogene in transgenic mice results in follicular tumors that progress to poorly differentiated carcinomas. *Oncogene* 25:5467-5474
192. Schlumberger M, Tubiana M, De Vathaire F, Hill C, Gardet P, Travagli JP, Fragu P, Lumbroso J, Caillou B, Parmentier C 1986 Long-term results of treatment of 283 patients with lung and bone metastases from differentiated thyroid carcinoma. *The Journal of clinical endocrinology and metabolism* 63:960-967

193. Mazzaferri EL, Jhiang SM 1994 Long-term impact of initial surgical and medical therapy on papillary and follicular thyroid cancer. *The American journal of medicine* 97:418-428
194. Schlumberger M, Baudin E 1998 Serum thyroglobulin determination in the follow-up of patients with differentiated thyroid carcinoma. *European journal of endocrinology / European Federation of Endocrine Societies* 138:249-252
195. Sherman SI 2003 Thyroid carcinoma. *Lancet* 361:501-511
196. Carvalho DP, Ferreira AC 2007 The importance of sodium/iodide symporter (NIS) for thyroid cancer management. *Arquivos brasileiros de endocrinologia e metabologia* 51:672-682
197. Simon D, Korber C, Krausch M, Segering J, Groth P, Gorges R, Grunwald F, Muller-Gartner HW, Schmutzler C, Kohrle J, Roher HD, Reiners C 2002 Clinical impact of retinoids in redifferentiation therapy of advanced thyroid cancer: final results of a pilot study. *European journal of nuclear medicine and molecular imaging* 29:775-782
198. Riesco-Eizaguirre G, Santisteban P 2006 A perspective view of sodium iodide symporter research and its clinical implications. *European journal of endocrinology / European Federation of Endocrine Societies* 155:495-512
199. Sebolt-Leopold JS, Dudley DT, Herrera R, Van Becelaere K, Wiland A, Gowan RC, Teclé H, Barrett SD, Bridges A, Przybranowski S, Leopold WR, Saltiel AR 1999 Blockade of the MAP kinase pathway suppresses growth of colon tumors in vivo. *Nature medicine* 5:810-816
200. Wang D, Boerner SA, Winkler JD, LoRusso PM 2007 Clinical experience of MEK inhibitors in cancer therapy. *Biochimica et biophysica acta* 1773:1248-1255
201. Allen LF, Sebolt-Leopold J, Meyer MB 2003 CI-1040 (PD184352), a targeted signal transduction inhibitor of MEK (MAPKK). *Seminars in oncology* 30:105-116
202. Rinehart J, Adjei AA, Lorusso PM, Waterhouse D, Hecht JR, Natale RB, Hamid O, Varterasian M, Asbury P, Kaldjian EP, Gulyas S, Mitchell DY, Herrera R, Sebolt-Leopold JS, Meyer MB 2004 Multicenter phase II study of the oral MEK inhibitor, CI-1040, in patients with advanced non-small-cell lung, breast, colon, and pancreatic cancer. *J Clin Oncol* 22:4456-4462
203. Lorusso PM, Adjei AA, Varterasian M, Gadgeel S, Reid J, Mitchell DY, Hanson L, DeLuca P, Bruzek L, Piens J, Asbury P, Van Becelaere K, Herrera R, Sebolt-Leopold J, Meyer MB 2005 Phase I and pharmacodynamic study of the oral MEK inhibitor CI-1040 in patients with advanced malignancies. *J Clin Oncol* 23:5281-5293
204. Solit DB, Garraway LA, Pratilas CA, Sawai A, Getz G, Basso A, Ye Q, Lobo JM, She Y, Osman I, Golub TR, Sebolt-Leopold J, Sellers WR, Rosen N 2006 BRAF mutation predicts sensitivity to MEK inhibition. *Nature* 439:358-362
205. Liu D, Liu Z, Jiang D, Dackiw AP, Xing M 2007 Inhibitory effects of the mitogen-activated protein kinase kinase inhibitor CI-1040 on the proliferation and tumor growth of thyroid cancer cells with BRAF or RAS mutations. *The Journal of clinical endocrinology and metabolism* 92:4686-4695
206. Ball DW, Jin N, Rosen DM, Dackiw A, Sidransky D, Xing M, Nelkin BD 2007 Selective growth inhibition in BRAF mutant thyroid cancer by the mitogen-activated protein kinase kinase 1/2 inhibitor AZD6244. *The Journal of clinical endocrinology and metabolism* 92:4712-4718
207. Ahmad T, Eisen T 2004 Kinase inhibition with BAY 43-9006 in renal cell carcinoma. *Clin Cancer Res* 10:6388S-6392S
208. Salvatore G, De Falco V, Salerno P, Nappi TC, Pepe S, Troncone G, Carlomagno F, Melillo RM, Wilhelm SM, Santoro M 2006 BRAF is a therapeutic target in aggressive thyroid carcinoma. *Clin Cancer Res* 12:1623-1629

209. Carlomagno F, Anaganti S, Guida T, Salvatore G, Troncone G, Wilhelm SM, Santoro M 2006 BAY 43-9006 inhibition of oncogenic RET mutants. *Journal of the National Cancer Institute* 98:326-334
210. Ouyang B, Knauf JA, Smith EP, Zhang L, Ramsey T, Yusuff N, Batt D, Fagin JA 2006 Inhibitors of Raf kinase activity block growth of thyroid cancer cells with RET/PTC or BRAF mutations in vitro and in vivo. *Clin Cancer Res* 12:1785-1793
211. Levitzki A 1999 Protein tyrosine kinase inhibitors as novel therapeutic agents. *Pharmacology & therapeutics* 82:231-239
212. Wedge SR, Ogilvie DJ, Dukes M, Kendrew J, Chester R, Jackson JA, Boffey SJ, Valentine PJ, Curwen JO, Musgrove HL, Graham GA, Hughes GD, Thomas AP, Stokes ES, Curry B, Richmond GH, Wadsworth PF, Bigley AL, Hennequin LF 2002 ZD6474 inhibits vascular endothelial growth factor signaling, angiogenesis, and tumor growth following oral administration. *Cancer research* 62:4645-4655
213. Carlomagno F, Vitagliano D, Guida T, Ciardiello F, Tortora G, Vecchio G, Ryan AJ, Fontanini G, Fusco A, Santoro M 2002 ZD6474, an orally available inhibitor of KDR tyrosine kinase activity, efficiently blocks oncogenic RET kinases. *Cancer research* 62:7284-7290
214. Weinstein IB, Joe AK 2006 Mechanisms of disease: Oncogene addiction--a rationale for molecular targeting in cancer therapy. *Nature clinical practice* 3:448-457
215. McKinstry R, Qiao L, Yacoub A, Dai Y, Decker R, Holt S, Hagan MP, Grant S, Dent P 2002 Inhibitors of MEK1/2 interact with UCN-01 to induce apoptosis and reduce colony formation in mammary and prostate carcinoma cells. *Cancer biology & therapy* 1:243-253
216. Qiao L, Yacoub A, McKinstry R, Park JS, Caron R, Fisher PB, Hagan MP, Grant S, Dent P 2002 Pharmacologic inhibitors of the mitogen activated protein kinase cascade have the potential to interact with ionizing radiation exposure to induce cell death in carcinoma cells by multiple mechanisms. *Cancer biology & therapy* 1:168-176
217. Yeh TC, Marsh V, Bernat BA, Ballard J, Colwell H, Evans RJ, Parry J, Smith D, Brandhuber BJ, Gross S, Marlow A, Hurley B, Lyssikatos J, Lee PA, Winkler JD, Koch K, Wallace E 2007 Biological characterization of ARRY-142886 (AZD6244), a potent, highly selective mitogen-activated protein kinase kinase 1/2 inhibitor. *Clin Cancer Res* 13:1576-1583
218. Ambesi-Impimbato FS, Parks LA, Coon HG 1980 Culture of hormone-dependent functional epithelial cells from rat thyroids. *Proceedings of the National Academy of Sciences of the United States of America* 77:3455-3459
219. Francis-Lang H, Zannini M, De Felice M, Berlingieri MT, Fusco A, Di Lauro R 1992 Multiple mechanisms of interference between transformation and differentiation in thyroid cells. *Molecular and cellular biology* 12:5793-5800
220. Cobellis G, Missero C, Di Lauro R 1998 Concomitant activation of MEK-1 and Rac-1 increases the proliferative potential of thyroid epithelial cells, without affecting their differentiation. *Oncogene* 17:2047-2057
221. Missero C, Pirro MT, Di Lauro R 2000 Multiple ras downstream pathways mediate functional repression of the homeobox gene product TTF-1. *Molecular and cellular biology* 20:2783-2793
222. Young L, Dong Q 2004 Two-step total gene synthesis method. *Nucleic acids research* 32:e59
223. Heckman KL, Pease LR 2007 Gene splicing and mutagenesis by PCR-driven overlap extension. *Nature protocols* 2:924-932
224. Martin KJ, Lillie JW, Green MR 1990 Evidence for interaction of different eukaryotic transcriptional activators with distinct cellular targets. *Nature* 346:147-152

225. Chun JT, Di Dato V, D'Andrea B, Zannini M, Di Lauro R 2004 The CRE-like element inside the 5'-upstream region of the rat sodium/iodide symporter gene interacts with diverse classes of b-Zip molecules that regulate transcriptional activities through strong synergy with Pax-8. *Molecular endocrinology* (Baltimore, Md 18:2817-2829
226. Dorfler P, Busslinger M 1996 C-terminal activating and inhibitory domains determine the transactivation potential of BSAP (Pax-5), Pax-2 and Pax-8. *The EMBO journal* 15:1971-1982
227. Vlaeminck-Guillem V, Ho SC, Rodien P, Vassart G, Costagliola S 2002 Activation of the cAMP pathway by the TSH receptor involves switching of the ectodomain from a tethered inverse agonist to an agonist. *Molecular endocrinology* (Baltimore, Md 16:736-746
228. Driegen S, Ferreira R, van Zon A, Strouboulis J, Jaegle M, Grosveld F, Philipsen S, Meijer D 2005 A generic tool for biotinylation of tagged proteins in transgenic mice. *Transgenic research* 14:477-482
229. Davidson D, Chow LM, Fournel M, Veillette A 1992 Differential regulation of T cell antigen responsiveness by isoforms of the src-related tyrosine protein kinase p59fyn. *The Journal of experimental medicine* 175:1483-1492
230. Wessel D, Flugge UI 1984 A method for the quantitative recovery of protein in dilute solution in the presence of detergents and lipids. *Analytical biochemistry* 138:141-143
231. Rutledge RG, Cote C 2003 Mathematics of quantitative kinetic PCR and the application of standard curves. *Nucleic acids research* 31:e93
232. Sandoval J, Rodriguez JL, Tur G, Serviddio G, Pereda J, Boukaba A, Sastre J, Torres L, Franco L, Lopez-Rodas G 2004 RNAPol-ChIP: a novel application of chromatin immunoprecipitation to the analysis of real-time gene transcription. *Nucleic acids research* 32:e88
233. Civitareale D, Lonigro R, Sinclair AJ, Di Lauro R 1989 A thyroid-specific nuclear protein essential for tissue-specific expression of the thyroglobulin promoter. *The EMBO journal* 8:2537-2542
234. Poleev A, Okladnova O, Musti AM, Schneider S, Royer-Pokora B, Plachov D 1997 Determination of functional domains of the human transcription factor PAX8 responsible for its nuclear localization and transactivating potential. *European journal of biochemistry / FEBS* 247:860-869
235. De Felice M, Postiglione MP, Di Lauro R 2004 Minireview: thyrotropin receptor signaling in development and differentiation of the thyroid gland: insights from mouse models and human diseases. *Endocrinology* 145:4062-4067
236. Ledent C, Parmentier M, Maenhaut C, Taton M, Pirson I, Lamy F, Roger P, Dumont JE 1991 The TSH cyclic AMP cascade in the control of thyroid cell proliferation: the story of a concept. *Thyroidology / APRI* 3:97-101
237. Opitz R, Trubiroha A, Lorenz C, Lutz I, Hartmann S, Blank T, Braunbeck T, Kloas W 2006 Expression of sodium-iodide symporter mRNA in the thyroid gland of *Xenopus laevis* tadpoles: developmental expression, effects of antithyroidal compounds, and regulation by TSH. *The Journal of endocrinology* 190:157-170
238. Southern JA, Young DF, Heaney F, Baumgartner WK, Randall RE 1991 Identification of an epitope on the P and V proteins of simian virus 5 that distinguishes between two isolates with different biological characteristics. *The Journal of general virology* 72 (Pt 7):1551-1557
239. Chubet RG, Brizzard BL 1996 Vectors for expression and secretion of FLAG epitope-tagged proteins in mammalian cells. *BioTechniques* 20:136-141

240. Witzgall R, O'Leary E, Bonventre JV 1994 A mammalian expression vector for the expression of GAL4 fusion proteins with an epitope tag and histidine tail. *Analytical biochemistry* 223:291-298
241. Beckett D, Kovaleva E, Schatz PJ 1999 A minimal peptide substrate in biotin holoenzyme synthetase-catalyzed biotinylation. *Protein Sci* 8:921-929
242. Nallamsetty S, Kapust RB, Tozser J, Cherry S, Tropea JE, Copeland TD, Waugh DS 2004 Efficient site-specific processing of fusion proteins by tobacco vein mottling virus protease in vivo and in vitro. *Protein expression and purification* 38:108-115
243. Cordingley MG, Callahan PL, Sardana VV, Garsky VM, Colonna RJ 1990 Substrate requirements of human rhinovirus 3C protease for peptide cleavage in vitro. *The Journal of biological chemistry* 265:9062-9065
244. de Boer E, Rodriguez P, Bonte E, Krijgsveld J, Katsantoni E, Heck A, Grosveld F, Strouboulis J 2003 Efficient biotinylation and single-step purification of tagged transcription factors in mammalian cells and transgenic mice. *Proceedings of the National Academy of Sciences of the United States of America* 100:7480-7485
245. Rodriguez P, Braun H, Kolodziej KE, de Boer E, Campbell J, Bonte E, Grosveld F, Philipsen S, Strouboulis J 2006 Isolation of transcription factor complexes by in vivo biotinylation tagging and direct binding to streptavidin beads. *Methods in molecular biology (Clifton, NJ)* 338:305-323
246. Jonkers J, Berns A 2004 Oncogene addiction: sometimes a temporary slavery. *Cancer cell* 6:535-538
247. Sharma SV, Settleman J 2007 Oncogene addiction: setting the stage for molecularly targeted cancer therapy. *Genes & development* 21:3214-3231
248. Weinstein IB, Joe A 2008 Oncogene addiction. *Cancer research* 68:3077-3080; discussion 3080
249. Avvedimento VE, Musti AM, Ueffing M, Obici S, Gallo A, Sanchez M, DeBrasi D, Gottesman ME 1991 Reversible inhibition of a thyroid-specific trans-acting factor by Ras. *Genes & development* 5:22-28
250. Berlingieri MT, Musti AM, Avvedimento VE, Di Lauro R, Di Fiore PP, Fusco A 1989 The block of thyroglobulin synthesis, which occurs upon transformation of rat thyroid epithelial cells, is at the transcriptional level and it is associated with methylation of the 5' flanking region of the gene. *Experimental cell research* 183:277-283
251. Colletta G, Pinto A, Di Fiore PP, Fusco A, Ferrentino M, Avvedimento VE, Tsuchida N, Vecchio G 1983 Dissociation between transformed and differentiated phenotype in rat thyroid epithelial cells after transformation with a temperature-sensitive mutant of the Kirsten murine sarcoma virus. *Molecular and cellular biology* 3:2099-2109
252. Daub H, Specht K, Ullrich A 2004 Strategies to overcome resistance to targeted protein kinase inhibitors. *Nat Rev Drug Discov* 3:1001-1010
253. Spitzweg C, Morris JC 2002 The sodium iodide symporter: its pathophysiological and therapeutic implications. *Clinical endocrinology* 57:559-574
254. Crespo P, Leon J 2000 Ras proteins in the control of the cell cycle and cell differentiation. *Cell Mol Life Sci* 57:1613-1636
255. Sansom OJ, Meniel V, Wilkins JA, Cole AM, Oien KA, Marsh V, Jamieson TJ, Guerra C, Ashton GH, Barbacid M, Clarke AR 2006 Loss of Apc allows phenotypic manifestation of the transforming properties of an endogenous K-ras oncogene in vivo. *Proceedings of the National Academy of Sciences of the United States of America* 103:14122-14127
256. Monaco C, Califano D, Chiappetta G, Mineo A, De Franciscis V, Vecchio G, Santelli G 1995 Mutated human Kirsten ras, driven by a thyroglobulin promoter, induces a

- growth advantage and partially dedifferentiates rat thyroid epithelial cells in vitro. *International journal of cancer* 63:757-760
257. Kupperman E, Wofford D, Wen W, Meinkoth JL 1996 Ras inhibits thyroglobulin expression but not cyclic adenosine monophosphate-mediated signaling in Wistar rat thyrocytes. *Endocrinology* 137:96-104
 258. Bruno R, Ferretti E, Tosi E, Arturi F, Giannasio P, Mattei T, Scipioni A, Presta I, Morisi R, Gulino A, Filetti S, Russo D 2005 Modulation of thyroid-specific gene expression in normal and nodular human thyroid tissues from adults: an in vivo effect of thyrotropin. *The Journal of clinical endocrinology and metabolism* 90:5692-5697
 259. Dumaz N, Marais R 2005 Integrating signals between cAMP and the RAS/RAF/MEK/ERK signalling pathways. Based on the anniversary prize of the Gesellschaft fur Biochemie und Molekularbiologie Lecture delivered on 5 July 2003 at the Special FEBS Meeting in Brussels. *The FEBS journal* 272:3491-3504
 260. Presta I, Arturi F, Ferretti E, Mattei T, Scarpelli D, Tosi E, Scipioni A, Celano M, Gulino A, Filetti S, Russo D 2005 Recovery of NIS expression in thyroid cancer cells by overexpression of Pax8 gene. *BMC cancer* 5:80
 261. Feliciello A, Giuliano P, Porcellini A, Garbi C, Obici S, Mele E, Angotti E, Grieco D, Amabile G, Cassano S, Li Y, Musti AM, Rubin CS, Gottesman ME, Avvedimento EV 1996 The v-Ki-Ras oncogene alters cAMP nuclear signaling by regulating the location and the expression of cAMP-dependent protein kinase IIbeta. *The Journal of biological chemistry* 271:25350-25359
 262. Gallo A, Benusiglio E, Bonapace IM, Feliciello A, Cassano S, Garbi C, Musti AM, Gottesman ME, Avvedimento EV 1992 v-ras and protein kinase C dedifferentiate thyroid cells by down-regulating nuclear cAMP-dependent protein kinase A. *Genes & development* 6:1621-1630
 263. Gallo A, Feliciello A, Varrone A, Cerillo R, Gottesman ME, Avvedimento VE 1995 Ki-ras oncogene interferes with the expression of cyclic AMP-dependent promoters. *Cell Growth Differ* 6:91-95
 264. Calebiro D, de Filippis T, Lucchi S, Martinez F, Porazzi P, Trivellato R, Locati M, Beck-Peccoz P, Persani L 2006 Selective modulation of protein kinase A I and II reveals distinct roles in thyroid cell gene expression and growth. *Molecular endocrinology (Baltimore, Md)* 20:3196-3211
 265. Mayr B, Montminy M 2001 Transcriptional regulation by the phosphorylation-dependent factor CREB. *Nature reviews* 2:599-609
 266. Garcia-Jimenez C, Zaballos MA, Santisteban P 2005 DARPP-32 (dopamine and 3',5'-cyclic adenosine monophosphate-regulated neuronal phosphoprotein) is essential for the maintenance of thyroid differentiation. *Molecular endocrinology (Baltimore, Md)* 19:3060-3072
 267. Woloshin PI, Walton KM, Rehfuss RP, Goodman RH, Cone RD 1992 3',5'-cyclic adenosine monophosphate-regulated enhancer binding (CREB) activity is required for normal growth and differentiated phenotype in the FRTL5 thyroid follicular cell line. *Molecular endocrinology (Baltimore, Md)* 6:1725-1733
 268. Nguyen LQ, Kopp P, Martinson F, Stanfield K, Roth SI, Jameson JL 2000 A dominant negative CREB (cAMP response element-binding protein) isoform inhibits thyrocyte growth, thyroid-specific gene expression, differentiation, and function. *Molecular endocrinology (Baltimore, Md)* 14:1448-1461
 269. Robbins RJ, Schlumberger MJ 2005 The evolving role of (131)I for the treatment of differentiated thyroid carcinoma. *J Nucl Med* 46 Suppl 1:28S-37S

270. Cornett WR, Sharma AK, Day TA, Richardson MS, Hoda RS, van Heerden JA, Fernandes JK 2007 Anaplastic thyroid carcinoma: an overview. *Current oncology reports* 9:152-158
271. Miccoli P, Materazzi G, Antonelli A, Panicucci E, Frustaci G, Berti P 2007 New trends in the treatment of undifferentiated carcinomas of the thyroid. *Langenbeck's archives of surgery / Deutsche Gesellschaft für Chirurgie* 392:397-404
272. Ciampi R, Nikiforov YE 2005 Alterations of the BRAF gene in thyroid tumors. *Endocrine pathology* 16:163-172
273. Fagin JA 2005 Genetics of papillary thyroid cancer initiation: implications for therapy. *Transactions of the American Clinical and Climatological Association* 116:259-269; discussion 269-271